Chemoenzymatic surface modification of liposomal drug carriers

Dissertation zur Erlangung des Doktorgrades
der Mathematisch-Naturwissenschaftlichen Fakultät
der Christian-Albrechts-Universität zu Kiel

vorgelegt von

Steffen Wöll

Mainz, 2019

This work was carried out from July 2014 until September 2017 at the Merck KGaA, Darmstadt, Germany in collaboration with the Department of Pharmaceutics and Biopharmaceutics, Kiel University, Kiel, Germany. The thesis was prepared under supervision of Prof. Dr. Regina Scherließ.

Submission of the PhD application:	14.03.2019
Date of examination:	06.05.2019
Accepted for publication:	06.05.2019

1st Referee:	Prof. Dr. Regina Scherließ
2nd Referee:	Prof. Dr. Susanne Sebens
3rd Referee:	Prof. Dr. Ulrich Massing

Für die drei Omas

Messen sei eine hohe Kunst, sagte Humboldt.

Eine Verantwortung, die man nicht leichtnehmen dürfe.

Alexander von Humboldt in „Die Vermessung der Welt“

(Daniel Kehlmann, Rowohlt Verlag, 2005)

Table of contents

Chapter 1
Introduction and aim of thesis

1. Introduction: Nanoparticulate drug delivery

"…, wir müssen zielen lernen, chemisch zielen lernen!" – "we have to learn how to aim chemically" [1]. This famous appeal, proclaimed by Paul Ehrlich in 1909, set the paradigm for a rational development of tailored drugs precisely targeting disease-affected sites in patients while circumventing adverse effects [2]. More than a century later, Ehrlich's concept of the "magic bullet" was most closely realized in nanoparticulate drug delivery systems, whose function as targeted drug carriers strive to advance the treatment and diagnosis of various diseases [3].

Drug encapsulation into a carrier system aims to refine drug characteristics via three major pathways. Firstly, physico-chemical properties may be improved. This includes improvement of solubility [4] or the prevention of drug degradation during storage and administration [5].

Secondly, pharmacokinetics can be controlled. This includes extension of systemic circulation time by a reduced glomerular filtration in the kidney [6] or prevention of drug metabolism during circulation [7]. Furthermore, prolonged release after local administration may be achieved [8, 9]. A major pharmacokinetic benefit, and key relation towards Paul Ehrlich's magic bullet, is the prevention of drug distribution in vulnerable healthy tissues [10, 11], and *vice versa* the option to selectively target the carrier towards disease-affected tissues and cells [12].

Thirdly, pharmacodynamics may be improved. This improvement may in some cases be primarily explained by pharmacokinetic effects [10, 13]. However, especially large, non-permeable drugs require particulate drug delivery systems to cross cell membranes and subsequently exhibit intracellular effects. This is due to the unique interaction of nanoparticles with cells, leading to cellular uptake by active processes including endocytosis, (macro-)pinocytosis and phagocytosis [14]. Prominent examples are nanoparticulate formulated vaccines [15-17] or nucleic acid-loaded vectors utilized in gene therapy [18].

These three principle mechanisms contribute – alone or in combination [13] – to the possibility to improve the efficacy and safety of drugs via encapsulation in carrier systems. Recent decades of research in biomedical nanotechnology resulted in a large selection of such colloidal drug carriers composed of a plethora of materials with different dimensions, shapes and surface varieties [3]. The following work will focus on liposomal drug carriers due to their marked versatility and biocompatibility among the currently available drug delivery systems.

2. Liposomal drug carriers

Within the nanotechnological toolbox, liposomes have been most extensively studied as drug carriers since their discovery by Alec Bangham et al. in 1964 [19] and have been commercialized in several products (Table 1). According to a definition by Vladimir Torchilin, liposomes are "spherical, self-closed structures formed by one or several concentric lipid bilayers with an aqueous phase inside and between the lipid bilayers" [12]. The presence of both aqueous and lipid compartments offers the potential to encapsulate either hydrophilic, hydrophobic or amphiphilic drugs into the carrier [5]. Therapeutic liposomes are typically composed of amphiphilic phospholipids, cholesterol and stabilizing components, such as charged or polymer-conjugated lipids [4]. Hence, the main building blocks of liposomes are naturally occurring cell membrane components. This may explain the popularity of liposomal drug delivery systems due to the material's inherent biocompatibility, represented e.g. through degradability and low toxicity. Liposome dimensions and bilayer number (lamellarity), composition or surface modalities such as charge or ligand coating are commonly used for classification of liposomes [5]. In general, the liposomal size can vary between 20 nm and several micrometers, with 100 nm and 1000 nm used as thresholds discriminating small, large and giant vesicles. Furthermore, a single liposome can consist of one (unilamellar) or several (oligo- to multilamellar) bilayers. Drugs can be encapsulated [5, 20] or adsorbed to the liposomal surface [21]. Drug encapsulation occurs passively during liposome formation, or via remote loading, which is based on drug accumulation in the liposomal interior due to pH- or salt-gradients over the liposome bilayer [20].

Intravenous application is the most important route of administration for liposomal formulations (Table 1). After injection or infusion, the liposomes are subsequently distributed via the systemic circulation through narrow capillaries or strongly vascularized tissues. Hence, the liposome size has a significant impact on the *in vivo* fate of the carrier and is therefore a crucial formulation parameter [22, 23]. The average liposome size as well as the heterogeneity of the underlying size distribution strongly depend on the liposome manufacturing strategy. Different techniques were developed over the recent years to facilitate the formation of liposomes in an aqueous system from lipid components. These include hydration of thin lipid films, (supercritical) reverse-phase evaporation, coacervation, detergent depletion, solvent injection, microfluidic techniques or spray-drying of proliposomes [5]. Additional sonication steps or vesicle extrusion through membranes with a defined pore size lead to a subsequent sizing of the liposomes, where large and occasionally oligolamellar structures are processed into small or large unilamellar vesicles [5]. Especially the latter group of liposomes, characterized by a monomodal size distribution with a

mean diameter around 100 nm and a single bilayer architecture, was revealed as most suitable for the systemic administration of liposomal drugs (Table 1, [22]).

Table 1: Marketed liposomal drugs (modified from [22]).

drug	route of administration	indication	diameter	reference
doxorubicin (Doxil®, Myocet®, Evacet®)	intravenous	Kaposi's sarcoma, ovarian and breast cancer	100 nm / 180 nm	[10]
daunorubicin (DaunoXome®)	intravenous	Kaposi's sarcoma	45 nm	[24]
vincristine (Marqibo®)	intravenous	acute lymphoblastic leukemia	100 nm	[13]
irinotecan (Onivyde®)	intravenous	metastatic adenocarcinoma of the pancreas	110 nm	[25]
amphotericin B (AmBisome®, Amphotec®)	intravenous	fungal infections	100 nm	[11]
mifamurtide (Mepact®)	intravenous	osteosarcoma	< 100 nm	[26]
verteporfin (Visudyne®)	intravenous	age-related macular degeneration	150-300 nm	[27]
daunorubicin, cytarabine (Vyxeos®)	intravenous	acute myeloid leukemia	100 nm	[28]
cytarabine (DepoCyte®)	intrathecal	neoplastic meningitis, lymphomatous meningitis	3-30 µm	[29]
bupivacaine (Exparel®)	subcutaneous	local anesthesia	24-31 µm	[9]
morphine sulfate (DepoDur®)	epidural	pain management	17-23 µm	[8]
inactivated hepatitis A virus (Epaxal®)	intramuscular	hepatitis A	150 nm	[16]
inactivated hemagglutinine (Inflexal V®)	intramuscular	influenza	150 nm	[17]

3. Liposomal drug targeting

The major indication for liposomal drugs is the treatment of cancer (Table 1). Chemotherapeutics typically have a low therapeutic index due to their unfavorable safety profile. Therefore, they can in particular profit from liposomal encapsulation if (i) the drug remains encapsulated in the carrier during circulation, (ii) the liposome is selectively delivered towards a tumor and (iii) the drug is able to reach its target and exhibit the pharmacodynamic effect [10]. Such behavior was observed for stable liposomes showing an extended systemic circulation, which is achieved by several key formulation attributes [10]. Firstly, this is the grafting of a polyethylene glycol (PEG) layer on the liposome surface, which avoids unspecific carrier uptake via the mononuclear phagocyte system (MPS). Furthermore, usage of high-melting lipids together with cholesterol and active loading technology leads to efficient and

stable drug encapsulation. Such long-circulating liposomes with an approximated size of 100 nm are known to exploit a passive targeting via the enhanced permeability and retention (EPR) effect [5]. The EPR effect is based on widely-fenestrated, “leaky” vascularization found in solid tumors, but also in inflammatory tissues [30]. Large molecules or nanoparticles can escape the circulation via a passage through endothelial gaps (extravasation) and reach the tumor interstitium [30]. This vascular hyperpermeability, together with an impaired lymphatic drainage, leads to an elevated interstitial fluid pressure. Latter reduces the convective transport of nanoparticles in the interstitium, while diffusion is hindered by a dense extracellular matrix [31]. Both mechanisms are responsible for an accumulation of drug carriers in the tumor interstitium [30]. After distribution in the tumor tissue, the drug may then be released from the carrier and permeate into surrounding cells. Alternatively, cellular uptake of the whole carrier occurs, followed by an intracellular drug release, e.g. promoted by enzymatic degradation in lysosomes [23]. Finally, both mechanisms lead to a site-selective availability of pharmacodynamically active drugs.

This EPR-based passive targeting is limited as it relies on specific physiological conditions, meaning the unique combination of leaky vascularization and low lymphatic drainage. It would, besides tremendous doubts on the overall clinical relevance [30], only be applicable to solid tumors and a limited number of other diseases [5] without any specificity towards special cell types. This cellular specificity of drug delivery can be increased by active targeting. Active targeting strives for a site-selective drug delivery by combining carriers with ligands binding towards disease-specific receptors. Specificity of active targeting is therefore closely correlated with expression patterns of the receptors of interest [32]. Especially tumor cells or tumor vasculature overexpress receptors which can be exploited as targets due to a virtual absence on healthy cells. This discovery has firstly led to the approval of a huge amount of biological entities such as monoclonal antibodies [2], which can bind to such targets with high specificity and thereby exhibit desired pharmacodynamic effects. In a second stage, these binders were conjugated with toxic molecules (antibody-drug conjugates, ADCs), combining the specificity of the ligand with the potency of the toxin, thereby increasing therapeutic indices of the latter [33]. The conjugation of ligands on the surface of liposomal carriers, yielding so called “immunoliposomes”, is therefore a reasonable approach to achieve a targeting effect additional on passive targeting. Furthermore, the targeting is independent from physiologic prerequisites such as tissues showing an EPR effect, what enables targeting of e.g. blood [34, 35] or endothelial cells [36].

Besides monoclonal antibodies (mAb), a huge variety of structures was employed as liposomal targeting moieties in the past. This includes antibody-derivatives such as fragment antigen-

binding (Fab or Fab'), single-chain variable fragment (scFv), single-domain antibodies or peptides, carbohydrate structures and small molecules (for a recent review see [37]). Choice of the ligand design can have significant impact on the *in vivo* behavior of the targeted liposomes. This is due to differences in ligand-induced immunogenicity, impact on pharmacokinetics (e.g. via Fc-receptor mediated clearance), opsonization or *in vivo* stability [37]. Furthermore, tumor penetration may strongly depend on the type of ligand used. Especially a homogenous tumor distribution was shown to be more effective with low-affine scFvs than high-affine mAbs or Fabs, explained via the so called "binding site barrier" phenomenon [37, 38]. This was also transferred to immunoliposomes, assuming that targeted carriers stick to the first encountered, target-positive cells after extravasation, preventing pervasive drug delivery throughout the tumor tissue [35, 39]. Hence, especially small binder formats such as Fab's or scFvs are nowadays preferred over whole antibodies when utilized as ligands on liposomes [35, 40-43].

Depending on the utilized receptor and ligand type, carriers may solely bind to target cells or undergo receptor-mediated internalization [37]. Especially for the delivery of permeable small molecules, internalization of the carrier may not be a prerequisite, since a liposomal drug release in target proximity can be sufficient for increasing therapeutic efficiency over non-liposomal drug [35]. In contrast, large impermeable macromolecules such as proteins will most likely require a drug delivery system which promotes internalization and cytosolic delivery of the cargo [44, 45].

Compared to direct conjugates of drug and targeting moiety, such as ADCs [33], actively targeted carriers may profit from two major benefits [45]. Firstly, this is the comparably high ratio of drug to ligand that can be achieved [46], especially when state-of-the-art remote loading techniques (such as the ammonium sulfate gradient method) are employed [20]. Secondly, nanoparticulate platforms bind in a multivalent fashion towards their target cells [45, 47, 48], meaning that a single carrier utilizes several surface receptors during interaction with the cell. This may lead to an enhanced internalization of carriers [44, 48]. Multivalent binding may also gain specificity over off-target tissues, as targeting ligands with low affinity can be utilized. The high avidity of the multivalent carrier counterbalances the low affinity of the individual ligand, and lead to a sufficiently strong binding. This allows avoidance of high-affinity ligands, which may also bind to off-target cells with a low target density [47].

4. Liposomal surface modifications

Actively targeted liposomes necessarily require a stable anchoring of the ligand in the outer liposomal bilayer. This consequently requires lipidation of the ligand, meaning the attachment of a hydrophobic tail via typically covalent [46, 49] or more rarely used high-affinity non-

covalent [50] bonds. Three general functionalization procedures can be distinguished, which can be titled as “pre-insertion”, “post-insertion” and “post-functionalization” approaches [46]. Pre- and post-insertion separate the lipidation reaction from the liposome formation process. Pre-insertion implies presence of the lipidated ligand in the lipid blend during the liposome formation, thereby integrating the targeting ligand into the inner and outer bilayer leaflet of the liposome. During post-insertion, the lipidated ligand is inserted into the outer bilayer leaflet of preformed liposomes, typically above the phase transition temperature of the liposome bilayer [51]. Post-functionalization implies introduction of head-group reactive lipids during liposome formation. The lipidation and ligand anchoring is then performed directly on the liposomal surface. All methods have advantages and disadvantages depending e.g. on chemical nature of the ligand, available ligand quantitiy, or effectivity (for a detailed discussion see [46]).

What they all have in common is the requirement to modify the chemical structure of the targeting ligand. The majority of targeting ligands has a proteinaceous origin. Proteins as macromolecules possess several reactive sites. Those may be accessible for lipid conjugation via amide bond, disulfide or thioether formation, either directly (cysteines, lysines) or after activating steps (such as thiolation, reduction, crosslinker-condensation or carboxylic-acid activation). These three linker principles are merely examples of the most abundantly used chemical conjugation strategies, whose vast diversity is summarized in several reviews [46, 49]. Importantly, due to the presence of manifold reactive sites per protein, most of these reactions suffer from poor chemical selectivity, leading to heterogeneous conjugation products. Besides regio-specific chemical conjugation methods (such as copper-assisted azide-alkyne cycloaddition, native chemical ligation (NCL) or the Staudinger ligation) [52], chemoenzymatic ligation is a promising tool to avoid unspecific conjugation products by yielding chemically well defined protein modifications due to the inherent site-selectivity of enzymes [53].

Among the chemoenzymatic tools, Sortase-A is one of the most established enzymes promoting a regio-specific protein modifciation. Sortases are transpeptidases, originally discovered as house-keeping enzymes in gram-positive bacteria, where they mediate protein anchoring on the peptidoglycan layer [53]. Sortase-A, derived from *Staphylococcus aureus*, recognizes a C-terminal LPxTG (leucine, proline, any amino acid, threonine, glycine)-motif in the target protein and forms a thioacyl intermediate with the threonine and a cysteine in the catalytic center of the enzyme [53].

Equation 1: General scheme of Sortase-A mediated transpeptidation.

$$\boldsymbol{Protein\text{-}LPxTG\text{-}R_1}\text{-}COOH + H_2N\text{-}\boldsymbol{G\text{-}R_2} \xrightarrow{Sortase\text{-}A} \boldsymbol{Protein\text{-}LPxTG\text{-}R_2} + H_2N\text{-}\boldsymbol{G\text{-}R_1}\text{-}COOH$$

The amide bond towards the glycine is cleaved and subsequently replaced during the transpeptidation reaction with an incoming nucleophilic N-Terminus (Equation 1), e.g. of oligoglycines [53] or other primary amines [54, 55].

After its discovery in 1994 by Schneewind et al. [56] and subsequent recognition of the technological value of the "sortagging" reaction, Sortase variants have been used for a vast diversity of applications. This includes for example protein-protein fusion, protein modification (e.g. with carbohydrates, dyes or lipids), drug conjugation to antibodies, *in vitro* labeling of living cells or intracellular transpeptidation (for a comprehensive review see [53]).

Also, particulate drug delivery and diagnostic systems have been modified using Sortase-A technology. A scFv binding specifically to activated platelets has been conjugated via Sortase-A mediated transpeptidation to iron-oxide particles. This targeted contrast agent was able to specifically image thrombi in mice [57]. Similar targeting was achieved using a PEGylated, polymer-based layer-by-layer nano-capsule conjugated to a thrombus-specific scFv via Sortase-A [58, 59]. In another example, microparticles were modified with glucose-oxidase via Sortase-A, resulting (together with a biotin-immobilized horseradish peroxidase) in a construct ready for detecting glucose [60]. Other reports related to drug delivery describe the use of Sortase-A for the labelling of lipid nanodiscs [61], surface functionalization of hydrogels [62] or ligand-conjugation to polymeric micelles [55]. Liposomes have also been modified using Sortase-A. Guo et al. firstly described the conjugation of a model protein to diglycine-modified liposomes [63]. Tabata et al. optimized reaction conditions of a novel recombinant Sortase-A variant on pentaglycine-polystyrene beads. This was followed by verifying these optimized conditions by conjugation of a biotinylated LPETG-peptide on a liposomal surface [64]. Afterwards, the same group successfully conjugated a lung-tumor binding peptide to liposomes via Sortase-A, showing a selective delivery of these targeted liposomes to a lung-cancer cell line *in vitro* [65]. In a more recent study, Silvius et al. investigated reaction kinetics and coupling yields of protein conjugation to liposomes equipped with differently composed oligopeptide-modified acceptor lipids [66]. The authors showed that especially a reversible pre-binding of Sortase-A to the liposomes can enhance coupling yields during the manufacturing of protein-modified liposomes.

These examples indicate the potentials of Sortase-A mediated conjugation applied for the manufacturing of drug delivery systems, thus making proceeding investigations on this technology attractive for the pharmaceutical technology.

5. Aim of thesis

The use of Sortase-A as conjugation tool to attach targeting ligands on liposomes was considered as promising research field due to the marked versatility, the conjugation feasibility at mild reaction conditions, and the inherent site-specificity of the reaction. Only a limited number of reports described Sortase-mediated transpeptidation for ligand grafting on liposomal drug delivery systems at the start of this thesis [63-65]. This encouraged the author to gain deeper insights into the analytical and manufacturing challenges of such chemoenzymatically produced immunoliposomes, but also into their potential to improve *in vitro* and *in vivo* delivery of marker molecules and drugs.

The sortagging of liposomes requires integration of suitable lipid-anchored peptide sequences in the bilayer, serving as recognition motif for the transpeptidase. The stable insertion of such pentaglycine-lipids into the liposomal membrane and the integrity of the whole liposomal bilayer composition during manufacturing is indispensable for reliable downstream processes and meaningful biological read-outs. The development and validation of a highly versatile chromatographic method for the quantification of the individual lipid components of several sortaggable liposomal formulations was therefore aimed and is described in **Chapter 2**.

Ligand conjugation to liposomes implies a reaction on a surface, whose kinetics or efficiency may be considerably different from reactions in solution. The influence of liposomal surface properties and further conditions on kinetics and efficiency of the Sortase-A catalyzed conjugation of llama-derived single-domain antibodies was investigated in detail. Furthermore, the selective binding and uptake of such single-domain antibody-modified liposomes targeted against the immune cell receptor CD11b was tested on human peripheral blood mononuclear cells (**Chapter 3**).

A drawback of Sortase-A transpeptidation is the reversibility of the reaction. Traces of the enzyme in a drug product can be responsible for cleavage of the ligand from the liposomal system and can therefore lead to a loss of the targeting function during storage. This function is essential for immunoliposomes to specifically deliver substances towards target cells in living organisms. Thus, different formulation properties and purification methods were screened regarding efficiency of Sortase-A depletion from the reaction bulk and influence on drug product stability (**Chapter 4**). Most importantly, the chapter investigates CD11b-targeted immunoliposomes for the *in vivo* delivery of marker molecules towards immune-regulatory myeloid-derived suppressors cells with regard to specificity over T and B cells.

Lipidated single-domain antibodies may be inserted into preformed liposomes to obtain immunoliposomes via the post-insertion technique, thus obviating above mentioned purification efforts. The post-insertion technique demands a method to isolate the lipidated ligand from Sortase-A and unreacted educts while retaining target affinity of the ligand. Furthermore, such lipidated but soluble ligands may be inserted into biological membranes, thereby promoting non-natural cell-cell interactions. Studies elucidating the synthesis and isolation of lipidated single-domain antibodies as well as their insertion into liposomal and cellular membranes are described in **Chapter 5**.

Liposomal encapsulation may enable cytosolic delivery of impermeable macromolecules such as proteins via different intracellular routing. *Pseudomonas* exotoxin A is a proteinaceous inhibitor of the protein biosynthesis with high cytotoxic potency as soon as it reaches the cytosol. **Chapter 6** reports the attempt to exhibit specific toxicity against myeloid-derived suppressor cells via the cytosolic delivery of the catalytic domain of *Pseudomonas* exotoxin A using diverse chemoenzymatically prepared immunoliposomal formulations.

Doxorubicin is an important chemotherapy medication that has been further refined by liposomal encapsulation. Conventional conjugates of liposomal doxorubicin and anti-epidermal growth factor receptor (EGFR) derived targeting ligands have recently reached clinical development. The usage of site-specific conjugation chemistries may improve such clinical assets by yielding products with higher homogenity. **Chapter 7** aims to explore the formulation development and remote-loading of doxorubicin into sortaggable liposomes. It gives insights into sortagging kinetics of full-length monoclonal antibodies to these liposomes and demonstrates the specific cytotoxicity of EGFR-targeted immunoliposomes on a cancer cell line.

References

[1] P. Ehrlich, Über den jetzigen Stand der Chemotherapie, Berichte der Deutschen Chemischen Gesellschaft, 42 (1909) 17-47.

[2] K. Strebhardt, A. Ullrich, Paul Ehrlich's magic bullet concept: 100 years of progress, Nature Reviews Cancer, 8 (2008) 473-480.

[3] D. Bobo, K.J. Robinson, J. Islam, K.J. Thurecht, S.R. Corrie, Nanoparticle-Based Medicines: A Review of FDA-Approved Materials and Clinical Trials to Date, Pharmaceutical Research, 33 (2016) 2373-2387.

[4] H.-I. Chang, M.-K. Yeh, Clinical development of liposome-based drugs: formulation, characterization, and therapeutic efficacy, International Journal of Nanomedicine, 7 (2012) 49-60.

[5] B.S. Pattni, V.V. Chupin, V.P. Torchilin, New Developments in Liposomal Drug Delivery, Chemical Reviews, 115 (2015) 10938-10966.

[6] R. Solomon, A.A. Gabizon, Clinical Pharmacology of Liposomal Anthracyclines: Focus on Pegylated Liposomal Doxorubicin, Clinical Lymphoma and Myeloma, 8 (2008) 21-32.

[7] D.C. Drummond, C.O. Noble, Z. Guo, K. Hong, J.W. Park, D.B. Kirpotin, Development of a Highly Active Nanoliposomal Irinotecan Using a Novel Intraliposomal Stabilization Strategy, Cancer Research, 66 (2006) 3271.

[8] B. Carvalho, L.M. Roland, L.F. Chu, V.A. Campitelli Iii, E.T. Riley, Single-dose, extended-release epidural morphine (DepoDur™) compared to conventional epidural morphine for post-cesarean pain, Anesthesia & Analgesia, 105 (2007) 176-183.

[9] M. Golf, S.E. Daniels, E. Onel, A phase 3, randomized, placebo-controlled trial of DepoFoam® bupivacaine (extended-release bupivacaine local analgesic) in bunionectomy, Advances in therapy, 28 (2011) 776.

[10] Y. Barenholz, Doxil® – The first FDA-approved nano-drug: Lessons learned, Journal of Controlled Release, 160 (2012) 117-134.

[11] F. Meunier, H.G. Prentice, O. Ringdén, Liposomal amphotericin B (AmBisome): safety data from a phase II/III clinical trial, Journal of Antimicrobial Chemotherapy, 28 (1991) 83-91.

[12] V.P. Torchilin, Recent advances with liposomes as pharmaceutical carriers, Nature Reviews Drug Discovery, 4 (2005) 145.

[13] J.A. Silverman, S.R. Deitcher, Marqibo® (vincristine sulfate liposome injection) improves the pharmacokinetics and pharmacodynamics of vincristine, Cancer Chemotherapy and Pharmacology, 71 (2013) 555-564.

[14] F. Zhao, Y. Zhao, Y. Liu, X. Chang, C. Chen, Y. Zhao, Cellular Uptake, Intracellular Trafficking, and Cytotoxicity of Nanomaterials, Small, 7 (2011) 1322-1337.

[15] C.R. Alving, Z. Beck, G.R. Matyas, M. Rao, Liposomal adjuvants for human vaccines, Expert Opinion on Drug Delivery, 13 (2016) 807-816.

[16] P.A. Bovier, Epaxal®: a virosomal vaccine to prevent hepatitis A infection, Expert Review of Vaccines, 7 (2008) 1141-1150.

[17] C. Herzog, K. Hartmann, V. Künzi, O. Kürsteiner, R. Mischler, H. Lazar, R. Glück, Eleven years of Inflexal® V – a virosomal adjuvanted influenza vaccine, Vaccine, 27 (2009) 4381-4387.

[18] H. Tian, J. Chen, X. Chen, Nanoparticles for Gene Delivery, Small, 9 (2013) 2034-2044.

[19] A.D. Bangham, R.W. Horne, Negative staining of phospholipids and their structural modification by surface-active agents as observed in the electron microscope, Journal of Molecular Biology, 8 (1964) 660-668.

[20] J. Gubernator, Active methods of drug loading into liposomes: recent strategies for stable drug entrapment and increased in vivo activity, Expert Opinion on Drug Delivery, 8 (2011) 565-580.

[21] M. Matsuura, Y. Yamazaki, M. Sugiyama, M. Kondo, H. Ori, M. Nango, N. Oku, Polycation liposome-mediated gene transfer in vivo, Biochimica et Biophysica Acta (BBA) – Biomembranes, 1612 (2003) 136-143.

[22] A. Gabizon, D.C. Price, J. Huberty, R.S. Bresalier, D. Papahadjopoulos, Effect of Liposome Composition and Other Factors on the Targeting of Liposomes to Experimental Tumors: Biodistribution and Imaging Studies, Cancer Research, 50 (1990) 6371.

[23] N. Bertrand, J.-C. Leroux, The journey of a drug-carrier in the body: An anatomo-physiological perspective, Journal of Controlled Release, 161 (2012) 152-163.

[24] E.A. Forssen, M.E. Ross, Daunoxome® Treatment of Solid Tumors: Preclinical and Clinical Investigations, Journal of Liposome Research, 4 (1994) 481-512.

[25] F.C. Passero Jr, D. Grapsa, K.N. Syrigos, M.W. Saif, The safety and efficacy of Onivyde (irinotecan liposome injection) for the treatment of metastatic pancreatic cancer following gemcitabine-based therapy, Expert review of anticancer therapy, 16 (2016) 697-703.

[26] K. Ando, K. Mori, N. Corradini, F. Redini, D. Heymann, Mifamurtide for the treatment of nonmetastatic osteosarcoma, Expert Opinion on Pharmacotherapy, 12 (2011) 285-292.

[27] P.K. Kaiser, Verteporfin PDT for subfoveal occult CNV in AMD: two-year results of a randomized trial, Current Medical Research and Opinion, 25 (2009) 1853-1860.

[28] E.J. Feldman, J.E. Lancet, J.E. Kolitz, E.K. Ritchie, G.J. Roboz, A.F. List, S.L. Allen, E. Asatiani, L.D. Mayer, C. Swenson, A.C. Louie, First-In-Man Study of CPX-351: A Liposomal Carrier Containing Cytarabine and Daunorubicin in a Fixed 5:1 Molar Ratio for the Treatment of Relapsed and Refractory Acute Myeloid Leukemia, Journal of Clinical Oncology, 29 (2011) 979-985.

[29] K.A. Jaeckle, T. Batchelor, S.J. O'Day, S. Phuphanich, P. New, G. Lesser, A. Cohn, M. Gilbert, R. Aiken, D. Heros, L. Rogers, E. Wong, D. Fulton, J.C. Gutheil, S. Baidas, J.M. Kennedy, W. Mason, P. Moots, C. Russell, L.J. Swinnen, S.B. Howell, An Open Label Trial of Sustained-release Cytarabine (DepoCyt™) for the Intrathecal Treatment of Solid Tumor Neoplastic Meningitis, Journal of Neuro-Oncology, 57 (2002) 231-239.

[30] F. Danhier, To exploit the tumor microenvironment: Since the EPR effect fails in the clinic, what is the future of nanomedicine?, Journal of Controlled Release, 244 (2016) 108-121.

[31] C.-H. Heldin, K. Rubin, K. Pietras, A. Östman, High interstitial fluid pressure — an obstacle in cancer therapy, Nature Reviews Cancer, 4 (2004) 806-813.

[32] F. Danhier, O. Feron, V. Préat, To exploit the tumor microenvironment: Passive and active tumor targeting of nanocarriers for anti-cancer drug delivery, Journal of Controlled Release, 148 (2010) 135-146.

[33] R.S. Zolot, S. Basu, R.P. Million, Antibody-drug conjugates, Nature Reviews Drug Discovery, 12 (2013) 259.

[34] E. Moles, S. Galiano, A. Gomes, M. Quiliano, C. Teixeira, I. Aldana, P. Gomes, X. Fernàndez-Busquets, ImmunoPEGliposomes for the targeted delivery of novel lipophilic drugs to red blood cells in a falciparum malaria murine model, Biomaterials, 145 (2017) 178-191.

[35] P. Sapra, T.M. Allen, Improved outcome when B-cell lymphoma is treated with combinations of immunoliposomal anticancer drugs targeted to both the CD19 and CD20 epitopes, Clinical Cancer Research, 10 (2004) 2530-2537.

[36] A. Gutkin, P. Decuzzi, D. Peer, Targeting central nervous system pathologies with nanomedicines, Journal of Drug Targeting, 28 (2018) 1-13.

[37] G.T. Noble, J.F. Stefanick, J.D. Ashley, T. Kiziltepe, B. Bilgicer, Ligand-targeted liposome design: challenges and fundamental considerations, Trends in Biotechnology, 32 (2014) 32-45.

[38] T. Yokota, D.E. Milenic, M. Whitlow, J. Schlom, Rapid Tumor Penetration of a Single-Chain Fv and Comparison with Other Immunoglobulin Forms, Cancer Research, 52 (1992) 3402.

[39] N. Emanuel, E. Kedar, E.M. Bolotin, N.I. Smorodinsky, Y. Barenholz, Targeted Delivery of Doxorubicin via Sterically Stabilized Immunoliposomes: Pharmacokinetics and Biodistribution in Tumor-bearing Mice, Pharmaceutical Research, 13 (1996) 861-868.

[40] W.W.K. Cheng, T.M. Allen, Targeted delivery of anti-CD19 liposomal doxorubicin in B-cell lymphoma: A comparison of whole monoclonal antibody, Fab' fragments and single chain Fv, Journal of Controlled Release, 126 (2008) 50-58.

[41] F. Pastorino, C. Brignole, D. Marimpietri, P. Sapra, E.H. Moase, T.M. Allen, M. Ponzoni, Doxorubicin-loaded Fab' Fragments of Anti-disialoganglioside Immunoliposomes Selectively Inhibit the Growth and Dissemination of Human Neuroblastoma in Nude Mice, Cancer Research, 63 (2003) 86.

[42] P. Simard, J.-C. Leroux, In Vivo Evaluation of pH-Sensitive Polymer-Based Immunoliposomes Targeting the CD33 Antigen, Molecular Pharmaceutics, 7 (2010) 1098-1107.

[43] S. Zalba, A.M. Contreras, A. Haeri, T.L.M. ten Hagen, I. Navarro, G. Koning, M.J. Garrido, Cetuximab-oxaliplatin-liposomes for epidermal growth factor receptor targeted chemotherapy of colorectal cancer, Journal of Controlled Release, 210 (2015) 26-38.

[44] W.Z. Jie Gao, Jinqiu He, Huimei Li, He Zhang, Guichen Zhou, Bohua Li, Ying Lu, Hao Zou, Geng Kou, Dapeng Zhang, Hao Wang, Yajun Guo, Yanqiang Zhong, Tumor-targeted PE38KDEL delivery via PEGylated anti-HER2 immunoliposomes, International Journal of Pharmaceutics, 374 (2009) 145-152.

[45] J. Gao, G. Kou, H. Wang, H. Chen, B. Li, Y. Lu, D. Zhang, S. Wang, S. Hou, W. Qian, J. Dai, J. Zhao, Y. Zhong, Y. Guo, PE38KDEL-loaded anti-HER2 nanoparticles inhibit breast tumor progression with reduced toxicity and immunogenicity, Breast Cancer Res Treat, 115 (2009) 29-41.

[46] R. Jølck, L. Feldborg, S. Andersen, S.M. Moghimi, T. Andresen, Engineering Liposomes and Nanoparticles for Biological Targeting, in: G.S. Nyanhongo, W. Steiner, G. Gübitz (Eds.) Biofunctionalization of Polymers and their Applications, Springer Berlin Heidelberg, 2011, pp. 251-280.
[47] R. Hennig, A. Ohlmann, J. Staffel, K. Pollinger, A. Haunberger, M. Breunig, F. Schweda, E.R. Tamm, A. Goepferich, Multivalent nanoparticles bind the retinal and choroidal vasculature, Journal of Controlled Release, 220 (2015) 265-274.
[48] S. Oliveira, R.M. Schiffelers, J. van der Veeken, R. van der Meel, R. Vongpromek, P.M.v.B. en Henegouwen, G. Storm, R.C. Roovers, Downregulation of EGFR by a novel multivalent nanobody-liposome platform, Journal of Controlled Release, 145 (2010) 165-175.
[49] P. Marques-Gallego, A.I. de Kroon, Ligation strategies for targeting liposomal nanocarriers, Biomed Research International, (2014) e129458.
[50] M.-H. Chen, Y. Soda, K. Izawa, S. Kobayashi, K. Tani, K. Maruyama, A. Tojo, S. Asano, A versatile drug delivery system using streptavidin-tagged pegylated liposomes and biotinylated biomaterials, International Journal of Pharmaceutics, 454 (2013) 478-485.
[51] D.L. Iden, T.M. Allen, In vitro and in vivo comparison of immunoliposomes made by conventional coupling techniques with those made by a new post-insertion approach, Biochimica et Biophysica Acta (BBA) - Biomembranes, 1513 (2001) 207-216.
[52] C.D. Hein, X.M. Liu, D. Wang, Click chemistry, a powerful tool for pharmaceutical sciences, Pharmaceutical Research, 25 (2008) 2216-2230.
[53] M. Ritzefeld, Sortagging: A Robust and Efficient Chemoenzymatic Ligation Strategy, Chemistry – A European Journal, 20 (2014) 8516-8529.
[54] J.E. Glasgow, M.L. Salit, J.R. Cochran, In Vivo Site-Specific Protein Tagging with Diverse Amines Using an Engineered Sortase Variant, Journal of the American Chemical Society, 138 (2016) 7496-7499.
[55] S.A. van Lith, S.M. van Duijnhoven, A.C. Navis, W.P. Leenders, E. Dolk, J.W. Wennink, C.F. van Nostrum, J.C. van Hest, Legomedicine-A Versatile Chemo-Enzymatic Approach for the Preparation of Targeted Dual-Labeled Llama Antibody-Nanoparticle Conjugates, Bioconjugate Chemistry, 28 (2017) 539-548.
[56] W. Navarre William, O. Schneewind, Proteolytic cleavage and cell wall anchoring at the LPXTG motif of surface proteins in Gram-positive bacteria, Molecular Microbiology, 14 (2006) 115-121.
[57] H.T. Ta, S. Prabhu, E. Leitner, F. Jia, D. von Elverfeldt, K. Jackson, T. Heidt, A. Nair, H. Pearce, C. von zur Muhlen, X. Wang, K. Peter, C.E. Hagemeyer, Enzymatic Single-Chain Antibody Tagging, Circulation Research, 109 (2011) 365-373.
[58] C.E. Hagemeyer, K. Alt, A.P. Johnston, Particle generation, functionalization and sortase A-mediated modification with targeting of single-chain antibodies for diagnostic and therapeutic use, Nature Protocols, 10 (2015) 90-105.
[59] M.K.M. Leung, C.E. Hagemeyer, A.P.R. Johnston, C. Gonzales, M.M.J. Kamphuis, K. Ardipradja, G.K. Such, K. Peter, F. Caruso, Bio-Click Chemistry: Enzymatic Functionalization of PEGylated Capsules for Targeting Applications, Angewandte Chemie International Edition, 51 (2012) 7132-7136.
[60] T. Matsumoto, T. Tanaka, A. Kondo, Sortase A-catalyzed site-specific coimmobilization on microparticles via streptavidin, Langmuir, 28 (2012) 3553-3557.
[61] A.I. Petrache, D. Machin, D.J. Williamson, M. Webb, P.A. Beales, Sortase-mediated labelling of lipid nanodiscs for cellular tracing, Molecular BioSystems, 12 (2016) 1760-1763.
[62] E. Gau, D.M. Mate, Z. Zou, A. Oppermann, A. Töpel, F. Jakob, D. Wöll, U. Schwaneberg, A. Pich, Sortase-Mediated Surface Functionalization of Stimuli-Responsive Microgels, Biomacromolecules, 18 (2017) 2789-2798.
[63] X. Guo, Z. Wu, Z. Guo, New method for site-specific modification of liposomes with proteins using sortase A-mediated transpeptidation, Bioconjugate Chemistry, 23 (2012) 650-655.
[64] A. Tabata, N. Anyoji, Y. Ohkubo, T. Tomoyasu, H. Nagamune, Investigation on the Reaction Conditions of Staphylococcus aureus Sortase A for Creating Surface-modified Liposomes as a Drug-delivery System Tool, Anticancer Research, 34 (2014) 4521-4527.
[65] A. Tabata, Y. Ohkubo, N. Anyoji, K. Hojo, T. Tomoyasu, Y. Tatematsu, K. Ohkura, H. Nagamune, Development of a Sortase A-mediated Peptide-labeled Liposome Applicable to Drug-delivery Systems, Anticancer Research, 35 (2015) 4411-4417.
[66] J.R. Silvius, R. Leventis, A Novel "Prebinding" Strategy Dramatically Enhances Sortase-Mediated Coupling of Proteins to Liposomes, Bioconjugate Chemistry, 28 (2017) 1271-1282.

Chapter 2

Pentaglycine lipid derivates – rp-HPLC analytics for bioorthogonal anchor molecules in targeted, multiple-composite liposomal drug delivery systems

This chapter is published as: Wöll, S., Schiller, S., Bachran, C., Swee, L. K., Scherließ, R.: Pentaglycine lipid derivates – rp-HPLC analytics for bioorthogonal anchor molecules in targeted, multiple-composite liposomal drug delivery systems.
International Journal of Pharmaceutics, 547 (2018), Issues 1-2, 602-610.
https://doi.org/10.1016/j.ijpharm.2018.05.052

Abstract

The quantification of lipids and assessment of lipid composition is an indispensable step during the pharmaceutical development of lipid-based drug delivery systems such as liposomes. Broad excipient screenings of such formulations raise the need for versatile analytical methods. Even more demanding complexity is generated by introduction of targeted systems requiring functionalized lipids. We addressed this demand by developing an rp-HPLC-based analytical method with evaporative light scattering detection (ELSD) for the simultaneous analysis of commonly used phosphatidylcholines, cholesterol and bilayer surface-modifying cationic, anionic or PEGylated lipids, which can be analyzed in combination with novel pentaglycine lipids suitable as targeting ligand anchor. The method was validated for specificity, precision, accuracy and sample stability. We monitor the continuous and scalable manufacturing of two pentaglycine-modified liposomal formulations and track the modification of these drug delivery systems with a single-domain antibody utilizing bioorthogonal Sortase-A technology. Both the presented analytical and preparative techniques can help to improve the quality control and to accelerate the pharmaceutical development of such targeted drug delivery systems.

1. Introduction

Lipid excipients have become an indispensable part of the formulation scientists' toolbox. Their versatility and broad applicability e.g. in topical [1], oral [2], parenteral [3, 4] or pulmonary [5] dosage forms has progressively led to the synthesis of functionalized lipids, depending on the formulation purpose. Especially in lipid-based nanoparticulate drug delivery systems like liposomes, head group modification and hydrophobic chain properties are crucial parameters for formulation characteristics and *in vivo* performance [6]. A thorough screening of the bilayer composition is therefore an important part of the formulation development, and corresponding lipid analytics are essential to monitor composition and concentration over the usually multi-step formulation processes. Although several rp-HPLC methods for lipid quantification have been published in the past, bilayer analyses are frequently carried out using unspecific colorimetric assays, which typically do not take phosphate-free lipids into account [7], or are not conducted at all. Mass-sensitive evaporative light scattering [8-13] is besides charged aerosol detection (CAD) [14] the detection method of choice for lipid structures having no or few chromophores. It is preferred over other mass-sensitive detectors using refractive index detection (e.g. due to the higher detectability and compatibility with gradient elution), or mass-spectrometers especially due to the low costs and convenience of operation and instrumentation [15]. Besides those advantages, ELSDs have several limitations, such as the requirement of volatile mobile phases, the destructive characteristic and the exponential relationship of analyte mass and signal intensity [15].

Due to this non-linear response and the influence of the atmospheric pressure in the lab on the signal intensity, a time consuming, frequent multi-point calibration is required. This is, together with tedious standard preparation, long chromatographic run durations and extensive data evaluation, a hurdle for the implementation of such analytical methods, which is further enhanced by a lack of method versatility. Previously reported chromatographic methods focused on the separation and quantification of phosphatidylcholines, phosphatidylglycerols and their lyso-forms [8], or on functionalized lipids like 1,2-dioleoyl-3-trimethylammonium-propane (R-DOTAP) [10, 13] or 1,2-distearoyl-sn-glycero-3-phosphoethanolamine-N-[methoxy(polyethylene glycol)-2000] (DSPE-mPEG) [9, 11]. However, none of the published methods provides a general approach to analyze vesicles with cationic, anionic and PEGylated surfaces, a versatility that would be helpful in early liposome development when the required bilayer composition is rather unknown and thus often varied. Furthermore, the quantification of "coupling-ready lipids" like maleimide-conjugated lipids or amino acid-modified lipids is

currently disregarded. Especially the latter novel class of lipids currently gains attraction as anchor molecules for bioorthogonal bilayer modification [16-18].

In the past, liposomes have been successfully modified with ligands to target the drug delivery system to specific cell surface structures [19]. For that purpose, mainly chemically-based conjugation methods are employed, making use of free thiol-, carboxy- or amino-groups in proteins or peptides [20]. As every accessible reactive amino acid side chain can participate in the reaction, a broad conjugation product profile might be obtained, as e.g. reported by Lukyanov et al., where up to 32 PEGylated phosphoethanolamines were conjugated to free amine groups of a full length antibody [21]. Unspecific protein modifications lead to product heterogeneity, an unfavorable hindrance for the transfer of targeted nanotherapeutics from bench to the clinic. For that reason site selective reactions, mainly driven from currently rising antibody-drug conjugate technology [22], are an emerging field in the bioconjugation research. Amongst them, enzyme-based, bioorthogonal Sortase-A transpeptidation technology has been established as versatile tool to promote efficient conjugation between LPxTG (leucine, proline, any amino acid, threonine, glycine) and oligoglycine amino acid motifs [23]. Working under mild conditions, Sortase-A conjugation offers a favorable approach to attach targeting ligands with the techniques inherent specificity to surfaces and was shown on various particulate constructs, amongst them iron oxide particles [24], polystyrene microparticles [25], silica nanoparticles [26] and liposomes [16-18].

In the present work, we firstly show the development of an rp-HPLC-ELSD method allowing us to analyze a broad variety of liposomal formulations which shall be ligand-modified by novel Sortase-A bioconjugation technique. We describe useful protocols to minimize time-consuming HPLC-standard preparation in daily lab-work while considering overall analysis times. As demonstration, we apply the method to an industry-relevant multi-step liposomal preparation process, which is especially challenging to be followed by analytics as composition can change in every step. We describe the formulation and characterization of two differently PEGylated pentaglycine-modified liposome types suitable for the active loading of weak bases. Furthermore, enzyme-mediated conjugation of a single-domain antibody of camelid heavy-chain only antibodies (VHH) is used as exemplary bilayer modification reaction. The presented method and manufacturing procedures can help to accelerate liposomal development processes as they provide suitable early-development analytics and scalable manufacturing for a targeted liposome platform that may be loaded with desired active-loading compatible drug and sortaggable ligand.

2. Materials

Pentaglycine-modified lipids (Figure 1) are based on two myristyl alcohols ether linked to an amino-propandiol moiety being coupled to the δ-carboxy-group of an iso-glutamine by an amide linkage. The pentaglycine motif is either directly (here called DMA-G5) C-terminally linked to the α-standing amino function of the iso-glutamine, or spaced via a 2000 Da monodisperse polyethylene linker (DMA-PEG-G5) [27]. Both compounds, as well as (R)-1,2-dioleoyl-3-trimethylammonium-propane (R-DOTAP) were obtained from Merck & Cie (Schaffhausen, Switzerland). 1,2-dipalmitoyl-sn-glycero-3-phosphocholine (DPPC), 1,2-dipalmitoyl-sn-glycero-3-phospho-(1'-rac-glycerol) (DPPG), 1,2-distearoyl-sn-glycero-3-phosphoethanolamine-N-[meth-oxy (polyethylene glycol)-2000] (DSPE-mPEG), 1,2-dioleoyl-sn-glycero-3-phospho-ethanolamine (DOPE), 1,2-distearoyl-sn-glycero-3-phosphocholine (DSPC), lyso-phosphatidyl-choline reference standard and hydrogenated soy phosphatidylcholine (HSPC) were from Lipoid GmbH (Ludwigshafen, Germany). Dulbecco's phosphate buffered saline (DPBS, D1408, tenfold stock), cholesterol and 3β-hydroxy-5-cholestene 3-hemisuccinate (CHEMS) were obtained from Sigma-Aldrich (St. Louis, MO, USA). 1,2-dipalmitoyl-sn-glycero-3-phosphoethanolamine-N-(lissamine rhodamine B sulfonyl) (Liss-Rhod-PE) and 1,2-distearoyl-sn-glycero-3-phospho-ethanolamine-N-[maleimide(polyethylene glycol)-2000] (DSPE-PEG-Mal) were obtained from Avanti Polar Lipids (Alabaster, AL, USA). Doxorubicin (DXR) was purchased from Ark Pharma (Arlington Heights, IL, USA). 1,1'-dioctadecyl-3,3,3',3'-tetramethyl-indotricarbocyanine iodide (DiR) was from Thermo Fisher Scientific (Waltham, MA, USA). Trifluoroacetic acid (TFA), methanol and ethanol (both gradient grade) as well as dimethylsulfoxide (DMSO) were obtained from Merck KGaA (Darmstadt, Germany). Water was purified by a Milli-Q system (Merck Millipore, Billerica, MA, USA).

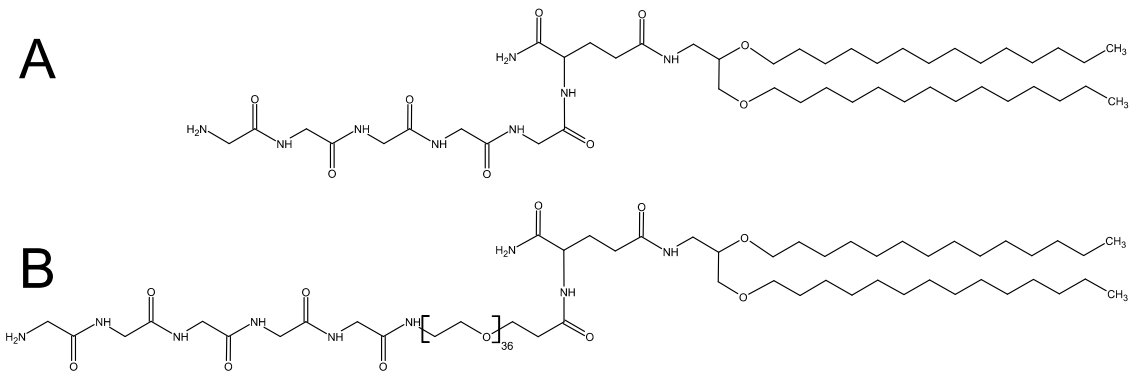

Figure 1: Chemical structure of A: DMA-G5, 897 Da and B: DMA-PEG-G5, 2554 Da.

3. Methods

3.1. Chromatographic conditions

Final method utilized an XSelect CSH C18 column with a particle size of 5 µm, an inner diameter of 4.6 mm, a length of 150 mm (Waters Corporation, Milford, MA, USA) and a binary pseudopolar gradient pattern (Table 1) for compound separation. Eluent A consisted of water-methanol (1:1 v/v), eluent B was methanol-ethanol (3:2 v/v) supplemented with 0.01 % TFA v/v. Analysis was performed on an Agilent 1260 Infinity HPLC system equipped with a degasser (G4225A), binary pump (G1312B), autosampler (G1329B), thermostat (G1330B), column oven (1316A), diode array detector VL+ (DAD, G1315C) and evaporative light scattering detector (ELSD, G4260B), controlled by EZChrom Elite Software. Column temperature was set to 35 °C, autosampler temperature was set to 4 °C. Standard injection volumes were 50 µL or 25 µL to adjust signal intensities between compounds occurring at very high (DPPC) and low molar fractions. Flow rate was 2.5 mL/min. Data was recorded using DAD set to 485, 560 and 750 nm to detect DXR and dyes. ELSD settings were 1.5 standard liter per minute for nitrogen nebulizer gas, 60 °C for nebulizer and 80 °C for evaporator, a sampling frequency of 10 Hz, detector-inherent signal smoothing of “30”, LED power of 100 % and a photomultiplier tube gain of “1”. All analyses were performed with duplicate runs. To avoid lipid carry-over on subsequent injections, injection needle was cleaned after each injection in a wash-vial filled with chloroform-methanol-water (4.5 : 4.5 : 1 v/v, further called diluent).

3.2. Analytical lipid blend ready mixes

Lipids shown in Table 3 were weighed on a daily calibrated balance (AG245, Mettler Toledo, Columbus, OH, USA), dissolved in methanol to the upper concentration and aliquoted in HPLC vials. Solvent was evaporated in a vacuum oven (VT 6060 M-BL, Thermo Scientific, Waltham, MA, USA) at 25 °C (0-2 h: 200 mbar, 1 h at 50 mbar, further 10 min at 1-2 mbar) to prepare ready-to-use blends. Blends were stored in a nitrogen atmosphere at -20 °C. For evaluation of separation and method optimization, single lipids or blends were dissolved in diluent and 50 µL were injected.

Table 1: Gradient pattern.

time [min]	gradient
0.0 – 1.0	100 % A
1.0 – 2.0	100 % A – 20 % A
2.0 – 12.0	20 % A – 0 % A
12.0 – 12.1	0 % A – 100 % A
12.1 – 17.0	100 % A

3.3. Calibration, accuracy, precision and sample stability

Ready-to-use lipid blends described in section 3.2 were dissolved in the diluent and injected with varying injection volumes to calibrate the ELSD over five levels, achieving calibration ranges from 60-125 % of each expected lipid concentration, related to its molar liposomal fraction (see section 3.4) of a target sample molarity of 1 mM total lipid. Signal-to-noise ratio (SNR) was determined for the lowest calibration point, no further chromatogram smoothening was applied. Limit of detection (LOD) was determined visually due to the ELS inherent non-linear signal response. Subsequently increasing amounts were injected on the column until a peak could be reliably detected. Accuracy of method was determined by quantification of individually weighed lipid blends over three days. Intra-day precision and retention robustness was determined as the relative standard deviation of the mean peak area of 10 consecutive injections, inter-day precision and retention robustness of equally concentrated samples analyzed in duplicate at three consecutive days. Sample stability in diluent was tested as the recovery rate of three samples analyzed over three consecutive days with daily-actual calibrations.

3.4. Liposome preparation

Liposome samples were prepared by a continuous solvent injection process. Lipid powder blends consisting of 59.4 mol% DPPC, 34.7 mol% cholesterol, 1.0 mol% DMA-PEG-G5 and either 5.0 mol% DSPE-mPEG (referred to as “PEG-NP”) or DPPG (referred to as “Anionic-NP”) were dissolved to 119 mM (PEG-NP) and 48 mM (Anionic-NP) in chloroform-methanol. The solution was aliquoted and vacuum-dried from 400 mbar subsequently to 2 mbar in a vacuum centrifuge (RVC 2-33 IR, Martin Christ, Osterode am Harz, Germany). The films were nitrogen gassed, sealed and stored at -20 °C as ready-to-use mixes. For solvent injection, lipids were redissolved to a target molarity of 90 mM in ethanol (PEG-NP) or 16 mM in methanol (Anionic-NP). Alcohol solutions were injected computer-controlled utilizing a syringe pump (PHD Ultra4400, Harvard Apparatus, Holliston, MA, USA) and a customized T-piece at a flow rate of 10 mL/min into a stream of ammonium sulfate buffer (pH 5.4, 250 mM) conveyed by a peristaltic pump (Ismatec IP65, Cole-Parmer, Wertheim, Germany) at 120 mL/min for PEG-NP or 200 mL/min for Anionic-NP.

3.5. Tangential flow filtration

Dispersions obtained from solvent injection were refined using a tangential flow filtration (TFF) system equipped with a MicroKros® Filter module (Spectrum Labs, Los Angeles, CA, USA) with a 500 kDa cut-off and 20 cm^2 surface area. The TFF was fed at a flow rate of 100 mL/min

pump speed and filtration pressure < 2 bar. A known amount of liposomal dispersion was concentrated to a target molarity of ≈30 mM, followed by purification of alcohol and replacement of the outer buffer by DPBS for 10 diafiltration volumes. For lipid analytics, liposomal samples were firstly diluted tenfold with chloroform-methanol (1:1 v/v), followed by a further dilution with diluent to an estimated concentration of 1 mM to maintain an equal aqueous sample content of 10 % (v/v), previously shown to be relevant for lipid analytics [11]. Lipid analytic was applied before and after TFF to control bilayer composition changes, and the lipid recovery was calculated by Equation 1. For Anionic-NP, lipid concentration before TFF was calculated from pump flow rate ratio during solvent injection due to the sample concentration being below the limit of quantification.

Equation 1

$$TFF\ yield\ [\%] = \frac{m_{dispersion}[mg] * c_{lipid}[mM](TFF\ out)}{m_{dispersion}[mg] * c_{lipid}\ [mM]\ (TFF\ in)} * 100$$

3.6. Ligand conjugation

Particles were surface-modified using a Sortase-A mediated transpeptidation approach. Ca^{2+}-independent Sortase-A variant SortA7m and LPETG (leucine, proline, glutamic acid, threonine, glycine)-modified VHH were prepared as described elsewhere [28, 29]. Purified liposomes (100 µM total pentaglycine) were mixed with 50 µM VHH and 25 µM Sortase-A. The mixture was incubated for 4 h at 4 °C, until the reaction was stopped by dilution (1:9) with chloroform-methanol (1:1 v/v). Precipitated proteins were removed by centrifugation (5 minutes at 10,000 × g), and the supernatant was analyzed for decrease of DMA-PEG-G5 in the bilayer. Statistical significance was tested using a paired t-test (SigmaPlot, Systat Sofware, San Jose, CA, USA).

3.7. Physical liposome characterization

Liposomal mean hydrodynamic diameter and polydispersity were measured by dynamic light scattering using a DynaPro Plate Reader II (Wyatt, Santa Barbara, CA, USA). Typically, liposomes were diluted to 0.1-1 mM total lipid in the respective surrounding buffer and measured in triplicate wells. Zeta potential was determined in triplicate using laser Doppler electrophoresis (Malvern Zetasizer, Worcestershire, UK) after a dilution of 30 µL sample in 970 µL 10 mM NaCl.

4. Results and discussion

4.1. Method development

During method development, focus was set on the separation of pentaglycine-modified lipids from common bilayer components used in liposome research to enable a fast and simple lipid quantification of highly diverse formulations in early composition screening. Previously published methods for versatile lipid analysis investigated neutral phospholipids and anionic phosphatidylglycerols, cholesterol and their hydrolysis products [8]. It was here in our interest to extend the analytical scope toward the simultaneous analysis of either cationic, anionic and PEGylated surface-modifying lipids in combination with different phospholipids and cholesterol. Versatility of such a method would allow a broad screening of formulations with wide applicability such as long-circulating PEGylated vesicles [30], controlled drug release through phosphatidylcholines with different chain lengths [31] as well as a vaccination purpose utilizing adjuvant-acting R-DOTAP [32]. The arbitrary combinability with novel pentaglycine-modified lipids (Figure 1) for enzymatic ligand attachment would allow easy transfer of such traditional liposome formulations toward immunoliposomes for targeted drug delivery without additional analytical development.

C18-phase rp-columns with ammonium acetate buffered pseudopolar eluents were previously used for separation of PEGylated lipids from cholesterol and phosphatidylcholines [9, 11]. Applying a method published by Oswald et al. [9], we were not able to separate DMA-G5 from DSPE-mPEG even after various optimization steps in the gradient profile. Therefore, a water-methanol gradient with TFA as ion-pairing additive [13] was selected as alternative eluent system. Decrease of polarity by addition of ethanol to eluent B led to the ability to elute DPPG and separate it from DSPE-mPEG, both structures with negative formal charge at the phosphate group, which might be lost due to TFA presence, leading to strong column interaction. We varied column temperature and decreased TFA content in eluent B, which had further promising influence on the separation of DPPG and DSPE-mPEG, as well as the two pentaglycine-modified lipids. Finally, we chose a column temperature of 35 °C and 40 % ethanol in eluent B supplemented with 0.01 % TFA, leading to the separation of DMA-G5 and DMA-PEG-G5 (R_S = 2.0) and DSPE-mPEG and DPPG (R_S = 1.5), as well as R-DOTAP, cholesterol and DPPC, the major lipid combinations applied in our lab (Figure 2A) within a short analysis time of 17 min.

CHEMS is a cholesterol ester that can be protonated in acidic environment leading to pH-dependent polymorphic states [33]. CHEMS is therefore used as membrane component in pH-sensitive formulations [34]. Eluting at 7.1 min, CHEMS is not separated from cholesterol (7.0 min), however CHEMS typically replaces cholesterol when combined with DOPE

in pH-sensitive formulations. As both CHEMS and DOPE are well separated (Figure 2B), the analysis of such pH-sensitive formulations can be provided by the presented method.

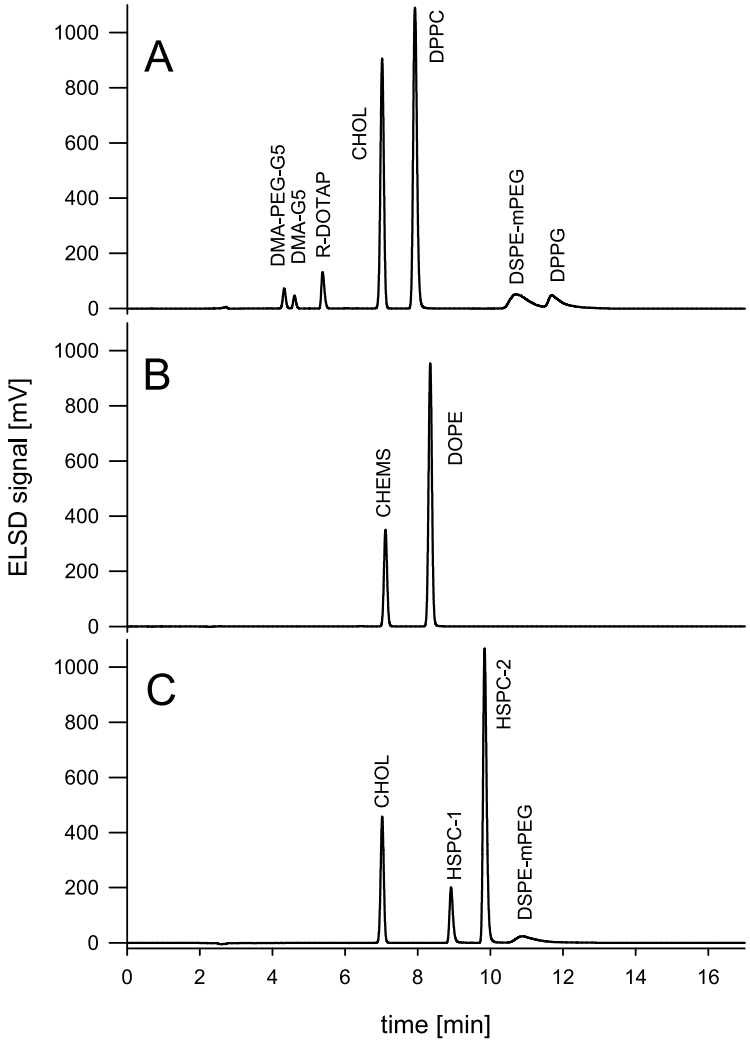

Figure 2: Representative chromatograms showing suitability to separate frequently literature-described liposomal formulations in combination with sortaggable pentaglycine lipids. **A**: Typical calibration standard relevant for the analysis of formulations consisting of 60 mol% DPPC, 35 mol% CHOL, 1 mol% DMA-PEG-G5 or DMA-G5 as well as 5 mol% R-DOTAP, DSPE-mPEG or DPPG. DPPC is calibrated with half of the expected molar fraction to align absolute signal intensities of different bilayer ingredients within the detector range. Liposomal sample is then analyzed for DPPC with decreased injection volume. **B**: CHEMS and DOPE (40:60 mol% at 0.8 mM total lipid shown), typical ingredients of pH-sensitive formulations, can be baseline-separated in combination with PEGylated lipids. **C**: Widely used formulation of 60 mol% HSPC, 35 mol% CHOL and 5 mol% DSPE-mPEG, with separation of the two major ingredients of naturally derived HSPC (concentration: 1 mM total lipid).

HSPC is a naturally derived palmitoyl and stearoyl phosphatidylcholine mix [11] forming rigid liposomes with low drug leakage together with cholesterol and DSPE-mPEG [35]. The method (Figure 2C) separates two peaks, from which HSPC-2 was identified as DSPC (18:0 PC, Figure 3) by a reference standard. HSPC-1 is assumed to be 1-palmitoyl-2-stearoyl-sn-glycero-3-phosphocholine (16:0-18:0 PC), according to the fatty acid distribution of HSPC [11] and the elution between DPPC (16:0 PC) and DSPC, related to its expected hydrophobicity. Excipients of both the pH-sensitive and rigid, HSPC-based formulation are well separated from the pentaglycine lipids, enabling a simultaneous bilayer analysis of such formulations with a targeting purpose.

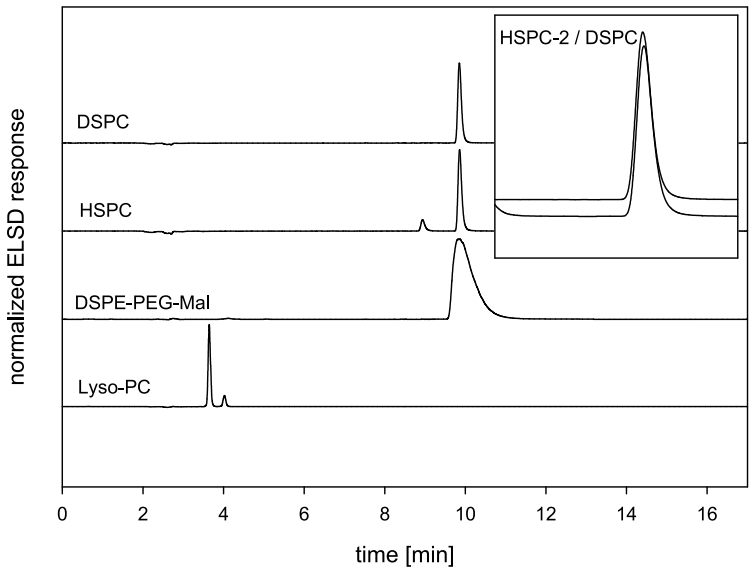

Figure 3: Elution profiles of lyso-PC reference and further frequently used lipids in liposome research. HSPC-2 was identified as DSPC by a reference standard.

DSPE-mPEG (Figure 2) or DSPE-PEG-Mal (Figure 3), latter used for conjugation of ligands with free thiol groups, show broader peak profiles probably due to the polydispersity of the polymer spacer. Comparable C18:0-chain carrying lipid DSPC (Table 2) has a similar elution time. This indicates a minor influence of the 2 kDa PEG-group on the column interaction, which seems to be predominantly determined by the C18-acyl-chains. Furthermore, common dyes DiR and Liss-Rhod-PE used in liposome bioimaging or fluorimetric studies may be analyzed with parallel UV-VIS detection (Figure 4), although peak tailing requires method optimization for Liss-Rhod-PE.

Table 2: Retention times of all tested compounds.

compound	**retention time [min]**
doxorubicin	2.6
lyso-PC reference standard	3.6, 4.0
DMA-PEG-G5	4.3
DMA-G5	4.6
R-DOTAP	5.4
CHOL	7.0
CHEMS	7.1
DPPC	7.9
DOPE	8.3
DiR	8.7
HSPC-1	8.9
DSPE-PEG-Mal	9.5-11.6
DSPC / HSPC-2	9.9
Liss-Rhod-PE	10.2-13.2
DSPE-mPEG	10.7
DPPG	12.1

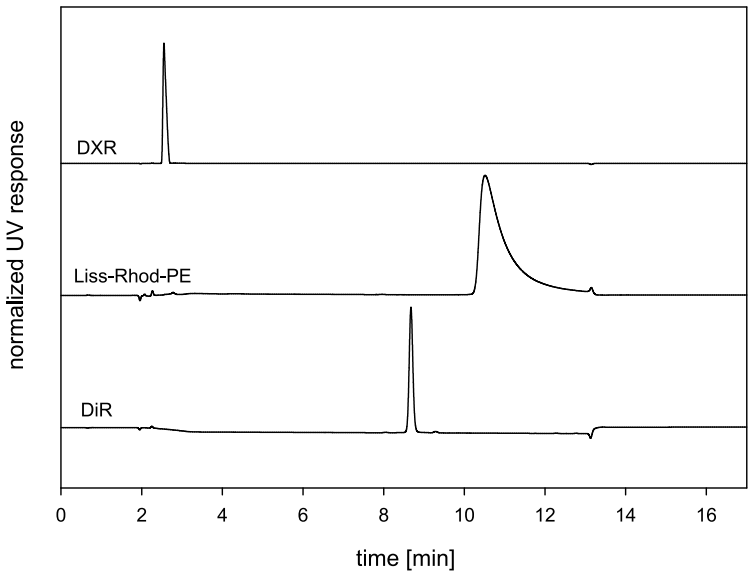

Figure 4: Analysis of dyes and DXR with parallel UV detection. DXR elutes at 2.6 min, indicating compatibility with analysis of pentaglycine lipids. Furthermore, frequently used dyes in liposome research may be quantified using parallel UV-VIS detection.

Typical degradation products of phospholipids are monoacylphosphatidylcholines or phosphoglycerol [36]. Specificity was therefore checked with a lyso-phosphatidylcholine standard containing relevant palmitoyl- and stearoyl fatty acid esters whether possible degradation products were also detectable and separated from the investigated lipids. We found the lyso-structures elute at 3.6 min and 4.0 min, indicating adequate separation to the pentaglycine lipids (Figure 3). A quantification of the lyso-forms was not of interest in this study. Finally, widely used liposomal drug doxorubicin (DXR) was found to elute at 2.6 min (Figure 4), indicating compatibility with the lipid analytic as well.

4.2. Precision, calibration and accuracy

It is known that ELS detection can be influenced by daily variabilities like device performance or lab conditions such as temperature and atmospheric pressure. Especially the latter is affected by night-time reduction of the lab's ventilation system, changing signal intensities by different droplet and particle formation during nebulization and evaporation processes. Improved exhaust conditions with reduced direct contact to the fume system led to decrease of those fluctuations down to 3-5 %, nonetheless we tried to avoid analyzes overnight. Use of an internal standard may circumvent such limitations, but adds further complexity to the analyte mixture and was therefore not considered here. Intra- and inter-day retention robustness and precision (Table 3) were both evaluated to investigate the reproducibility of the chromatography and ELSD. We found the RSD (relative standard deviation) of the retention time of 10 consecutive injections less than 0.2 % for all tested compounds, and slightly higher (< 0.6 %) for 6 injections on three different days, indicating minor influences of different eluent preparations.

Table 3: Intra- and inter-day retention time robustness and precision, expressed as relative standard deviation of 10 consecutive analyses or 6 analyses on three different days, respectively.

	retention time (RSD)		precision (RSD)	
compound	**intra-day**	**inter-day**	**intra-day**	**inter-day**
DMA-PEG-G5	0.07 %	0.30 %	1.02 %	1.88 %
DMA-G5	0.06 %	0.27 %	1.82 %	6.11 %
R-DOTAP	0.06 %	0.25 %	1.15 %	1.86 %
CHOL	0.04 %	0.04 %	0.96 %	2.53 %
DPPC	0.04 %	0.04 %	1.13 %	2.70 %
DSPE-mPEG	0.13 %	0.44 %	1.30 %	1.45 %
DPPG	0.17 %	0.59 %	1.76 %	7.23 %

Similar results were observed for precision analysis, which was found to be reproducible (RSD < 2 %) within a daily analysis, but less reproducible over three days. Increases were observed for DPPG and DMA-G5, and might be due to fluctuations in TFA content of eluent B [13], or indicate the need to increase the injected sample mass to improve the low signal-to-noise ratio for these two lipids (Table 4). The results obtained from precision analysis are comparable to those published earlier [8] and indicate suitability of this method for early research purposes.

The described method was calibrated automatically by decreasing injection volumes for lipids given in Table 4 on three different days using a five-point calibration (Figure 5). Alteration of injection volume had no impact on retention times (Supplementary Table 1).

Table 4: Calibration range and curve characteristics. Lower limit of calibration represents the here stated limit of quantification (LOQ). Slope, intercept, correlation coefficient and SNR of lowest calibration point are reported as mean ± standard deviation of three daily-actual calibrations using a logarithmic fit of the equation $area = concentration^{slope} * intercept$. LOD was determined by injection of decreasing quantities on the column until a peak could be reliably recognized.

compound	**ng on column / µM**	**slope**	**intercept**	**correlation**	**SNR**	**LOD [ng]**
DMA-PEG-G5	1115 - 2322 / 9 - 18	1.6589 ± 0.0204	7.9458 ± 0.0477	0.9997 ± 0.0004	137 ± 10	139
DMA-G5	269 - 561 / 6 - 13	1.4766 ± 0.0593	7.3009 ± 0.0987	0.9991 ± 0.0003	28 ± 2	135
R-DOTAP	1084 - 2258 / 31 - 65	1.5221 ± 0.0131	7.0739 ± 0.0350	0.9994 ± 0.0003	307 ± 25	45
CHOL	3964 - 8258 / 205 - 427	1.4393 ± 0.0148	6.7772 ± 0.0731	0.9994 ± 0.0003	2248 ± 165	83
DPPC	6043 - 12590 / 165 - 343	1.4321 ± 0.0323	7.4575 ± 0.1579	0.9997 ± 0.0002	2842 ± 197	126
DSPE-mPEG	4282 - 8920 / 31 - 64	1.7430 ± 0.0058	6.9389 ± 0.0027	0.9999 ± 0.0000	76 ± 5	535
DPPG	1321 - 2752 / 35 - 74	1.8183 ± 0.0416	4.3966 ± 0.2332	0.9984 ± 0.0009	15 ± 1	660

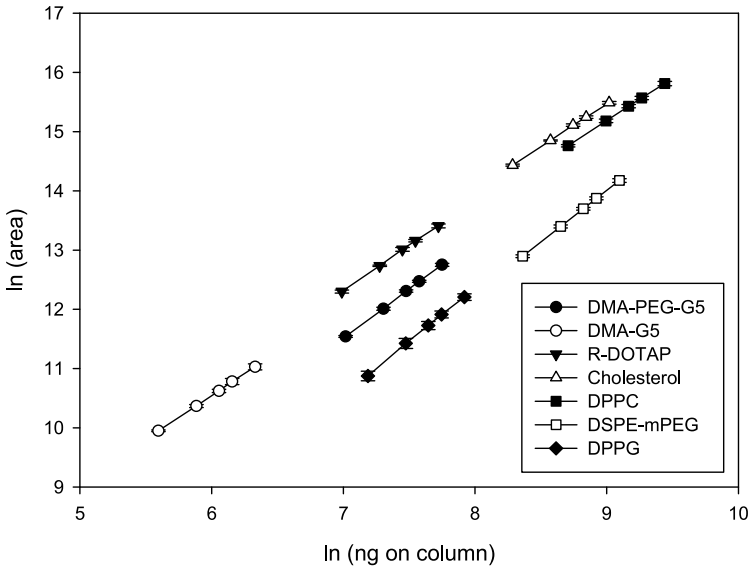

Figure 5: Calibration curves for simultaneous composition assessment of commonly used formulations modified with pentaglycine lipids. Calibration was performed in narrow ranges between 60-125 % of the expected sample concentration (1 mM total lipid) to enable simultaneous and rapid determination of low- and high-containing lipids. Linear relationships (Table 4) were obtained using a logarithmic fit according to the ELSD manufactures instruction, error bars show standard deviations of three calibrations on three different days.

As the signal-mass response during evaporative light scattering detection typically follows an exponential relationship, we obtained good linearity ($R^2 > 0.999$) after a logarithmic fit for every lipid except DPPG, which had slightly higher variability ($R^2 > 0.998$). We checked the accuracy (Table 5) of the calibration over three consecutive days with freshly dissolved blends and found recovery rates between 97-100 % at day 0 for all lipids.

Table 5: Accuracy. The recovery rate of the actual calibration was tested by analyzing individually prepared lipid solutions on three consecutive days. Standard deviations shown of three independent experiments.

compound	day 0	day 1	day 2
DMA-PEG-G5	98.6 ± 0.9 %	98.8 ± 1.6 %	98.2 ± 1.2 %
DMA-G5	98.9 ± 1.6 %	99.4 ± 4.5 %	97.1 ± 4.2 %
R-DOTAP	100.7 ± 0.9 %	99.9 ± 0.9 %	99.0 ± 1.0 %
CHOL	100.0 ± 0.8 %	99.4 ± 1.6 %	98.9 ± 2.2 %
DPPC	100.0 ± 0.9 %	99.8 ± 1.9 %	99.6 ± 3.5 %
DSPE-mPEG	100.3 ± 0.5 %	99.1 ± 0.3 %	98.0 ± 0.7 %
DPPG	98.9 ± 0.9 %	94.8 ± 0.7 %	92.2 ± 0.9 %

Similar recovery rates which resulted from calibration with analytical lipid blend ready mixes (Section 3.2) were achieved with blends stored up to 6 months at the described conditions, indicating the stability of the blends. Accuracy was constant for analysis over 3 consecutive days, only DPPG showed slightly decreasing recovery rates over time (Table 5).

As we observed relevant degradation of an ethanolic R-DOTAP sample stored in ambient-temperature autosampler in previous method developments (data not shown), we decreased the sample temperature to 4 °C in this method and investigated the sample stability, expressed as recovery rates of autosampler-stored samples with daily-actual calibrations (Table 6). We

found the lipids to be stable indicated by recovery rates ranging from 97 % to 100 %, however DPPG showed decreasing recovery rates down to 91 %. Sample instability may occur over time, for example precipitation of the sparingly soluble DPPG. Nevertheless, this does not explain the lower DPPG recovery of freshly prepared samples after inter-day-calibration analysis (Table 5). Furthermore, lipid precipitation in the diluent was excluded after visual inspection of HPLC vials stored for 2 days in the cooled autosampler using a cold light source. Avoidance of TFA fluctuations, increase of the injected sample mass to improve the SNR (Table 4) or slight gradient adaptions to enhance separation from DSPE-mPEG could be means to further improve the quantification of DPPG.

Table 6: Sample stability. Stability of lipids in chloroform-methanol-water (4.5 : 4.5 : 1 v/v/v) was investigated as recovery rate of lipid solutions (n=3) of known concentrations stored in HPLC autosampler at 4 °C over two days.

compound	day 0	day 1	day 2
DMA-PEG-G5	98.3 ± 0.7 %	97.3 ± 0.7 %	97.6 ± 0.3 %
DMA-G5	98.9 ± 2.0 %	97.7 ± 0.8 %	96.9 ± 0.7 %
R-DOTAP	100.4 ± 0.9 %	98.0 ± 1.7 %	96.9 ± 0.6 %
CHOL	100.1 ± 0.9 %	99.2 ± 0.6 %	98.9 ± 0.2 %
DPPC	100.0 ± 1.1 %	100.4 ± 0.7 %	100.1 ± 0.7 %
DSPE-mPEG	100.2 ± 0.6 %	98.9 ± 1.1 %	97.6 ± 0.6 %
DPPG	98.9 ± 1.1 %	97.7 ± 2.4 %	91.3 ± 1.8 %

4.3. Application of the analytical method

The preparation of liposomal formulations is a multistep process, involving blending of numerous lipids, the dissolution in organic solvents, extrusion or other homogenization processes, functionalization and purification steps. As lipids tend to be sticky compounds with the potential to adsorb to surfaces [37], the composition may change over the process. A proper analytical method for process monitoring is required. This is especially relevant for functionalized lipids like DSPE-mPEG, whose function as shield-layer around the drug carrier against the reticuloendothelial system of humans is widely described, and where definite correlations between molecular fraction in the bilayer and biological effect were revealed [30]. Same relevance has the quantification of lipids for the conjugation of targeting ligands, whose exact concentration is required for controlling consistent downstream process conditions. We applied an industry-relevant continuous solvent injection process [38] for the formation of pentaglycine-modified liposomes, followed by an easily scalable [39] tangential flow filtration step for purification and concentration. Here concentration changes may occur due to imperfect pump conveying, adsorption to the syringe, tubing or the membrane of the TFF device, as well as a wash-out of lipids during long-lasting crossflow process. Lipids for conjugation need to be inserted into the liposomal bilayer only to minor amounts, making the preparation of such blends in early development (usually small-scale) a demanding task due to very low weighed

portions. Larger exact blends were therefore prepared for two DMA-PEG-G5 containing formulations, aliquoted and dried as lipid film to be used as ready-to-use mix. The developed HPLC method was applied to monitor lipid amounts and composition throughout the preparation process (Table 7). It confirmed an accurate film preparation and re-dissolution in alcohols for injection with a DMA-PEG-G5 fraction of 1.0 mol%. Absolute lipid concentrations were in a suitable range for both formulations (recoveries > 95 %). Especially latter is highly relevant for reproducible particle size distributions during solvent injection processes [40]. The concentration of DPPG was about 1 mol% lower than expected from weighing. Jeschek et al. reported slight losses of phosphatidylglycerols during a film hydration and extrusion process and attributed the differences to weight and transfer losses or solubility reasons [8]. Those or above-mentioned recovery issues may explain the observed decrease here.

Table 7: Purification of liposomes using tangential flow filtration. Particles were prepared by solvent injection and purified and concentrated by TFF. Lipid composition and lipid mass recovery was evaluated by monitoring lipid concentration during liposome preparation. Analyses for lipid stock values done for two (PEG-NP) or one (Anionic-NP) individual blend preparations analyzed in triplicate. Analyses of liposomes after solvent injection and TFF done for three liposomal batches.

PEG-NP	*molecular bilayer composition [mol%]*			
	theoretical	*lipid stock*	*solvent injection*	*TFF*
DMA-PEG-G5	1.0	1.0 ± 0.0	1.0 ± 0.0	1.0 ± 0.0
CHOL	34.7	34.4 ± 0.3	34.0 ± 0.4	33.8 ± 0.4
DPPC	59.4	59.9 ± 0.5	60.2 ± 0.4	60.6 ± 0.3
DSPE-mPEG	5.0	4.7 ± 0.1	4.7 ± 0.1	4.6 ± 0.1
absolute conc. [mM]	90.1	85.7 ± 1.9	6.7 ± 0.1	25.4 ± 4.3
recovery [%]		95.1 ± 2.0	97.4 ± 2.7	92.0 ± 7.0

Anionic-NP	*molecular bilayer composition [mol%]*			
	theoretical	*lipid stock*	*solvent injection*	*TFF*
DMA-PEG-G5	1.0	1.0 ± 0.0	n.d.	1.0 ± 0.0
CHOL	34.7	34.6 ± 0.1	n.d.	34.5 ± 0.2
DPPC	59.3	60.5 ± 0.1	n.d.	60.6 ± 0.2
DPPG	5.0	4.0 ± 0.1	n.d.	3.9 ± 0.1
absolute conc. [mM]	16.0	16.0 ± 0.1	n.d.	26.2 ± 2.9
recovery [%]		99.7 ± 0.7	n.d.	88.4 ± 9.9

We were able to reproducibly prepare and purify liposomes within a size range of 150 nm (± 10 %) with acceptable polydispersity (< 0.25) without applying any further homogenization steps (Table 8). Zeta potential was -8 mV for PEGylated and -23 mV for liposomes being stabilized via a pronounced anionic surface charge, respectively, which is comparable to previously reported formulations [41, 42]. The pumps for solvent injection worked with good reliability, shown by the 97 % lipid recovery calculated from the theoretical concentration based on the flow rates.

Tangential flow filtration was used to exchange the external buffer ammonium sulfate to DPBS and to concentrate the liposomal dispersions to a target concentration of 30 mM, required for

downstream processes like drug loading and ligand modification. The lipid composition did not change during processing, especially the relevant conjugation-lipid DMA-PEG-G5 maintained its molar fraction of 1.0 mol%. Furthermore, good lipid yields around 90 % were obtained from TFF equipment, indicating low loss due to adsorption to the membrane or hold-up volume of the system.

Active loading is the state of the art technology in liposomal drug delivery achieving high drug loads and encapsulation efficacies for small molecules that can be retained interior of vesicles by charge, salt formation, precipitation or complexation mechanisms [43]. The combination of scalable manufacturing techniques for sortaggable liposomes, widely applicable active loading and versatile analytics would offer a broad platform for the industrial development of targeted, toxin-loaded liposomes. We therefore analyzed if the pentaglycine-modified liposomes could be actively loaded with a model compound, acridine orange, and fluorescence analysis [44] showed a quick accumulation inside the liposomes for both formulations (*data not shown in publication, meanwhile displayed in Chapter 6, Figure 2*). This indicates a stable ammonium sulfate gradient generation by tangential flow filtration, suitable for the active loading of weak bases like doxorubicin [43], an active compound compatible with the presented analytical method (Figure 4).

Sortase-A technology [23] was then used to modify the pentaglycine-liposomes with a LPETG-modified model VHH specific for the enhanced green fluorescent protein (eGFP) [45]. This transpeptidation reaction offers site-specific ligand conjugation to the drug delivery system yielding a homogenous product profile, what is highly desired for quality controls and regulatory authorities. A mix of Sortase-A, LPTEG-modified VHH and pentaglycine-modified liposomes was incubated for 4 h to allow VHH coupling. Dynamic light scattering showed no relevant changes of the hydrodynamic diameter or the polydispersity index, indicating that no sub-visible precipitation or aggregation occurred (Table 8).

Table 8: Physical properties of liposomes before and after incubation of liposomes with 25 µM Sortase-A and 50 µM VHH. Standard deviations shown for experiments done with three liposome batches.

formulation	process step	d_h [nm]	PDI	zeta potential [mV]
PEG-NP	before reaction	143 ± 5	0.24 ± 0.00	-8.1 ± 0.4
	after reaction	138 ± 4	0.24 ± 0.01	-6.1 ± 0.4
Anionic-NP	before reaction	148 ± 1	0.24 ± 0.02	-23.3 ± 0.6
	after reaction	152 ± 1	0.23 ± 0.01	-18.1 ± 1.2

Furthermore, minor changes (PEG-NP: -2 mV, Anionic-NP: -5 mV) in zeta potential were detected, hinting at surface modifications, however the small absolute changes can also be attributed to measurement fluctuations. Influence of the reaction on the molar fraction of

DMA-PEG-G5 in the bilayer of three liposomal batches was analyzed after dissolution of the liposomes in diluent and removal of precipitated protein by centrifugation. This procedure had no impact on the accuracy as verified by analysis of an accuracy sample spiked with VHH and Sortase-A prior diluent addition (Supplementary Table 2). Statistically significant decreases down to 0.87 ± 0.02 mol% for PEG-NP ($p < 0.005$) and 0.88 ± 0.01 mol% for Anionic-NP ($p < 0.009$) were found. Roughly half of the pentaglycine molecules are expected to be present at the outer bilayer leaflet due to homogenous lipid distribution during vesicle formation after solvent injection. As only those are accessible for Sortase-A reaction, this decrease indicates that about 24 % of the accessible lipids have reacted with the VHH, however further protein-based methods for direct protein quantification are required to give valid statements on reaction efficacy and VHH-load on the drug delivery system.

5. Conclusion and outlook

A versatile rp-HPLC-based analytical method applying evaporative light scattering detection was developed for numerous liposomal concepts. It covers formulations with different particle surface properties by separation of positive (R-DOTAP), negative (DPPG) or PEGylated lipids (DSPE-mPEG) from frequently used phosphatidylcholines (DPPC, HSPC, DSPC) and cholesterol. Furthermore, pH-sensitive lipid combinations of CHEMS with DOPE or dye-labeled (DiR, Liss-Rhod-PE) formulations can be analyzed. Conjugation of ligands towards liposomes for a targeted drug delivery requires integration of reactive lipid anchors in the bilayer. These lipids include novel pentaglycine lipids for Sortase-A mediated chemoenzymatic conjugation (sortagging) of proteinaceous ligands. Two variants of pentaglycine lipids could be quantified simultaneously with above mentioned excipients, ensuring analyzability of various bilayer combinations. This completes the proposed analytical method as a supportive tool in formulation screens for targeted drug delivery.

The method validation for the pentaglycine lipids and selected helper lipids showed good analytical performance. The bilayer fraction of DMA-PEG-G5 in an anionic and in a PEGylated, DPPC-based liposomal formulation was tracked over an industry-relevant manufacturing process. Results obtained with the newly developed method indicated no adsorption to surfaces of the instruments and materials being in use in production, or wash-out during cross-flow filtration. This shows a stable bilayer anchoring of the pentaglycine moiety by the two myristyl chains. A subsequent sortagging reaction was monitored by following the decrease of the pentaglycine substrate fraction in the bilayer due to the coupling with a single-domain antibody.

Besides the here extensively described process monitoring of rigid, DPPC-based liposomal formulations, we utilized the method in our lab to successfully analyze other sortaggable liposomal constructs. This included analysis of a Doxil® like doxorubicin-loaded stealth liposome formulation (DMA-PEG-G5 : DSPE-mPEG : CHOL : HSPC) and PEGylated, pH-sensitive liposomes (DMA-PEG-G5 : DSPE-mPEG : CHEMS : DOPE).

Proceeding work for the lipid characterization of sortaggable liposomes may involve the separation and quantification of lipid degradation products. This would be especially relevant after the required lipid combination was chosen from first *in vitro* or *in vivo* screenings. Within the current method, analysis of lipid degradation products may be feasible by expansion of the gradient towards more hydrophilic fractions. However, this will probably lead to extended analysis times, which is less desired for preliminary formulation screening experiments and was therefore not in scope of this method development.

On the contrary, due to the fast and versatile approach, the here presented reliable quantification of numerous lipid combinations together with sortaggable lipids can help to accelerate a rational early formulation development of targeted liposomal systems.

References

[1] M. Ashtikar, K. Nagarsekar, A. Fahr, Transdermal delivery from liposomal formulations – Evolution of the technology over the last three decades, Journal of Controlled Release, 242 (2016) 126-140.

[2] G. Fricker, T. Kromp, A. Wendel, A. Blume, J. Zirkel, H. Rebmann, C. Setzer, R.-O. Quinkert, F. Martin, MC, Phospholipids and lipid-based formulations in oral drug delivery, Pharmaceutical Research, 27 (2010) 1469-1486.

[3] T.M. Allen, P.R. Cullis, Liposomal drug delivery systems: from concept to clinical applications, Advanced drug delivery reviews, 65 (2013) 36-48.

[4] P. van Hoogevest, X. Liu, A. Fahr, M.L.S. Leigh, Role of phospholipids in the oral and parenteral delivery of poorly water soluble drugs, Journal of Drug Delivery Science and Technology, 21 (2011) 5-16.

[5] L. Willis, D. Hayes, H.M. Mansour, Therapeutic liposomal dry powder inhalation aerosols for targeted lung delivery, Lung, 190 (2012) 251-262.

[6] V.P. Torchilin, Recent advances with liposomes as pharmaceutical carriers, Nature reviews Drug discovery, 4 (2005) 145-160.

[7] Y. Barenholz, S. Amselem, Quality control assays in the development and clinical use of liposome-based formulations, Liposome technology, 1 (1993) 527-616.

[8] D. Jeschek, G. Lhota, J. Wallner, K. Vorauer-Uhl, A versatile, quantitative analytical method for pharmaceutical relevant lipids in drug delivery systems, Journal of pharmaceutical and biomedical analysis, 119 (2016) 37-44.

[9] M. Oswald, M. Platscher, S. Geissler, A. Goepferich, HPLC analysis as a tool for assessing targeted liposome composition, International journal of pharmaceutics, 497 (2016) 293-300.

[10] M. Riehl, M. Harms, A. Hanefeld, K. Mäder, Investigation of the stabilizer elimination during the washing step of charged PLGA microparticles utilizing a novel HPLC-UV-ELSD method, European Journal of Pharmaceutics and Biopharmaceutics, 94 (2015) 468-472.

[11] H. Shibata, C. Yomota, H. Okuda, Simultaneous determination of polyethylene glycol-conjugated liposome components by using reversed-phase high-performance liquid chromatography with UV and evaporative light scattering detection, AAPS PharmSciTech, 14 (2013) 811-817.

[12] K. Vorauer-Uhl, D. Jeschek, G. Lhota, A. Wagner, S. Strobach, H. Katinger, Simultaneous quantification of complex phospholipid compositions containing monophosphoryl lipid-A by RP-HPLC, Journal of Liquid Chromatography & Related Technologies, 32 (2009) 2203-2215.

[13] Z. Zhong, Q. Ji, J.A. Zhang, Analysis of cationic liposomes by reversed-phase HPLC with evaporative light-scattering detection, Journal of pharmaceutical and biomedical analysis, 51 (2010) 947-951.

[14] C. Schönherr, S. Touchene, G. Wilser, R. Peschka-Suss, G. Francese, Simple and precise detection of lipid compounds present within liposomal formulations using a charged aerosol detector, Journal of Chromatography A, 1216 (2009) 781-786.

[15] N.C. Megoulas, M.A. Koupparis, Twenty years of evaporative light scattering detection, Critical Reviews in Analytical Chemistry, 35 (2005) 301-316.

[16] X. Guo, Z. Wu, Z. Guo, New method for site-specific modification of liposomes with proteins using sortase a-mediated transpeptidation, Bioconjugate chemistry, 23 (2012) 650-655.

[17] J.R. Silvius, R. Leventis, A Novel "Prebinding" Strategy Dramatically Enhances Sortase-Mediated Coupling of Proteins to Liposomes, Bioconjugate Chemistry, 28 (2017) 1271-1282.

[18] A. Tabata, N. Anyoji, Y. Ohkubo, T. Tomoyasu, H. Nagamune, Investigation on the Reaction Conditions of Staphylococcus aureus Sortase A for Creating Surface-modified Liposomes as a Drug-delivery System Tool, Anticancer Research, 34 (2014) 4521-4527.

[19] J.O. Eloy, R. Petrilli, L.N.F. Trevizan, M. Chorilli, Immunoliposomes: A review on functionalization strategies and targets for drug delivery, Colloids and Surfaces B: Biointerfaces, 159 (2017) 454-467.

[20] P. Marques-Gallego, A.I. de Kroon, Ligation strategies for targeting liposomal nanocarriers, Biomed Research International, (2014) e129458.

[21] A.N. Lukyanov, T.A. Elbayoumi, A.R. Chakilam, V.P. Torchilin, Tumor-targeted liposomes: doxorubicin-loaded long-circulating liposomes modified with anti-cancer antibody, Journal of Controlled Release, 100 (2004) 135-144.

[22] N. Jain, S.W. Smith, S. Ghone, B. Tomczuk, Current ADC Linker Chemistry, Pharmaceutical Research, 32 (2015) 3526-3540.

[23] M. Ritzefeld, Sortagging: A Robust and Efficient Chemoenzymatic Ligation Strategy, Chemistry – A European Journal, 20 (2014) 8516-8529.

[24] H.T. Ta, S. Prabhu, E. Leitner, F. Jia, D. von Elverfeldt, K. Jackson, T. Heidt, A. Nair, H. Pearce, C. von zur Muhlen, X. Wang, K. Peter, C.E. Hagemeyer, Enzymatic Single-Chain Antibody Tagging, Circulation Research, 109 (2011) 365-373.
[25] T. Matsumoto, T. Tanaka, A. Kondo, Sortase A-catalyzed site-specific coimmobilization on microparticles via streptavidin, Langmuir, 28 (2012) 3553-3557.
[26] C.E. Hagemeyer, K. Alt, A.P. Johnston, Particle generation, functionalization and sortase A-mediated modification with targeting of single-chain antibodies for diagnostic and therapeutic use, Nature Protocols, 10 (2015) 90-105.
[27] M.W. Platscher, R. Behrendt, V. Groehn, S.R. Hoertner, M.S. Passafaro, F. Bauer, Targeting aminoacid lipids, in: Google Patents, Merck Patent Gmbh, US, 2014.
[28] C. Bachran, M. Schröder, L. Conrad, J.J. Cragnolini, F.G. Tafesse, L. Helming, H.L. Ploegh, L.K. Swee, The activity of myeloid cell-specific VHH immunotoxins is target-, epitope-, subset- and organ dependent, Scientific Reports, 7 (2017) 17916.
[29] M. Rashidian, E.J. Keliher, A.M. Bilate, J.N. Duarte, G.R. Wojtkiewicz, J.T. Jacobsen, J. Cragnolini, L.K. Swee, G.D. Victora, R. Weissleder, H.L. Ploegh, Noninvasive imaging of immune responses, Proceedings of the National Academy of Sciences, 112 (2015) 6146-6151.
[30] M.L. Immordino, F. Dosio, L. Cattel, Stealth liposomes: review of the basic science, rationale, and clinical applications, existing and potential., International Journal of Nanomedicine, 1 (2006) 297-315.
[31] Y. Zhao, J. May, I.W. Chen, E. Undzys, S.-D. Li, A Study of Liposomal Formulations to Improve the Delivery of Aquated Cisplatin to a Multidrug Resistant Tumor, Pharmaceutical Research, 32 (2015) 3261-3268.
[32] D. Christensen, K.S. Korsholm, P. Andersen, E.M. Agger, Cationic liposomes as vaccine adjuvants, Expert Review of Vaccines, 10 (2011) 513-521.
[33] I.M. Hafez, P.R. Cullis, Cholesteryl hemisuccinate exhibits pH sensitive polymorphic phase behavior, Biochimica et Biophysica Acta (BBA) - Biomembranes, 1463 (2000) 107-114.
[34] T. Ishida, M.J. Kirchmeier, E.H. Moase, S. Zalipsky, T.M. Allen, Targeted delivery and triggered release of liposomal doxorubicin enhances cytotoxicity against human B lymphoma cells, Biochimica et Biophysica Acta (BBA) - Biomembranes, 1515 (2001) 144-158.
[35] Y. Barenholz, Doxil® – The first FDA-approved nano-drug: Lessons learned, Journal of Controlled Release, 160 (2012) 117-134.
[36] M. Grit, D.J.A. Crommelin, Chemical stability of liposomes: implications for their physical stability, Chemistry and Physics of Lipids, 64 (1993) 3-18.
[37] A.L. Carneiro, M.H.A. Santana, Production of liposomes in a multitubular system useful for scaling up of processes, in: Surface and Colloid Science, Springer Berlin Heidelberg, 2004, pp. 273-277.
[38] A. Wagner, K. Vorauer-Uhl, Liposome technology for industrial purposes, Journal of drug delivery, 2011 (2010) 591325.
[39] S. Schiller, A. Hanefeld, M. Schneider, C.-M. Lehr, Focused Ultrasound as a Scalable and Contact-Free Method to Manufacture Protein-Loaded PLGA Nanoparticles, Pharmaceutical Research, 32 (2015) 2995-3006.
[40] A.S. Domazou, P.L. Luisi, Size distribution of spontaneously formed liposomes by the alcohol injection method, Journal of Liposome Research, 12 (2002) 205-220.
[41] H.D. Han, A. Lee, C.K. Song, T. Hwang, H. Seong, C.O. Lee, B.C. Shin, In vivo distribution and antitumor activity of heparin-stabilized doxorubicin-loaded liposomes, International Journal of Pharmaceutics, 313 (2006) 181-188.
[42] M. Ionov, Z. Garaiova, I. Waczulikova, D. Wróbel, Pędziwiatr-Werbicka, R. Gomez-Ramirez, F.J. de la Mata, B. Klajnert, T. Hianik, M. Bryszewska, siRNA carriers based on carbosilane dendrimers affect zeta potential and size of phospholipid vesicles, Biochimica et Biophysica Acta (BBA) - Biomembranes, 1818 (2012) 2209-2216.
[43] J. Gubernator, Active methods of drug loading into liposomes: recent strategies for stable drug entrapment and increased in vivo activity, Expert Opinion on Drug Delivery, 8 (2011) 565-580.
[44] G. Haran, R. Cohen, L.K. Bar, Y. Barenholz, Transmembrane ammonium sulfate gradients in liposomes produce efficient and stable entrapment of amphipathic weak bases, Biochimica et Biophysica Acta (BBA) – Biomembranes, 1151 (1993) 201-215.
[45] A. Kirchhofer, J. Helma, K. Schmidthals, C. Frauer, S. Cui, A. Karcher, M. Pellis, S. Muyldermans, C.S. Casas-Delucchi, M.C. Cardoso, Modulation of protein properties in living cells using nanobodies, Nature Structural & Molecular Biology, 17 (2010) 133-138.

Supplementary Data

Supplementary Table 1: Retention time is independent of the applied injection volume.

	retention time [min]						
injection volume [µL]	**DMA-PEG-G5**	**DMA-G5**	**R-DOTAP**	**CHOL**	**DPPC**	**DSPE-mPEG**	**DPPG**
50	4.37	4.65	5.43	6.98	7.88	10.67	12.17
42	4.38	4.67	5.45	7.01	7.92	10.74	12.24
38	4.37	4.65	5.44	7.00	7.91	10.79	12.25
32	4.36	4.65	5.44	7.00	7.91	10.84	12.39
24	4.36	4.65	5.44	7.00	7.91	10.88	12.09

Supplementary Table 2: Influence of protein presence on lipid quantification accuracy. 50 µM VHH ENH and 25 µM Sortase-A were spiked to an aqueous lipid blend, and the reaction was immediately quenched by dilution of the blend in the diluent methanol-chloroform (1:1, v/v). Precipitated proteins were removed by centrifugation. Two individual mixtures were analyzed in duplicate runs.

compound	**target [µM]**	**recovery n1**	**recovery n2**
DMA-PEG-G5	13.7	101 %	102 %
DMA-G5	12.5	103 %	97 %
R-DOTAP	49.5	101 %	102 %
CHOL	276.7	104 %	103 %
DPPC	264.2	104 %	105 %
DSPE-mPEG	51.5	105 %	106 %
DPPG	60.7	92 %	98 %

Chapter 3

Sortaggable liposomes: Evaluation of reaction conditions for single-domain antibody conjugation by Sortase-A and targeting of CD11b$^+$ myeloid cells

This chapter is published as: Wöll, S., Bachran, C., Schiller, S., Schröder, M., Conrad, L., Swee, L.K., Scherließ, R.: Sortaggable liposomes: Evaluation of reaction conditions for single-domain antibody conjugation by Sortase-A and targeting of CD11b$^+$ myeloid cells.
European Journal of Pharmaceutics and Biopharmaceutics, 133 (2018), 138-150.
https://doi.org/10.1016/j.ejpb.2018.09.017

Abstract

Active targeting with ligand coated liposomal drug delivery systems is a means to increase the therapeutic index of drugs. Stable ligand coating requires bilayer anchorage of the commonly proteinaceous ligands and hence a conjugation of lipid structures towards amino acids. This often leads to heterogeneous reaction products especially when chemical coupling methods are employed. Chemoenzymatic Sortase-A mediated transpeptidation (sortagging) is a useful tool to avoid this protein heterogeneity through its site-specific, bioorthogonal ligation mechanism. Manufacturing of such sortaggable, pentaglycine-modified liposomes was developed by adaption of a scalable solvent injection technique. The pentaglycine liposomes were prepared with different degrees of PEGylation and steric accessibility of the pentaglycine motif. Comparable hydrodynamic diameters (146-188 nm) of the different formulations were obtained after a flow rate screening. The sortagging reactivity of a single-domain antibody (VHH) towards the pentaglycine liposomes was strongly dependent on the steric accessibility of the pentaglycine nucleophile. Adjusting the pentaglycine to ligand ratio improved conversion rates up to 80 %. The liposome-bound VHH was accessible for its soluble antigen as shown by a chromatography-based binding assay. Mono- and granulocytes could be selectively targeted *in vitro* by conjugation of BMX1, a VHH directed towards human myeloid cell surface marker CD11b. Confocal microscopy revealed intracellular localization of the targeted liposomes. The developability of those pentaglycine liposomes as well as their proof of principle for targeted drug delivery shows their potential for further investigation, for example as delivery platform for diagnostics or drugs into the tumor microenvironment.

1. Introduction

The therapeutic index is one of the most crucial criteria for a novel drug. A means to increase the therapeutic index is the site-selective delivery of drugs to affected cells while avoiding side effects on healthy tissues. This “concept of the magic bullet” introduced by Paul Ehrlich remains a highly desirable aim in pharmaceutical research [1]. Significant progress has been achieved with targeted therapies utilizing antibody-drug conjugates [2] or “actively”, meaning ligand mediated targeted drug delivery systems such as liposomes [3]. A key technology in the design of actively targeted liposomes is the conjugation between ligand and drug carrier [4]. The conjugation reaction between labile ligands and liposomes should be feasible under mild conditions in aqueous environment, it should conjugate expensive proteins with high yields and deliver homogenous reaction products that are reliably anchored in the bilayer. First attempts attached targeting motifs in an adsorptive fashion [5, 6], followed by covalent IgG coupling with unspecific amine-cross linkers [7], disulfide [8] and thiol-maleimide chemistry [9] or more sophisticated methods, as reviewed by Marques-Gallego et al. [4]. Although conjugation methods evolved towards regio-specific reactions [10], these strategies are still not routinely used for ligand attachment in current scientific reports. This is probably due to their superior applicability for small targeting entities [11-13] rather than large proteins and the requirement of substrates with difficult commercial accessibility [14]. Amongst other enzymatic methods [15], the chemo-selective, bioorthogonal Sortase-A mediated conjugation (sortagging) of proteins to liposomes [14] or lipid anchors [16, 17] has been shown as a convenient and efficient tool to overcome these hurdles. Sortase-A transpeptidase is derived from *Staphylococcus aureus*, where it physiologically anchors surface proteins in the bacterial cell wall. It recognizes a C-terminal LPxTG (leucine, proline, any amino acid, threonine, glycine) motif and forms a thioacyl intermediate with the threonine while cleaving the amide bond towards the glycine. This is followed by the transpeptidation reaction with an incoming nucleophilic N-Terminus of oligoglycines [18] or other primary amines [19, 20]. Sortase-A is used in several isoforms developed with different technological advantages such as Ca^{2+}-independency [21] or a shift of the pH-optimum to the weakly acidic spectrum [22]. Several studies have investigated Sortase-A as a tool to promote linkage between model proteins or ligands and single lipid structures [16], recognition motif carrying vesicles [14, 22-24] or even whole cells [17]. Main advantage of the Sortase-A reaction is the inherent site-selectivity, which leads to homogeneous conjugation products [18]. This is a decisive advantage over traditional chemical linkage approaches considering regulatory demands on product uniformity and quality controls.

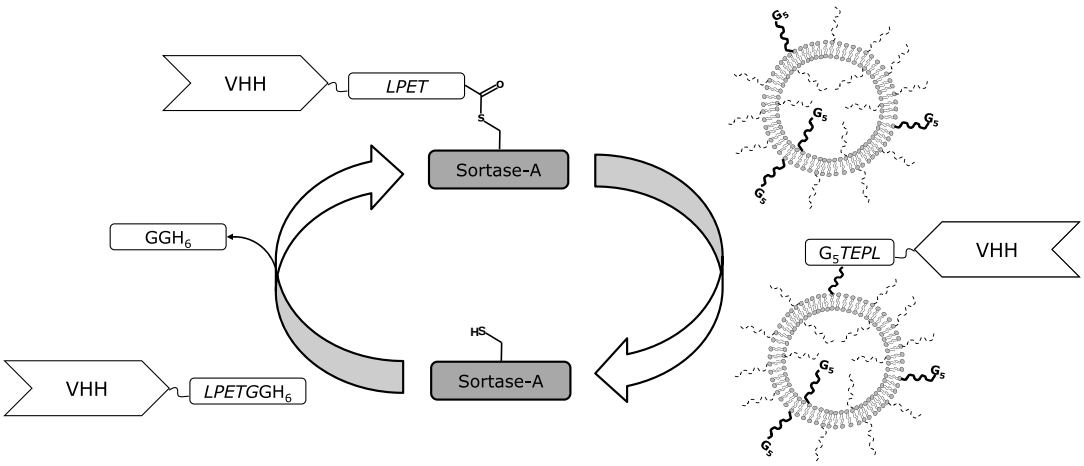

Scheme 1: Sortase-A mediated reaction of a LPETG-modified VHH with pentaglycine-modified liposomes. Sortase-A recognizes LPETG-modified single-domain antibodies (VHHs) and forms a thioester-intermediate between the VHH's threonine and a cysteine residue at the active site of the enzyme. The amino-group of a liposome-anchored oligoglycine serves as nucleophile, which forms a peptide bond between the targeting ligand (the VHH) and the liposome in a transpeptidation reaction.

To apply Sortase-A technology for manufacturing of targeted liposomes (Scheme 1), the relevant transpeptidation motif, typically an oligoglycine, is conjugated to a lipid component serving as anchor molecule [14, 16, 24]. The synthesis of such amino acid lipids circumvents involvement of labile proteins and liposomal structures during the critical linkage between amino acids and the lipid anchor. Therefore, it can be conducted as chemical synthesis, e.g. on a solid phase [25]. The subsequent conjugation between ligand and amino acid lipid can be done on enzymatic, meaning site-selective basis by a transpeptidation, forming a peptide bond between the protein and amino acid lipid [4]. This approach yields chemically defined reaction products without implications on ligands paratope regions. Sortase-A reaction conditions for modification of soluble substrates have been investigated in various studies [18]. However, the enzymatic reaction behavior of artificial surfaces, such as differently polyethylene glycol coated (PEGylated) bilayers, might greatly differ from the ideal reaction behavior of soluble substrates. Silvius et al. [23] examined various glycine-nucleophiles integrated in non-PEGylated, fluid DOPC/POPG vesicles for their reaction kinetics with a model protein (green fluorescent protein, GFP) or a human enzyme. The authors showed a dramatic increase of conversion rates for membrane-bound Sortase-A over a soluble one. Furthermore, Guo et al. [14] revealed a drastically reduced reaction efficacy of a glycine-motif hidden by a surrounding PEG-layer for the conjugation of GFP. As PEGylation is a key factor for the *in vivo* fate of nanotherapeutics [26], it is of high importance to carefully adjust the degree of PEGylation for targeted liposomes. To gain deeper insights in PEG- and surface dependent Sortase-A reactivity, we altered a liposomal surface either by integration of PEGylated (2 kDa) distearoyl-phosphatidylethanolamine (DSPE) or anionic dipalmitoyl-phosphoglycerol (DPPG) as an alternative stabilizing agent. A PEG-spaced or a bilayer-proximal located pentaglycine motif was

integrated in the composition. This enabled the investigation of the reaction conditions of Sortase-A mediated ligand attachment towards liposomes with closely similar bilayer properties, but clear differences in surface properties and steric accessibility of the reaction partner (Scheme 2). Tabata et al. [22] investigated reaction conditions of a pH-sensitive Sortase-A mutant with a model protein (GFP) or a peptide for lung cancer targeting [24]. As the latter was the only report where a liposomal drug delivery system was modified by Sortase-A with a targeting ligand, it was here the intention to gain further insights into the conjugation of antibody-derived ligands with respect to the liposomal surface properties. Therefore, we here employed a sortaggable single-domain antibody [27] for kinetic investigations of the conjugation towards liposomal surfaces differing in PEGylation and steric accessibility of the pentaglycine motif. Single-domain antibodies or VHHs (single-domain antibody of camelid heavy-chain only antibodies) are promising candidates as novel targeting ligands for drug delivery systems [28]. They provide favorable physicochemical properties like high refolding capacity [29], high solubility, affinity and specificity comparable to Fab' ligands [30, 31] while their molecular weight is drastically reduced to ≈15 kDa. This is advantageous for the colloidal stability and physiologic behavior of nanomedicines due to the low impact on size and weight of the particulate construct, even at high ligand densities. VHHs have been reported as liposomal targeting ligands against model proteins [32] and the cellular targets HER2 [33], EGFR [34-37] and HIV-1 env [38].

To demonstrate proof of concept for a targeted drug delivery with the presented sortaggable liposomes, dye-labeled liposomes were modified with a novel VHH against human CD11b and tested *in vitro* for their selective binding and uptake in human peripheral blood mononuclear cells (hPBMCs). CD11b is a cell surface marker found on myeloid cells in the tumor microenvironment such as myeloid-derived suppressor cells (MDSC). MDSC are a heterogeneous cell population involved in the control of immune responses of several inflammatory and proliferative diseases [39]. A drug targeting to such cells would therefore offer new opportunities in the treatment of cancer or autoimmune diseases via an immunomodulatory approach [40].

In the presented work, a solvent injection process was chosen to prepare pentaglycine-modified liposomes due to the technique's inherent scalability and the option to control product characteristics by rational parameter selection [41]. Firstly, this tunable process was adjusted to obtain liposomes with comparable size distribution, but different surface structures, in particular the steric accessibility of the pentaglycine moiety (Scheme 2). Secondly, we thoroughly evaluated the reaction kinetics and optimized conditions of Sortase-A mediated VHH conjugation for these formulations. To investigate whether the VHHs grafted on the liposome

surface maintained their ability to bind their corresponding antigen, a size exclusion chromatography-based assay was employed. Finally, the CD11b-dependent specific binding and uptake of selected formulations by hPBMCs was investigated. The presented work therefore provides a profound development of sortaggable liposomal formulations combined with a detailed investigation of a novel conjugation technique. In addition, proof of principle for a targeted drug delivery utilizing a promising class of antibody species against an exploratory target is demonstrated, enabling a deeper investigation of nanoparticulate drug delivery systems in rising therapeutic areas like immuno-oncology.

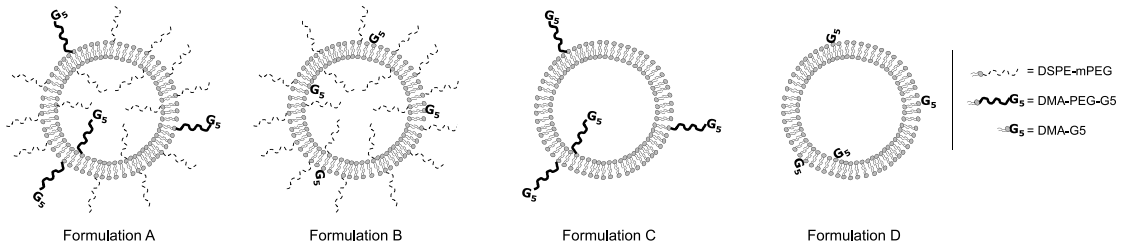

Scheme 2: Differently PEGylated, pentaglycine-modified formulations. Formulation A and B are stabilized through a PEG-shell, whereas formulation C and D are stabilized via an anionic phosphoglycerol (DPPG).

2. Materials

Pentaglycine-modified lipids (Merck & Cie, Schaffhausen, Switzerland) consist of a dimyristyl-amino-propandiol scaffold (DMA) linked directly (DMA-G5, 897 Da, formulation B and D, Scheme 2) or via a 2 kDa PEG spacer (DMA-PEG-G5, 2554 Da, formulation A and C, Scheme 2) to a pentaglycine-motif (G5) and are described in detail in [42]. 1,2-dipalmitoyl-sn-glycero-3-phosphocholine (DPPC), 1,2-dipalmitoyl-sn-glycero-3-phospho-(1'-rac-glycerol) (DPPG), 1,2-distearoyl-sn-glycero-3-phosphoethanolamine-N-[methoxy (polyethylene glycol)-2000] (DSPE-mPEG) were a kind gift of Lipoid GmbH (Ludwigshafen, Germany). Dulbecco's phosphate buffered saline (DPBS D1408, 10fold stock), FITC-dextran 10 kDa, cholesterol (CHOL) and Triton X-100 were obtained from Sigma-Aldrich (St. Louis, MO, USA). 1,2-dipalmitoyl-sn-glycero-3-phosphoethanolamine-N-(lissamine rhodamine B sulfonyl) (Liss-Rhod-PE) was obtained from Avanti Polar Lipids (Alabaster, AL, USA). Acetonitrile, trifluoroacetic acid (TFA), sodium chloride (NaCl), hydrochloric acid (HCl), methanol and ethanol (both gradient grade) as well as dimethylsulfoxide (DMSO) were obtained from Merck KGaA (Darmstadt, Germany). Water was purified by a Milli-Q system (Merck Millipore, Billerica, MA, USA). LPETG (leucine, proline, glutamic acid, threonine, glycine)-modified single-domain antibodies of camelid heavy-chain only antibodies (VHH) VHH ENH (14237 Da), VHH BMX1 (16541 Da) and Sortase-A variant SortA7m were prepared as described in [40]. VHH BMX1 was obtained by phage display from an alpaca immune library (supplementary information). Enhanced green fluorescent protein (eGFP) was prepared as described in [43].

3. Methods

3.1. Liposomal formulation development

Pentaglycine-modified liposomes were prepared by a continuous solvent injection process. Either DMA-PEG-G5 or DMA-G5 were combined with a DSPE-mPEG or DPPG containing lipid blend (Table 1). Lipid blends for formulation A and B were dissolved in ethanol to 90 mM, blends for formulation C and D were dissolved in methanol to 32 mM. Due to solubility reasons, DMA-G5 was spiked to the alcohol solution from a DMSO solution (5 mg/mL). Lipid solutions were filled into a plastic syringe (B. Braun, Melsungen, Germany) and injected utilizing a syringe pump (PHD Ultra4400, Harvard Apparatus, Holliston, MA, USA) into a stream of DPBS pH 7.4 conveyed by a peristaltic pump (Ismatec IP65, Cole-Parmer, Wertheim, Germany). A combination of flexible tubing (3.2 mm inner diameter, PharMed BPT, Saint Gobain, Courbevoie, France) and rigid tubing (2.0 mm inner diameter, Bola FEP, Bohlender GmbH, Grünsfeld, Germany) was used to reduce overall dead volume. Lipid and buffer stream were connected via a stainless-steel T-piece (Unimed SA, Lausanne, Switzerland), which was customized with a 27 G needle for lipid injection. Different flow rate combinations were applied to screen the resulting dispersions for hydrodynamic diameter (d_h) and polydispersity index (PDI) with short injection times of 1-2 s. Selected flow rates (formulation A and B: 80 and 10 mL/min, formulation C and D: 90 and 13.5 mL/min for buffer and lipid flow rate, respectively) were used to prepare four different formulations in larger scales applying injection times of 12 s (formulation A and B, yielding ≈130 mg total lipid) or 19 s (formulation C and D, yielding ≈87 mg total lipid). The dispersions were purified from alcohol and concentrated using a tangential flow filtration process (TFF) as described in [42]. Liposomes were stored in Teflon-sealed vials at 4 °C and analyzed regarding physical stability. For *in vitro* experiments, formulation A and C were labeled in a dual dye approach. FITC-Dextran 10 kDa was dissolved to 10 mg/mL in the injection buffer to label the aqueous liposomal core. The liposomal bilayer was stained by adding 0.1 mol% Liss-Rhod-PE to the alcohol stock solution. Labeled liposomes were purified by tangential flow filtration as described above.

Table 1: Theoretical molecular lipid compositions (mol%) of differently PEGylated and charged formulations A-D.

formulation	DMA-PEG-G5	DMA-G5	DPPC	CHOL	DSPE-mPEG	DPPG
A	1.0	-	59.4	34.7	5.0	-
B	-	1.0	59.4	34.7	5.0	-
C	1.0	-	59.4	34.7	-	5.0
D	-	1.0	59.4	34.7	-	5.0

3.2. Liposome characterization

Liposomal mean hydrodynamic diameter (d_h) and PDI were measured by dynamic light scattering using the DynaPro Plate Reader II (Wyatt, Santa Barbara, CA, USA) in a 96-half-well plate (#3679, Corning Inc., Corning, NY, USA). Liposomes were diluted with DPBS in triplicate wells to 3 % (v/v) of the initial lipid concentration to diminish influence of alcohol on measurement and to obtain dispersions with suitable turbidity (normalized intensity: 10^7-10^9 counts/s) for dynamic light scattering. Laser power and attenuation were determined automatically. 100 µL sample per well were equilibrated at 25 °C, rested for 5 min, and data was acquired over 10 acquisitions with each 5 s. Data was processed with Dynals cumulants analysis (Dynamics V7.1.7), results of each well were averaged.

Zeta potential was determined by laser Doppler electrophoresis (Malvern Zetasizer Nano ZS, Worcestershire, UK). 30 µL liposomal sample were diluted in 970 µL 10 mM NaCl (resulting sample pH: 7.4) and filled into a capillary cell (DTS1070). The sample was equilibrated at 25 °C for 1 min, after which zeta potential was measured with minimum 10 runs and automatic attenuation and voltage selection. Typical conductivity and count rate were between 1-2 mS/cm and 60-400 kcounts/s. Data was analyzed using Smoluchowski model, three measurements per sample were averaged.

Pentaglycine and further lipid quantification was performed using an rp-HPLC-ELSD chromatographic method as described in [42]. FITC-dextran content was determined by fluorimetry (M200 plate reader, Tecan Group, Männedorf, Switzerland) after lysis of the liposomes with Triton X-100.

3.3. Ligand conjugation, monitoring of transpeptidation and final purification

Sortase-A variant SrtA7m was used to promote transpeptidation between LPETG-modified single-domain antibodies and pentaglycine-modified liposomes. To investigate reaction kinetics, liposomes (100 µM, based on pentaglycine content) were mixed with 5-50 µM VHH ENH, 25 µM Sortase-A and incubated at 4 or 37 °C over 14 h. Reaction was monitored in 30 min intervals by an rp-HPLC-based method that separated Sortase-A and unbound VHH from lipid-modified VHH and further liposomal components. This method utilized an Aeris Widepore column (stationary phase: C4, particle size: 3.6 µm, dimensions: 100 mm x 2.1 mm, manufacturer: Phenomenex, Torrance, CA, USA). Eluent A was 0.1 % TFA in water, eluent B 0.05 % TFA in acetonitrile. Eluent profile started with 95 % of eluent A with a gradient phase to 45.5 % A (5.5 min), followed by a shallow gradient phase to 18.5 % eluent A (15.0 min), a steep shift to 5 % eluent A until 18.0 min, followed by a flushing step at initial conditions until 27.5 min.

5 µL of the reaction mixture were injected and analyzed for the reaction product using UV-detection at 280 nm. Conversion rate was calculated according to Equation 1, where t_i is the timepoint of interest, $A_{conjugate}$ the peak area of the conjugate and A_{VHH} the peak area of the native VHH at the initial concentration (c_0) at the start of reaction. No relevant shift in UV-absorption coefficient by the lipid modification was observed. All reactions were monitored in triplicate. Statistical analysis (One-Way Anova, all pairwise multiple comparison procedures using the Holm-Sidak method) was conducted for 14 h values of all recorded reaction kinetics and showed significant differences ($p < 0.05$) for all combinations.

Equation 1

$$conversion\,[\%]\;at\;t_i = \frac{A_{conjugate}(t_i)}{A_{VHH}(c_0)} * 100$$

To verify the reaction product by mass spectrometry, the method was transferred to a similar HPLC system equipped with an ESI-MS (amaZon SL, Bruker Corporation, Billerica, Massachusetts, USA). Ion source type was set to ESI with positive polarity. Capillary exit was 140 V, trap drive was set to "94". The mass range mode was set to enhanced resolution, with a scanning range from 100-2200 m/z. 5 spectra were averaged per run and the molecular masses were determined by deconvolution.

Absolute concentrations of VHH on the liposomes were determined from the conjugate peak area and a calibration curve based on unmodified VHH (4 point, 5-50 µM, $R^2 = 0.999$). Liposome count per volume was estimated from lipid content, an average lipid headgroup area of 0.6 nm^2, a bilayer thickness of 5 nm, the hydrodynamic diameter and the assumption of spherical, unilamellar liposome appearance [44].

To evaluate Sortase-A concentration influence on reaction, 30 µL of 10 µM VHH ENH, liposomes (100 µM of pentaglycine lipid) and various concentrations of Sortase-A were incubated in DPBS for 4 h at 4 °C. The reaction was stopped by addition of 15 µL 1 N HCl as described by Kruger et al. [45]. Effective suppression of transpeptidation was tested by spiking equal amounts of HCl to the reaction mixture prior to Sortase-A addition. No enzyme activity was found at these conditions (pH < 1.0). Conversion extent was determined based on the peak area at 280 nm of 6.66 µM VHH ENH.

For *in vitro* experiments, liposomes were incubated with either 50 µM of non-binding isotype control VHH ENH ("ENH-liposomes") or human CD11b binding VHH BMX1 ("BMX1-liposomes") and 25 µM Sortase-A for 4 h at 4 °C. Liposomes for *in vitro* experiments were purified from unbound VHH and Sortase-A by dialysis (Float-A-Lyzer, MWCO 1000 kDa, G235037, Spectrum

Labs, Los Angeles, CA, USA) against 100-200fold acceptor medium (DPBS) with three buffer changes over 24 h.

3.4. Liposomal antigen capturing

The four liposomal types (Scheme 2) with differently accessible pentaglycine motif were incubated (100 µM pentaglycine lipid) with 50 µM VHH ENH and with or without 25 µM Sortase-A for 4 h at 4 °C to assess the effect of covalent, Sortase-A mediated VHH conjugation compared to a potential passive VHH adsorption. After dialysis and lipid quantification, 1 mM liposomes (based on total lipid content) were mixed with 15 µM eGFP (enhanced green fluorescent protein) and incubated for at least 30 min. Liposome-eGFP mixture was then separated by analytical size exclusion chromatography based on a method published earlier [46] utilizing a Tosoh TSKgel PWxL G4000 (length: 30 cm, diameter: 7.8 mm, particle size: 10 µm). Column temperature was set to 25 °C, eluent was the liposomal medium buffer DPBS pH 7.4, flow rate was 0.6 mL/min and the overall run time 30 min. eGFP was detected using a fluorescence detector (Agilent Technologies, Santa Clara, California, USA) with excitation set to 494 nm, emission 510 nm and gain of photomultiplier tube set to 8. Chromatograms were merged to visualize differences in eGFP binding.

3.5. Cell culture and *in vitro* binding

hPBMCs were obtained from remainders of blood donations from healthy volunteers. Written consent was obtained from all donors. Human whole blood leukocytes were isolated by lysis of red blood cells. 1 mL of blood was incubated with 9 mL ACK lysis buffer (Thermo Fisher Scientific, #A1049201) for 5 min at room temperature and centrifuged for 5 min at 300 × g. The pellet was resuspended in FACS buffer (1 × PBS with 2 % heat-inactivated fetal bovine serum (Life Technologies, #10270106) and cells were counted after pipetting through cell strainer (Corning, #352350).

For FACS binding experiments, 0.5×10^6 cells were seeded in a total volume of 200 µL complete RPMI: RPMI1640 medium (Life Technologies, #21875-034) supplemented with 10 % heat-inactivated fetal bovine serum, 100 U/mL penicillin (Life Technologies, #15140122), 100 µg/mL streptomycin (Life Technologies, #15140122), 1 mM sodium pyruvate (Life Technologies, #11360070), 50 µM 2-mercaptoethanol (Life Technologies, #31350-010), and 1 × non-essential amino acids (Life Technologies, #11140-035). 100 µM liposomes (based on total lipid content of FITC- and rhodamine-labeled formulation A and C, either as pentaglycine-coated control, VHH ENH-coated or VHH BMX1-coated sample) were added to each sample in V-bottom-shaped 96-well plates and incubated at 37 °C for 4 h in the presence of 5 % CO_2. Medium containing

unbound liposomes was removed by centrifugation (300 × g for 1 min) and cells were washed with FACS buffer. Antibody staining of cells was performed in presence of Fc receptor block (TruStain fcX BioLegend, #422302) in FACS buffer. SytoxBlue (Thermo Fisher Scientific, S34857) was used for exclusion of dead cells. Following antibodies from BioLegend were used for flow cytometry: allophycocyanin (APC)-Cy7-anti-CD14 (#325620) or APC-anti-CD15 (#323008) or biotin-anti CD3 (#317320) or biotin-anti-CD19 (#302203) and streptavidin-APC (#405207) for biotin-conjugated antibodies.

3.6. Confocal microscopy

For confocal microscopy, 0.5×10^6 cells were seeded in a total volume of 200 µL complete RPMI. 100 µM liposomes were added to each sample in V-bottom-shaped 96-well plates and incubated at 37 °C for 4 h in the presence of 5 % CO_2. Cells were stained with CellMask Deep Red Plasma membrane stain (1:5000) (Life Technologies, #C10046) and Hoechst 33342 (1:2000) (Thermo Scientific, #62249) for 15 min at 37 °C in the presence of 5 % CO_2. The medium was removed by centrifugation (1 min at 300 × g), cells washed with FACS buffer and transferred in 100 µL FACS buffer on polyethyleneimine-coated cover slips (microscope cover glasses from Marienfeld, 18 mm diameter, #0117580) and incubated for 10 min at 37 °C. Cells were fixed on cover slips with paraformaldehyde (final concentration 4 %) for 15 min. Cover slips were washed with 1fold PBS and mounted on cover glass (neoLab, #1-6273) using anti-fade ProLong Diamond mounting medium (Invitrogen, #P36961). The cells were analyzed after 18 h with a Leica TCS SP5 confocal microscope using HCX Plan APO 40 × /1.30 Oil CS objective. For image analysis Leica Application Suite software was used.

4. Results and discussion

4.1. Liposomal formulation development

Adapting a continuous solvent injection technique, differently PEGylated and pentaglycine-modified liposomes (Table 1, Scheme 2) in comparable size ranges were prepared as substrates for kinetic investigations. The formation of liposomes via solvent injection is based on a solvent-antisolvent mixing process followed by a self-assembly [41] of the lipids in an aqueous buffer. Therefore, this technique requires a complete solution of lipid excipients in a water miscible organic solvent to ensure homogenous lipid distribution upon liposome formation. Major lipids DPPC, cholesterol and DSPE-mPEG (formulation A and B) were well soluble in ethanol. DPPG has low solubility in alcohols and limited the choice of solvents for formulation C and D to methanol with a maximum total lipid concentration of 32 mM. DMA-PEG-G5 easily dissolved in aforementioned solvents. Due to its limited solubility, non-PEGylated DMA-G5 was spiked from

a DMSO stock solution to the alcoholic solutions of major lipids prior solvent injection. No precipitation was observed before the solvent injection procedure as analyzed by visual inspection with cold light.

To obtain liposomes with different degree of PEGylation and pentaglycine accessibility (Scheme 2), but comparable physical properties such as d_h and PDI, d_h was screened for formulation A-D by flow rate alteration (Table 2).

Table 2: Flow rate screening. Different combinations of flow rates during solvent injection were screened to obtain liposomes with comparable hydrodynamic diameter and polydispersity (mean ± standard deviation shown for different solvent injections).

formulation	flow rate buffer	flow rate lipid	$C_{lipid\ dispersion}$	production rate	d_h	PDI	reps
	[mL/min]	*[mL/min]*	*[mM]*	*[g/h]*	*[nm]*	*A.U.*	
A	40	5.00	10.0	20	200 ± 20	0.18 ± 0.03	n=4
	80	10.00	10.0	40	149 ± 7	0.22 ± 0.01	n=4
	100	12.50	10.0	50	132 ± 11	0.24 ± 0.01	n=4
	150	12.50	6.9	50	125 ± 2	0.23 ± 0.00	n=4
	180	12.50	5.8	50	106	0.24	n=1
B	40	5.00	10.0	19	200 ± 18	0.21 ± 0.01	n=3
	80	10.00	10.0	39	150 ± 6	0.23 ± 0.01	n=3
	100	12.50	10.0	48	137 ± 3	0.23 ± 0.01	n=3
	150	12.50	6.9	48	126 ± 7	0.24 ± 0.00	n=3
C	45	6.75	4.2	8	230 ± 20	0.22 ± 0.01	n=4
	90	13.50	4.2	16	180 ± 3	0.20 ± 0.02	n=4
	135	13.50	2.9	16	163 ± 13	0.19 ± 0.01	n=4
	180	13.50	2.2	16	153	0.19	n=1
D	45	6.75	4.2	8	188 ± 21	0.18 ± 0.06	n=4
	90	13.50	4.2	16	145 ± 13	0.18 ± 0.02	n=4
	135	13.50	2.9	16	130 ± 3	0.19 ± 0.02	n=4
	180	13.50	2.2	16	95	0.19	n=1

Increase of the total flow rate with constant flow rate ratio of buffer-to-lipid = 8 (formulation A) led to subsequent decrease of the d_h down to 125 nm while maintaining acceptable PDIs < 0.25 (Table 2). Further increase of the buffer flow decreased the d_h to ≈100 nm, previously found as most suitable liposome size for *in vivo* tumor targeting with liposomes [47]. This decrease is due to an increased shearing and turbulence at the injection site [41]. The lipid concentration after injection was 10 mM for formulation A, representing a high value compared to other reports on liposome production by solvent injection [41, 48]. The lipid concentration after injection is an important factor to consider for the encapsulation of hydrophilic compounds. Here, the encapsulation efficacy is mainly determined by the volume ratio of the aqueous liposome interior to the surrounding buffer. This ratio is determined by the liposome diameter and the lipid concentration. Hence, high lipid concentrations after liposome formation are favorable for efficient cargo encapsulation. The production rate ranged for formulation A and B from 19-50 g/h (Table 2). In solvent injection processes, the production rate is dependent on the

injection speed and the concentration of the lipid solution. Although this rate can impact the final process duration, it should be kept in mind that during large-scale preparations other downstream processes (like tangential flow filtration with a low filtration rate [49]) may determine the absolute production rate. Formulation A and B were prepared with similar size distributions, indicating minor influence of the different pentaglycine lipids, probably due to the low fraction in the bilayer of 1 mol%.

Due to the limited solubility of DPPG, formulation C and D had an overall lower final lipid concentration and production rate. Thus, lipid flow was set to the maximum pump rate of 13.5 mL/min for small (2-5 mL) syringes in most experiments. Interestingly, a high influence of the PEGylated pentaglycine lipid on mean size was observed for formulation C. The d_h of formulation C was 30-50 nm larger compared to the non-PEGylated formulation D (Table 2), although other parameters (solvent, lipid concentration, flow rates) were similar. A comparable 1.9 kDa PEG-group was previously reported to increase the d_h of liposomes by 3-15 nm after a post insertion processes, depending on the bilayer fraction and further experimental conditions [50]. In the present study, not only the PEG-group, but also the pentaglycine group (0.375 kDa) may contribute to the extension of the d_h.

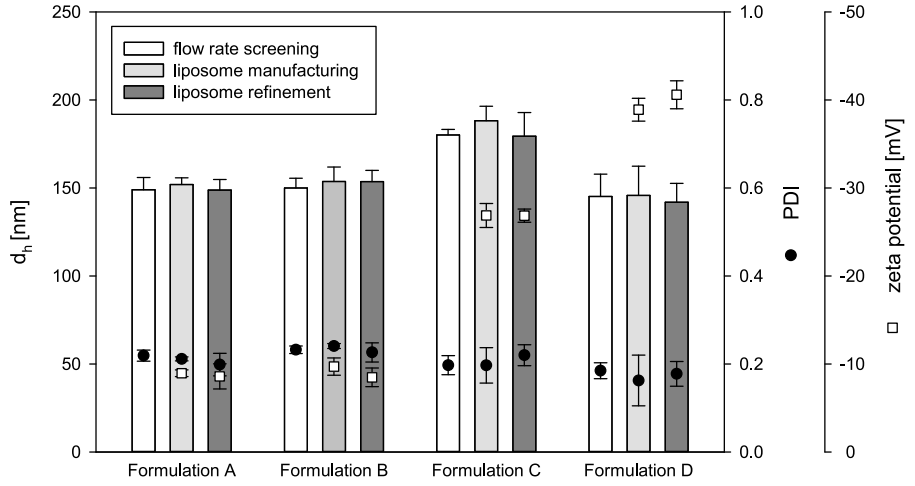

Figure 1: Predictivity of flow rate screening experiments towards manufacturing of the pentaglycine-modified liposomes. Flow rates yielding comparable d_h and PDI in the screening were applied to prepare formulations A-D in larger scale. DLS confirmed the screening results for larger scale manufacturing with mean sizes between 150 nm and 180 nm. Furthermore, subsequent purification and concentration utilizing tangential flow filtration did not alter size, PDI or zeta potential of the formulations (data shown as mean ± standard deviations of three experiments).

Flow rates predicting comparable d_h and PDI were selected with respect to final lipid concentration from screening experiments and applied to prepare formulations A-D in a larger scale. Similar d_h and PDI were obtained in screening and larger scale preparation (Figure 1), indicating predictivity of the screening experiment. Tangential flow filtration was used to concentrate and purify the dispersion from residual alcohol. No relevant changes of physical properties (size, PDI, zeta potential) occurred over the process (Figure 1). Zeta potential was

≈-10 mV for formulation A and B, and distinctly more negative for formulation C (-27 mV) and D (-40 mV) due to the anionic stabilizer DPPG.

The bilayer composition was analyzed by rp-HPLC-ELSD and did not show relevant changes over TFF processing (Table 3). Most important, the pentaglycine lipids showed sufficient bilayer anchorage, maintaining their bilayer fraction of 1 mol%. Physical stability of the four pentaglycine-modified formulations was investigated over 8 weeks at 2-8 °C. As result, neither d_h, PDI nor zeta potential showed relevant changes over time (Figure 2).

Table 3: Bilayer compositions after tangential flow filtration, determined by rp-HPLC-ELSD (mean ± standard deviations shown for three batches).

formulation	G5 lipid [mol%]	CHOL [mol%]	DPPC [mol%]	DSPE-mPEG / DPPG [mol%]
theoretical	*1.0*	*34.7*	*59.4*	*5.0*
A	1.0 ± 0.1	33.5 ± 0.5	61.1 ± 0.5	4.4 ± 0.2
B	1.0 ± 0.1	33.7 ± 1.3	60.1 ± 0.9	5.2 ± 0.7
C	1.0 ± 0.0	33.9 ± 1.1	60.4 ± 0.8	4.7 ± 0.4
D	1.0 ± 0.1	33.9 ± 1.7	60.5 ± 1.0	4.6 ± 0.7

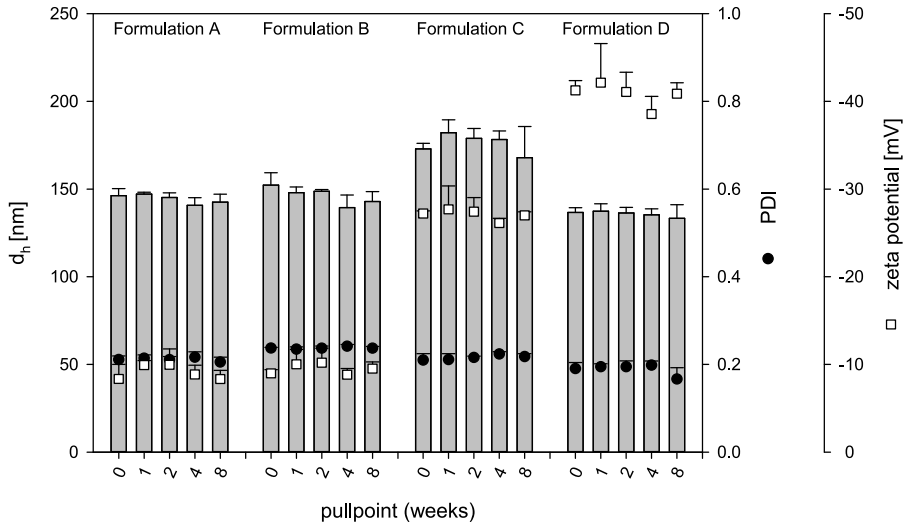

Figure 2: Physical stability (size, PDI and zeta potential) of pentaglycine-modified liposomes over an 8 weeks storage at 2-8 °C (mean ± standard deviations shown for three batches).

4.2. Investigation of reaction kinetics on liposomes

We monitored the conjugation of a model VHH (VHH ENH) towards differently PEGylated liposomal formulations (Scheme 2) over 14 h by rp-HPLC (Figure 3A). ESI-MS confirmed the calculated theoretical molecular masses for the PEGylated or non-PEGylated lipid-modified antibody structure (Figure 4A and B). Low reaction efficacies (< 10 %) were found for a pentaglycine motif hidden by surrounding PEG-groups (Figure 3B, formulation B). Formulation D, lacking the shielding PEG-groups, had a higher steric accessibility of the bilayer-proximal nucleophile and showed an increased conversion extent of ≈15 % after 4 h. In contrast, both formulations equipped with the PEG-spaced pentaglycine showed much higher reaction

rate and overall reactivity, reaching educt conversion of 40 ± 1 % (formulation A) or 33 ± 3 % (formulation C) after 4 h. This is probably due to the increased steric accessibility of the pentaglycine moiety towards Sortase-A, and a higher degree of freedom through the flexible PEG-spacer. This might enable conformational changes that facilitate the access of the amino-function to the thioester intermediate at the active site.

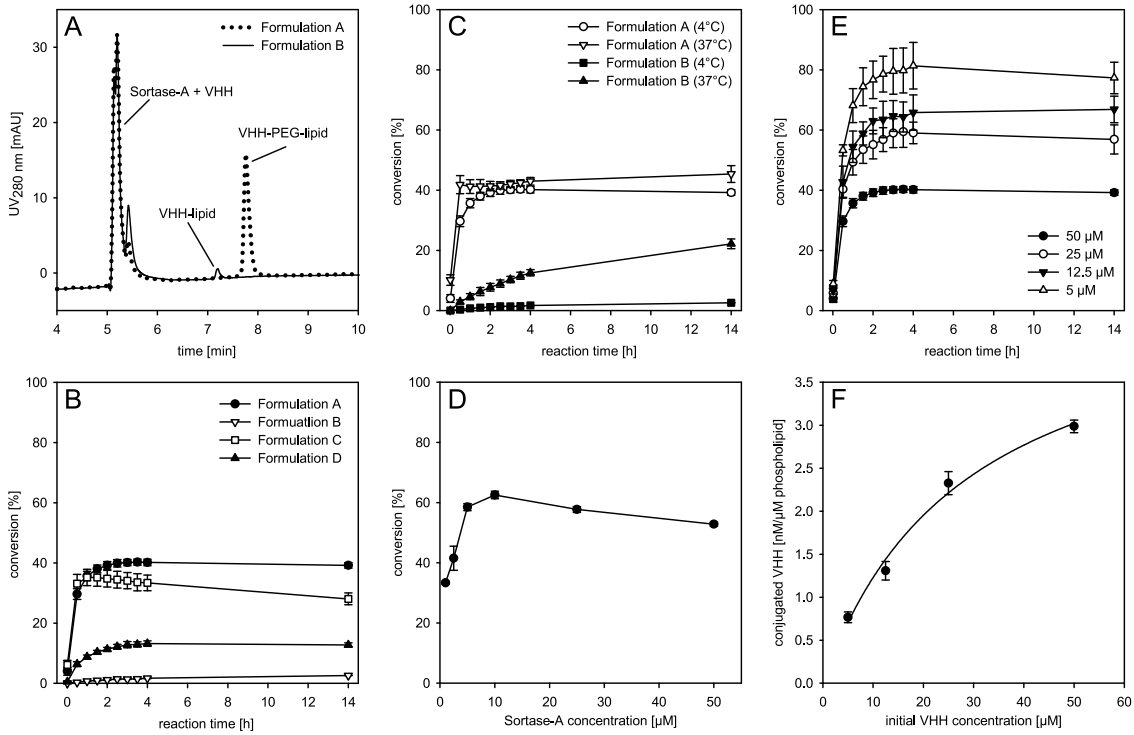

Figure 3: **A**: Representative rp-HPLC chromatograms of DMA-G5 (solid line)- or DMA-PEG-G5 (dotted line)-modified, PEGylated liposomes after 14 h incubation with 50 µM VHH ENH and 25 µM Sortase-A. **B**: Influence of PEGylation status on Sortase-A reaction kinetics (100 µM pentaglycine, 50 µM VHH ENH and 25 µM Sortase-A, 4 °C). **C**: Influence of temperature on reaction kinetics of PEG-shielded (formulation B) or exposed (formulation A) pentaglycine motifs (100 µM pentaglycine, 50 µM VHH ENH and 25 µM Sortase-A). **D**: Optimization of Sortase-A concentration (100 µM pentaglycine of formulation A, 10 µM VHH ENH, 4 °C). After 4 h, reaction was stopped by HCl and the dispersion analyzed for the reaction product. **E**: Optimization of targeting ligand reaction efficacy (100 µM pentaglycine of formulation A, 25 µM Sortase-A, 4 °C). **F**: Calculated ligand density on the drug delivery system based on conversion data (4 h) of experiment in 6E. All data: mean ± standard deviation of three experiments.

Interestingly, the fully PEGylated formulation A showed slightly higher conversion rate and extent than formulation C. This may be explained by the observation of Silvius et al. [23], who showed that bilayer-immobilization of Sortase-A drastically enhanced the reaction efficacy compared to soluble Sortase-A . We observed unspecific binding of Sortase-A towards PEGylated liposomal bilayer surfaces, indicated by Sortase-A residuals after a dialysis step (Figure 5). This may lead to an increased conversion rate and extent for formulation A, comparable to Silvius et al. [23]. Whether attraction of Sortase-A towards the PEGylated formulations is due to an interaction with PEG or electrostatics remains unclear. As the zeta potential of formulation A and C distinctly differ from each other by ≈17 mV, charge may also be a reason for Sortase-A interaction with PEGylated formulations.

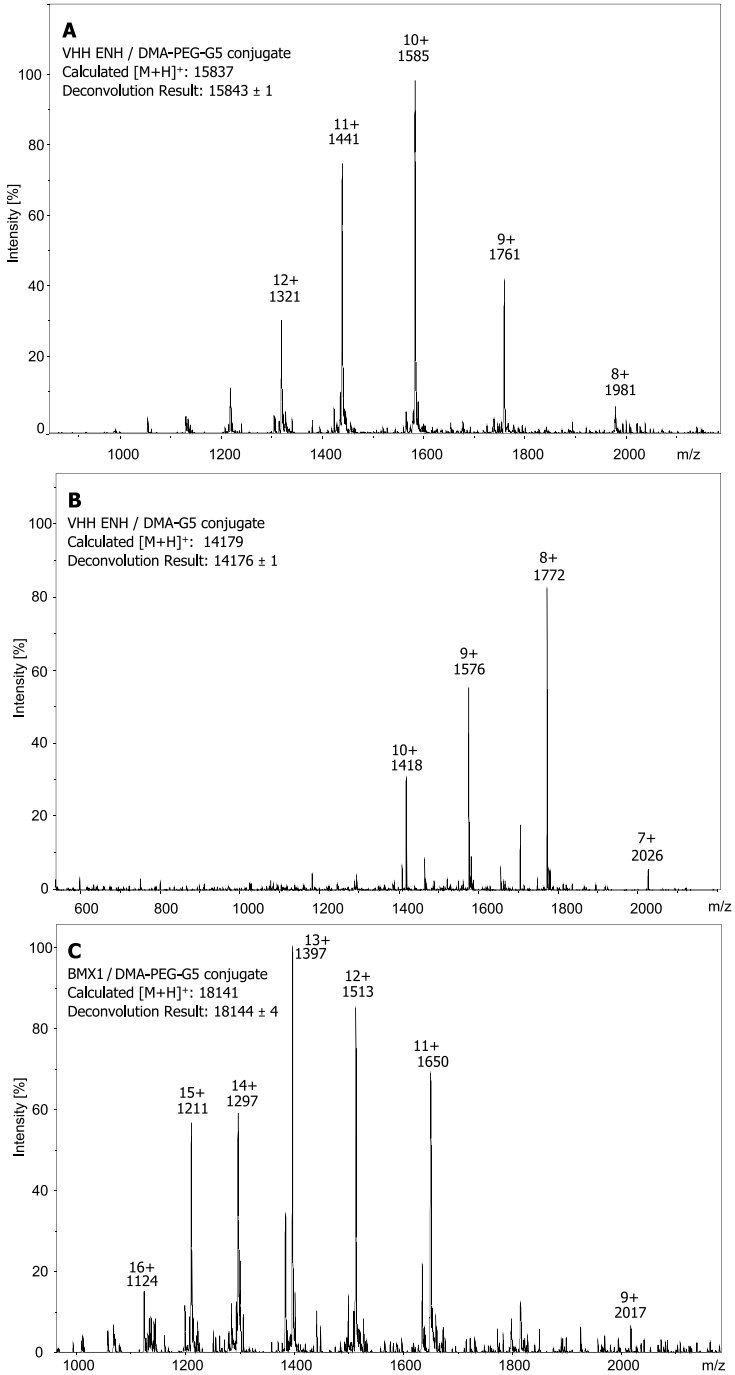

Figure 4: Confirmation of conjugation products by ESI-MS. Target mass was calculated as native VHH mass plus lipid mass minus mass of the his-tag cleaved from the native VHH during transpeptidation (GGH_6, 955 Da). **A**: Conjugate of VHH ENH (14237 Da) and DMA-PEG-G5 (2554 Da). **B**: Conjugate of VHH ENH and DMA-G5 (897 Da). **C**: Conjugate of BMX1 (16541 Da) and DMA-PEG-G5.

Formulation C showed a tendency for the reverse reaction, indicated by a decrease of the conjugate product after 14 h. The reverse reaction occurs after a re-recognition of the newly formed $LPETG_5$-motif between VHH and lipid anchor by Sortase-A. Subsequently, a thioester is formed and hydrolyzed through the attack of a water molecule as alternative nucleophile [18]. It was concluded that the higher degree of flexibility of the PEG-pentaglycine in formulation C compared to A leads to a higher accessibility of the LPETG-motif after transpeptidation, and therefore a higher rate of the reverse reaction.

Negligible impact of temperature was previously described for Sortase-A variant SortA7m [40]. Low reaction temperature of 4 °C was therefore chosen as standard condition to reduce overall impact on the liposomes and their potentially labile cargos. However, to overcome low reactivity of PEG-shielded pentaglycine-motifs, the impact of temperature (namely an increase from 4 °C to 37 °C) on the conversion extent (Figure 3C) was analyzed. Interestingly, in case of a freely accessible nucleophile (formulation A), slight increase in conversion rate, but low impact on final VHH conversion over 14 h was observed. Formulation B showed a drastic increase in reaction efficacy by increase of temperature. This effect can be attributed to a higher accessibility of the hidden pentaglycine motif to the active site of the enzyme due to a higher mobility of the PEG-groups. Their decreased viscosity at elevated temperature may lead to a less rigid shielding layer of the pentaglycine-coated bilayer surface, therefore increasing overall conversion over time. This effect might enable manufacturing of multi-layered liposomes by integration of additional DMA-G5 lipid in formulation A. One could firstly saturate an outer layer of PEG-spaced glycine motifs at low temperature and subsequently modify a PEG-shielded nucleophilic layer by increasing temperature. This would add a further dimension of selectivity towards enzyme-mediated bilayer modification.

Sortase-A concentration was evaluated between 1-50 µM for the reaction of 10 µM VHH ENH to formulation A (Figure 3D). Optimal conversion was found for 10 µM Sortase-A. At higher concentrations, decreasing conversion extents were observed. A possible reason may be an increased reverse reaction over the 4 h incubation time, indicating that increased enzyme concentrations require decreased incubation times.

Initial VHH concentration was evaluated between 5-50 µM (Figure 3E). Increased conversion up to 80 % was achieved with a decrease of VHH concentration. This can be explained by the higher ratio of the nucleophile pentaglycine to the electrophilic thioester intermediate of the Sortase-A-VHH complex. Interestingly, the higher standard deviations observed with decreasing VHH concentrations hint at a less uniform reaction process. This might be explained by a heterogeneous educt distribution during the reaction due to slow diffusion at low temperatures and indicate the need for stirring during conjugation.

The ligand density on the liposomal surface is an important parameter for an efficient targeting effect. Furthermore, it plays a critical role for the colloidal stability and also determines the drug-to-ligand ratio. Here, ligand density could be controlled by variation of the initial VHH concentration (Figure 3F). The density ranged from 0.6-3 nM ligand per µM phospholipid, corresponding to 110-430 VHHs per liposome. This covers a ligand density previously described as suitable for the targeting of immunoliposomes to raji cells [51].

4.3. Purification from Sortase-A and target binding

Pentaglycine-modified formulations were sortagged with VHH ENH and purified by dialysis. Samples incubated without Sortase-A served as controls. DLS and LDE (Table 4) indicated physical stability over the reaction although a slight increase in PDI of formulation B was observed. Furthermore, conjugated samples had a slightly less negative zeta potential, probably due to the charge of the conjugated VHH ENH. As described above, PEGylated formulations A and B tended to bind a much higher amount of Sortase-A which was thus not removed by the dialysis process (Figure 5).

Table 4: Physicochemical properties of liposomes after ligand conjugation and dialysis (with / without Sortase-A, data shown as mean ± standard deviation of three measurements).

formulation	d_h [nm]	PDI	zeta potential [mV]
A	143 ± 2 / 151 ± 1	0.23 ± 0.00 / 0.22 ± 0.01	-7.0 ± 0.2 / -8.5 ± 0.2
B	146 ± 6 / 161 ± 2	0.32 ± 0.06 / 0.24 ± 0.00	-7.4 ± 0.3 / -8.6 ± 0.8
C	174 ± 2 / 173 ± 2	0.23 ± 0.01 / 0.22 ± 0.01	-18.3 ± 1.2 / -26.3 ± 1.7
D	139 ± 1 / 138 ± 1	0.19 ± 0.01 / 0.20 ± 0.02	-32.8 ± 1.7 / -40.0 ± 2.2

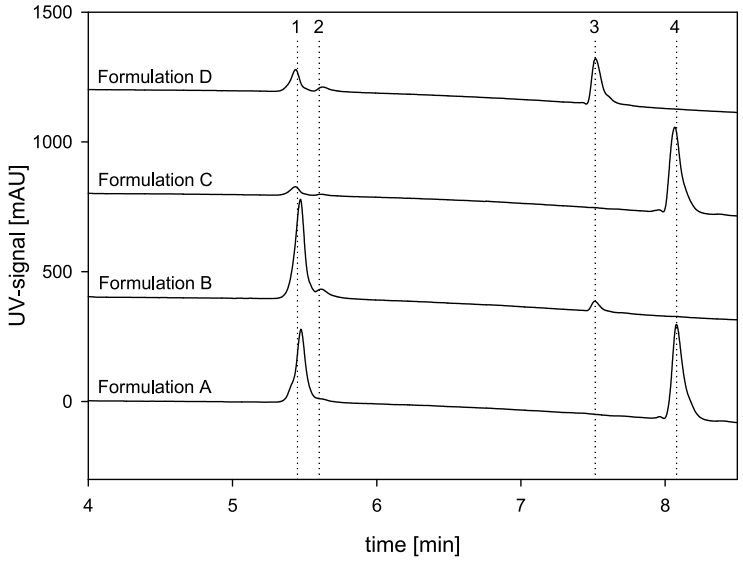

Figure 5: Effectivity of Sortase-A removal by dialysis. Formulations A-D were incubated with 50 µM VHH ENH and 25 µM Sortase-A and purified by dialysis (cut-off: 1000 kDa) overnight with 3 buffer changes. Substantial residuals of Sortase-A (peak 1) and, to a minor degree, native VHH (peak 2) were found by rp-HPLC analysis in the PEGylated formulations A and B. Furthermore, PEGylation and spacer dependent conversion efficacy is obvious when peak areas of non-spaced (peak 3) and PEG-spaced (peak 4) VHH-lipid conjugate are compared.

This interaction may be a critical factor influencing stability of the targeted system as Sortase-A is known for pronounced reverse reaction [18], which would cleave the targeting ligand from the liposome during storage. Additionally, liposome associated Sortase-A is likely to act as a strong immunogen, since it is derived from *Staphylococcus aureus*, a widespread pathogen bacterium. Traces of this protein may lead to serious adverse events like allergic reactions, antibody-formation against the drug delivery system or in worst case, fatal anaphylactic shocks. Initial evaluations revealed that up to 6.0 µM of Sortase-A remained in formulation A after

dialysis. Improvement of Sortase-A purification from liposomal drug carriers is therefore required to ensure a safe application to patients, and is currently under investigation with regard to the liposomal surface properties.

To investigate the ability of the immunoliposomes to bind towards antigens, the VHH ENH-modified dispersions were incubated with the target protein eGFP. Free eGFP and liposomes were separated by analytical size exclusion chromatography (Figure 6) and analyzed by fluorescence detection.

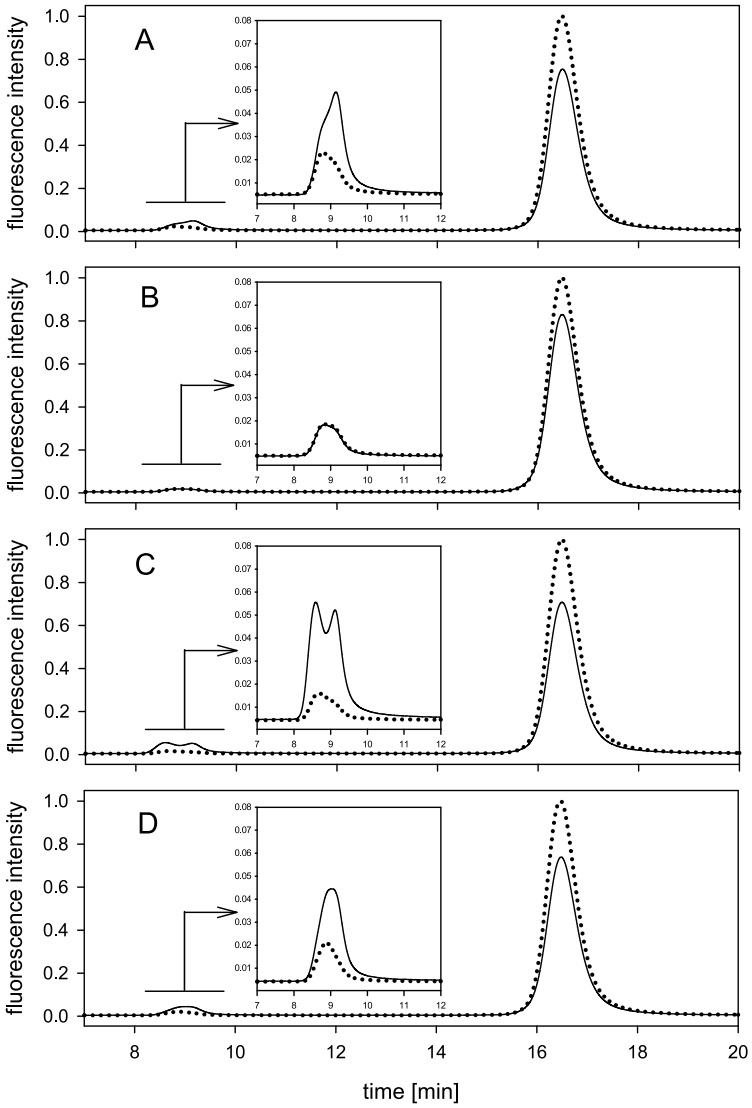

Figure 6: Binding of eGFP to VHH ENH-modified liposomes. Liposomes (1 mM total lipid) precedingly incubated with VHH ENH and with (solid) or without (dotted) 25 µM Sortase-A were mixed with 15 µM eGFP and separated by size exclusion chromatography. Increase of liposome peak intensity (8-10 min) as well as decrease of free eGFP fluorescence (15-18 min) indicates eGFP binding to the formulations. Formulation A-D as assigned in chromatograms.

Although sole presence of unmodified liposomes in the fluorescence detector caused background noise, probably through light scattering effects, a clear increase in fluorescence of the liposome peak was found for the sortagged liposomes for formulation A, C and D. Hardly any increase was observed for formulation B, reflecting the lower reactivity of the PEG-shielded

nucleophile, though height of free eGFP peak of formulation B was decreased for sortagged liposomes. This should consequently indicate a binding towards the sortagged liposome higher than for the control formulation. VHH ENH is known to enhance the intrinsic fluorescence of eGFP [43]. Higher amounts of residual, unbound VHH ENH in the control formulation might therefore have led to increased fluorescence intensities of free eGFP. These considerations hamper the use of this assay for absolute quantification of ligand activity on the liposomes. However, if one can work with a ligand-target system without mutual influence on the fluorescence intensity, such as other fluorescent proteins or fluorophore-labeled target proteins, the presented SEC method might serve as convenient quantitative tool for liposome-target protein interaction studies.

4.4. *In vitro* targeting of myeloid cells

Formulation A and C were investigated regarding their ability to bind *in vitro* towards a relevant target, namely CD11b$^+$ human myeloid cells. For that purpose, both bilayer and liposomal core were stained with fluorescent dyes. Encapsulation efficiency of FITC-dextran 10 kDa was determined by fluorimetry after TX-100 lysis and was < 1 % for both formulations, indicating a complete passive encapsulation during solvent injection without any specific bilayer interaction. Liss-Rhod-PE content was analyzed after TFF and maintained its molar fraction of 0.1 mol%. Dye-labeled formulations were modified with VHH BMX1, a VHH binding CD11b (Supplementary Figure 1), or with VHH ENH as isotype control. Staining and ligand conjugation had no influence on physicochemical properties of the liposomes. Furthermore, liposomes were physically stable for 4 weeks (Supplementary Table 1). Mass spectrometry showed successful conjugation of VHH BMX1 towards the lipid anchor molecule DMA-PEG-G5 (Figure 4). hPBMCs were collected from the buffy coat of blood donations from healthy donors. Subsequent co-staining of surface receptors for T cells, B cells, monocytes and granulocytes enabled a simultaneous assessment of targeting feasibility and specificity. According to the CD11b expression (CD11b is expressed on myeloid-derived CD14$^+$ granulocytes and CD15$^+$ monocytes, but not on lymphoid-derived CD3$^+$ T cells and CD19$^+$ B cells), we found specific targeting towards CD14$^+$CD11b$^+$ and CD15$^+$CD11b$^+$ cells (Figure 7). Neither isotype control VHH ENH nor unmodified liposomes bound to a relevant extent. It is difficult to estimate from the current data whether the fully PEGylated formulation A or minimally PEGylated formulation C (by the PEG-spacer between ligand and bilayer) showed different behavior in binding. There might be a trend for a higher interaction of formulation C, indicated by stronger shifts in FACS analysis. This could be reasoned in the overall decreased unspecific uptake of PEGylated particulate systems [26].

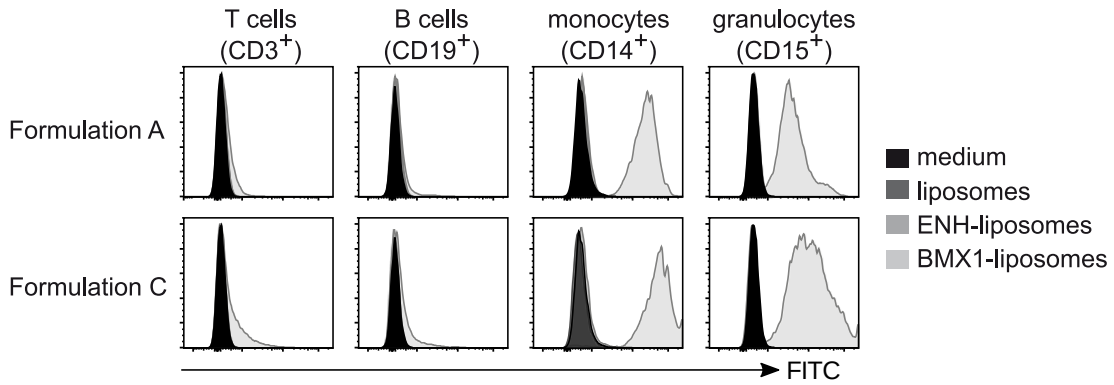

Figure 7: Targeting of CD11b⁺ myeloid cells. FITC-labeled formulation A and C were incubated with hPBMCs. FACS analysis of $CD3^+CD11b^-$ (T lymphocytes), $CD19^+CD11b^-$ (B lymphocytes), $CD14^+CD11b^+$ (monocytes) and $CD15^+CD11b^+$ (granulocytes) cells revealed selective binding of VHH BMX1-modified liposomes towards the $CD11b^+$ mono- and granulocytes.

Confocal microcopy revealed a selective staining of the cells (Figure 8) only by BMX1-liposomes with intracellular aggregations of liposomes (Supplementary Video 1 and 2). Co-localization of liposome-labels Liss-Rhod-PE (liposome bilayer) and FITC-dextran (liposome core / cargo) showed internalization of intact liposomes. These focal spots of intact liposomes rather than confluent FITC-fluorescence over the cytosol may indicate the necessity to improve the intracellular cargo release in further formulation developments. However, as focus of this work was the investigation of reaction conditions and proof of concept for targeting feasibility with chemoenzymatically VHH-modified liposomes, these considerations were not part of this work.

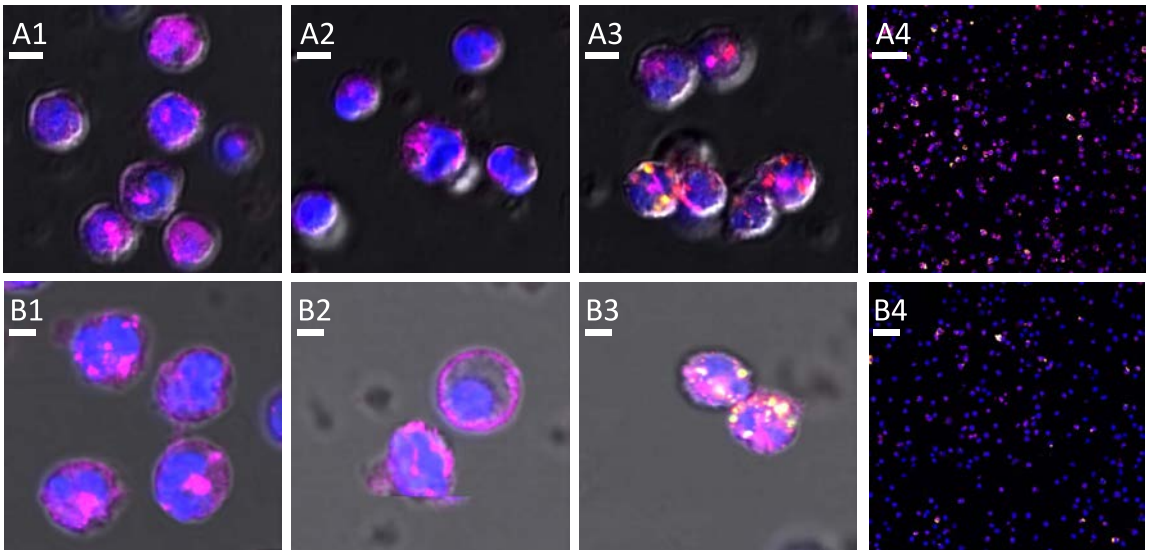

Figure 8: Confocal microscopy of hPBMCs incubated with formulation A (A1-4, upper row) and formulation C (B1-4, lower row). 1: uncoated liposomes, 2: ENH-liposomes, 3 and 4: BMX1-liposomes. Yellow and red fluorescence of liposomal core and bilayer, respectively, was solely observed on cells incubated with BMX1-liposomes (A3/4, B3/4). Co-localization of liposomal membrane dye Liss-Rhod-PE and liposome-core dye FITC-dextran indicated internalization of intact liposomes. Only selected cells were stained through the liposomes (A4 / B4). This is due to the presence of CD11b-positive and CD11b-negative cells in the hPBMC culture. Color code: yellow: liposomal core, red: liposomal bilayer, blue: nucleus, purple: plasma membrane. White scale bars: A1-3: 5 µm, A4: 50 µm, B1-3: 2.5 µm, B4: 100 µm.

5. Conclusion and outlook

In the present study, Sortase-A "conjugation-ready" or sortaggable liposomes with different surface properties like PEGylation and steric accessibility of the pentaglycine moiety were successfully prepared by solvent injection. A flow rate screening allowed us to prepare different pentaglycine formulations with comparable size distributions. This enabled us to thoroughly investigate reaction conditions and kinetics for the Sortase-A reaction with sole dependency of the liposomal surface properties. A single-domain antibody was used as reaction partner during transpeptidation, representing a promising novel class of targeting ligands for drug delivery systems. Adjusting the pentaglycine to ligand ratio improved conversion extents up to 80 %. We further found high dependency of conversion extent on the surface properties and steric accessibility of the pentaglycine, which could, in case of a PEG-shielding, be overcome by a temperature increase. This gives implications for further research on the modification of PEGylated surfaces by Sortase-A, e.g. for the manufacturing of multilayer surfaces, what may be realized by utilization of the here presented PEG-spaced and non-spaced pentaglycine lipids. The findings in this study further revealed formulation dependent effectivity of Sortase-A purification. This indicates need for a deeper investigation of liposome purification processes, since Sortase-A residuals may cause serious immunogenic reactions. Additionally, storage stability of the protein-lipid conjugate in presence of trace amounts of Sortase-A may be impaired, as the enzyme is known for its hydrolytic activity on the LPxTG recognition site.

Pharmaceutical relevance of the presented work was shown by an effective, specific binding towards CD11b$^+$ cells. CD11b is a promising cellular surface marker of myeloid cells in inflammatory or proliferative tissues. The presented drug delivery system might be used for delivery of toxic payloads or diagnostics towards the tumor microenvironment [27, 39, 40]. For this purpose, further improvements like a screening of the bilayer composition, e.g. usage of pH-sensitive or fusogenic lipids could be useful to improve intracellular release characteristics. Furthermore, investigation of liposomal surface properties, meaning degree of PEGylation as well targeting ligand density are relevant formulation parameters for improvement of *in vitro* and *in vivo* performance. With the presented work, we provide a profound and detailed basis for a further rationale formulation development of such drug delivery systems suitable for chemoenzymatic ligand modifications.

References

[1] K. Strebhardt, A. Ullrich, Paul Ehrlich's magic bullet concept: 100 years of progress, Nature Reviews Cancer, 8 (2008) 473-480.

[2] A. Beck, L. Goetsch, C. Dumontet, N. Corvaïa, Strategies and challenges for the next generation of antibody–drug conjugates, Nature Reviews Drug Discovery, 16 (2017) 315.

[3] N. Bertrand, J. Wu, X. Xu, N. Kamaly, O.C. Farokhzad, Cancer nanotechnology: The impact of passive and active targeting in the era of modern cancer biology, Advanced drug delivery reviews, 66 (2014) 2-25.

[4] P. Marques-Gallego, A.I. de Kroon, Ligation strategies for targeting liposomal nanocarriers, Biomed Research International, (2014) e129458.

[5] E. Gregory Gregoriadis, D. Neerunjun, Homing of liposomes to target cells, Biochemical and Biophysical Research Communications, 65 (1975) 537-544.

[6] G. Weissmann, D. Bloomgarden, R. Kaplan, C. Cohen, S. Hoffstein, T. Collins, A. Gotlieb, D. Nagle, A general method for the introduction of enzymes, by means of immunoglobulin-coated liposomes, into lysosomes of deficient cells, Proceedings of the National Academy of Sciences, 72 (1975) 88-92.

[7] V.P. Torchilin, V.S. Goldmacher, V.N. Smirnov, Comparative studies on covalent and noncovalent immobilization of protein molecules on the surface of liposomes, Biochemical and Biophysical Research Communications, 85 (1978) 983-990.

[8] F.J. Martin, W.L. Hubbell, D. Papahadjopoulos, Immunospecific targeting of liposomes to cells: a novel and efficient method for covalent attachment of Fab' fragments via disulfide bonds, Biochemistry, 20 (1981) 4229–4238.

[9] F.J. Martin, D. Papahadjopoulos, Irreversible coupling of immunoglobulin fragments to preformed vesicles. An improved method for liposome targeting, Journal of Biological Chemistry, 257 (1982) 286-288.

[10] C.D. Hein, X.M. Liu, D. Wang, Click chemistry, a powerful tool for pharmaceutical sciences, Pharmaceutical Research, 25 (2008) 2216-2230.

[11] L. Bourel-Bonnet, H. Gras-Masse, O. Melnyk, A novel family of amphilic α-oxo aldehydes for the site-specific modification of peptides by two palmitoyl groups in solution or in liposome suspensions, Tetrahedron Letters, 42 (2001) 6851-6853.

[12] Y. Ma, H. Zhang, X.-L. Sun, Surface-Bound Cytomimetic Assembly Based on Chemoselective and Biocompatible Immobilization and Further Modification of Intact Liposome, Bioconjugate Chemistry, 21 (2010) 1994-1999.

[13] F. Said Hassane, B. Frisch, F. Schuber, Targeted Liposomes: Convenient Coupling of Ligands to Preformed Vesicles Using “Click Chemistry”, Bioconjugate Chemistry, 17 (2006) 849-854.

[14] X. Guo, Z. Wu, Z. Guo, New method for site-specific modification of liposomes with proteins using sortase A-mediated transpeptidation, Bioconjugate Chemistry, 23 (2012) 650-655.

[15] S.A. Walper, K.B. Turner, I.L. Medintz, Enzymatic bioconjugation of nanoparticles: developing specificity and control, Current Opinion in Biotechnology, 34 (2015) 232-241.

[16] J.M. Antos, G.M. Miller, G.M. Grotenbreg, H.L. Ploegh, Lipid Modification of Proteins through Sortase-Catalyzed Transpeptidation, Journal of the American Chemical Society, 130 (2008) 16338-16343.

[17] U. Tomita, S. Yamaguchi, Y. Maeda, K. Chujo, K. Minamihata, T. Nagamune, Protein cell-surface display through in situ enzymatic modification of proteins with a poly(Ethylene glycol)-lipid, Biotechnology and Bioengineering, 110 (2013) 2785-2789.

[18] M. Ritzefeld, Sortagging: A Robust and Efficient Chemoenzymatic Ligation Strategy, Chemistry – A European Journal, 20 (2014) 8516-8529.

[19] J.E. Glasgow, M.L. Salit, J.R. Cochran, In Vivo Site-Specific Protein Tagging with Diverse Amines Using an Engineered Sortase Variant, Journal of the American Chemical Society, 138 (2016) 7496-7499.

[20] S.A. van Lith, S.M. van Duijnhoven, A.C. Navis, W.P. Leenders, E. Dolk, J.W. Wennink, C.F. van Nostrum, J.C. van Hest, Legomedicine-A Versatile Chemo-Enzymatic Approach for the Preparation of Targeted Dual-Labeled Llama Antibody-Nanoparticle Conjugates, Bioconjugate Chemistry, 28 (2017) 539-548.

[21] H. Hirakawa, S. Ishikawa, T. Nagamune, Ca2+-independent sortase-A exhibits high selective protein ligation activity in the cytoplasm of Escherichia coli, Biotechnology Journal, 10 (2015) 1487-1492.

[22] A. Tabata, N. Anyoji, Y. Ohkubo, T. Tomoyasu, H. Nagamune, Investigation on the Reaction Conditions of Staphylococcus aureus Sortase A for Creating Surface-modified Liposomes as a Drug-delivery System Tool, Anticancer Research, 34 (2014) 4521-4527.
[23] J.R. Silvius, R. Leventis, A Novel "Prebinding" Strategy Dramatically Enhances Sortase-Mediated Coupling of Proteins to Liposomes, Bioconjugate Chemistry, 28 (2017) 1271-1282.
[24] A. Tabata, Y. Ohkubo, N. Anyoji, K. Hojo, T. Tomoyasu, Y. Tatematsu, K. Ohkura, H. Nagamune, Development of a Sortase A-mediated Peptide-labeled Liposome Applicable to Drug-delivery Systems, Anticancer Research, 35 (2015) 4411-4417.
[25] M.W. Platscher, R. Behrendt, V. Groehn, S.R. Hoertner, M.S. Passafaro, F. Bauer, Targeting aminoacid lipids, in: Google Patents, Merck Patent Gmbh, US, 2014.
[26] M.L. Immordino, F. Dosio, L. Cattel, Stealth liposomes: review of the basic science, rationale, and clinical applications, existing and potential., International Journal of Nanomedicine, 1 (2006) 297-315.
[27] M. Rashidian, E.J. Keliher, A.M. Bilate, J.N. Duarte, G.R. Wojtkiewicz, J.T. Jacobsen, J. Cragnolini, L.K. Swee, G.D. Victora, R. Weissleder, H.L. Ploegh, Noninvasive imaging of immune responses, Proceedings of the National Academy of Sciences of the United States of America, 112 (2015) 6146-6151.
[28] S. Krah, C. Schröter, S. Zielonka, M. Empting, B. Valldorf, H. Kolmar, Single-domain antibodies for biomedical applications, Immunopharmacology and Immunotoxicology, 38 (2016) 21-28.
[29] E. Dolk, C. van Vliet, J.M.J. Perez, G. Vriend, H. Darbon, G. Ferrat, C. Cambillau, L.G.J. Frenken, T. Verrips, Induced refolding of a temperature denatured llama heavy-chain antibody fragment by its antigen, Proteins: Structure, Function, and Bioinformatics, 59 (2005) 555-564.
[30] M.M. Harmsen, H.J. De Haard, Properties, production, and applications of camelid single-domain antibody fragments, Applied Microbiology and Biotechnology, 77 (2007) 13-22.
[31] S. Oliveira, R. Heukers, J. Sornkom, R.J. Kok, P.M.P. van Bergen en Henegouwen, Targeting tumors with nanobodies for cancer imaging and therapy, Journal of Controlled Release, 172 (2013) 607-617.
[32] S. Kobayashi, T. Terai, Y. Yoshikawa, R. Ohkawa, M. Ebihara, M. Hayashi, K. Takiguchi, N. Nemoto, In vitro selection of random peptides against artificial lipid bilayers: a potential tool to immobilize molecules on membranes, Chemical Communications, 53 (2017) 3458-3461.
[33] S. Khaleghi, F. Rahbarizadeh, D. Ahmadvand, H.R.M. Hosseini, Anti-HER2 VHH Targeted Magnetoliposome for Intelligent Magnetic Resonance Imaging of Breast Cancer Cells, Cellular and Molecular Bioengineering, 10 (2017) 263-272.
[34] M. Broekgaarden, R. van Vught, S. Oliveira, R.C. Roovers, P.M. van Bergen en Henegouwen, R.J. Pieters, T.M. Van Gulik, E. Breukink, M. Heger, Site-specific conjugation of single domain antibodies to liposomes enhances photosensitizer uptake and photodynamic therapy efficacy, Nanoscale, 8 (2016) 6490-6494.
[35] S. Oliveira, R.M. Schiffelers, J. van der Veeken, R. van der Meel, R. Vongpromek, P.M.P. van Bergen en Henegouwen, G. Storm, R.C. Roovers, Downregulation of EGFR by a novel multivalent nanobody-liposome platform, Journal of Controlled Release, 145 (2010) 165-175.
[36] R. van der Meel, S. Oliveira, I. Altintas, R. Haselberg, J. van der Veeken, R.C. Roovers, P.M. van Bergen en Henegouwen, G. Storm, W.E. Hennink, R.M. Schiffelers, R.J. Kok, Tumor-targeted Nanobullets: Anti-EGFR nanobody-liposomes loaded with anti-IGF-1R kinase inhibitor for cancer treatment, Journal of Controlled Release, 159 (2012) 281-289.
[37] R. van der Meel, S. Oliveira, I. Altintas, R. Heukers, E.H. Pieters, P.M. van Bergen en Henegouwen, G. Storm, W.E. Hennink, R.J. Kok, R.M. Schiffelers, Inhibition of tumor growth by targeted anti-EGFR/IGF-1R nanobullets depends on efficient blocking of cell survival pathways, Molecular Pharmaceutics, 10 (2013) 3717-3727.
[38] S.X. Wang, J. Michiels, K.K. Arien, R. New, G. Vanham, I. Roitt, Inhibition of HIV Virus by Neutralizing Vhh Attached to Dual Functional Liposomes Encapsulating Dapivirine, Nanoscale Research Letters, 11 (2016) 350.
[39] D.I. Gabrilovich, S. Nagaraj, Myeloid-derived suppressor cells as regulators of the immune system, Nature Reviews Immunology, 9 (2009) 162.
[40] C. Bachran, M. Schröder, L. Conrad, J.J. Cragnolini, F.G. Tafesse, L. Helming, H.L. Ploegh, L.K. Swee, The activity of myeloid cell-specific VHH immunotoxins is target-, epitope-, subset- and organ dependent, Scientific Reports, 7 (2017) 17916.
[41] D. Carugo, E. Bottaro, J. Owen, E. Stride, C. Nastruzzi, Liposome production by microfluidics: potential and limiting factors, Scientific Reports, 6 (2016) 25876.

[42] S. Wöll, S. Schiller, C. Bachran, L.K. Swee, R. Scherließ, Pentaglycine lipid derivates – rp-HPLC-analytics for bioorthogonal anchor molecules in targeted, multiple-composite liposomal drug delivery systems, International Journal of Pharmaceutics, 547 (2018) 602-610.

[43] A. Kirchhofer, J. Helma, K. Schmidthals, C. Frauer, S. Cui, A. Karcher, M. Pellis, S. Muyldermans, C.S. Casas-Delucchi, M.C. Cardoso, Modulation of protein properties in living cells using nanobodies, Nature Structural & Molecular Biology, 17 (2010) 133-138.

[44] F. Szoka, D. Papahadjopoulos, Procedure for preparation of liposomes with large internal aqueous space and high capture by reverse-phase evaporation, Proceedings of the National Academy of Sciences, 75 (1978) 4194-4198.

[45] R.G. Kruger, B. Otvos, B.A. Frankel, M. Bentley, P. Dostal, D.G. McCafferty, Analysis of the Substrate Specificity of the Staphylococcus aureus Sortase Transpeptidase SrtA, Biochemistry, 43 (2004) 1541-1551.

[46] C. Grabielle-Madelmont, S. Lesieur, M. Ollivon, Characterization of loaded liposomes by size exclusion chromatography, Journal of biochemical and biophysical methods, 56 (2003) 189-217.

[47] A. Gabizon, D.C. Price, J. Huberty, R.S. Bresalier, D. Papahadjopoulos, Effect of Liposome Composition and Other Factors on the Targeting of Liposomes to Experimental Tumors: Biodistribution and Imaging Studies, Cancer Research, 50 (1990) 6371.

[48] J.-M. Lim, A. Swami, L.M. Gilson, S. Chopra, S. Choi, J. Wu, R. Langer, R. Karnik, O.C. Farokhzad, Ultra-High Throughput Synthesis of Nanoparticles with Homogeneous Size Distribution Using a Coaxial Turbulent Jet Mixer, ACS Nano, 8 (2014) 6056-6065.

[49] R. Peschka, T. Purmann, R. Schubert, Cross-flow filtration – an improved detergent removal technique for the preparation of liposomes, International Journal of Pharmaceutics, 162 (1998) 177-183.

[50] P.S. Uster, T.M. Allen, B.E. Daniel, C.J. Mendez, M.S. Newman, G.Z. Zhu, Insertion of poly(ethylene glycol) derivatized phospholipid into pre-formed liposomes results in prolonged in vivo circulation time, FEBS Letters, 386 (1996) 243-246.

[51] W.W.K. Cheng, T.M. Allen, Targeted delivery of anti-CD19 liposomal doxorubicin in B-cell lymphoma: A comparison of whole monoclonal antibody, Fab' fragments and single chain Fv, Journal of Controlled Release, 126 (2008) 50-58.

Supplementary Data

Isolation and characterization of VHH BMX1

VHH BMX1 was generated by immunization of an alpaca with human myeloid cells following standard procedures (PMID24577359). Human myeloid cells were isolated by fluorescence activated cell sorting using antibodies against CD33 and CD14 for positive selection and CD3, CD19, CD56, and HLA-DR for negative selection. Cells were isolated by Ficoll-density gradient centrifugation from human blood donations from several donors, pooled and killed by radiation. Panning of the VHH library was performed with similar non-radiated cells.

The specificity of VHH BMX1 for myeloid cells was determined by flow cytometry using CD11b as myeloid marker on human peripheral blood mononuclear cells obtained by Ficoll-density gradient centrifugation from human blood donations. VHH BMX1 binding was detected by anti-His FITC antibody and was restricted to CD11b-positive cells. The staining pattern indicates binding of VHH BMX1 to CD11b.

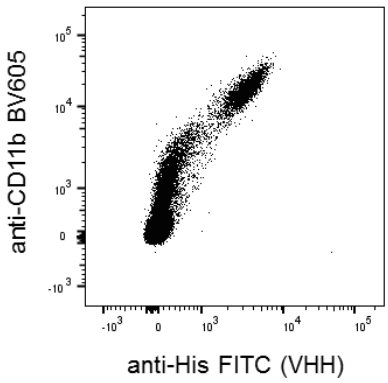

Supplementary Figure 1: Binding of VHH BMX1 (stained by anti-His FITC) to human peripheral blood mononuclear cells stained by anti-CD11b.

VHH BMX1 Sequence:

AAAQVQLVETGGGLVQAGGSLRLSCAASGRSFSSYDMGWYRQTPGKEREFVAAISWRGGNPDYADSVKG
RFTISRDNAANSLYLQMNSLKPEDTAIYYCNAGVYSDPDWGAESGSWGQGTQVTVSSEPKTPKPQPAR

Physical properties and stability of targeted liposomes

Supplementary Table 1: Size, PDI and zeta potential of dye-labeled and VHH-modified formulation A and C (data shown as mean ± standard deviation of three measurements). Liposomes were at least stable for four weeks.

	d_h [nm]		**PDI**		**zeta potential [mV]**	
pull point [weeks]	0	4	0	4	0	4
formulation A						
- G5-liposomes	141 ± 2	140 ± 5	0.23 ± 0.00	0.23 ± 0.01	-8 ± 1	-9 ± 1
- VHH ENH-modified	135 ± 2	147 ± 2	0.24 ± 0.00	0.22 ± 0.01	-6 ± 0	-7 ± 1
- VHH BMX1-modified	130 ± 14	155 ± 4	0.24 ± 0.00	0.22 ± 0.00	-13 ± 3	-7 ± 1
formulation C						
- G5-liposomes	194 ± 2	198 ± 3	0.21 ± 0.02	0.23 ± 0.00	-26 ± 2	-25 ± 1
- VHH ENH-modified	205 ± 2	197 ± 1	0.22 ± 0.02	0.22 ± 0.01	-19 ± 1	-20 ± 1
- VHH BMX1-modified	193 ± 4	194 ± 2	0.23 ± 0.01	0.23 ± 0.01	-20 ± 1	-20 ± 1

In vitro uptake of BMX1-liposomes in hPBMCs (confocal microscopy)

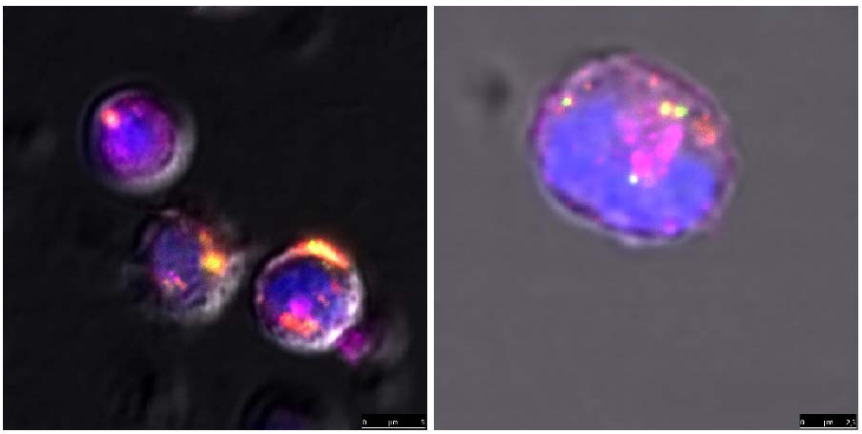

Supplementary Video 1 can be accessed online at https://doi.org/10.1016/j.ejpb.2018.09.017 and shows hPMBCs incubated with BMX1-liposomes. Confocal microscopy reveals the intracellular localization of intact liposomes, indicated by the co-localization of the liposomal dyes Liss-Rhod-PE (red) for liposomal bilayer and FITC-dextran (yellow) for liposomal core. Formulation A: left video, formulation C: right video. Color code: yellow: liposomal core, red: liposomal bilayer, blue: nucleus, purple: plasma membrane. Scale bars: formulation A: 5 µm, formulation C: 2.5 µm. Replay requires Adobe Flash®.

Chapter 4

Sortagging of liposomes with a murine CD11b-specific VHH increases *in vitro* and *in vivo* targeting specificity of myeloid cells

This chapter is published as: Wöll, S., Bachran, C., Schiller, S., Schröder, M., Conrad, L., Scherließ, R., Swee, L.K.: Sortagging of liposomes with a murine CD11b-specific VHH increases *in vitro* and *in vivo* targeting specificity of myeloid cells.
European Journal of Pharmaceutics and Biopharmaceutics, 134 (2019), 190-198.
https://doi.org/10.1016/j.ejpb.2018.11.014

Abstract

The therapeutic index of drugs can be increased via drug encapsulation in actively targeted, meaning ligand modified drug delivery systems. The manufacturing of such targeted drug delivery systems, in particular the conjugation between drug carrier and ligand, can be done by enzymatic conjugation methods, exploiting the site-specific, bioorthogonal nature of these reactions. The use of such enzymes like Sortase-A transpeptidase requires efficient purification methods, as residuals of the enzyme may be responsible for immunogenic potential and drug product instabilities. These instabilities may be based on the enzymatic reverse reaction, meaning here a cleavage between ligand and drug carrier. In the presented work, two differently PEGylated formulations were modified with variable fragments of camelid heavy chain-only antibodies (VHH) via Sortase-A, purified by different methodologies and tested for ligand cleavage upon storage. Strongly PEGylated liposomes (PEG^{high}-LS) were found to retain higher amounts of Sortase-A than lowly PEGylated ones (PEG^{low}-LS) after dialysis purification. Surprisingly, this did not correlate with ligand stability during storage. PEG^{high}-LS were less prone for degradation, compared to PEG^{low}-LS, which showed a ligand cleavage of 20 % after an 8 weeks storage at 2-8 °C. Nonetheless, overall degradation could be minimized by an additional affinity bead purification procedure. Liposomes modified with a CD11b-specific VHH were tested for their *in vitro* and *in vivo* targeting ability towards $CD11b^{+}$ cells. Specific targeting of CD11b was achieved *in vitro* and *in vivo* on various cell types. PEGylation decreased the targeting effect *in vitro*, however no differences between PEG^{high} or PEG^{low} formulations were observed *in vivo*. The obtained results underline the need for a thorough physico-chemical characterization of novel conjugation strategies as well as an early *in vivo* characterization of such targeted drug delivery systems.

1. Introduction

The use of enzyme-mediated transpeptidation techniques has proven valuable for protein modifications in many examples. These include payload [1] or fluorophore conjugation [2] for antibody-drug conjugates and diagnostics, the lipidation [3] and glycosylation [4] of proteins and the decoration of drug delivery systems with targeting ligands [5-9]. Amongst other enzymes such as transglutaminase [10] and butelase [11], Sortase-A is the most widely used enzyme for such applications [3, 12]. The main advantages of Sortase-catalyzed reactions are the inherent site-specificity, mild conjugation conditions and short recognition motifs in substrate proteins [3, 12]. Sortase variants have been extensively studied regarding structure [13], substrate specificity [9], reaction kinetics [14] and conditions [12]. Sortase-A recognizes a C-terminal amino acid sequence of LPxTG (leucine, proline, any amino acid, threonine, glycine) and forms a thioester as intermediate between threonine and glycine. Subsequently, a nucleophile, typically an oligoglycine, forms a peptide bond between threonine's carboxylic acid group and the oligoglycine's free amine [3, 12]. A major drawback of Sortase-A reaction is the reversibility of the transpeptidation [11]. The reverse reaction can be defined as the formation of the thioester intermediate of a newly formed LPxTG motif, followed by a nucleophilic attack of a) the previously cleaved sequence from the substrate with the N-terminal glycine, b) the desired glycine-nucleophile again leading to the reaction product, or c) a water molecule [15, 16]. Latter causes hydrolysis of the LPxTG motif and loss of recognition for the transpeptidation reaction. This reverse reaction can therefore decrease overall conversion rates [7, 11]. Furthermore, although Sortase-A reaction is considered as site-specific and reaction products should be homogeneous, structural variants of the product are obtained by reverse reactions especially if substrates carry several LPxTG motifs. This is typically the case in the synthesis of antibody-drug conjugates [1], where equilibrium processes between payload conjugation and hydrolysis may lead to different drug-to-antibody ratio species. Reversibility of the reaction further necessitates high demands on product purification. Besides the immunogenic potential of Sortase-A residuals in drug products, traces of the enzyme may be responsible for chemical instabilities, manifested in the subsequent hydrolysis of the LPxTG motif between the conjugated substrates. This would, in case of antibody-drug conjugates, lead to an increase of the free drug, or in case of drug delivery systems, cleavage of the targeting ligand from the particulate construct. A robust and efficient purification from Sortase-A is therefore of utmost importance for the use of this technology.

We recently demonstrated high dependency of liposomal surface properties on the transpeptidation reactivity of pentaglycine-liposomes towards LPETG-modified single-domain

antibodies of camelid heavy chain only antibodies (VHHs) [17]. PEG-shielding of a pentaglycine moiety on the bilayer surface led to a drastically decreased conversion rate. Furthermore, reaction kinetics indicated influence of the PEGylation status on the extent of the reverse reaction during the ligand conjugation. Besides this, we observed retention of Sortase-A over dialysis purification, which occurred preferentially for 2 kDa PEG-derivatized liposomes. We therefore investigated here the stability of the VHH bound to the liposomal system to analyze if purification methods or liposomal surface properties influence hydrolysis stability of the targeting ligand upon storage.

In vitro targeting of CD11b$^+$ human myeloid cells with an CD11b-specific VHH-modified liposomal system was recently achieved with high specificity [17]. To further demonstrate the feasibility to target desired cell types *in vivo* with sortaggable liposomes, a VHH (VHH DC13) which binds murine myeloid cell surface receptor CD11b [2, 18] was employed as targeting ligand. CD11b is an integrin expressed on various myeloid cells such as monocytes, granulocytes, dendritic cells, macrophages and myeloid-derived suppressor cells (MDSC). MDSC are a heterogeneous cell population expanding under pathologic conditions such as cancer, trauma or sepsis that can inhibit the function of effector T cells [19]. Specific delivery of cargos such as antigens or toxins to myeloid cells can be used for therapeutic purposes as vaccines to increase adaptive immune response (antigen cargo) or to deplete cells (toxin cargo) that contribute to cancer progression (e.g. MDSC). Recently, VHHs against myeloid cell surface markers Gr-1 and CD11b were conjugated to the catalytic domains of *Pseudomonas* exotoxin A, a potent bacterial toxin. The immunotoxins were able to deplete mono- or granulocytes *in vivo* with a target-, cell- and organ-dependent activity [18]. In the present work, we investigated whether the described sortaggable liposomal drug delivery systems can be decorated with VHH DC13 by Sortase-A and directed towards murine CD11b$^+$Gr-1$^+$ myeloid cells. For that purpose, binding of fluorescence-labeled liposomes was tested *in vitro* with different immune cell lines and primary splenocytes. Furthermore, specificity of targeting myeloid cells was investigated *in vivo* and analyzed with flow cytometry by staining murine splenocytes for myeloid (Gr-1$^+$/CD11b$^+$) or lymphoid (CD3$^+$ or CD19$^+$) subpopulations. With the present work, we analyzed for the first time the active *in vivo* targeting of CD11b$^+$ myeloid cells via a liposomal system. Our results demonstrate feasibility for a cell-selective drug delivery towards these immune cells and can be useful for novel therapeutic approaches in immuno-oncology.

2. Materials

Pentaglycine-modified lipid DMA-PEG-G5 was obtained from Merck & Cie (Schaffhausen, Switzerland) and is described in detail elsewhere [17]. In brief, the lipid consists of a pentaglycine

structure conjugated to a 2 kDa monodisperse PEG-spacer, followed by a bilayer anchor (dimyristyl-amino-propandiol; DMA). 1,2-dipalmitoyl-sn-glycero-3-phosphocholine (DPPC), 1,2-dipalmitoyl-sn-glycero-3-phospho-(1'-rac-glycerol) (DPPG) and 1,2-distearoyl-sn-glycero-3-phosphoethanolamine-N-[methoxy(polyethylene glycol)-2000] (DSPE-mPEG) were a gift of Lipoid GmbH (Ludwigshafen, Germany). DPBS (Dulbecco's phosphate buffered saline, D1408, 10fold stock), FITC-dextran 10 kDa and cholesterol were purchased from MilliporeSigma (St. Louis, Missouri, USA). Acetonitrile, trifluoroacetic acid (TFA), methanol and ethanol (both gradient grade) were obtained from Merck KGaA (Darmstadt, Germany). MilliQ water was taken from a Millipore Advantage A 10 with Q-Pod apparatus (Merck KGaA, Darmstadt, Germany). Sortase-A and LPETG (leucine, proline, glutamic acid, threonine, glycine)-modified VHH ENH and VHH DC13 were prepared as described in [18].

3. Methods

3.1. Liposome preparation

Pentaglycine-modified liposomes were prepared by a solvent injection process described in detail elsewhere [17]. Liposomes consisted of 1 mol% DMA-PEG-G5, DPPC (59.4 mol%), cholesterol (34.7 mol%) and 5.0 mol% of either DSPE-mPEG (referred to as "PEG^{high}-LS") or DPPG (referred to as "PEG^{low}-LS"). In brief, the lipids were dissolved to 90 mM in ethanol (PEG^{high}-LS) or to 32 mM in methanol (PEG^{low}-LS). The lipid solutions were injected by a syringe pump (PHD Ultra4400, Harvard Apparatus, Holliston, Massachusetts, USA) into a stream of DPBS pH 7.4 conveyed by a peristaltic pump (Ismatec IP65, Cole-Parmer, Wertheim, Germany). Lipid and buffer streams were connected via a stainless steel, luer-lock T-piece (Unimed S.A., Lausanne, Switzerland), customized with a 27 G needle for lipid injection. 10 mg/mL FITC-dextran was added to the injection buffer for the manufacturing of FITC-labeled liposomes. Dispersions obtained from injection were purified and concentrated by tangential flow filtration [17].

3.2. Ligand conjugation and purification

For analysis of purification dependent ligand stability, PEG^{high}-LS and PEG^{low}-LS were conjugated to the model single-domain antibody VHH ENH [20]. Liposomes (100 µM total pentaglycine), VHH ENH (50 µM) and 25 µM of Ca^{2+}-independent, 6-histidin (his) tagged Sortase-A variant SortA7m were incubated for 4 h at 4 °C. An aliquot of the reaction mixture was retained for further analysis, remaining liposomes were dialyzed (Float-A-Lyzer, MWCO 1000 kDa, G235037, Spectrum Labs, Los Angeles, California, USA) against 100-200fold acceptor medium (DPBS) with five buffer changes over 24 h. A further aliquot was additionally refined with his-tag binding magnetic sepharose-nickel beads (GE Healthcare, Chaltfont St Giles, UK) to remove residual

amounts of Sortase-A or VHH. For that, 100 µL bead slurry was washed three times with DPBS using a magnetic rack. Supernatant was removed, and the beads were redispersed with 200 µL of the liposomal dispersion. After 2 h incubation at 4 °C and gentle shaking, magnetic beads were removed. Non-purified, dialyzed and additional bead purified liposomes were stored in Teflon-sealed glass vials for analysis of physical liposome stability (hydrodynamic diameter, polydispersity index, zeta potential) and chemical stability of the targeting ligand. For *in vitro* and *in vivo* experiments, FITC-labeled liposomes were either modified with VHH ENH (isotype control) or murine CD11b binding VHH DC13, followed by dialysis purification.

3.3. Liposome characterization

Liposomes were analyzed for hydrodynamic diameter d_h and polydispersity index (PDI) using a DynaPro Plate Reader II, Wyatt Technology Corporation, Santa Barbara, California, USA. Zeta potential was measured after dilution to 3 % v/v in 10 mM NaCl using a Malvern Zetasizer Nano ZS, Worcestershire, UK. Detailed measurement settings are described elsewhere [17]. Molecular bilayer compositions were determined by an rp-HPLC method (based on a C18-column) with evaporative light scattering as described earlier [17].

For quantification of conjugated VHH on the liposomes, a second rp-HPLC method (based on a C4 column), which separates proteins, DMA-PEG-G5-modified VHHs and lipid components of the liposome from each other was used [17]. For that, non-liposomal conjugates were synthesized, isolated by rp-HPLC and redispersed in water. Concentration was determined by UV-spectroscopy (NP80, Implen, Westlake Village, California, USA) using calculated extinction coefficients (ExPASy ProtParam, SIB, Lausanne, Switzerland). Isolated conjugates were used as HPLC-reference standard at 280 nm to determine concentration of VHH-lipid conjugates on liposomes after injection of 5 µL liposomal dispersion. VHH-conjugate content was normalized on phospholipid content, and the reaction efficacy was calculated (Equation 1, t_i : after sortagging and purification, t_0 : start of the reaction).

Equation 1

$$reaction\ efficacy\ [\%] = \frac{\frac{c_{VHH-conjugate}}{c_{lipid}}(t_i)}{\frac{c_{VHH}}{c_{lipid}}(t_0)} * 100$$

Furthermore, residual amounts of Sortase-A after dialysis or bead purification were determined by rp-HPLC based on a 25 µM Sortase-A reference measured at 280 nm. Limit of quantification (LOQ) of this method was 3.1 µM for a signal to noise ratio of 10:1 as determined by the chromatography software (OpenLab CDS EZChrom, Agilent Technologies).

To investigate stability of the targeting ligand regarding hydrolytic cleavage, liposomal samples were stored at 2-8 °C for 8 weeks and analyzed by rp-HPLC for change in the relative area of the lipidated VHH. Stability was calculated according to Equation 2, where t_i is the actual pull point and t_0 the start value of the study. Results of three batches were averaged.

Equation 2

$$stability\ S_{rel} = \frac{area\%_{VHH-conjugate}(t_i)}{area\%_{VHH-conjugate}(t_0)}$$

Total FITC content of dye-labeled batches was determined by fluorimetry (M200 plate reader, Tecan Group, Männedorf, Switzerland) after a lysis of the liposomes in Triton X-100. Free FITC-dextran was determined by analytical size exclusion chromatography described in [17] with fluorescence detection (excitation: zero order, emission: 510 nm) separating liposomes and non-encapsulated FITC-dextran. Encapsulated FITC-dextran was calculated as total minus free FITC-dextran. Encapsulation efficiency was calculated as the ratio of FITC-dextran per lipid of the final dispersion, divided by the theoretical ratio of FITC-dextran per lipid after solvent injection.

3.4. *In vitro* characterization of VHH DC13-liposomes

In cell culture DC2.4 cells and RAW macrophages were maintained in DMEM (Life Technologies, #61965026) supplemented with 10 % heat-inactivated fetal bovine serum (FBS, Life Technologies, #10270106), 100 U/mL penicillin (Life Technologies, #15140122), and 100 µg/mL streptomycin (Life Technologies, #15140122). NUP progenitor cells (hematopoietic progenitors immortalized using a NUP98/HOXB4 transgene, described in [21]) and NUP-derived myeloid-derived suppressor cells (MDSC) were cultured in complete RPMI consisting of RPMI 1640 medium (Life Technologies, #21875-034) supplemented with 10 % FBS, 100 U/mL penicillin, 100 µg/mL streptomycin, 1 mM sodium pyruvate (Life Technologies, #11360070), 50 µM 2-mercaptoethanol (Life Technologies, #31350-010) and 1 × non-essential amino acids (Life Technologies, #11140-035). MDSC were differentiated from NUP cells by 4 days of incubation in the presence of 20 ng/mL IL-6 (Biolegend, #570802) and 20 ng/mL murine GM-CSF (Biolegend, #576304) [22]. Splenocytes were isolated from a C57BL6/J mouse by mashing the spleen in a 70 µm cell strainer (Corning, #352350) and washing cells in FACS buffer (1fold PBS (Life Technologies, #14190-094) with 2 % FBS). Cells were resuspended in 1 mL ACK (ammonium-chloride-potassium) lysing buffer (Thermo Fisher Scientific, #A10492-01) to remove red cells, incubated 5 min at room temperature, followed by addition of 5 mL FACS buffer and re-centrifuged.

For binding experiments 1 × 10^5 DC2.4 cells or RAW macrophages were seeded in a 96-well plate in 200 µL medium and kept overnight at 37 °C in the presence of 5 % CO_2 before addition of liposomes. 2 × 10^5 NUP cells, MDSC or splenocytes were seeded in a 96-well plate in 200 µL. 100 µM of PEG^{high}-LS or PEG^{low}-LS (based on total lipid content of FITC-labeled formulation, either as ligand free control (G5-LS), VHH ENH-decorated or VHH DC13-decorated liposomes) in 200 µL complete RPMI medium were added to each sample in V-bottom-shaped 96-well plates and incubated at 37 °C for 4 h in the presence of 5 % CO_2. Afterwards, cells were centrifugated (300 x g for 1 min). The supernatant containing unbound liposomes was removed, followed by redispersion of the cells in FACS buffer by multiple pipetting cycles. Antibody staining of cells was performed in presence of Fc receptor block (TruStain fcX BioLegend, #422302) in FACS buffer. SytoxBlue (Thermo Fisher Scientific, S34857) was used for exclusion of dead cells. Following antibodies from BioLegend were used for flow cytometry: Brilliant Violet 605 anti-Gr-1 (#108439), PerCP-anti-CD11b (#101229), BV605-anti-CD3 (#100237) and APC-anti-CD19 (#115511).

For confocal microscopy, 0.5 × 10^6 RAW macrophages were seeded in a total volume of 200 µL complete RPMI. 100 µM liposomes were added to each sample in V-bottom-shaped 96-well plates and incubated at 37 °C for 4 h in the presence of 5 % CO_2. Cells were stained with CellMask Deep Red Plasma membrane stain (1:5000) (Life Technologies, #C10046) and Hoechst 33342 (1:2000) (Thermo Scientific, #62249) for 15 min at 37 °C in the presence of 5 % CO_2. The medium was removed by centrifugation (1 min at 300 × g), cells were washed with FACS buffer, transferred in 100 µL FACS buffer on polyethyleneimine-coated cover slips (microscope cover glasses from Marienfeld, 18 mm diameter, #0117580) and incubated for 10 min at 37 °C. Cells were fixed on cover slips with paraformaldehyde (final concentration 4 %) for 15 min and washed with 1 × PBS. Cover slips were mounted on cover glass (neoLab, #1-6273) using anti-fade ProLong Diamond mounting medium (Invitrogen, #P36961) and analyzed 18 h later with a Leica TCS SP5 confocal microscope using an HCX Plan APO 40 × /1.30 Oil CS objective. For image analysis the Leica Application Suite software was used.

3.5. *In vivo* targeting of MDSC

C57BL/6J mice were maintained under specific pathogen-free conditions in the animal facility of the University of Heidelberg. All animal experiments were done in accordance with German legislation governing animal studies (approved project G-250/14 by the Regierungspräsidium Karlsruhe). Female C57BL/6J mice (8 weeks old, Charles River) were injected intravenously with PBS (one animal) or 0.6 mM (based on total lipid content) of either VHH ENH-PEG^{low}-LS, VHH DC13-PEG^{high}-LS or VHH DC13-PEG^{low}-LS in 200 µL PBS (each 3 animals per group). After 2 h,

mice were sacrificed and splenocytes were isolated as described above. Splenocytes were stained for flow cytometry analysis using the same antibodies as described above. Statistically significant differences ($p < 0.05$) of FACS measurements were determined by unpaired t-test (Graph Pad Prism 7.03).

4. Results and discussion

4.1. VHH conjugation, purification and stability of the immunoliposomes

To investigate the formulation- and purification-dependent stability of liposomes conjugated with VHHs via Sortase-A, two sortaggable liposome types differing in the bilayer surface properties were prepared by solvent injection. Physicochemical parameters are described in Table 1. Sortase-A was used to ligate a LPETG-modified VHH (VHH "enhancer", described in [20]) towards the liposomes, followed by a dialysis step to remove the enzyme and unbound VHH. The sortagging and dialysis process had no relevant influence on size or PDI (Figure 1A) as relative changes were below 10 %. Zeta potential showed a shift towards neutral values with relative changes > 30 %, however absolute changes were small (Table 1).

Table 1: Physico-chemical properties of unmodified and VHH-modified PEG^{high}-LS and PEG^{low}-LS (data shown as mean ± standard deviation of three reactions from one liposome bulk)

formulation	d_h [nm]	PDI	zeta potential [mV]
PEG^{high}-LS			
PEG^{high}-LS (unmodified)	140	0.22	-9.3
VHH ENH-PEG^{high}-LS (dialysis)	141 ± 1	0.22 ± 0.01	-5.7 ± 0.3
VHH ENH-PEG^{high}-LS (bead)	143 ± 0	0.22 ± 0.02	-6.1 ± 0.1
PEG^{low}-LS			
PEG^{low}-LS (unmodified)	175	0.23	-25.8
VHH ENH-PEG^{low}-LS (dialysis)	186 ± 4	0.23 ± 0.01	-17.3 ± 0.8
VHH ENH-PEG^{low}-LS (bead)	187 ± 2	0.23 ± 0.01	-17.2 ± 0.7

We previously observed a formulation dependent retention of Sortase-A after a dialysis purification step [17]. This encouraged us here to add an additional magnetic bead purification step [18] after the dialysis protocol to enhance removal of free Sortase-A from the liposomal dispersion. Here, his-tagged Sortase-A is bound towards Ni^{2+}-chelate beads. As the use of such magnetic bead systems for purification of liposomes was previously not described, we investigated compatibility regarding physical (size, PDI and zeta potential) and chemical properties (bilayer composition and VHH-density) of the liposomes. Neither size, PDI nor zeta potential showed relevant changes during the incubation process, indicating no alteration of the particle size distribution or surface properties by shear forces or other impacts through the beads (Figure 1, Table 1). Furthermore, we investigated the influence of the sortagging and purification processes on the bilayer composition of the liposomes. The bilayer fraction of the

reaction educt DMA-PEG-G5 showed a clear decrease after sortagging, showing the consumption of this lipid by the transpeptidation reaction. No other major changes occurred, indicating no adsorption to the dialysis membrane or device housing. Absolute lipid yields from dialysis devices were > 88 % for PEG^{high}-LS and > 97 % for PEG^{low}-LS. Bead purification was compatible with both liposomal compositions as the bilayer compositions were maintained (Table 2). This and the high overall lipid yields (> 90 % for both formulation types, Table 2) indicated no adsorption of lipids to the sepharose bead material.

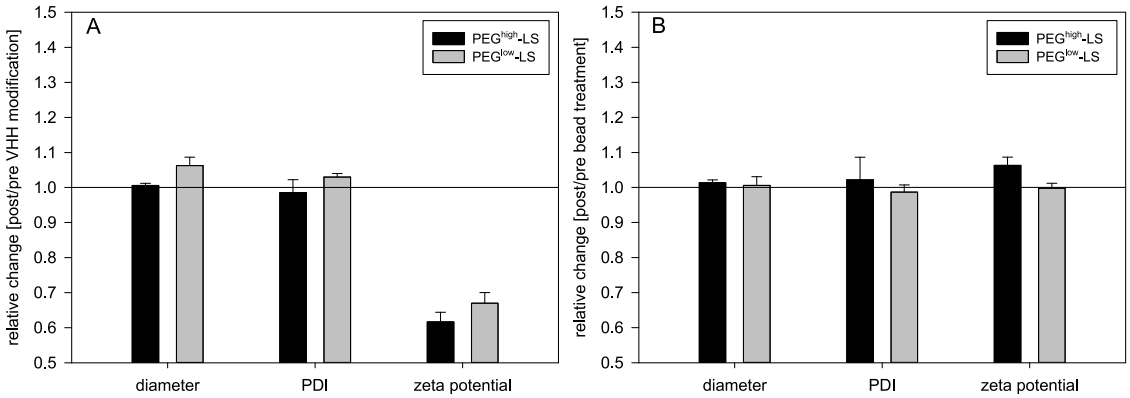

Figure 1: Physico-chemical impact of VHH conjugation (A) and bead purification (B) on PEG^{high}-LS and PEG^{low}-LS. **A**: Minor affection of hydrodynamic diameter and PDI indicates colloidal stability of the nanoparticulate dispersion during ligand modification. Zeta potential showed low absolute, but clear relative changes due to surface modification and thereby charge alteration. **B**: His-tag affinity-based magnetic bead purification does not affect integrity of targeted liposomal formulations as neither d_h, PDI nor zeta potential showed relevant changes. Data shown as mean ± standard deviation of three reactions and purifications from one liposome bulk.

Table 2: Molecular composition and purification yield of VHH ENH-modified formulations (data shown as mean ± standard deviation of three reactions and purification procedures).

	DMA-PEG-G5 [mol%]	CHOL [mol%]	DPPC [mol%]	DPPG/DSPE-mPEG [mol%]	yield [%]
PEG^{high}-LS					
PEG^{high}-LS (unmodified)	1.0	35.2	59.4	4.5	
VHH ENH-PEG^{high}-LS (dialysis)	0.6 ± 0.0	34.8 ± 0.3	60.4 ± 0.2	4.2 ± 0.1	88.1 ± 1.4
VHH ENH-PEG^{high}-LS (bead)	0.6 ± 0.0	35 ± 0.6	60.5 ± 0.6	3.8 ± 0.1	90.4 ± 4.0
PEG^{low}-LS					
PEG^{low}-LS (unmodified)	1.0	35.2	59.5	4.3	
VHH ENH-PEG^{low}-LS (dialysis)	0.7 ± 0.0	34.3 ± 0.6	60.9 ± 0.9	4.2 ± 0.4	97.2 ± 2.5
VHH ENH-PEG^{low}-LS (bead)	0.7 ± 0.0	34.9 ± 0.4	60.1 ± 0.3	4.4 ± 0.1	96.8 ± 3.6

Residual Sortase-A levels were analyzed after dialysis and bead purification. PEG^{high}-LS retained high amounts of Sortase-A after dialysis (Figure 2, Table 3). This is a surprising result as the cut-off of the dialysis device was ≈50fold larger than the molecular weight of this Sortase-A variant (20.9 kDa). It is expected that an unspecific binding towards the PEG^{high}-LS may have occurred. The DPPG-stabilized formulation did hardly retain any non-lipidated protein over the dialysis process. A reason for the lower adsorption tendency of Sortase-A to the DPPG stabilized bilayers may be the significantly lower zeta potential. This may lead to a higher repulsion

between Sortase-A and liposome surface, and finally a more effective dialysis purification. It was tested whether an additional affinity-based bead purification could further reduce Sortase-A residuals in the liposomal formulations. Though the Ni^{2+}-chelate beads should bind and therefore be able to remove the his-tagged enzyme, Sortase-A content in PEG^{high}-LS formulation was reduced only to a minor extent (Table 3).

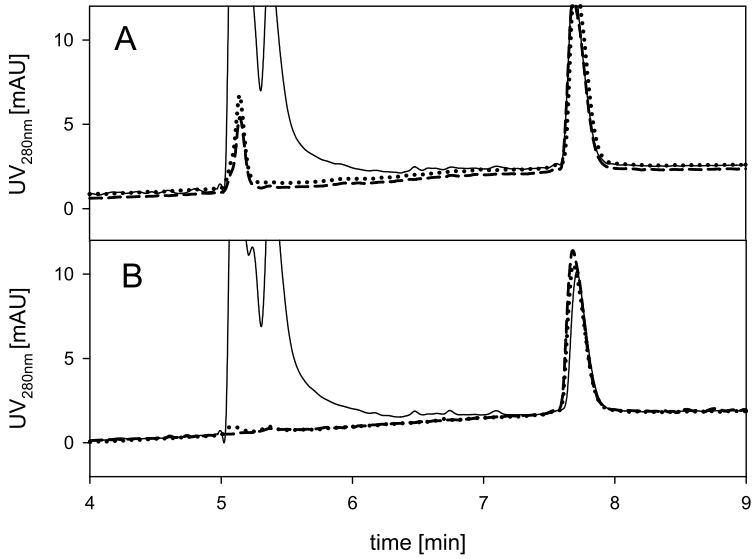

Figure 2: Purification of PEG^{high}-LS (**A**) and PEG^{low}-LS (**B**) by dialysis (dotted) and magnetic beads (dashed). Solid chromatogram indicates unpurified reaction bulk. Peak at 5.0-5.3 min: Sortase-A, peak at 5.3-6.5 min: unbound VHH, peak at 7.8 min: lipidated VHH.

Table 3: Purification and VHH conjugation efficacy. Residual Sortase-A levels were below limit of quantification (LOQ) for PEG^{low}-LS. PEG^{high}-LS retained considerable amounts of the enzyme over dialysis and the additional bead purification procedure. Data shown as mean ± standard deviation of three reactions and purification procedures.

formulation	residual Sortase-A [µM]	reaction efficacy [%]
VHH ENH-PEG^{high}-LS (dialysis)	6.0 ± 0.6	33 ± 2
VHH ENH-PEG^{high}-LS (bead)	4.8 ± 0.6	34 ± 1
VHH ENH-PEG^{low}-LS (dialysis)	< 3.1 (LOQ)	28 ± 1
VHH ENH-PEG^{low}-LS (bead)	< 3.1 (LOQ)	28 ± 4

This indicates a strong interaction with the liposomal surface, and may be origin of product instabilities, meaning a cleavage of the targeting ligand from the liposomal system via the reverse reaction of Sortase-A. Stability of the differently purified liposomal dispersions were therefore analyzed for cleavage of the targeting ligand upon storage at 2-8 °C. Non-purified feedstock from conjugation bulk of both formulations showed a pronounced loss of targeting ligand over storage (Figure 3). Degradation rates were significantly higher for PEG^{low}-LS compared to PEG^{high}-LS. This is in congruence with results obtained earlier for the monitoring of the reaction kinetics on these two formulations, which showed a predominant reverse reaction for PEG^{low}-LS already after 14 h [17]. Most surprisingly, extent of targeting cleavage was independent of residual Sortase-A content. Although PEG^{high}-LS contained significant amounts of Sortase-A after both dialysis and bead purification steps, hardly any cleavage of the lipidated

VHH was observed over the stability study (Figure 3). In contrast to that, dialyzed PEG^{low}-LS showed a decrease of the VHH conjugated to the liposomes over 8 weeks (Figure 3B, triangles). Assuming a homogenous loss of ligand over the liposomal dispersion, the average ligand density on a single liposome decreased about 20 % during storage. As latter is a critical value for an effective targeting [23], such a decrease would be inacceptable for a commercial product. Though not correlated in a quantitative manner with residual Sortase-A levels due to the quantification limit of the rp-HPLC method, this instability was overcome by the additional bead purification, since the bead purified PEG^{low}-LS did not show degradation over the study time.

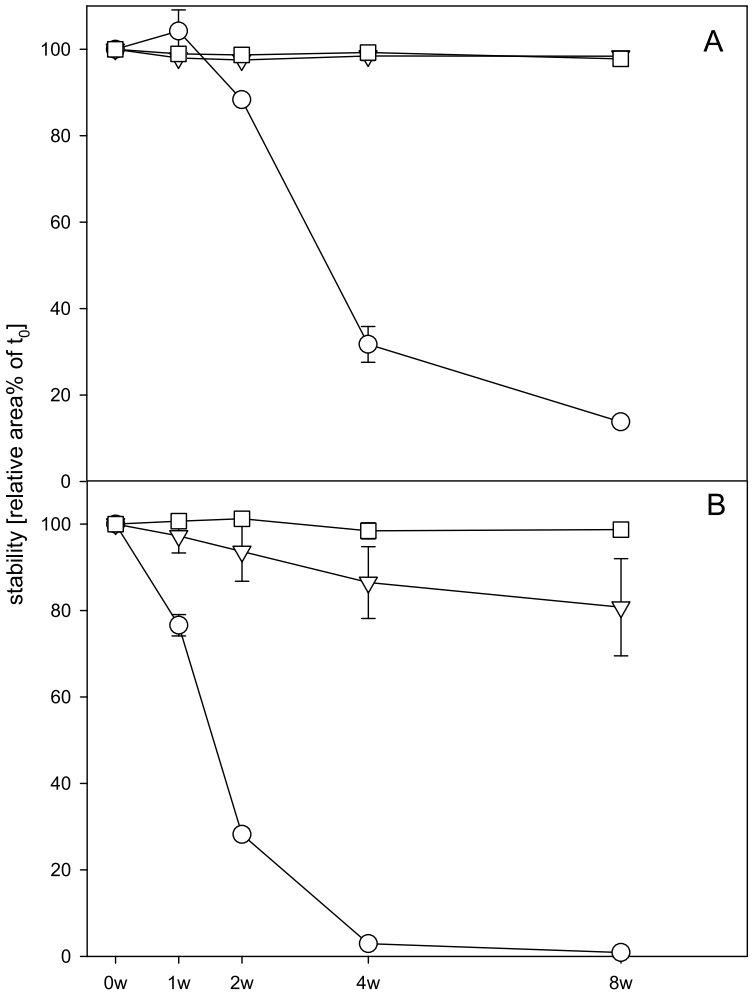

Figure 3: Stability of VHH conjugated to the liposomes. Extent of targeting ligand cleavage by Sortase-A during storage is dependent on the PEGylation status. **A**: PEG^{high}-LS. **B**: PEG^{low}-LS. Circles: unpurified feedstock containing Sortase-A, triangles: dialyzed feedstock, squares: dialyzed and bead purified feedstock. Data shown as mean ± standard deviation of three reactions and purification procedures.

It is suggested that a further reduction of the Sortase-A residuals by a his-tag mediated removal through the Ni^{2+}-chelate beads increased overall storage stability. It remains unclear why PEG^{low}-LS are more prone to the reverse reaction and hence lability during storage. Comparing surface properties of both formulations, PEG^{high}-LS contain an additional 2 kDa PEG-layer, that may protect the newly formed LPETG-motif after transpeptidation against a second recognition via Sortase-A. It is known that PEG-layers adopt different conformations (brush, mushroom) on

liposomes [24]. These depend on the molar fraction of the PEGylated lipid due to interactions between adjacent polymer chains, leading to a brush-like conformation at a total PEG-densities > 4 mol% [25]. Suggesting this extended polymer conformation for DSPE-mPEG in PEG^{high}-LS, this could explain the resistance of this formulation against the reverse reaction via a steric shielding of the LPETG motif (Scheme 1) by neighboring PEG-groups.

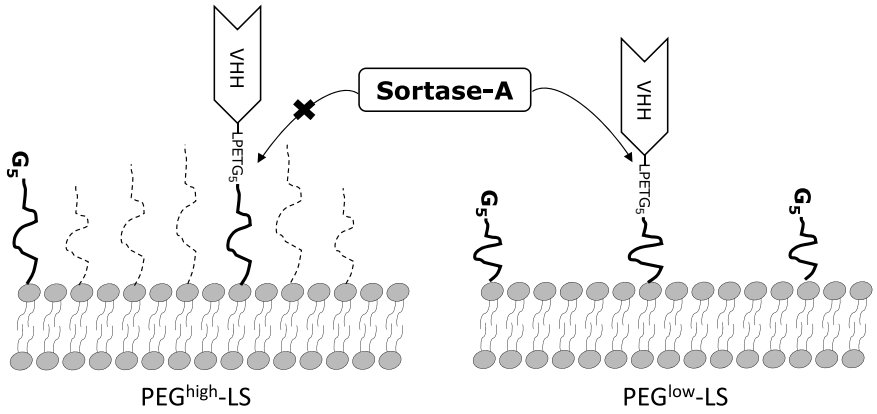

Scheme 1: Steric accessibility of LPETG-motifs on differently PEGylated bilayers. Neighboring PEG-groups in PEG^{high}-LS may shield the LPETG-motif from re-recognition by Sortase-A and therefore reduce the propensity of the reverse reaction. PEG^{low}-LS exhibit higher steric accessibility and are therefore prone for ligand cleavage by residuals of Sortase-A.

Furthermore, polydispersity of PEG-groups in DSPE-mPEG, but not in DMA-PEG-G5 [17], may extent this shielding effect by presence of PEG-chains in DSPE-mPEG with a molecular weight larger than the 2 kDa spacer in DMA-PEG-G5. Interestingly, the PEG-layer seems to inhibit only the reverse reaction and not the recognition of the pentaglycine motif prior transpeptidation, as overall reaction efficacy of both formulations was comparable (Table 3). Compared to that, PEG^{low}-LS probably possess an exposed LPETG-motif in mushroom conformation due to the low (DMA-PEG-G5 derived) PEG-fraction of 1 mol%. Low interaction with neighboring polymer coils could enhance steric accessibility of the LPETG-motif between VHH and lipid anchor, leading to a pronounced reverse reaction. We furthermore tested d_h, PDI and zeta potential during storage. No relevant changes were observed over the tested time (size and PDI changes < 10 %, absolute zeta potential changes < 4 mV, Figure 4).

Sortase-A is currently gaining attraction as versatile tool to conjugate ligands on particulate drug delivery systems [5-7, 9, 12, 17, 26]. Due to the immunogenic potential of bacteria-derived protein residuals and the enzyme's inherent reversibility of the reaction, efficient purification methods are essential to ensure drug product stability and quality.

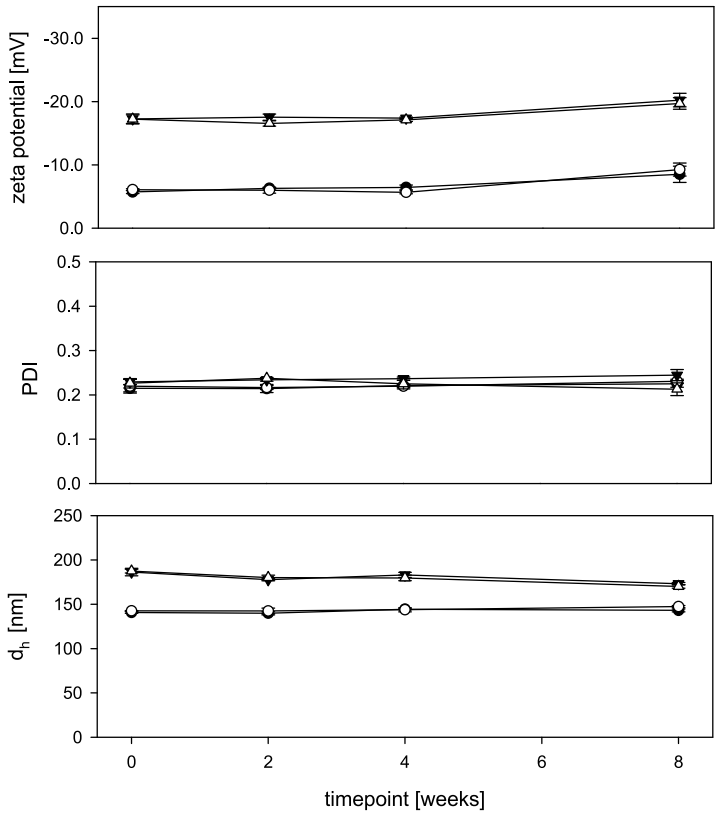

Figure 4: Stability of VHH ENH-modified liposomes after different purification protocols. No considerable changes in size, PDI or zeta potential occurred over an 8 weeks storage at 2-8 °C (circles: PEG^{high}-LS, triangles: PEG^{low}-LS, black filling: dialysis, white filling: bead purification). Data shown as mean ± standard deviation of three reactions and purification procedures.

Such methods may include, especially in larger production scale, size exclusion or affinity-based chromatography. Our results indicate that especially latter frequently used method may be challenging, since considerable residuals of Sortase-A remained in the highly PEGylated formulation after affinity bead purification. Estimating a lipid dosing for the presented dialyzed PEG^{high}-LS comparable to marketed liposomal doxorubicin (Doxil®; maximum dose for the treatment of ovarian carcinoma is 50 mg doxorubicin or 400 mg total lipid per square meter of body surface), this would result in an application of 20 mg Sortase-A residuals to an average patient (1.73 m^2). The presented results therefore raise the consciousness on the drawbacks of the use of such novel conjugation techniques, which obviously put special demands on manufacturing and purification protocols. Especially the separation of Sortase or other catalytic proteins from nanoparticulate drug delivery systems can be challenging due to unspecific adsorption to the large surface of the nano-sized dispersions. Besides improvements of purification techniques, advancement of the manufacturing strategies may contribute to an avoidance of drug product instabilities by enzymatic reverse reactions. For Sortase-A, this may include the usage of primary amines (e.g. a DSPE-PEG-amine) instead of oligoglycine acceptor motifs. Primary amines are known as alternative nucleophiles during the transpeptidation [27]. As the final product would not contain a LPxTG-motif, the so obtained constructs may not be

susceptible for the reverse reaction, avoiding at least stability, but not immunogenic problems. Other strategies, especially suitable for liposome modification, could involve post-insertion processes, meaning a separation of ligand lipidation and particle modification [28]. This would avoid exposure of the particulate surface with Sortase-A, thereby avoiding unspecific adsorption. Also, pre-immobilization of Sortase-A on sepharose beads could help to simplify the downstream purification of sortaggable nanoparticulate drug delivery systems [29-31].

4.2. VHH DC13-liposomes show cell type specific binding *in vitro* and *in vivo*

Liposomes functionalized with the CD11b-specific VHH DC13 or a control VHH (eGFP-specific enhancer) were tested for specific binding to cells that are CD11b positive or negative. $CD11b^+$ cells included DC2.4 murine dendritic cell line [32], RAW macrophage cell line [33] and MDSC differentiated from NUP cells [22] while CD11b-negative cells included undifferentiated NUP cells [22], T cells [34] and B cells [35]. Cell lines or primary splenocytes were incubated with 100 µM FITC-labeled liposomes (based on total lipid content) for 4 h and analyzed by FACS and microscopy.

Untargeted PEG^{low} or PEG^{high} pentaglycine liposomes (G5-LS) and isotype control-modified VHH ENH-LS did not bind to any cell type (Figure 5A). The minor shift of the FITC signal on DC2.4 and RAW cells might be due to the ability of these antigen presenting cells to phagocytose small particles without any specific surface binding. Decoration with VHH DC13 induced specific surface binding on cell lines expressing CD11b (DC2.4, RAW). NUP cells did not show any superior interaction with the VHH DC13-modified formulations. In contrast, both VHH DC13-modified formulations were able to bind towards $CD11b^+Gr\text{-}1^+$ MDSC differentiated from NUP cells [22].

Specificity of binding was tested using a murine splenocyte mix containing $CD11b^+Gr\text{-}1^+$ cells, $CD11b^-CD3^+$ T cells and $CD11b^-CD19^+$ B cells. Parallel staining of their relevant cell surface receptors and simultaneous analysis for the liposomal FITC fluorescence revealed a specific binding towards $CD11b^+Gr\text{-}1^+$ cells, while other cell types like T cells and B cells were unaffected (Figure 5A).

In all cases, VHH DC13-PEG^{low}-LS showed superior binding compared to VHH DC13-PEG^{high}-LS. We demonstrated comparable VHH loading (Table 3) and antigen capturing [17] of both formulations, however, FITC-dextran encapsulation efficiency was higher for VHH DC13-PEG^{low}-LS (0.42 %) than for VHH DC13-PEG^{high}-LS (0.25 %). As concentrations of the dye were kept similar during solvent injection, these differences may be due to the slightly larger liposome diameter of the PEG^{low}-LS. Despite the different FITC-dextran loadings, the observed differences of *in vitro* binding may be due to a decreased uptake of the PEGylated liposomes

after binding. PEGylation is a widely used method to prevent uptake of the formulation by the mononuclear phagocyte system (MPS), thereby increasing *in vivo* circulation times [24]. *In vitro*, PEGylation was previously shown to reduce the uptake of liposomes by macrophages even at low molar bilayer ratios (0.5 mol%) [36]. It might therefore be that here the PEG-layer decreased uptake of the liposomes, e.g. via a PEG-induced hindrance of an effective liposome internalization. Furthermore, the additional PEG layer may reduce the steric flexibility of the conjugated VHH, and thereby decrease the cell-VHH interaction compared to the PEG^{low}-LS.

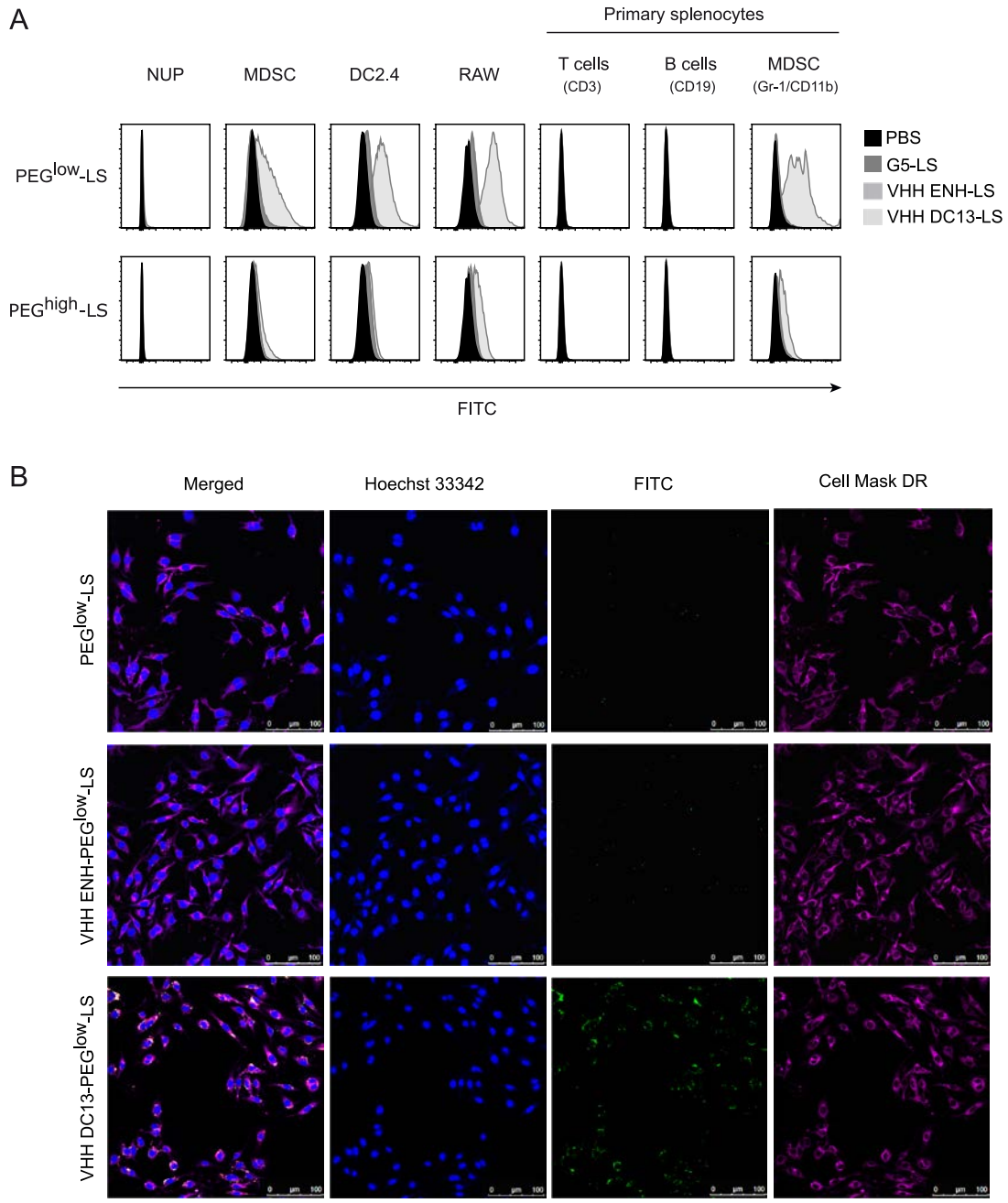

Figure 5: *In vitro* binding of CD11b-targeted liposomes. **A**: CD11b-positive (MDSC, DC2.4, RAW) and CD11b-negative (NUP cells) cell lines were tested for the specific binding of liposomes modified with anti-CD11b VHH DC13. Furthermore, specificity of binding was investigated on isolated splenocytes including CD11b$^+$ MDSC and CD11b$^-$ T and B cells. Both PEG^{high}-LS and PEG^{low}-LS bound to the cells in a ligand dependent fashion. **B**: Incubation of G5-PEG^{low}-LS, VHH ENH-PEG^{low}-LS and VHH DC13-PEG^{low}-LS with RAW macrophages. Confocal microscopy revealed cellular surface and cytosolic localization of VHH DC13-PEG^{low}-LS, but not of the control groups.

Confocal microscopy was used to investigate the specific uptake of VHH DC13-PEG^{low}-LS into RAW cells (Figure 5B). Association with the cell surface and internalization to the cytosol was observed for VHH DC13 targeted liposomes, but not for the isotype or uncoated control. This indicates that the sortagging of liposomes with VHH DC13 enabled the specific delivery of FITC-loaded liposomes to target cells.

Although surface marker specific targeting and cellular uptake did work *in vitro* this may be different *in vivo* as the liposomes might encounter additional hurdles, such as unspecific attachment to endothelial cells, loss of target specificity, fast clearance from circulation via the MPS or blockage of the antigen-ligand interaction via plasma proteins. We injected 3 mice each intravenously with 0.6 mM of the respective VHH-conjugated liposomes (VHH ENH-LS, VHH DC13-LS, either as PEG^{low}-LS or PEG^{high}-LS) in 200 µL PBS and isolated the spleen 2 hours later. The splenocytes were then stained for flow cytometry analysis to differentiate between CD11b$^-$ T cells and B cells or CD11b$^+$Gr-1$^+$ cells. ENH-PEG^{low}-LS were used as isotype control and did not bind to any analyzed cell type (Figure 6).

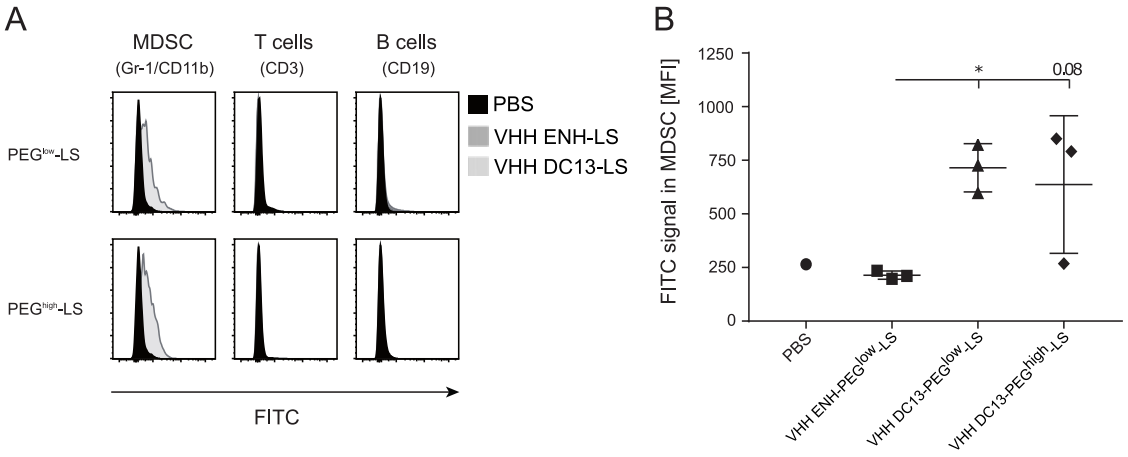

Figure 6: *In vivo* targeting of splenic CD11b$^+$Gr-1$^+$ MDSC. C57BL/6J mice were injected with 0.6 mM (total lipid) of VHH DC13-modified, FITC-dextran-labeled PEG^{high}-LS or PEG^{low}-LS. After 2 h incubation, mice were sacrificed and the splenocytes were analyzed for the liposomal FITC fluorescence by flow cytometry after co-staining of MDSC, T and B cell determining surface markers. **A**: Representative flow cytometry histograms. **B**: Threefold increase in MFI over the isotype control group was found for both VHH DC13 targeted formulations (significant for VHH DC13-PEG^{low}-LS ($p < 0.05$)).

The uptake of VHH DC13-PEG^{low}-LS was increased significantly leading to a threefold increased FITC signal compared to VHH ENH-PEG^{low}-LS (Figure 6B). Surprisingly this was true to the same extent for both liposomal surface types and not increased with the PEG^{low}-LS as it was the case *in vitro*. This might be due to different pharmacokinetic behavior of the strongly PEGylated and the anionic, charge stabilized formulation. It is known that increasing amounts of 2 kDa PEG grafting on liposomal surfaces increase the circulation time of the drug delivery system [37]. The increased circulation may therefore compensate a decreased overall binding and uptake of PEGylated formulations by the target cells. Furthermore, the presence of a broad variety of

plasma proteins *in vivo* (which cannot be entirely simulated by the presence of FBS *in vitro*) may lead to enhanced alteration of lowly PEGylated surfaces due to increased unspecific protein adsorption [38]. This may lead to a decreased accessibility of the VHH on the liposomal surface and subsequently a decreased recognition of the targeted cells. These considerations indicate the need for thorough and early *in vivo* characterization of such targeted nanoparticulate drug delivery systems.

5. Conclusion and outlook

In the present study, Sortase-A was used to conjugate single-domain antibodies (VHHs) towards two differently PEGylated, pentaglycine-modified liposomal surfaces. The resulting immunoliposomes were analyzed regarding stability against the Sortase-A inherent reverse reaction. DSPE-mPEG stabilized liposomal formulations revealed resistance against the reverse reaction, though considerable enzyme residuals were detected after a dialysis purification. DPPG stabilized PEG^{low}-LS having low PEGylation degree were prone for ligand cleavage by Sortase residuals. This could be overcome by improvement of the purification procedure and demonstrates challenges in the usage of enzyme-based conjugation methods for drug delivery system modification.

We investigated the *in vitro* and *in vivo* targeting potential of the sortagged, VHH carrying liposomes. *In vitro*, liposomes modified with an anti-CD11b single-domain antibody were targeted to various $CD11b^+$ myeloid cells. This observation was successfully verified *in vivo*, where splenic $CD11b^+Gr\text{-}1^+$ cells were targeted with clear specificity over $CD11b^-$ cells. High degree of PEGylation seemed to decrease the target cell binding *in vitro*. Surprisingly, this was not observed when splenic $CD11b^+Gr\text{-}1^+$ cells were targeted *in vivo*, as both formulations performed equally. It is assumed that the extension of circulation time and reduction of unspecific plasma protein adsorption via the PEG-shell is responsible for this contrary observation. This indicates the need for an early *in vivo* characterization of nanoparticulate drug delivery systems, with a special regard to formulation parameters such as particle surface design.

The $CD11b^+$ and $Gr\text{-}1^+$ phenotype determines murine myeloid-derived suppressors cells. This cell population exhibits the ability to suppress T cells, leading to a negative impact on the individual immune response in diseases such as cancer [19]. Thus, the here presented approach to target MDSC is attractive, e.g. for the delivery of toxins which may diminish immune suppression in the tumor microenvironment. Since CD11b is present on various other myeloid cells, a more specific targeting of MDSC may be achieved with ligands binding epitopes of Gr-1. VHHs specific for this

target were recently described [18], and a combination of such ligands with nanoparticulate drug delivery systems would be a favorable option for further development. Nevertheless, $CD11b^+$ targeting may involve other promising applications such as a selective vaccine delivery [39, 40] or delivery of drugs towards atherosclerotic plaques [41].

With the presented work, manufacturing demands and formulation parameters determining the *in vivo* targeting of sortagged, VHH-modified liposomes were highlighted. They underline important challenges, but also the potential of such novel targeted drug delivery systems.

References

[1] R.R. Beerli, T. Hell, A.S. Merkel, U. Grawunder, Sortase enzyme-mediated generation of site-specifically conjugated antibody drug conjugates with high in vitro and in vivo potency, PloS one, 10 (2015) e0131177.

[2] M. Rashidian, E.J. Keliher, A.M. Bilate, J.N. Duarte, G.R. Wojtkiewicz, J.T. Jacobsen, J. Cragnolini, L.K. Swee, G.D. Victora, R. Weissleder, H.L. Ploegh, Noninvasive imaging of immune responses, Proceedings of the National Academy of Sciences of the United States of America, 112 (2015) 6146-6151.

[3] J.M. Antos, M.C. Truttmann, H.L. Ploegh, Recent advances in sortase-catalyzed ligation methodology, Current Opinion in Structural Biology, 38 (2016) 111-118.

[4] Z. Wu, X. Guo, Q. Wang, B.M. Swarts, Z. Guo, Sortase A-Catalyzed Transpeptidation of Glycosylphosphatidylinositol Derivatives for Chemoenzymatic Synthesis of GPI-Anchored Proteins, Journal of the American Chemical Society, 132 (2010) 1567-1571.

[5] X. Guo, Z. Wu, Z. Guo, New method for site-specific modification of liposomes with proteins using sortase a-mediated transpeptidation, Bioconjugate chemistry, 23 (2012) 650-655.

[6] C.E. Hagemeyer, K. Alt, A.P. Johnston, Particle generation, functionalization and sortase A-mediated modification with targeting of single-chain antibodies for diagnostic and therapeutic use, Nature Protocols, 10 (2015) 90-105.

[7] J.R. Silvius, R. Leventis, A Novel “Prebinding” Strategy Dramatically Enhances Sortase-Mediated Coupling of Proteins to Liposomes, Bioconjugate Chemistry, 28 (2017) 1271-1282.

[8] H.T. Ta, S. Prabhu, E. Leitner, F. Jia, D. von Elverfeldt, K. Jackson, T. Heidt, A. Nair, H. Pearce, C. von zur Muhlen, X. Wang, K. Peter, C.E. Hagemeyer, Enzymatic Single-Chain Antibody Tagging: a universal approach to targeted molecular imaging and cell homing in cardiovascular disease, Circulation Research, (2011) 365-373.

[9] A. Tabata, N. Anyoji, Y. Ohkubo, T. Tomoyasu, H. Nagamune, Investigation on the Reaction Conditions of Staphylococcus aureus Sortase A for Creating Surface-modified Liposomes as a Drug-delivery System Tool, Anticancer Research, 34 (2014) 4521-4527.

[10] S. Panowski, S. Bhakta, H. Raab, P. Polakis, J.R. Junutula, Site-specific antibody drug conjugates for cancer therapy, mAbs, 6 (2014) 34-45.

[11] M. Schmidt, A. Toplak, P.J.L.M. Quaedflieg, T. Nuijens, Enzyme-mediated ligation technologies for peptides and proteins, Current Opinion in Chemical Biology, 38 (2017) 1-7.

[12] M. Ritzefeld, Sortagging: A Robust and Efficient Chemoenzymatic Ligation Strategy, Chemistry – A European Journal, 20 (2014) 8516-8529.

[13] U. Ilangovan, H. Ton-That, J. Iwahara, O. Schneewind, R.T. Clubb, Structure of sortase, the transpeptidase that anchors proteins to the cell wall of Staphylococcus aureus, Proceedings of the National Academy of Sciences, 98 (2001) 6056-6061.

[14] X. Huang, A. Aulabaugh, W. Ding, B. Kapoor, L. Alksne, K. Tabei, G. Ellestad, Kinetic mechanism of Staphylococcus aureus sortase SrtA, Biochemistry, 42 (2003) 11307-11315.

[15] S. Möhlmann, C. Mahlert, S. Greven, P. Scholz, A. Harrenga, In vitro sortagging of an antibody fab fragment: overcoming unproductive reactions of sortase with water and lysine side chains, ChemBioChem, 12 (2011) 1774-1780.

[16] W.L. Popp Maximilian, M. Antos John, L. Ploegh Hidde, Site-Specific Protein Labeling via Sortase-Mediated Transpeptidation, Current Protocols in Protein Science, 56 (2009) 15.13.11-15.13.19.

[17] S. Wöll, C. Bachran, S. Schiller, M. Schröder, L. Conrad, L.K. Swee, R. Scherließ, Sortaggable liposomes: Evaluation of reaction conditions for single-domain antibody conjugation by Sortase-A and targeting of $CD11b^+$ myeloid cells, European Journal of Pharmaceutics and Biopharmaceutics, 133 (2018) 138-150.

[18] C. Bachran, M. Schröder, L. Conrad, J.J. Cragnolini, F.G. Tafesse, L. Helming, H.L. Ploegh, L.K. Swee, The activity of myeloid cell-specific VHH immunotoxins is target-, epitope-, subset- and organ dependent, Scientific Reports, 7 (2017) 17916.

[19] D.I. Gabrilovich, S. Nagaraj, Myeloid-derived suppressor cells as regulators of the immune system, Nature Reviews Immunology, 9 (2009) 162-174.

[20] A. Kirchhofer, J. Helma, K. Schmidthals, C. Frauer, S. Cui, A. Karcher, M. Pellis, S. Muyldermans, C.S. Casas-Delucchi, M.C. Cardoso, Modulation of protein properties in living cells using nanobodies, Nature Structural & Molecular Biology, 17 (2010) 133-138.

[21] C. Ruedl, H.J. Khameneh, K. Karjalainen, Manipulation of immune system via immortal bone marrow stem cells, International Immunology, 20 (2008) 1211-1218.

[22] M. Schröder, S. Loos, S.K. Naumann, C. Bachran, M. Krötschel, V. Umansky, L. Helming, L.K. Swee, Identification of inhibitors of myeloid-derived suppressor cells activity through phenotypic chemical screening, OncoImmunology, 6 (2017) e1258503.

[23] C. Mamot, D.C. Drummond, U. Greiser, K. Hong, D.B. Kirpotin, J.D. Marks, J.W. Park, Epidermal Growth Factor Receptor (EGFR)-targeted Immunoliposomes Mediate Specific and Efficient Drug Delivery to EGFR- and EGFRvIII-overexpressing Tumor Cells, Cancer Research, 63 (2003) 3154-3161.

[24] M.L. Immordino, F. Dosio, L. Cattel, Stealth liposomes: review of the basic science, rationale, and clinical applications, existing and potential, International Journal of Nanomedicine, 1 (2006) 297-315.

[25] O. Garbuzenko, Y. Barenholz, A. Priev, Effect of grafted PEG on liposome size and on compressibility and packing of lipid bilayer, Chemistry and Physics of Lipids, 135 (2005) 117-129.

[26] S. Wöll, S. Schiller, C. Bachran, L.K. Swee, R. Scherließ, Pentaglycine lipid derivates – rp-HPLC analytics for bioorthogonal anchor molecules in targeted, multiple-composite liposomal drug delivery systems, International Journal of Pharmaceutics, 547 (2018) 602-610.

[27] J.E. Glasgow, M.L. Salit, J.R. Cochran, In Vivo Site-Specific Protein Tagging with Diverse Amines Using an Engineered Sortase Variant, Journal of the American Chemical Society, 138 (2016) 7496-7499.

[28] D.L. Iden, T.M. Allen, In vitro and in vivo comparison of immunoliposomes made by conventional coupling techniques with those made by a new post-insertion approach, Biochimica et Biophysica Acta (BBA) - Biomembranes, 1513 (2001) 207-216.

[29] M. Steinhagen, K. Zunker, K. Nordsieck, A.G. Beck-Sickinger, Large scale modification of biomolecules using immobilized sortase A from Staphylococcus aureus, Bioorganic & Medicinal Chemistry, 21 (2013) 3504-3510.

[30] X. Zhao, H. Hong, X. Cheng, S. Liu, T. Deng, Z. Guo, Z. Wu, One-step purification and immobilization of extracellularly expressed sortase A by magnetic particles to develop a robust and recyclable biocatalyst, Scientific Reports, 7 (2017) 6561.

[31] M.D. Witte, T. Wu, C.P. Guimaraes, C.S. Theile, A.E.M. Blom, J.R. Ingram, Z. Li, L. Kundrat, S.D. Goldberg, H.L. Ploegh, Site-specific protein modification using immobilized sortase in batch and continuous-flow systems, Nature Protocols, 10 (2015) 508.

[32] M. Merad, P. Sathe, J. Helft, J. Miller, A. Mortha, The Dendritic Cell Lineage, Annual Review of Immunology, 31 (2013) 563-604.

[33] L.J. Berghaus, J.N. Moore, D.J. Hurley, M.L. Vandenplas, B.P. Fortes, M.A. Wolfert, G.-J. Boons, Innate immune responses of primary murine macrophage-lineage cells and RAW 264.7 cells to ligands of Toll-like receptors 2, 3, and 4, Comparative Immunology, Microbiology and Infectious Diseases, 33 (2010) 443-454.

[34] H.I. McFarland, S.R. Nahill, J.W. Maciaszek, R.M. Welsh, CD11b (Mac-1): a marker for CD8+ cytotoxic T cell activation and memory in virus infection, The Journal of Immunology, 149 (1992) 1326.

[35] L.L. Rumfelt, Y. Zhou, B.M. Rowley, S.A. Shinton, R.R. Hardy, Lineage specification and plasticity in CD19(−) early B cell precursors, The Journal of Experimental Medicine, 203 (2006) 675-687.

[36] H. Xu, J.W. Paxton, Z. Wu, Enhanced pH-Responsiveness, Cellular Trafficking, Cytotoxicity and Long-circulation of PEGylated Liposomes with Post-insertion Technique Using Gemcitabine as a Model Drug, Pharmaceutical Research, 32 (2015) 2428-2438.

[37] P.S. Uster, T.M. Allen, B.E. Daniel, C.J. Mendez, M.S. Newman, G.Z. Zhu, Insertion of poly(ethylene glycol) derivatized phospholipid into pre-formed liposomes results in prolonged in vivo circulation time, FEBS Letters, 386 (1996) 243-246.

[38] N. Bertrand, J.-C. Leroux, The journey of a drug-carrier in the body: An anatomo-physiological perspective, Journal of Controlled Release, 161 (2012) 152-163.

[39] Y.J. Kwon, E. James, N. Shastri, J.M.J. Fréchet, In vivo targeting of dendritic cells for activation of cellular immunity using vaccine carriers based on pH-responsive microparticles, Proceedings of the National Academy of Sciences of the United States of America, 102 (2005) 18264-18268.

[40] J.N. Duarte, J.J. Cragnolini, L.K. Swee, A.M. Bilate, J. Bader, J.R. Ingram, A. Rashidfarrokhi, T. Fang, A. Schiepers, L. Hanke, H.L. Ploegh, Generation of Immunity against Pathogens via Single-Domain Antibody–Antigen Constructs, The Journal of Immunology, 197 (2016) 4838.

[41] S. Katsuki, T. Matoba, S. Nakashiro, K. Sato, J.-i. Koga, K. Nakano, Y. Nakano, S. Egusa, K. Sunagawa, K. Egashira, Nanoparticle-mediated delivery of pitavastatin inhibits atherosclerotic plaque destabilization/rupture in mice by regulating the recruitment of inflammatory monocytes, Circulation, 129 (2013) 896-906.

Chapter 5

Sortase-A mediated chemoenzymatic lipidation of single-domain antibodies for cell membrane engineering

This chapter is intended to be published as: Wöll, S. and Bachran, C., Schiller, M., Conrad, L., Scherließ, R., Swee, L.K.: Sortase-A mediated chemoenzymatic lipidation of single-domain antibodies for cell membrane engineering.

Abstract

Purpose: Membrane engineering has versatile applications in adoptive cell therapies, immune therapy or drug delivery. Incorporation of lipidated ligands into cells may enforce supraphysiological cell interactions that offer new therapeutic approaches. A challenge is the defined synthesis of lipidated ligands that effectively interact with such membranes.

Methods: Sortase-A was used to attach a PEGylated, dimyristyl anchor on single-domain antibodies (VHH). The membrane insertion was investigated on artificial liposomal bilayers, myeloid-derived suppressor cells (MDSC) and T cells.

Results: The lipidated VHHs remodeled artificial liposomal as well as cellular membranes. The VHH carrying liposomes were successfully targeted towards epitope-positive cells. MDSC and T cells were both modified with lipidated VHHs as detected with an FITC-anti-llama antibody. T cells that carried an anti-CD11b VHH showed cellular association *in vitro* with $CD11b^{+}Gr\text{-}1^{+}$ MDSC in a two-dimensional magnetic activated cell sorting / flow-cytometry assay.

Conclusion: The applied combination of chemoenzymatic ligation, PEGylated lipid and single-domain antibody delivers water-soluble and chemically defined lipidated ligands. Since the membrane-inserted constructs enabled liposomal targeting or cell-cell interactions, they are suitable for further application in the field of drug delivery and cell-based therapies.

1. Introduction

Cell membrane engineering is a means to induce or enforce cell-cell or cell-extracellular matrix interactions [1, 2]. This has been proven valuable for cell-based therapies such as chimeric antigen receptor (CAR)-T cell therapy [3], the regulation of immune responses by surface-modified cells [2] or in the field of regenerative medicine [1]. A prerequisite of such membrane engineering is the anchoring of typically proteinaceous structures into the cell membrane. One option for this anchorage is genetic engineering, leading to the expression of the protein of choice together with a transmembrane domain and intracellular sequences for signal transduction as applied in (CAR)-T cell therapies. In this approach, T cells are transfected with a construct that contains an extracellular scFv fragment linked to activating domains that induce T cell activation upon target engagement on tumor cells [3]. However, genome engineering has several drawbacks including safety related to genome editing [4, 5] or over-activation due to constitutive expression [6]. Additionally, display of proteins via genetic engineering may be challenging, since correct protein transduction across the cell membrane is required after a susceptible protein expression, folding, and intracellular trafficking process [7]. If the protein to be displayed on cells does not require an intracellular signal transduction or genetic inheritability, it can also be engineered to the cell surface by non-genetic techniques [1]. Possible applications include the support of immune therapies by anchorage of cytokines [8], increased chemotaxis for mesenchymal stem cells during regenerative therapies [9, 10] or treatment of autoimmune diseases [11, 12].

Non-genetic techniques for cell surface engineering are the covalent anchorage through on-site reactions with other components of the cell membrane [2, 11, 13, 14], or a spontaneous hydrophobic insertion of the structure of interest into the bilayer due to a previously attached lipid group [1, 15]. The latter strategy offers high control of the density of the displayed protein, avoids exposure of cells to toxic reagents and works in a rapid fashion [7]. Further advantages are the negligible toxicity, the maintenance of normal cellular activities and the participation of the inserted molecules in the cell membrane dynamics, although the latter may also lead to an undesired endocytosis of the inserted compound [1]. Despite these advantages, protein lipidation is technically difficult, since established chemical conjugation techniques (relying on reactive amino acid side chains) suffer from poor selectivity, leading to heterogeneous reaction products [16]. A further problem is the low solubility of lipophilic anchors [15] that causes strong increases of hydrophobicity of the lipidated protein. This can lead to a high aggregation tendency. Such solubility issues may be alleviated by the use of detergents such as

n-dodecyl-maltoside [15], however with unfavorable impact on the application of such lipidated proteins on living systems.

Therefore, in this study a PEGylated dimyristyl anchor was attached to single-domain antibodies of camelid heavy chain only antibodies (VHH) using chemoenzymatic ligation via the bacterial enzyme Sortase-A (Scheme 1). The inherent site-specificity of Sortase-A leads to highly defined reaction products [17]. Furthermore, PEGylated lipid anchors with two medium length (C14) alkyl chains [18], together with highly soluble VHHs [19], deliver reaction products with good aqueous solubility. This avoids usage of detergents or organic co-solvents, and hence enables direct application of such lipidated proteins on living cells while providing reliable anchorage in membranes [15, 20]. Sortaggable VHHs binding the enhanced green fluorescent protein eGFP (VHH ENH) or a myeloid cell surface receptor CD11b (VHH DC13) have been previously described [21, 22]. Therefore, the influence of the lipidation and isolation process on product purity, yield and binding activity was investigated here. Membrane insertion of lipidated VHHs into an artificial bilayer of fluorophore-labeled liposomes was analyzed via the binding of the so obtained immunoliposomes towards $CD11b^+$ myeloid-derived suppressor cells (MDSC). *In vitro* display of lipidated VHHs on MDSC and T cells was investigated by detection of the VHHs on the cells using an antibody directed against the VHHs. Furthermore, it was in question whether the VHHs retain their ability to recognize the corresponding antigen if inserted into the cellular membrane. For that purpose, cells remodeled with lipidated VHH ENH were analyzed for their ability to capture the antigen eGFP. Finally, to demonstrate the ability of the lipidated VHHs to mediate cell-cell interactions, purified murine T cells were modified with VHH DC13 and analyzed by a two-dimensional magnetic activated cell sorting (MACS) / flow cytometry assay to determine interaction with $CD11b^+$ myeloid-derived suppressor cells.

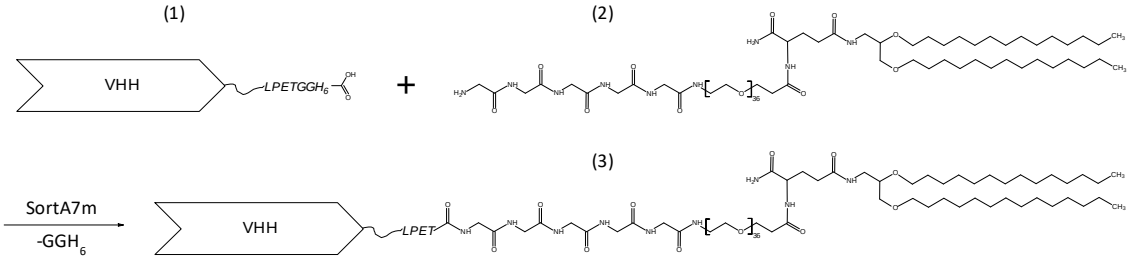

Scheme 1: Sortase-A mediated conjugation of LPETG-modified VHH with the pentaglycine-modified lipid anchor DMA-PEG-G5.

2. Materials

Sortase-A variant SortA7m and LPETG (leucine, proline, glutamic acid, threonine, glycine)-modified single-domain antibodies (Structure 1 in Scheme 1) of camelid heavy chain only antibodies (VHH) VHH ENH and VHH DC13 were prepared as described elsewhere [23]. VHH ENH

binds to enhanced green fluorescent protein eGFP whose fluorescence intensity increases upon binding [21]. VHH DC13 recognizes the myeloid cell surface receptor CD11b [24]. DMA-PEG-G5 (Structure 2 in Scheme 1, 2554 Da) is a 2 kDa PEG-spacer modified on one end with a pentaglycine motif and on the other end with a dimyristyl lipid anchor and was obtained from Merck & Cie (Schaffhausen, Switzerland). Lipoid GmbH (Ludwigshafen, Germany) was supplier of 1,2-dipalmitoyl-sn-glycero-3-phosphocholine (DPPC) and 1,2-dipalmitoyl-sn-glycero-3-phospho-(1'-rac-glycerol) (DPPG). Sigma-Aldrich (St. Louis, MO, USA) was supplier of Dulbecco's phosphate buffered saline (DPBS, D1408), fluorescein isothiocyanate-dextran (FITC-dextran) 10 kDa and cholesterol. Chloroform, acetonitrile, trifluoroacetic acid (TFA), methanol and ethanol (both gradient grade) were obtained from Merck KGaA (Darmstadt, Germany). Milli-Q, MilliporeSigma (Billerica, MA, USA) was used for the preparation of purified water.

3. Methods

3.1. Conjugate synthesis, isolation and analysis

DMA-PEG-G5 stock (25 mg/mL in chloroform) was aliquoted in a HPLC vial. Chloroform was evaporated under a gentle stream of nitrogen creating a thin lipid film, which was hydrated with DPBS pH 7.4 as micellar aqueous lipid dispersion (2 mM). 400 µL of 50 µM VHH, 25 µM Sortase-A and 1 mM DMA-PEG-G5, which corresponded to a target product mass of 320 µg, were incubated for 4 h at 4 °C, until the conjugate was isolated using reversed-phase HPLC (rp-HPLC). Reaction bulk and product were separated utilizing an Aeris Widepore C4 column (3.6 µm particle size, 100 mm length, 2.1 mm diameter, Waters Corporation, Milford, Massachusetts, USA) and a binary gradient pattern (Table 1).

Table 1: rp-HPLC gradient pattern for separation of reaction bulk and product (A: water with 0.1 % TFA v/v, B: acetonitrile with 0.05 % TFA v/v).

time [min]	solvent composition
0.0	95.0 % A
5.5	45.5 % A
15.0	18.5 % A
15.1	5.0 % A
18.0	5.0 % A
18.1	95.0 % A
20.0	95.0 % A

Eluent A was water with 0.1 % TFA, eluent B was acetonitrile with 0.05 % TFA. Analysis was performed on an Agilent 1110 HPLC system equipped with a degasser, binary pump, temperature controlled autosampler, column oven, diode array detector (DAD) and an analytical fraction collector (AFC), controlled by EZChrom Elite Software (Agilent Technologies, Santa Clara, CA, USA). Column temperature was set to 30 °C, autosampler temperature was 4 °C. Standard

analytical or isolation injection volume was 5 µL or 25-100 µL, respectively. Flow rate was 0.5 mL/min. Data was recorded using DAD at 214 and 280 nm.

The conjugate peak was collected either manually or using an automated fraction collector. Collections of single injections were stored on ice, until the eluent mixture was removed using a vacuum centrifuge (RVC 2-33 IR, Martin Christ, Osterode am Harz, Germany; speed: 1500 rpm, temperature: 40 °C, pressure settings: 100 mbar for 10 min, followed by 20 mbar for 20 min and further evaporation at 2 mbar). The resulting pellet was hydrated with water, and protein concentrations were determined by UV spectroscopy (NP80, Implen, Westlake Village, CA, USA) using extinction coefficients calculated by ExPASy ProtParam web application (https://web.expasy.org/protparam, SIB, Lausanne, Switzerland). Yield was calculated based on the mass and concentration of the recovered protein solution and the target product mass. Purity was determined by rp-HPLC analysis at 214 nm with automated peak detection between 2-15 min and a threshold level obtained from background noise of a water blank.

3.2. Mass spectroscopy

To verify the reaction product, the method was transferred to a similar HPLC system equipped with an electrospray ionization mass spectrometer (ESI-MS, amaZon SL, Bruker Corporation, Billerica, Massachusetts, USA). Ion source type was set to ESI with positive polarity. Capillary exit was 140 V, trap drive was set to “94”. The mass range mode was set to enhanced resolution, with a scanning range from 100-2200 m/z. 5 spectra were averaged per run. Masses were calculated using deconvolution of raw spectra.

3.3. Activity of lipidated VHH ENH

The isolated VHH ENH conjugate or native VHH ENH (100 nM) was spiked to 100 nM eGFP. Increase in fluorescence intensity compared to sole eGFP was measured in a black 96-well plate (Thermo Fisher Scientific, Waltham, Massachusetts, USA) utilizing a Spark Plate Reader (Tecan Group, Männedorf, Switzerland) with excitation and emission set to 485 nm and 535 nm, respectively.

3.4. Liposome preparation and post-insertion

FITC (fluorescein isothiocyanate)-labeled liposomes were prepared as described elsewhere [25]. In brief, a mixture of DPPC, cholesterol, DPPG and DMA-PEG-G5 (59.4 : 34.6 : 5.0 : 1.0, molar fractions) was dissolved to 32 mM in methanol and injected via a computer-controlled binary pumping system into a 10 mg/mL FITC-dextran solution in DPBS pH 7.4 utilizing a customized T-piece with a 27 G needle. The dispersion was purified and concentrated by tangential flow

filtration. Lipid concentration was determined by an rp-HPLC method with evaporative light scattering detection described elsewhere [18]. To prepare immunoliposomes, the lipidated VHH ENH or VHH DC13 were added to the liposomal dispersion to 0.25-2 nM VHH per µM phospholipid (PL). The mixture was thoroughly vortexed and incubated at 50 °C for 30 min. Hydrodynamic diameter (d_h) and polydispersity index (PDI) were measured by dynamic light scattering (DLS) using a Zetasizer Nano ZS (Malvern Instruments, Worcestershire, UK).

3.5. Immunoliposome binding and VHH display on MDSC

Murine myeloid-derived suppressor cells (MDSC) were derived from bone marrow-derived NUP-progenitor cells [26]. MDSC were differentiated for four days in complete RPMI (RPMI 1640 medium, Life Technologies, #21875-034, Carlsbad, CA, USA) supplemented with 10 % heat-inactivated fetal bovine serum, 100 U/mL penicillin (Life Technologies, #15140122), 100 µg/mL streptomycin (Life Technologies, #15140122), 1 mM sodium pyruvate (Life Technologies, #11360070), 50 µM 2-mercaptoethanol (Life Technologies, #31350-010), and 1 × non-essential amino acids (Life Technologies, #11140-035) supplemented with 20 ng/mL interleukine-6 and 20 ng/mL granulocyte-macrophage colony-stimulating factor (Biolegend, #576304, San Diego, USA). To investigate membrane insertion of lipidated VHHs, MDSC (10^7 cells/mL) were incubated for 30 min at 4 °C with 500 nM of native or lipidated VHH ENH or VHH DC13. To investigate binding of VHH-modified liposomes, MDSC were incubated with 500 µM of the liposomes (based on total lipid content) for 4 h at 4 °C. In both cases, cells were washed with FACS buffer (1 × PBS + 2 % heat-inactivated fetal bovine serum) and antibody staining of cells was performed in presence of Fc receptor block (TruStain FcX, BioLegend, #422302) in FACS buffer. SytoxBlue (Thermo Fisher Scientific, S34857) was used for exclusion of dead cells. Liposomes were detected via encapsulated FITC-dextran. Lipidated VHH inserted into the cell membrane was detected by a FITC-anti-llama antibody (Invitrogen, #A16061). Alternatively, cells were incubated with 100 µg/mL eGFP at 4 °C for 30 min to detect binding of eGFP to lipidated VHH ENH being inserted into the cell membrane. All analyses of cells were performed by flow cytometry. Flow cytometry was performed on a FACSAria II (Beckton, Dickinson and Company, Franklin Lakes, NJ, USA) and results were analyzed by FlowJo (Tree Star, V.10.0.8).

3.6. Display of VHHs on T cells and cell-cell interaction experiments

For cell-cell interaction experiments, T cells were isolated from spleens of C57BL/6j mice maintained under specific pathogen-free conditions at the animal facility of the University of Heidelberg and euthanized under the registered protocol T47/16. Spleens were mashed and $CD8^+$ cells isolated after red cell lysis (ACK lysing buffer, #A1049201, Thermo Fisher Scientific)

using a mouse CD8a$^+$ T cell isolation kit (#130-104-075, Miltenyi Biotec, Bergisch-Gladbach, Germany) and magnetic cell isolation (LS columns, #130-042-401, Miltenyi Biotec) used according to manufacturer's instructions. Purified CD8$^+$ T cells were stained by 1 nM Cell Tracer Far Red (#C34564, Thermo Fisher Scientific) for 5 min at 35 °C and washed with FACS buffer. Stained T cells (1.65×10^8 cells/mL) were incubated with 650 nM native or lipidated VHH DC13 and VHH ENH for 1 h at 4 °C. Lipidated VHH binding to T cells was detected by an FITC-anti-llama antibody. VHH-labeled T cells were washed twice with FACS buffer and 3×10^7 T cells were incubated with 1.1×10^7 MDSC for 1 h at 4 °C. T cells and MDSC were loaded on LS columns for magnetic bead isolation of CD8$^+$ T cells and co-purification of MDSC bound to T cells. Eluted cells were stained by anti-CD11b-Brilliant Violet 605 and anti-Gr-1-FITC (#101237 and #108405, Biolegend) and analyzed by flow cytometry as described above.

4. Results

4.1. VHH lipidation, isolation and activity

VHHs were conjugated to the PEGylated dimyristyl anchor DMA-PEG-G5 lipid using chemoenzymatic Sortase-A mediated transpeptidation (Scheme 1). For that purpose, DMA-PEG-G5 was dissolved in chloroform, aliquoted, dried by solvent evaporation and hydrated with DPBS in an ultrasonic bath. This film hydration yielded a micellar dispersion with a colloidal hydrodynamic diameter of 18-32 nm (measured by DLS). 1 mM DMA-PEG-G5 was incubated with 25 µM Sortase-A and 50 µM LPETG-VHH to achieve a high conversion yield through surplus of the pentaglycine nucleophile. Two different VHHs were tested for conjugation, namely VHH ENH, binding to eGFP and enhancing its fluorescence [21], or VHH DC13, binding to cell surface marker CD11b of myeloid cells [24]. An analytical rp-HPLC column with large pore size (200 Å) and low hydrophobicity (C4) provided adequate separation of Sortase-A (5.2 min), unconjugated VHH (5.6 min) and DMA-PEG-G5 (8.4 min) from the reaction product (7.6 min). Rp-HPLC analysis showed effective lipidation of the VHHs (Figure 1A), indicated by a hydrophobic shift of the retention time of the VHH. The expected peak of the lipidated VHHs was analyzed by LC-ESI-MS and good accuracy was found with the calculated mass for the two examined VHHs (Figure 1B, calculated / determined mass for VHH DC13: 15804 Da/ 15812 Da; VHH ENH 15835 Da / 15843 Da *(data for VHH ENH conjugate available in Chapter 3, Figure 4)*).

The described rp-HPLC method was compatible with injection volumes up to 100 µL (equalizing a maximum of 80 µg product) and therefore suitable for small scale purification of the lipidated VHH in sub milligram batch sizes. Up to four collected peak fractions were combined, and the eluent was removed by vacuum centrifugation. The pellets were dissolved in water to 1 mg/mL

and showed high purity (> 95 %, Figure 1C, Table 2). Yield was typically above 50 % for both VHH types. Lot #3 of VHH ENH conjugate was collected using a fraction collector and had a lower yield (27 %). Furthermore, slightly increased turbidity was measured during UV-quantification ($A_{350\ nm,\ 10\ mm}$ = 0.06 for lot #3 and < 0.02 for lot #2 and #3). VHH ENH is known for its ability to increase the fluorescence intensity of eGFP upon binding [21].This characteristic was employed as tool to test whether the isolated, lipidated VHH ENH recognize and bind its target protein comparably to the native VHH ENH. Native VHH ENH increased the fluorescence intensity by a factor of 1.9. No significant differences ($p > 0.3$) in fluorescence intensity increase were obtained comparing lot # 1, lot #2 of the isolated, lipidated VHH ENH and the native VHH ENH (Figure 1D). Lot #3 showed a lower increase in fluorescence ($p = 0.013$). It may be that lack of cooling of the column effluent in the AFC is responsible for lower yield and loss of activity of lot #3.

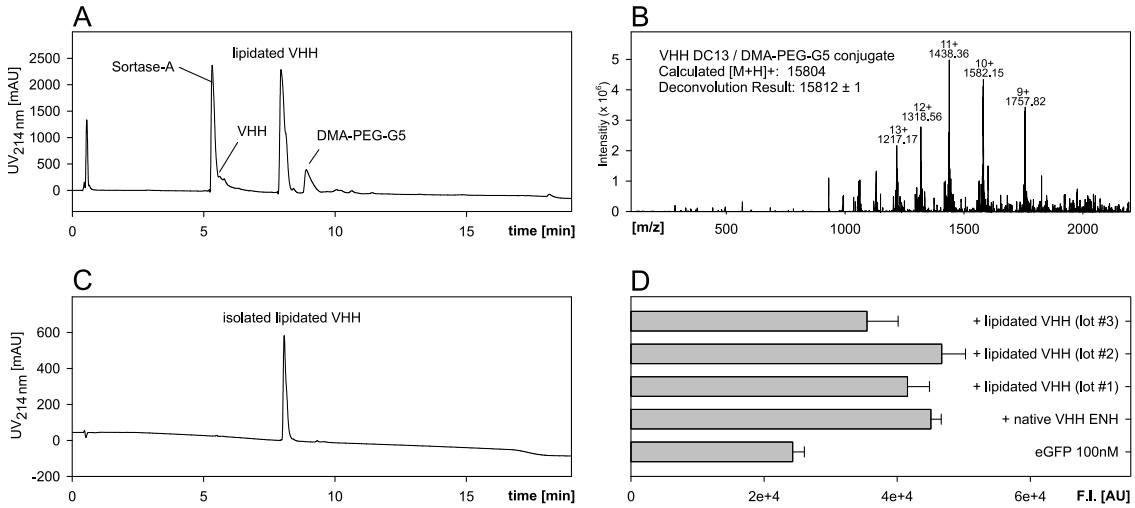

Figure 1: **A**: rp-HPLC analysis of reaction bulk containing Sortase-A, LPETG-modified VHH ENH, the lipidated VHH ENH and unconjugated DMA-PEG-G5. **B**: ESI-MS verification of VHH DC13 lipidation. Target mass was calculated as native VHH mass plus lipid mass minus mass of the his-tag cleaved off from the native VHH during transpeptidation (GGH_6, 955 Da). **C**: rp-HPLC of the isolated lipidated VHH ENH revealed high purity of the final product. **D**: Activity of VHH ENH after lipidation. Either native or conjugated and isolated VHH ENH bound eGFP and increased its fluorescence signal at 525 nm after excitation at 485 nm (mean ± standard deviation, n=3).

Table 2: Isolation of lipidated VHHs via rp-HPLC.

conjugate	purity [area%]	yield
VHH ENH lot #1	96 %	50 %
VHH ENH lot #2	97 %	52 %
VHH ENH lot #3	95 %	27 %
VHH DC13 lot #1	97 %	60 %

4.2. VHH insertion in liposomal bilayers

It was of interest whether the VHH can be anchored in membranes after the Sortase-A mediated lipidation. Therefore, dipalmitoyl-phosphatidylcholine-based, fluorophore-labeled liposomes (d_h = 149 nm, PDI = 0.23) were used as artificial membrane system [25]. The liposomes were incubated above the phase transition temperature of the lipid blend (determined to be 42 °C by

differential scanning calorimetry) at 50 °C for 30 min either with lipidated VHH ENH or VHH DC13 at different VHH to phospholipid ratios (Figure 2A). Dynamic light scattering was used to investigate influence of membrane insertion on the d_h of the dispersion. An increase of d_h with increasing ligand density of up to 20 nm at 2 nM VHH / µM PL was observed for VHH DC13-modified liposomes (Figure 2A, bars), indicating insertion of the ligand into the liposomal membrane. Since the PDI (Figure 2A, dots) did not change during the incubation process, the ligand insertion had no negative impact on the polydispersity of the dispersion.

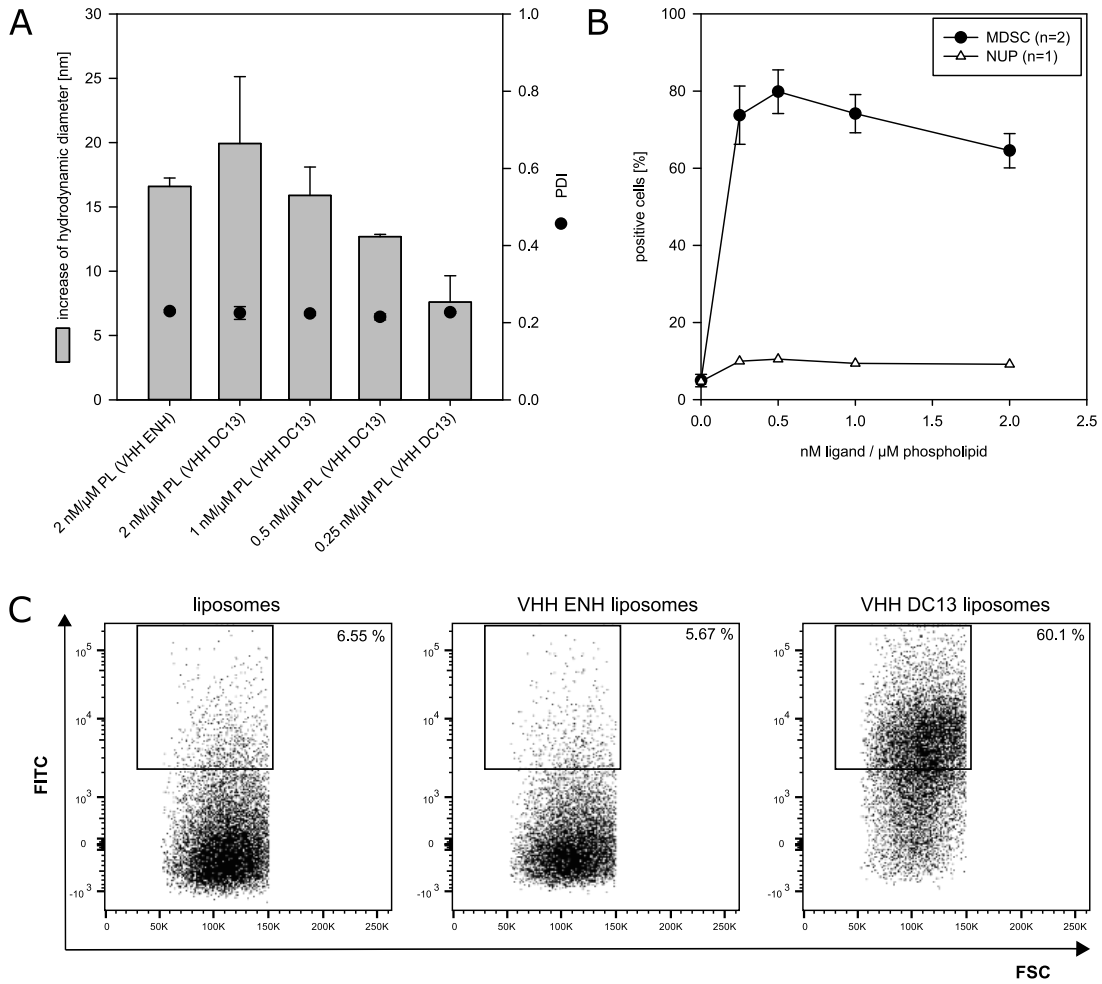

Figure 2: Liposome modification with lipidated VHHs and cellular binding. **A**: Post-insertion of lipidated VHHs monitored by dynamic light scattering. Slight increases in liposome diameter were observed depending on targeting ligand density (error bars indicate standard deviations of triplicate measurements; PL: phospholipid)). **B**: Influence of ligand density on cellular binding of VHH DC13-modified liposomes on myeloid-derived suppressor cells. Error bars indicate range of two experiments. **C**: Flow cytometry dot plots of binding of unmodified liposomes, isotype control (VHH ENH) and CD11b-targeted VHH DC13 liposomes (2 nM/µM phospholipid) towards MDSC. Detection of liposome binding using liposome-encapsulated FITC-dextran. The number within each dot plot indicates the percentage of events within the marked gate.

To investigate whether post-inserted VHH DC13 can target liposomes towards $CD11b^+$ cells, the ligand-modified, FITC-dextran-labeled liposomes were incubated with $CD11b^-$ NUP cells or $CD11b^+$ MDSC for 4 h at 4 °C. NUP cells are MDSC progenitors that can be differentiated to express MDSC characteristic surface markers (CD11b and Gr-1) [26]. Binding towards these off-target cells occurred only to a negligible extent and independent of the VHH DC13 density

on the liposomes (Figure 2B). Compared to that, a significant binding (> 60 % FITC-positive cells) was observed for all VHH DC13-modified liposomes on $CD11b^+$ MDSC. The binding efficiency was ligand-density dependent with a maximum at 0.5 nM VHH per µM phospholipid. VHH-free liposomes or VHH ENH isotype control liposomes did not stain cells to a relevant degree (< 4 %, Figure 2B and C). This indicates the specificity of the binding of VHH DC13-modified liposomes towards $CD11b^+$ MDSC.

4.3. Display of lipidated VHHs on cells

It was in question whether the lipidated VHHs can also interact with biological membranes of living cells. It was therefore tested if lipidated VHH ENH or VHH DC13 can associate with cellular membranes of $CD11b^+$ MDSC or $CD8^+$ T cells. MDSC were found positive for lipidated VHH ENH, as detected with a FITC-labeled antibody against llama antibody epitopes after incubation of lipidated VHH ENH and cells (Figure 3A).

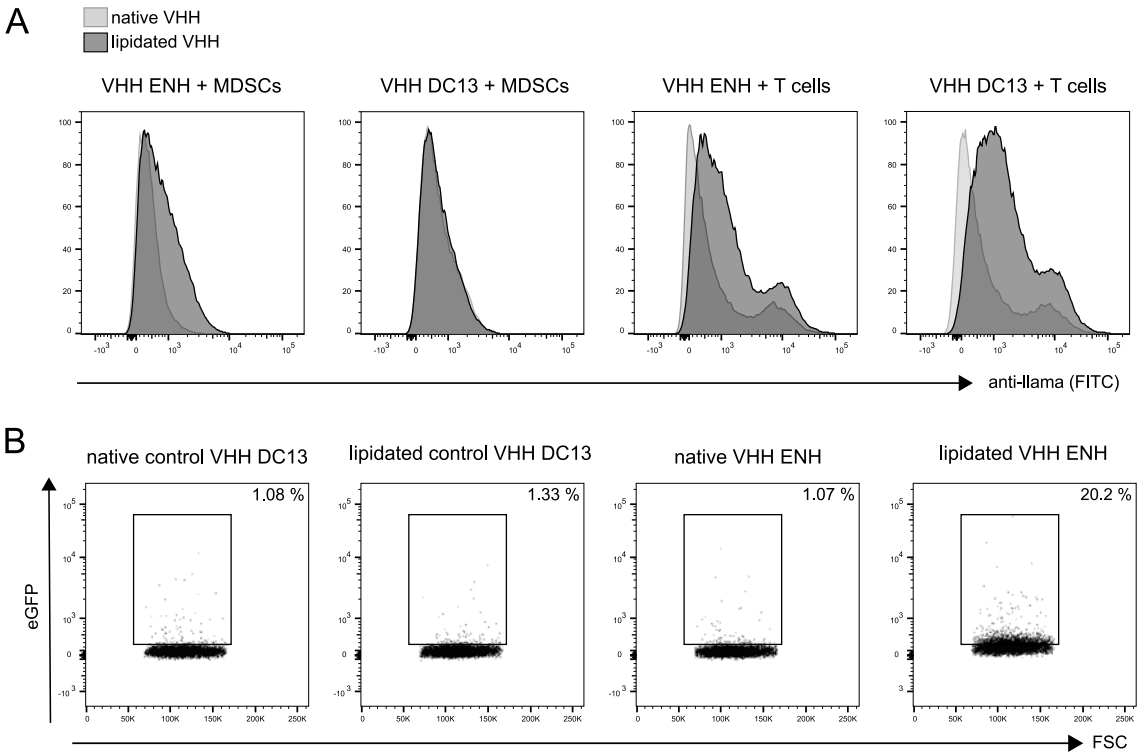

Figure 3: Display of lipidated VHHs on cell membranes. **A**: Display of lipidated VHH ENH and VHH DC13 on MDSC and T cells. Detection by FITC-anti-llama antibody. **B**: Antigen capturing ability of native and lipidated VHH ENH in cell membranes of MDSC compared with native and lipidated control VHH DC13. Detection of eGFP (intrinsic fluorescence) binding to MDSC. The number within each dot plot indicates the percentage of events within the marked gate.

Unspecific cell association of native VHH occurred only to a negligible degree, as no difference of native VHH and buffer control without VHH was observed (data not shown). Incubation with lipidated and native VHH DC13 with CD11b expressing MDSC resulted in detection of VHH DC13 by anti-llama antibody without differences (Figure 3A). The binding to its antigen masked the

potential additional insertion of lipidated VHH in the cell membrane. Compared to that, a successful display of both lipidated VHHs on CD11b$^-$ T cells was detected (Figure 3A).

It was in question whether the VHH-engineered cells can capture the VHH-corresponding antigen. Therefore, MDSC were incubated with 500 nM of lipidated VHH ENH, followed by incubation with eGFP (Figure 3B). The VHH ENH-modified cells bound to eGFP by obtaining a significant eGFP signal in flow cytometry (20 % positive cells). Control groups included cells which had been incubated with native VHH ENH or native or lipidated VHH DC13, serving here as a non-binding VHH. All showed an approximately 20fold lower eGFP-signal.

4.4. Lipidated VHH DC13 promotes supraphysiological cell-cell interaction

The enforcement of cellular accumulations in desired tissues through cell membrane engineering may offer novel therapeutic approaches, e.g. in adoptive cell therapies. It was therefore investigated whether the lipidated VHH DC13 can promote cellular interaction between MDSC and T cells. For that, murine T cells were isolated using ferromagnetic CD8 affinity beads for MACS. The isolated T cells were modified with lipidated VHH DC13 or controls, further incubated with CD11b$^+$ MDSC and again separated via MACS utilizing CD8 affinity beads present on the cell surface. The CD8$^+$ retentate was stained for CD11b and Gr-1 with fluorophore-labeled antibodies and analyzed by flow cytometry (Figure 4).

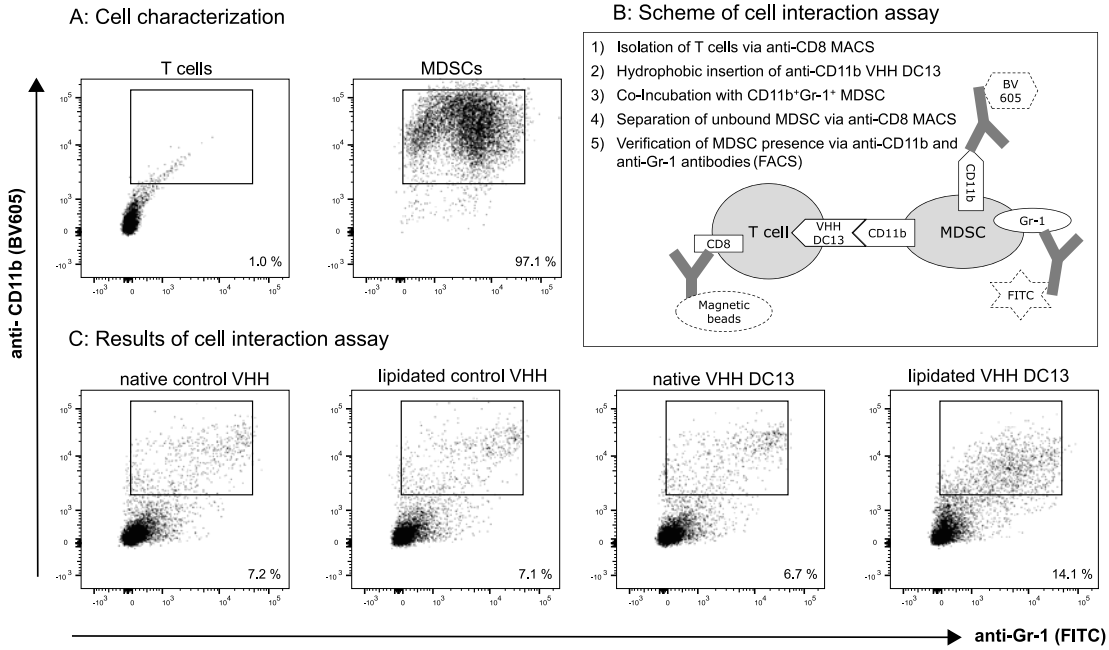

Figure 4: Lipidated VHH DC13 promotes T cell-MDSC interaction. **A**: T cells and MDSC were stained by anti-CD11b and anti-Gr-1 antibodies for flow cytometry analysis. Both markers are expressed only by MDSC. **B** and **C**: CD8$^+$CD11b$^-$Gr-1$^-$ T cells were labeled by anti-CD8 ferromagnetic beads for MACS isolation. Isolated T cells were incubated with lipidated anti-CD11b VHH DC13 or controls (native VHH ENH, lipidated VHH ENH, native VHH DC13), followed by incubation with CD11b$^+$Gr-1$^+$ MDSC and again purified by MACS isolation. CD8$^+$ retentate was stained for CD11b and Gr-1 and analyzed by flow cytometry. Cellular populations pre-incubated with lipidated VHH DC13 caused higher signals for MDSC in the LS column retentate, indicating that VHH DC13 promoted cellular interaction between MDSC and T cells. Percentages given in the dot plots indicate the fraction of cells in CD11b$^+$ / Gr-1$^+$ subset.

This two-dimensional approach of MACS and FACS enabled the detection of the interaction between $CD8^+$ T cells and $CD11b^+$ MDSC mediated by the inserted lipidated VHH. As expected, isolated, single T cells hardly showed any CD11b or Gr-1 expression compared to MDSC (Figure 4A). T cells which were incubated with either native or lipidated control VHH or native VHH DC13 showed a subset of approximately 7 % positive cells which were retained by the column on the magnet, probably due to unspecific cell-column interaction (Figure 4C). This subset doubled to 14 % $CD11b^+Gr\text{-}1^+$ events when the T cells were pre-treated with lipidated VHH DC13. This indicates that lipidated anti-CD11b VHH DC13 was efficiently inserted into cell membranes of T cells, and that the paratope region of DC13 was further sterically accessible for interaction with the $CD11b^+$ MDSC.

5. Discussion

The results reported in this study reveal important perspectives for the use of lipidated single-domain antibodies for membrane engineering. The lipidation of proteins is a challenging step, as heterogeneity of the reaction product is strongly dependent on the applied ligation method. Most protein modification reactions are chemically-based, making use of amino acid side chains to be conjugated either directly or after a preceding activation step towards the lipid. These activations include introduction of sulfhydryl groups by simple reduction [27] or thiolation reagents [28], oxidation of hydroxyl groups from carbohydrate, serine or threonine to aldehydes [29] or frequently used carboxylic-acid activation by 1-ethyl-3-(3-dimethylaminopropyl)-carbodiimide (EDC) [30]. However, reaction conditions and lack of site-specificity may influence paratope regions going along with affinity losses, stability issues and finally a heterogeneous product profile due to a huge and undefined number of lipid molecules per protein [31]. Heterogeneous product profiles were revealed as critical safety hurdle in the design of antibody-drug conjugates [16] and led to increased research efforts in development of site-specific conjugation techniques [32, 33]. Amongst them, Sortase-A transpeptidase is established as versatile “swiss army” promoting chemo-selective, bioorthogonal conjugation between C-terminal LPxTG-modified and N-terminal glycine-carrying peptides or proteins [17]. This technology was previously used by Antos et al. to ligate via 1 % (w/v) n-dodecyl maltoside solubilized triglycine-lipid nucleophiles to LPETG-modified eGFP with good yields between 60-90 % [15]. The lipidated eGFP molecules did then readily insert into HeLa cells with an increasing efficiency with increase in lipid tail length. Compared to that study, the here presented PEGylated dimyristyl anchor has good aqueous solubility, hence detergents were omitted without the risk of product precipitation. Antos et al. further reported the removal of His_6-tagged Sortase-A via a Ni-NTA resin, and also non-conjugated substrate protein (the His_6-tag

is cleaved during the transpeptidation reaction). Although this is a very gentle approach to remove enzyme and non-tagged protein, such a strategy disregards purification from non-conjugated lipid. Reversed-phase HPLC was previously described for the isolation of lipopeptides [34]. Therefore rp-HPLC was here chosen for product purification from Sortase-A, unreacted VHH and pentaglycine lipid. We used an analytical chromatographic system and column for purification of low volume (400 µL) and minimal mass (320 µg) batch sizes, which was found to be suitable for protein handling in early research (product yields from conjugation and subsequent purification were above 50 %). The reaction and purification process did not impact the binding of the model VHH ENH to its corresponding antigen eGFP. This was demonstrated by an equal ability of both native and lipidated VHH to increase the fluorescence of eGFP, as long the column effluent was treated under cooled conditions during conjugate purification.

The isolated VHH-lipid conjugates were inserted into the artificial bilayer of a liposomal drug delivery system [25]. This "post-insertion" technique enables a combinatorial approach to derivatize non-targeted liposomes into immunoliposomes. This is very suitable for small-scale screenings in lab-scale. Furthermore, it opens the perspective towards patient-individual or stratified nanomedicine. Here, a bulk of drug-loaded liposomes may be transformed to different immunoliposomal formulations without the need of separate manufacturing lines [35, 36]. We incubated FITC-labeled liposomes with various concentrations of the micellar ligand dispersion and found an increasing hydrodynamic diameter dependent on the ligand density (Figure 2A). Size increase of liposomes is known from the insertion of PEG-derivatized distearyl-phosphoethanolamine [37], where 2-16 nm net diameter increases were reported, related to the molar fraction of the applied PEGylated lipid and the resulting PEG-conformation at the bilayer. Sterically stabilized liposomes containing 6 % PEG-lipids (2 kDa) previously showed a size increase of 32-36 nm when modified with PEG-spaced full-length antibodies [38]. Compared to that, lower absolute diameter increases were found here which ranged from 8-20 nm with increasing ligand density. We attribute this increase in part to the additional VHH-layer on the liposomes, whose dimensions are about 2.5 x 4 nm and hence significantly smaller than a full length antibody of 8.5 x 14.2 nm [19]. Furthermore, additional conformational changes of the PEG-pentaglycine groups in our formulation may occur upon insertion of the PEGylated ligand. The binding efficacy to $CD11b^+$ MDSC had a ligand-density dependent maximum at 0.5 nM VHH per µM phospholipid (Figure 2B). Latter corresponds to ≈129 VHHs per liposome, calculated from the assumption of an average lipid headgroup area of 0.6 nm^2, the lipid concentration and the d_h of the unmodified liposomes. Effective targeting at comparable ligand densities between 0.2-0.7 nM / µM PL was described for Fab', scFv or mAb ligands on doxorubicin-loaded liposomes. Those were targeted against CD19 on human B cells and exhibited good activity

against raji-tumors in mice [35, 39]. The binding maximum at 0.5 nM VHH / µM PL (Figure 2B) may be explained by a steric interaction and a subsequent hindrance of paratope-epitope interaction between liposome and cell if a higher density is applied [40]. Furthermore, there may be a fraction of lipidated DC13 which did not integrate into the liposome and may therefore decrease the availability of free CD11b receptors on the cellular surfaces. A thorough optimization of the ligand density on the drug delivery system was not purpose of this study. Instead, it should be noted that here described post-insertion offers several advantages over previously reported, on-site sortagging of ligands to liposomes [25, 41-44]. As one can expect high insertion rates (> 80 % in liposomes with a PEGylation degree below 2 mol%) for lipidated ligands [38], subsequent purification steps to remove unbound ligands are not necessary. This enables minimization of batch sizes, what is extremely helpful in early research phases, since experiments can be conducted without regard to device design of dialysis chambers or ultracentrifugation filter devices. Furthermore, Sortase-A has no contact to the drug delivery system itself. This is highly appreciated, since large-surface nanoparticle dispersions are known to adsorb proteins in relevant quantities in an unspecific fashion, hence making complete enzyme removal challenging. Such Sortase-A residuals may cause immunogenic reactions or stability issues due to the enzymatic reverse reaction [17, 25, 43].

Besides the above discussed display of lipidated eGFP on cells [15], Sortase technology was used to attach functional proteins on living cells. Tomita et al. inserted a triglycine bearing lipid in murine thymoma cells (E.G7), which was then conjugated to a LPETG-modified Fc domain via Sortase-A [7]. The so modified tumor cells underwent a fourfold higher phagocytosis rate after co-culture with dendritic cells [7]. In a very recent study, Pishesha et al. used CRISPR/Cas9 to genetically introduce a LPETG-motif in the Kell-protein of red blood cells (RBC) in a murine germ line. The RBCs were then sortagged with various disease-associated autoantigens, and autologous treatment with those cells protected the mice against the respective autoimmune disease (encephalomyelitis, diabetes type 1) [11]. Swee et al. utilized a biotinylated LPETG-probe to firstly investigate the general sortagging feasibility of endogenous, exposed glycine residues on various cells. The authors reported that presumably most cells have glycines that are amenable for sortagging [14]. This sheds light on bioorthogonality of Sortase-A reaction, which is per se a site-specific reaction for the LPETG-carrying educt, however loses specificity in living systems where alternative nucleophiles such as endogenous proteins with N-terminal glycines are ubiquitously present. The authors further demonstrated that grafting a VHH specific for murine class-II MHC on activated T cells led to a specific, VHH-density related killing of MHC-II^{+} B cells, but not of MHC-II^{-} CD4 T cells. This indicated a cellular redirection of cytotoxic T cells to the lymphocytes via the VHH. Similar results were obtained by Shi et al., who directed red blood

cells (RBCs) equipped with the same VHH towards B cells [13]. In the study presented here, MDSC were successfully remodeled with the lipidated VHH ENH specific for eGFP. Compared to that, the lipidated VHH DC13 specific for the MDSC epitope CD11b did not show a superior presence on the MDSC surface compared to its native form. This is most likely due to the predominant binding between antibody and antigen, which masks the membrane insertion process. Although the lipidated VHH ENH was detected on the MDSC surface with a FITC-anti-llama antibody, the activity of the paratope regions after cell insertion was unknown. It was therefore tested whether the VHH ENH-functionalized MDSC can capture the corresponding antigen eGFP. A specific binding of eGFP to VHH ENH-modified MDSC was found by flow cytometry. This shows that the paratope regions remain accessible for soluble target proteins on cellular surfaces after membrane insertion, hence enabling artificial interactions between proteins and cells.

Besides MDSC, also T cells were successfully remodeled with the lipidated VHH ENH and VHH DC13. T cells which displayed VHH DC13 showed association with $CD11b^{+}Gr\text{-}1^{+}$ MDSC in a co-incubation assay. A functional cytotoxicity read-out (which would have required activated T cells) was not focus of the study here. Both MDSC and T cells rather served as model cell types to demonstrate an artificial cell-cell interaction introduced by hydrophobic insertion of lipidated VHHs, and that this process has decisive advantages over the “on-cell” sortagging approach demonstrated in the above explained studies [13, 14]. Firstly, reaction with various endogenous available glycines is obviated, since the enzyme has no contact to cells. This avoids formation of unspecific reaction products and alleviates hazards through auto-immunogenic response or impairment of cellular functions. Also, no removal of Sortase-A from the cells is required. This is especially useful for clinical application, where additional steps such as enzyme depletion in cell preparations for autologous therapies increase risks and costs of such procedures. Furthermore, risk of immunogenic reactions against potential Sortase-A residuals is drastically reduced. Hydrophobic insertion of a lipidated ligand is a rapid process [10] and is most likely easier to control than on-site reactions on genetically introduced LPETG-motifs [11, 13] or endogenous glycines [14]. Usage of lipidated ligands may therefore offer a better control of the density on the cells. Additionally, no genetic modification of cells is required. This is particularly suitable for therapies requiring only temporary modifications of the cell surface and avoids risks related to genetic engineering, such as *de novo* tumorigenesis. Therapeutic areas with a promising applicability to hydrophobic insertion-based cell membrane engineering include, besides the already discussed treatment of autoimmune diseases [11], cancer immunotherapy or regenerative medicine. Tang et al. reported an increased therapeutic index when a interleukin-15 superagonist was administered as nanogel immobilized via an anti-CD45 antibody

on T cells [8]. This led to increased tumor clearance by (CAR)-T cell therapies *in vivo*. Hydrophobic insertion of interleukins may be an important alternative due to the straightforward manufacturability and therewith related lower safety and regulatory hurdles. In order to improve the treatment of myocardial infarctions in a regenerative manner, Won et al. conjugated a recombinant CXC chemokine receptor 4 (CXCR4) to PEGylated lipids and modified the surface of mesenchymal stem cells (MSC) [10]. This improved the migration of the MSCs in an *in vitro* assay, thus potentially increasing the homing of MSCs to ischemic sites in the myocardium [1]. Since CXCR4 possesses 8 cysteines which are accessible for reaction with the utilized maleimide linker, several structural isomers of lipidated CXCR4 or multiple-conjugated species can be expected after lipid modification [10]. These may have different biological activities or may interact in different manner with the cellular bilayer, leading to different steric accessibilities of the binding regions. Such heterogeneity may be mitigated with the here proposed bioorthogonal conjugation strategy. Further therapeutic objectives of hydrophobically inserted compounds on cells include the combination of cell-based immunotherapy and antibody-drug conjugates [45] or diagnostic approaches like cell tracking using membrane-inserted contrast agents [9]. Also the immobilization of enzymes on cells may be a promising application for the here proposed protein lipidation and membrane insertion process, since an islet surface modification with urokinase suppressed an islet graft loss after transplantation [12].

6. Conclusion

A concept to attach a PEGylated dimyristyl-motif on single-domain antibodies (VHH) by means of Sortase-A is presented. The water-soluble, lipidated VHH was successfully inserted into the artificial bilayer of liposomes, which led to a targeting of the drug delivery system towards antigen-positive cells. Furthermore, the lipidated VHHs successfully remodeled the cell surface of myeloid-derived suppressor cells and T cells. T cells that carried an anti-CD11b VHH were redirected towards $CD11b^+$ myeloid-derived suppressor cells. Since the installation of the lipidated ligand worked reliably on the different bilayer and cell types, the presented anchor and conjugation system opens the door for display of other functional proteins on cells or bilayer-based drug delivery systems.

References

[1] D.Y. Lee, B.-H. Cha, M. Jung, A.S. Kim, D.A. Bull, Y.-W. Won, Cell surface engineering and application in cell delivery to heart diseases, Journal of Biological Engineering, 12 (2018) 28.

[2] P.Y. Li, Z. Fan, H. Cheng, Cell Membrane Bioconjugation and Membrane-Derived Nanomaterials for Immunotherapy, Bioconjugate Chemistry, 29 (2018) 624-634.

[3] J. Curran Kevin, J. Pegram Hollie, J. Brentjens Renier, Chimeric antigen receptors for T cell immunotherapy: current understanding and future directions, The Journal of Gene Medicine, 14 (2012) 405-415.

[4] S. Hacein-Bey-Abina, C. Von Kalle, M. Schmidt, M.P. McCormack, N. Wulffraat, P. Leboulch, A. Lim, C.S. Osborne, R. Pawliuk, E. Morillon, R. Sorensen, A. Forster, P. Fraser, J.I. Cohen, G. de Saint Basile, I. Alexander, U. Wintergerst, T. Frebourg, A. Aurias, D. Stoppa-Lyonnet, S. Romana, I. Radford-Weiss, F. Gross, F. Valensi, E. Delabesse, E. Macintyre, F. Sigaux, J. Soulier, L.E. Leiva, M. Wissler, C. Prinz, T.H. Rabbitts, F. Le Deist, A. Fischer, M. Cavazzana-Calvo, LMO2-Associated Clonal T Cell Proliferation in Two Patients after Gene Therapy for SCID-X1, Science, 302 (2003) 415.

[5] M. Ruella, J. Xu, D.M. Barrett, J.A. Fraietta, T.J. Reich, D.E. Ambrose, M. Klichinsky, O. Shestova, P.R. Patel, I. Kulikovskaya, F. Nazimuddin, V.G. Bhoj, E.J. Orlando, T.J. Fry, H. Bitter, S.L. Maude, B.L. Levine, C.L. Nobles, F.D. Bushman, R.M. Young, J. Scholler, S.I. Gill, C.H. June, S.A. Grupp, S.F. Lacey, J.J. Melenhorst, Induction of resistance to chimeric antigen receptor T cell therapy by transduction of a single leukemic B cell, Nature Medicine, 24 (2018) 1499-1503.

[6] W.-y. Zhang, Y. Liu, Y. Wang, J. Nie, Y.-l. Guo, C.-m. Wang, H.-r. Dai, Q.-m. Yang, Z.-q. Wu, W.-d. Han, Excessive activated T-cell proliferation after anti-CD19 CAR T-cell therapy, Gene Therapy, 25 (2018) 198-204.

[7] U. Tomita, S. Yamaguchi, Y. Maeda, K. Chujo, K. Minamihata, T. Nagamune, Protein cell-surface display through in situ enzymatic modification of proteins with a poly(Ethylene glycol)-lipid, Biotechnology and Bioengineering, 110 (2013) 2785-2789.

[8] L. Tang, Y. Zheng, M.B. Melo, L. Mabardi, A.P. Castaño, Y.-Q. Xie, N. Li, S.B. Kudchodkar, H.C. Wong, E.K. Jeng, M.V. Maus, D.J. Irvine, Enhancing T cell therapy through TCR-signaling-responsive nanoparticle drug delivery, Nature Biotechnology, 36 (2018) 707.

[9] K.S. Lim, D.Y. Lee, G.M. Valencia, Y.-W. Won, D.A. Bull, Cell surface-engineering to embed targeting ligands or tracking agents on the cell membrane, Biochemical and Biophysical Research Communications, 482 (2017) 1042-1047.

[10] Y.-W. Won, A.N. Patel, D.A. Bull, Cell surface engineering to enhance mesenchymal stem cell migration toward an SDF-1 gradient, Biomaterials, 35 (2014) 5627-5635.

[11] N. Pishesha, A.M. Bilate, M.C. Wibowo, N.-J. Huang, Z. Li, R. Deshycka, D. Bousbaine, H. Li, H.C. Patterson, S.K. Dougan, T. Maruyama, H.F. Lodish, H.L. Ploegh, Engineered erythrocytes covalently linked to antigenic peptides can protect against autoimmune disease, Proceedings of the National Academy of Sciences, 114 (2017) 3157.

[12] N. Takemoto, Y. Teramura, H. Iwata, Islet Surface Modification with Urokinase through DNA Hybridization, Bioconjugate Chemistry, 22 (2011) 673-678.

[13] J. Shi, L. Kundrat, N. Pishesha, A. Bilate, C. Theile, T. Maruyama, S.K. Dougan, H.L. Ploegh, H.F. Lodish, Engineered red blood cells as carriers for systemic delivery of a wide array of functional probes, Proceedings of the National Academy of Sciences, 111 (2014) 10131.

[14] L.K. Swee, S. Lourido, G.W. Bell, J.R. Ingram, H.L. Ploegh, One-Step Enzymatic Modification of the Cell Surface Redirects Cellular Cytotoxicity and Parasite Tropism, ACS Chemical Biology, 10 (2015) 460-465.

[15] J.M. Antos, G.M. Miller, G.M. Grotenbreg, H.L. Ploegh, Lipid Modification of Proteins through Sortase-Catalyzed Transpeptidation, Journal of the American Chemical Society, 130 (2008) 16338-16343.

[16] A.C. Braun, M. Gutmann, T. Lühmann, L. Meinel, Bioorthogonal strategies for site-directed decoration of biomaterials with therapeutic proteins, Journal of Controlled Release, 273 (2018) 68-85.

[17] M. Ritzefeld, Sortagging: A Robust and Efficient Chemoenzymatic Ligation Strategy, Chemistry – A European Journal, 20 (2014) 8516-8529.

[18] S. Wöll, S. Schiller, C. Bachran, L.K. Swee, R. Scherließ, Pentaglycine lipid derivates – rp-HPLC-analytics for bioorthogonal anchor molecules in targeted, multiple-composite liposomal drug delivery systems, International Journal of Pharmaceutics, 547 (2018) 602-610.

[19] S. Oliveira, R. Heukers, J. Sornkom, R.J. Kok, P.M.P.v.B. en Henegouwen, Targeting tumors with nanobodies for cancer imaging and therapy, Journal of Controlled Release, 172 (2013) 607-617.
[20] K. Tatsumi, K. Ohashi, Y. Teramura, R. Utoh, K. Kanegae, N. Watanabe, S. Mukobata, M. Nakayama, H. Iwata, T. Okano, The non-invasive cell surface modification of hepatocytes with PEG-lipid derivatives, Biomaterials, 33 (2012) 821-828.
[21] A. Kirchhofer, J. Helma, K. Schmidthals, C. Frauer, S. Cui, A. Karcher, M. Pellis, S. Muyldermans, C.S. Casas-Delucchi, M.C. Cardoso, Modulation of protein properties in living cells using nanobodies, Nature Structural & Molecular Biology, 17 (2010) 133-138.
[22] M. Rashidian, E.J. Keliher, A.M. Bilate, J.N. Duarte, G.R. Wojtkiewicz, J.T. Jacobsen, J. Cragnolini, L.K. Swee, G.D. Victora, R. Weissleder, H.L. Ploegh, Noninvasive imaging of immune responses, Proceedings of the National Academy of Sciences of the United States of America, 112 (2015) 6146-6151.
[23] C. Bachran, M. Schröder, L. Conrad, J.J. Cragnolini, F.G. Tafesse, L. Helming, H.L. Ploegh, L.K. Swee, The activity of myeloid cell-specific VHH immunotoxins is target-, epitope-, subset- and organ dependent, Scientific Reports, 7 (2017) 17916.
[24] M. Rashidian, E.J. Keliher, A.M. Bilate, J.N. Duarte, G.R. Wojtkiewicz, J.T. Jacobsen, J. Cragnolini, L.K. Swee, G.D. Victora, R. Weissleder, H.L. Ploegh, Noninvasive imaging of immune responses, Proceedings of the National Academy of Sciences, 112 (2015) 6146-6151.
[25] S. Wöll, C. Bachran, S. Schiller, M. Schröder, L. Conrad, L.K. Swee, R. Scherließ, Sortaggable liposomes: Evaluation of reaction conditions for single-domain antibody conjugation by Sortase-A and targeting of CD11b+ myeloid cells, European Journal of Pharmaceutics and Biopharmaceutics, 133 (2018) 138-150.
[26] M. Schröder, S. Loos, S.K. Naumann, C. Bachran, M. Krötschel, V. Umansky, L. Helming, L.K. Swee, Identification of inhibitors of myeloid-derived suppressor cells activity through phenotypic chemical screening, OncoImmunology, 6 (2017) e1258503.
[27] F.J. Martin, D. Papahadjopoulos, Irreversible coupling of immunoglobulin fragments to preformed vesicles. An improved method for liposome targeting, Journal of Biological Chemistry, 257 (1982) 286-288.
[28] J.T.P. Derksen, G.L. Scherphof, An improved method for the covalent coupling of proteins to liposomes, Biochimica et Biophysica Acta (BBA) - Biomembranes, 814 (1985) 151-155.
[29] E. Moles, S. Galiano, A. Gomes, M. Quiliano, C. Teixeira, I. Aldana, P. Gomes, X. Fernàndez-Busquets, ImmunoPEGliposomes for the targeted delivery of novel lipophilic drugs to red blood cells in a falciparum malaria murine model, Biomaterials, 145 (2017) 178-191.
[30] N. Nakajima, Y. Ikada, Mechanism of Amide Formation by Carbodiimide for Bioconjugation in Aqueous Media, Bioconjugate Chemistry, 6 (1995) 123-130.
[31] A.N. Lukyanov, T.A. Elbayoumi, A.R. Chakilam, V.P. Torchilin, Tumor-targeted liposomes: doxorubicin-loaded long-circulating liposomes modified with anti-cancer antibody, Journal of Controlled Release, 100 (2004) 135-144.
[32] N. Jain, S.W. Smith, S. Ghone, B. Tomczuk, Current ADC Linker Chemistry, Pharmaceutical Research, 32 (2015) 3526-3540.
[33] K. Tsuchikama, Z. An, Antibody-drug conjugates: recent advances in conjugation and linker chemistries, Protein & Cell, 9 (2016) 33-46.
[34] L. Bourel-Bonnet, H. Gras-Masse, O. Melnyk, A novel family of amphilic α-oxo aldehydes for the site-specific modification of peptides by two palmitoyl groups in solution or in liposome suspensions, Tetrahedron Letters, 42 (2001) 6851-6853.
[35] D.L. Iden, T.M. Allen, In vitro and in vivo comparison of immunoliposomes made by conventional coupling techniques with those made by a new post-insertion approach, Biochimica et Biophysica Acta (BBA)-Biomembranes, 1513 (2001) 207-216.
[36] M. Oswald, S. Geissler, A. Goepferich, Determination of the activity of maleimide-functionalized phospholipids during preparation of liposomes, International Journal of Pharmaceutics, 514 (2016) 93-102.
[37] P.S. Uster, T.M. Allen, B.E. Daniel, C.J. Mendez, M.S. Newman, G.Z. Zhu, Insertion of poly(ethylene glycol) derivatized phospholipid into pre-formed liposomes results in prolonged in vivo circulation time, FEBS Letters, 386 (1996) 243-246.
[38] T. Ishida, D.L. Iden, T.M. Allen, A combinatorial approach to producing sterically stabilized (Stealth) immunoliposomal drugs, FEBS Letters, 460 (1999) 129-133.

[39] W.W.K. Cheng, T.M. Allen, Targeted delivery of anti-CD19 liposomal doxorubicin in B-cell lymphoma: A comparison of whole monoclonal antibody, Fab' fragments and single chain Fv, Journal of Controlled Release, 126 (2008) 50-58.
[40] B. Saha, T.H. Evers, M.W. Prins, How antibody surface coverage on nanoparticles determines the activity and kinetics of antigen capturing for biosensing, Analytical chemistry, 86 (2014) 8158-8166.
[41] X. Guo, Z. Wu, Z. Guo, New method for site-specific modification of liposomes with proteins using sortase A-mediated transpeptidation, Bioconjugate Chemistry, 23 (2012) 650-655.
[42] A. Tabata, N. Anyoji, Y. Ohkubo, T. Tomoyasu, H. Nagamune, Investigation on the Reaction Conditions of Staphylococcus aureus Sortase A for Creating Surface-modified Liposomes as a Drug-delivery System Tool, Anticancer Research, 34 (2014) 4521-4527.
[43] S. Wöll, C. Bachran, S. Schiller, M. Schröder, L. Conrad, R. Scherließ, L.K. Swee, Sortagging of liposomes with a murine CD11b-specific VHH increases in vitro and in vivo targeting specificity of myeloid cells, European Journal of Pharmaceutics and Biopharmaceutics, 134 (2019) 190-198.
[44] S. Wöll, S. Dickgiesser, N. Rasche, S. Schiller, R. Scherließ, Sortagged anti-EGFR immunoliposomes exhibit increased cytotoxicity on target cells, European Journal of Pharmaceutics and Biopharmaceutics, 136 (2019) 203-212.
[45] D.Y. Lee, K.S. Lim, G.M. Valencia, M. Jung, D.A. Bull, Y.-W. Won, One-Step Method for Instant Generation of Advanced Allogeneic NK Cells, Advanced Science, 5 (2018) 1800447.

Chapter 6

Manufacturing and cytotoxicity of *Pseudomonas* exotoxin A-loaded immunoliposomes

Abstract

Purpose: *Pseudomonas* exotoxin A, more precisely it's subunit PE38, is a potent cytotoxin. It may effectively suppress distinct cell populations, such as cancer cells or immune cells if delivered cell-specifically to the cytosol. Here, different actively targeted liposomal drug delivery systems (immunoliposomes) are evaluated for the specific PE38 delivery to murine $CD11b^{+}Gr\text{-}1^{+}$ cells.

Methods: PE38-loaded liposomes differing in surface properties and lipid composition were prepared by the solvent injection method. The PE38-loaded liposomes were conjugated by means of Sortase-A transpeptidation with a single-domain antibody specific for CD11b, a myeloid cell marker. The cytotoxicity of the immunoliposomes was assessed on murine $CD11b^{+}Gr\text{-}1^{+}$ cells.

Results: The preparation of PE38-loaded liposomes by solvent injection was feasible yielding liposomes with hydrodynamic diameters between 141 nm and 162 nm (polydispersity index: < 0.25). Sortase-A modified all formulation concepts with single-domain antibodies as verified by rp-HPLC. None of the constructs exhibited a specific cytotoxic effect on murine $CD11b^{+}Gr\text{-}1^{+}$ cells. Reasons for the lack of toxicity are discussed.

Conclusion: Despite a successful manufacturing of PE38-loaded immunoliposomes and the previously shown proof of targeting with model compounds, no specific cytotoxicity on target cells was achieved. This report therefore describes challenges faced when a cargo is switched from a model to an active ingredient and discusses reasons and further options for formulation improvement.

1. Introduction

Plants, fungi or bacteria can produce highly potent enzymatic cytotoxins whose pharmaceutical application as anti-cancer agents is a desirable aim [1]. Prominent examples are *Pseudomonas* exotoxin A (origin: *Pseudomonas aeruginosa*), diphtheria toxin (origin: *Corynebacterium diphtheriae*), ricin (origin: seeds of *Ricinus communis*) and saporin (origin: *Saponaria officinalis*) [1]. The toxins are enzymes and hence of proteinaceous nature, what hinders them from a passive membrane permeation. Therefore, the toxins are typically composed of several subunits, which possess catalytic, but also cell-binding and internalization-mediating functions [1]. For example, *Pseudomonas* exotoxin A consists in its natural form of four structural domains [2]. Domain Ia and II are responsible for binding the cellular target structure (CD91) and further intracellular processing over the endosome, the Golgi apparatus and the endoplasmic reticulum (ER) [2]. As soon as the catalytic domains Ib and III are delivered from ER to the cytosol, they inhibit the protein biosynthesis by ADP-ribosylation of the eukaryotic elongation factor-2 (eEF-2) at the ribosomes, leading to apoptosis of the host cell [2]. Therapeutic immunotoxins aim at exploiting the high potency of such natural derived toxins while increasing their specificity [1]. For that purpose, the cell-binding domain is replaced through antibodies or their substructures, e.g. via molecular genetic means. Those may bind selected anti-cancer targets with high specificity, leading to an internalization of the toxic domain and subsequently cause cell death.

Despite a proven efficacy in cancer treatment and clinical success of some immunotoxins [3], the maximum parenteral dose is often limited by an unspecific toxicity, e.g. towards to liver cells [4, 5]. Also, immunogenicity is a major concern, related to the development of toxin neutralizing antibodies or strong allergic reactions [4, 5]. Although these drawbacks may partly be alleviated by local, intratumoral administration, such a strategy would only be applicable to solid tumors accessible for external medical interventions (e.g. melanoma [6]). Additionally, laborious administration procedures would likely decrease the patient acceptance towards the therapy and also decrease the pharmacoeconomic efficiency of the potential drug.

Targeted nanoparticulate drug delivery systems may be a promising alternative to counterbalance the prementioned disadvantages [7-9]. The encapsulation of the catalytic domains into a carrier decreases immunogenicity compared to administration of free immunotoxins [7]. Furthermore, drug delivery systems of various formats (such as liposomes or poly(lactic-co-glycolic acid)-based nanoparticles) have demonstrated to decrease unspecific drug toxicity, e.g. for doxorubicin or docetaxel [10, 11]. Active targeting of such drug carriers via

conjugation of disease-specific ligands on the particle-surface aids improvement in target specificity and intracellular delivery of the cargo [12].

Myeloid-derived suppressor cells (MDSC) have been described to decrease immune responses against tumors, hence making the selective killing of such cell populations an attractive target in immuno-oncology [13]. In mice, MDSC are characterized by a $CD11b^{+}Gr\text{-}1^{+}$ phenotype. In this study, a truncated form of *Pseudomonas* exotoxin A (PE38) lacking the cell-binding domain was encapsulated into different liposomal formulations. The liposomes were targeted to $CD11b^{+}Gr\text{-}1^{+}$ cells using a CD11b-specific single-domain antibody [14]. This antibody was conjugated to the liposomes using the site-specific Sortase-A technology, requiring the integration of a pentaglycine-modified lipid in the formulation [15]. The liposomal surface properties such as polyethylene glycol (PEG) presence were altered to investigate the impact on the cytotoxicity of the immunoliposomes. Furthermore, the liposomal lipid composition may have significant influence on the cytosolic delivery of large molecules such as proteins [16]. Therefore, "rigid" liposomes composed of saturated dipalmitoyl-phosphatidylcholine and cholesterol were compared with liposomes composed of a mixture of 2-dioleoyl-sn-glycero-3-phosphotethanolamine (DOPE) and 3β-hydroxy-5-cholestene 3-hemisuccinate (CHEMS). Latter lipids are known for their pH-responsiveness and may exhibit enhanced cytosolic delivery after an endosomal uptake and endo-lysosomal acidification [16-19]. The presented results highlight challenges faced in the transfer of binding studies with fluorophore-labeled liposomes (Chapter 3 and 4) towards the delivery of actually "active" pharmaceutical ingredients.

2. Materials

DMA-PEG-G5 is a pentaglycine-modified lipid suitable for Sortase-A mediated transpeptidation [20]. It was obtained from Merck & Cie (Schaffhausen, Switzerland) and consisted of a dimyristyl-amino-propandiol scaffold (DMA) linked via a 2 kDa PEG spacer to a pentaglycine-motif (G5). 1,2-dipalmitoyl-sn-glycero-3-phosphocholine (DPPC), 1,2-dipalmitoyl-sn-glycero-3-phospho-(1'-rac-glycerol) (DPPG), 2-dioleoyl-sn-glycero-3-phosphotethanolamine (DOPE) and 1,2-distearoyl-sn-glycero-3-phosphoethanolamine-N-[methoxy(polyethylene glycol)-2000] (DSPE-mPEG) were a kind gift of Lipoid GmbH (Ludwigshafen, Germany). 3β-hydroxy-5-cholestene 3-hemisuccinate (CHEMS), Triton X-100, acridine orange and Dulbecco's phosphate buffered saline (DPBS, D1408, 10fold stock) was obtained from Sigma-Aldrich (St. Louis, MO, USA). Water was purified by a Milli-Q system (Merck Millipore, Billerica, MA, USA). LPETG (leucine, proline, glutamic acid, threonine, glycine)-modified single-domain antibodies of camelid heavy-chain only antibodies (VHH) VHH ENH, VHH DC13, Sortase-A variant SortA7m and a truncated variant of *Pseudomonas* exotoxin A (PE38) were provided by BioMed X GmbH (Heidelberg, Germany) and were prepared as described in [14].

3. Methods

3.1. Liposome preparation and ligand conjugation

Liposomes were prepared by solvent injection using a binary pumping system as described in detail in Chapter 3 [21]. Therefore, the following section provides only a brief overview of the applied manufacturing and analytical procedures. Three different liposomal formulations (Table 1) were prepared in DPBS pH 7.4 supplemented with different concentrations of PE38 (Table 2). Alternatively, PEG^{high}-LS were loaded with doxorubicin. The formulation development and manufacturing of these liposomes is described in Chapter 7.

Table 1: Liposomal compositions.

formulation	composition [mol%]
PEG^{high}-LS	DPPC : CHOL : DSPE-mPEG : DMA-PEG-G5 (59.4 : 34.7 : 5.0 : 1.0)
PEG^{low}-LS	DPPC : CHOL : DPPG : DMA-PEG-G5 (59.4 : 34.7 : 5.0 : 1.0)
pH-sensitive-LS	DOPE : CHEMS : DSPE-mPEG : DMA-PEG-G5 (57.6 : 38.4 : 3.0 : 1.0)

Table 2: Liposomal manufacturing parameters (FR: flow rate).

formulation	lipid solvent and total lipid concentration	buffer for injection	FR buffer [mL/min]	FR lipid [mL/min]
PEG^{high}-LS	ethanol (90 mM)	DPBS (0, 0.1 or 2 mg/mL PE38)	80.0	10.0
	ethanol (90 mM)	250 mM $(NH_4)_2SO_4$ pH 5.4 rebuffered to 10 mM HEPES pH 7.0	120.0	10.0
PEG^{low}-LS	ethanol (32 mM)	DPBS (0 or 0.1 mg/mL PE38)	90.0	13.5
pH-sensitive-LS	ethanol (75 mM)	DPBS (0 or 0.5 mg/mL PE38)	80.0	10.0
	ethanol (50 mm)	250 mM $(NH_4)_2SO_4$ pH 9.0 rebuffered to 10 mM HEPES pH 7.4	120.0	15.0

To adjust the mean hydrodynamic diameter of pH-sensitive-LS according to previously described PEG^{high}-LS and PEG^{low}-LS, a flow rate screening was conducted. Finally applied manufacturing parameters can be found in Table 2. After solvent injection, the liposomes were purified and concentrated by TFF (tangential flow filtration, MicroKros® filter module, 500 kDa cut-off, Spectrum Labs, Los Angeles, CA, USA). Subsequently, ligands were conjugated to the liposomes. For that purpose, 100 µM of liposomes (based on pentaglycine lipid content) were incubated with 50 µM VHH and 25 µM Sortase-A at 4 °C. Afterwards, the liposome dispersion was purified using dialysis chambers (Float-A-Lyzer, 1000 kDa cut-off, G235037, Spectrum Labs, Los Angeles, CA, USA).

3.2. Liposome characterization

Lipid-individual content of the different formulations was simultaneously assessed via an rp-HPLC-ELSD method [20]. Hydrodynamic diameter (d_h), polydispersity index (PDI) and zeta potential (zp) were determined by dynamic light scattering (DynaPro Plate Reader II, Wyatt, Santa Barbara, CA, USA) or laser Doppler electrophoresis (Malvern Zetasizer Nano ZS, Worcestershire, UK), respectively. PE38 content was determined after solvent injection and after the sortagging and purification process. An rp-HPLC method based on a C4-column which separated proteinaceous formulation components (residual Sortase-A, VHHs and PE38) and lipid components was utilized (Figure 3, method details described in Chapter 3). Theoretical drug load after injection ($DL_{t;\ a.i.}$) includes the sum of encapsulated and non-encapsulated PE38 and was calculated according to Equation 1.

Equation 1

$$DL_{t;\ a.i.}\ \left[\%\frac{m}{m}\right] = \frac{c_{PE38}(buffer) * FR_{buffer}}{c_{lipid}(organic\ stock) * FR_{lipid}} * 100$$

The actual, measured drug load DL_a was calculated as follows:

Equation 2

$$DL_a\ [\%\frac{m}{m}] = \frac{c_{PE38}\ [\frac{mg}{mL}]}{c_{lipid}[\frac{mg}{mL}]} * 100$$

To estimate the amount of PE38 encapsulated inside the liposome, the interior volume (V_i) of an "ideal" liposome (spherical, unilamellar and monomodal liposomes with a bilayer thickness of 5 nm) was calculated according to Equation 3.

Equation 3

$$V_i\ [mL] = \frac{4}{3} * \pi * \left(\frac{d_h}{2} - 5\ nm\right)^3 : 10^{21}$$

To estimate the number of liposomes per volume, first the average number of lipids per liposome (n_l) was calculated using the liposomal hydrodynamic diameter d_h, the number of lipids per inner and outer bilayer leaflet and the assumption of an average lipid headgroup density of 0.6 nm^2 (Equation 4). The concentration of the liposomes was then calculated using the total lipid concentration (Equation 5, N_A = Avogadro constant).

Equation 4

$$n_l = \left(4 *\ \pi * \left(\frac{d_h}{2}\right)^2 + 4 *\ \pi * \left(\frac{d_h - 2 * 5\ nm}{2}\right)^2\right) : 0.6\ nm^2$$

Equation 5

$$c_{liposomes}\left[\frac{liposomes}{mL}\right] = \frac{(c_{lipid}\,[M]\ * N_A)}{n_l} : 1000$$

The total interior liposome volume per volume increment equals the theoretically, passively encapsulated fraction (EF_t, Equation 6).

Equation 6

$$EF_t\,[\%] = V_l * c_{liposomes} * 100$$

None of the encapsulated cargo is assumed to be lost during processing, and all non-encapsulated material should in theory be washed off during purification. Hence, the theoretical drug load after final purification ($DL_{t;\,f}$) is calculated according to Equation 7.

Equation 7

$$DL_{t;f}\left[\%\frac{m}{m}\right] = DL_{t;a.i.} * EF_t$$

3.3. Acridine orange release assay

pH-sensitive-LS and PEG^{high}-LS were prepared in ammonium sulfate buffer and rebuffered to 10 mM HEPES pH 7.4 (Table 2). This led to a pH- and salt-gradient over the liposomal bilayer, suitable for the "active" entrapment of weak bases in the liposome interior [22]. The pH-sensitivity was then investigated using the fluorescence of acridine orange, which changes upon liposomal entrapment and subsequent release (quenching / dequenching) [23]. The liposomes were diluted in HEPES pH 7.4 in a black 96 well plate to 90 µL (1.11 mM total lipid). 10 µL of an acridine orange stock solution (1 mM) were injected using a binary autotitration system connected to a fluorescence plate reader (F200, Tecan Group, Männedorf, Switzerland), so that final liposome concentration was 1 mM total lipid. The fluorescence was tracked at an excitation of 485 nm and emission of 535 nm for 150 s, until a second injection of either 18 µL 0.025 N HCl (leading to a pH of 5.5 +/- 0.04) or 100 µL Triton X-100 (TX-100) 5 % (final 2.5 % v/v) was performed. The fluorescence was then further tracked for 30 s. The fluorescence intensities of the liposomal samples were normalized on the fluorescence intensity of a similarly treated buffer reference. All samples were analyzed in triplicate wells.

3.4. Cell culture and cytotoxicity assays

Murine $CD11b^{+}Gr\text{-}1^{+}$ MDSC were cultured in RPMI complete and 20 ng/mL mGM-CSF (mouse granulocyte macrophage colony stimulating factor) as described elsewhere [14, 24]. For cytotoxicity experiments, 50,000 cells were seeded per well (final volume: 100 µL). The cells

were incubated for 24 h (PEG^{high}-LS and PEG^{low}-LS with low drug load) or 48 h (PEG^{high}-LS with high drug load and pH-sensitive-LS) with VHH-free, isotype control (VHH ENH) or CD11b-specific VHH DC13-modified liposomes at different PE38 concentrations at 37 °C. Alternatively, the cells were incubated with 0.001-100 µg/mL doxorubicin-loaded liposomes (based on doxorubicin) for 48 h. In two cases, a washout was performed. For that purpose, the cell culture medium with unbound liposomes was removed after 1 h or 4 h, cells were washed once in 200 µL PBS and resuspended in 100 µL RPMI complete and 20 ng/mL mGM-CSF. Cells were then further incubated at 37 °C to a total incubation time of 48 h.

To assess cell viability, 20 µL of Cell Titer Blue Cell Viability Assay reagent (#G8080, Promega, Madison, WI, USA) was added to each well and the samples were incubated for 2 h (pH-sensitive-LS: 1 h). Subsequently, the fluorescence was measured according to the manufacturer's protocol in a GloMax Multi plate reader (Promega). The relative survival (survival index) was calculated by comparison of the fluorescence values to untreated controls after subtraction of background value. All experiments were conducted in triplicate wells.

4. Results and discussion

4.1. PE38 loading to rigid liposomes

Three liposomal formulations (Table 1) were screened for suitability as actively targeted, PE38-loaded drug delivery system. PEG^{high}-LS and PEG^{low}-LS are primary composed of the saturated 1,2-dipalmitoyl-sn-glycero-3-phosphocholine (DPPC, transition temperature: 41 °C [25]) and cholesterol. Hence, both can be considered as liposomes having a "rigid" bilayer at physiological temperatures (37 °C) since the main transition temperature was determined at 43.7 ± 1.8 °C (Chapter 7). Both differ in their surface properties and stabilization mechanism. PEG^{high}-LS carry 2 kDa PEG-groups, which are derived from DSPE-mPEG (5 mol%). PEG is known to decrease unspecific uptake of liposomes by the mononuclear phagocyte system (MPS) [10]. Therefore, increases of *in vivo* half-life can be expected. PEG further serves as steric stabilizer of the liposomal dispersion [10]. PEG^{low}-LS are modified with DPPG, an anionic phosphoglycerol that leads to stable dispersions via charge-mediated stabilization. PEG^{low}-LS served as control formulation to investigate whether PEG may hinder an efficient delivery of PE38 to cells [26]. Both formulations effectively delivered a fluorescence marker towards humane and murine myeloid cells when they were modified with a myeloid cell specific single-domain antibody (Chapter 3 and 4). In those reports, PEG^{high}-LS had a mean hydrodynamic diameter of ≈140 nm, whereas PEG^{low}-LS appeared slightly larger (≈190 nm). To load PE38 into liposomes having a

similar composition and a comparable manufacturing process, differently concentrated PE38 solutions were used as aqueous phase during solvent injection (Table 3).

Table 3: Physico-chemical characterization of PE38-loaded liposomes after the final processing including solvent injection, tangential flow filtration, ligand conjugation and dialysis (data shown as mean ± standard deviation of three measurements).

PE38 conc. [mg/mL]	**d_h** [nm]	**PDI**	**zp** [mV]	**d_h** [nm]	**PDI**	**zp** [mV]	**d_h** [nm]	**PDI**	**zp** [mV]
PEG^{high}-LS	**VHH-free**			**+ control VHH**			**+ VHH DC13**		
0.1	141 ± 1	0.22 ± 0.01	-15 ± 0	135 ± 4	0.23 ± 0.01	-7 ± 0	138 ± 2	0.23 ± 0.01	-6 ± 0
2.0	149 ± 4	0.23 ± 0.01	-13 ± 0	148 ± 15	0.26 ± 0.06	-12 ± 1	149 ± 5	0.21 ± 0.04	-10 ± 0
PEG^{low}-LS	**VHH-free**			**+ control VHH**			**+ VHH DC13**		
0.1	162 ± 1	0.22 ± 0.01	-25 ± 1	199 ± 7	0.50 ± 0.44	-16 ± 1	171 ± 1	0.21 ± 0.01	-16 ± 1
pH-sensitive-LS	**VHH-free**			**+ control VHH**			**+ VHH DC13**		
0.5	159 ± 0	0.24 ± 0.00	-38 ± 2	180 ± 0	0.25 ± 0.01	-29 ± 2	165 ± 5	0.85 ± 0.26	-31 ± 2

PE38 presence had no relevant impact on the liposome formation, since the injection process was feasible without aggregation for both PEG^{high}-LS (at 0.1 and 2 mg/mL PE38 concentration) and PEG^{low}-LS (at 0.1 mg/mL PE38 concentration). Mean hydrodynamic diameters were in a similar range compared with previous manufactured batches in pure DPBS or 10 mg/mL FITC-Dextran in DPBS (compare with Table 2, Chapter 3). PDI values below 0.25 indicated a low polydispersity of the dispersion. As expected, the zeta potential was negative for both PE38-loaded formulations due to the anionic formal charges of the phospho-groups of DPPG and DSPE-mPEG, respectively.

4.2. Formulation development of pH-sensitive liposomes

To investigate whether the bilayer composition of the liposomes had an impact on the cytotoxicity of PE38-loaded liposomes, a third formulation composed of DOPE, CHEMS and DSPE-mPEG ("pH-sensitive-LS") was additionally selected. Lipid combinations of DOPE and CHEMS have been previously described as pH-sensitive [16-18]. This means these drug carriers exhibit a destabilization of the liposomal bilayer upon acidification and hence a release of encapsulated cargo. This may improve the cargo release inside the acidic environment of endosomes after drug carrier internalization, and subsequently an increase of the cytosolic availability of the toxin. To obtain pH-sensitive-LS in physical dimensions comparable to PEG^{high}-LS and PEG^{low}-LS, flow rates for the solvent injection of the ethanolic lipid stock into DPBS were screened (Figure 1). A decrease of the mean hydrodynamic diameter was observed with

increasing total flow rates. All applied flow rates delivered liposomes between 200 nm and 100 nm, and the polydispersity index was maintained below 0.25. The flow rate combination of 80 mL/min (buffer flow) : 10 mL/min (lipid flow) was chosen for PE38 loading (0.5 mg/mL in the aqueous phase). As expected from the size screening with pure buffer, liposomes with a mean hydrodynamic diameter of 159 ± 0 nm were obtained (Table 3). The zeta potential was strongly negative (-38 mV), what is due to the negatively charged acid groups of CHEMS, which is integrated to a high molar extent (38.4 mol%).

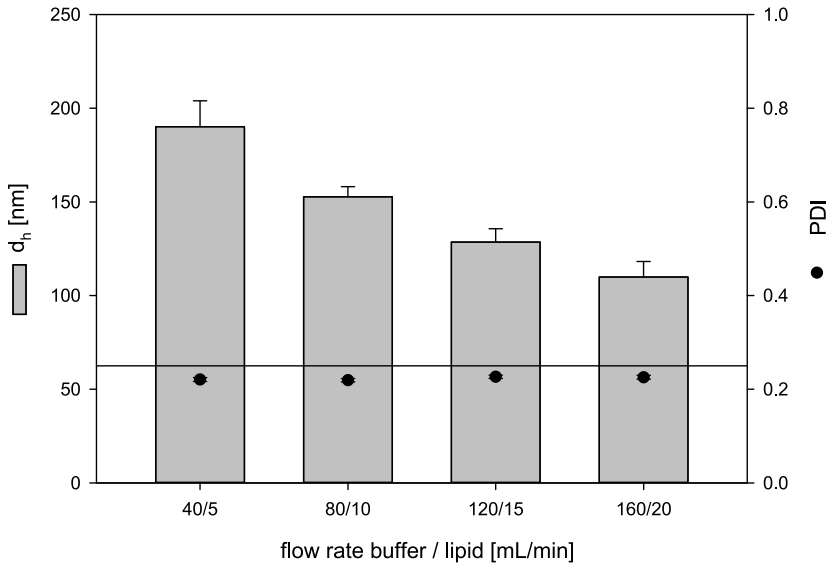

Figure 1: Size adjustment of DOPE and CHEMS-based, PEGylated and pentaglycine-modified liposomes by variation of flow rates during solvent injection of 75 mM lipid solution into DPBS. Standard deviations shown for the manufacturing of three batches.

PEGylation was previously reported to be compatible with the pH-sensitive function of DOPE-CHEMS liposomes [18], although there are concerns whether PEG may decrease the pH-responsiveness of such drug carriers [19, 27]. It was here in question whether pH-sensitive-LS (carrying PEG-groups and an additional pentaglycine modification) show a release of encapsulated material after acidification to a pH of 5.5, which is present in late endosomes [28]. For that purpose, pH-sensitive-LS were prepared in ammonium sulfate buffer (manufacturing parameters: Table 2), and an ammonium sulfate gradient was established over the membrane to yield liposomes compatible with active loading techniques [22]. Acridine orange is a fluorescent dye which can accumulate inside such gradient liposomes. Upon accumulation, the fluorescence quantum yield is drastically decreased (quenching). Acridine orange was therefore spiked either to gradient PEG^{high}-LS or to gradient pH-sensitive-LS with an autotitration system. The fluorescence intensity was monitored online. PEG^{high}-LS showed a time-dependent decrease of the fluorescence intensity, indicating a diffusion of the dye inside the vesicles within 20 s (Figure 2). This was going along with a pronounced quenching. Interestingly, this kinetic fluorescence loss was not observed for pH-sensitive-LS, which showed a weak fluorescence

signal directly after dye injection. This may be due to the primary used lipid DOPE, which has a transition temperature of -16 °C [29]. Hence, the fluidity of the pH-sensitive-LS is higher than those of PEG^{high}-LS, and accumulation of acridine orange can occur quicker. After a plateau time of 150 s, the acridine orange-loaded liposomes were exposed to HCl or TX-100, which served as acridine orange release stimuli. After detergent addition, both pH-sensitive-LS and PEG^{high}-LS showed a pronounced increase in fluorescence. This indicates the unspecific, detergent induced bilayer interference, which leads to dye release and subsequent de-quenching of the fluorescence. In contrast to that, only the pH-sensitive-LS, but not the PEG^{high}-LS changed their fluorescence intensity upon injection of HCl. This shows the pH-sensitivity of the formulation. However, the overall increase in fluorescence was weak compared to the TX-100 control, hence pH-sensitivity may offer room for optimization of this drug delivery system.

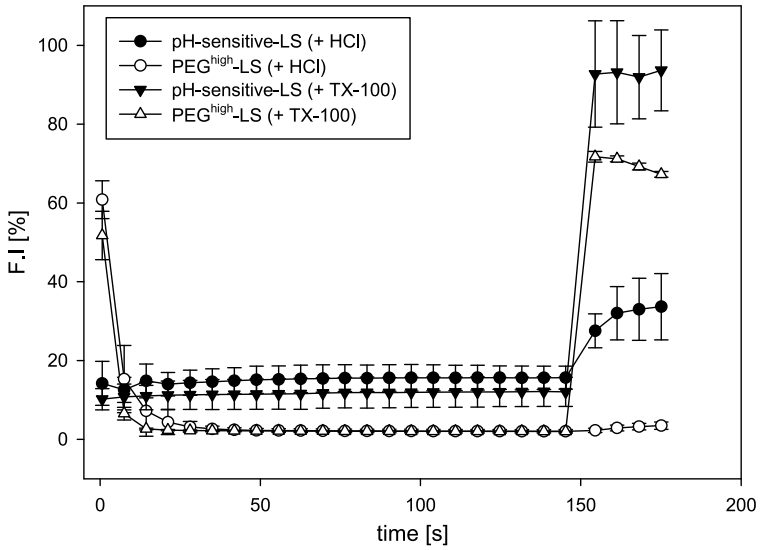

Figure 2: Evaluation of pH-sensitivity of PEG^{high}-LS and pH-sensitive-LS. 0 s: addition of acridine orange, 150 s: addition of HCl or TX-100. Only each 8th data point shown due to clarification. Data shown as mean ± standard deviation of three experiments conducted with one liposomal batch.

4.3. PE38 drug load analysis

The drug load, defined as the ratio of PE38 mass to lipid mass, was measured after solvent injection and after the final liposome purification step. Slightly lower drug loads compared to the theoretical values were determined after solvent injection. This may indicate a protein loss, e.g. due to adsorption to the tubing in use or due to denaturation through the organic solvent or shear stress during pumping. Interestingly, the drug load showed only slight decrease after the final dialysis compared to the value after injection. The measured drug loads exceed the ones expected from a sole passive encapsulation process by more than an order of magnitude (Table 4, brackets. Detailed calculations are described in methods.). This indicates that PE38 loading during solvent injection is predominantly based on adsorption processes between the liposomal bilayer and the proteinaceous toxin. This was especially observed for the PEG^{high}-LS,

whose drug load did not decrease by more than 25 % after dialysis. A comparable protein adsorption to PEG^{high}-LS was previously observed for Sortase-A and single-domain antibodies (Chapter 3 and 4). Though PEG is known to reduce the overall extent of (serum) protein adsorption to surfaces, it also shifts the affinity towards different protein populations, e.g. from coagulation factors towards lipoproteins [30, 31]. This change in composition of the protein corona is finally responsible for the stealth effect. It is therefore likely that the PEG-group of DSPE-mPEG increases the affinity of PE38 towards the liposome surface.

Table 4: PE38 drug load (DL, defined as PE38 mass divided by calculated or measured total lipid mass) during the different processing steps of immunoliposome preparation. In brackets: theoretical drug load after final processing, assuming a passive encapsulation process ($DL_{t;\,f}$).

formulation	c_{PE38} (in buffer)	$DL_{t,\,a.i.}$	$DL_{a,\,a.i.}$	$DL_{a,\,f}$ (brackets: $DL_{t,\,f}$)		
				VHH-free	+ control VHH	+ VHH DC13
PEG^{high}-LS	0.1 mg/mL	1.2 %	1.0 %	1.1 % (0.05 %)	1.0 %	1.0 %
	2.0 mg/mL	24.2 %	19.9 %	17.5 % (1.01 %)	14.9 %	15.6 %
PEG^{low}-LS	0.1 mg/mL	3.3 %	2.7 %	1.4 % (0.06 %)	1.5 %	1.4 %
pH-sensitive-LS	0.5 mg/mL	7.4 %	n.a.	3.7 % (0.28 %)	2.8 %	3.6 %

4.4. Sortagging of PE38-loaded liposomes

Sortase-A transpeptidation was applied to anchor targeting ligands on the three liposomal formulations. This chemoenzymatic technique offers site-specific conjugation between LPETG-motif carrying proteins and glycine nucleophiles under mild conditions in aqueous media [15]. For that purpose, all formulations carried a pentaglycine-modified lipid to 1 mol% in the liposomal bilayer. The liposomes were incubated with Sortase-A and LPETG-modified single-domain antibodies (VHHs) at 4 °C. Afterwards, the reaction bulk was purified from enzyme and unbound VHH by dialysis. An rp-HPLC method (Chapter 3 and 4) was used to separate proteinaceous and lipid ingredients of the formulations (Figure 3). It confirmed the presence of the lipidated VHH (retention time: 7.9 min, peak 3, mass spectroscopic peak identification described in Chapter 3 and 5) on all PE38-loaded liposomal constructs. This indicates that the pentaglycine motifs are accessible for the Sortase-A reaction. This was not self-evident, as above described PE38 adsorption on the liposome may have hindered an effective conjugation. In case of PEG^{high}-LS and pH-sensitive-LS, no relevant changes in the d_h or PDI occurred after conjugation, indicating physical stability during ligand conjugation (Table 3). PEG^{low}-LS showed increases in d_h and PDI for modification with VHH ENH, what indicates that subvisible aggregation may have occurred whereas no visible aggregation was observed. Similar to previously described liposome modifications with VHH ENH and DC13 (Chapter 3 and 4), slight changes in the zeta potential towards neutral values were observed (Table 3). This additionally indicates surface alteration of the liposomes through VHH-conjugation.

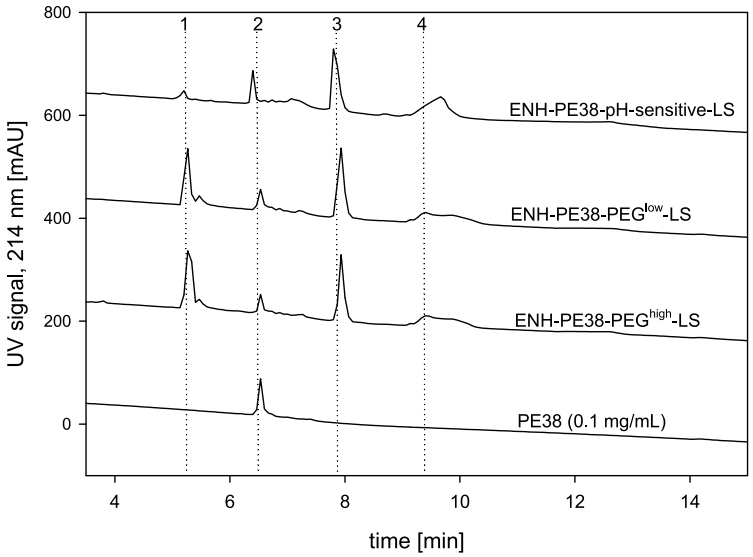

Figure 3: Separation of proteinaceous formulation ingredients by rp-HPLC: (1) - residuals of Sortase-A and VHH after dialysis, (2) - PE38 main peak, (3) - VHH conjugated to the lipid anchor DMA-PEG-G5, (4) - lipid excipients of liposomes. Presence of conjugate peak (3) indicates that the conjugation was feasible on all different PE38-loaded, pentaglycine-modified formulations.

4.5. Cytotoxicity of PE38-loaded liposomes

An immunotoxin conjugate of VHH DC13 and PE38 has previously been described to kill CD11b$^+$ cells [14]. Furthermore, VHH DC13 targeted immunoliposomes loaded with a fluorescent marker showed a specific targeting of CD11b$^+$ cells *in vitro* and *in vivo* (Chapter 3 and 4). It was therefore expected that PE38-loaded, via VHH DC13 targeted liposomes of similar composition and dimension offer a suitable drug delivery system for PE38.

PE38-loaded liposomes, either as VHH-free control, modified with an unspecific control VHH (VHH ENH) or with the CD11b-specific VHH DC13 were incubated with CD11b$^+$Gr-1$^+$ cells. Subsequently, cell viability was assessed. PEG^{high}-LS and PEG^{low}-LS loaded with 1.0-1.5 % PE38 (Table 4) were screened *in vitro* up to 1 µg/mL toxin, however without cytotoxic effect on the cells (Figure 4). Hence, the drug load was increased for PEG^{high}-LS. Only ≈40 % of the cells survived at the highest applied concentration (100 µg/mL), however without any specific effect for the CD11b-specific immunoliposomes. In this high concentration, PE38 is known to cause unspecific toxicity even without internalization-promoting domain [14]. It was suggested that the rigid bilayer composition of PEG^{high}-LS and PEG^{low}-LS is responsible for the low cytotoxicity, as this may lead to insufficient intracellular toxin release. Hence, pH-sensitive-LS composed of low-melting and pH-sensitive lipid combination DOPE and CHEMS were tested (Figure 4). pH-sensitive-LS did not exhibit CD11b-target related cytotoxicity as well, but a higher unspecific toxicity was observed (≈30 % survival at 10 µg/mL PE38) compared to PEG^{high}-LS (Figure 4). This indicates that the pH-sensitive formulation may exhibit higher cytotoxic potential than the rigid liposomes, especially if the 5-6fold lower drug loads (compared to PEG^{high}-LS, Table 4) are

considered. It was further verified that drug free PEG^{high}-LS, PEG^{low}-LS or pH-sensitive-LS do not exhibit cytotoxicity within the here applied lipid concentrations (data not shown). Furthermore, a PE38 sample recovered from the filtrate of the TFF was tested against loss of enzymatic activity using an assay described in [32]. Compared to a PE38 sample that did not face stress during solvent injection and purification, similar inhibition of the protein biosynthesis was observed (data not shown). This excludes that the manufacturing process has activity-decreasing influence on PE38 and indicates that stress from manufacturing is not responsible for lower cytotoxicity.

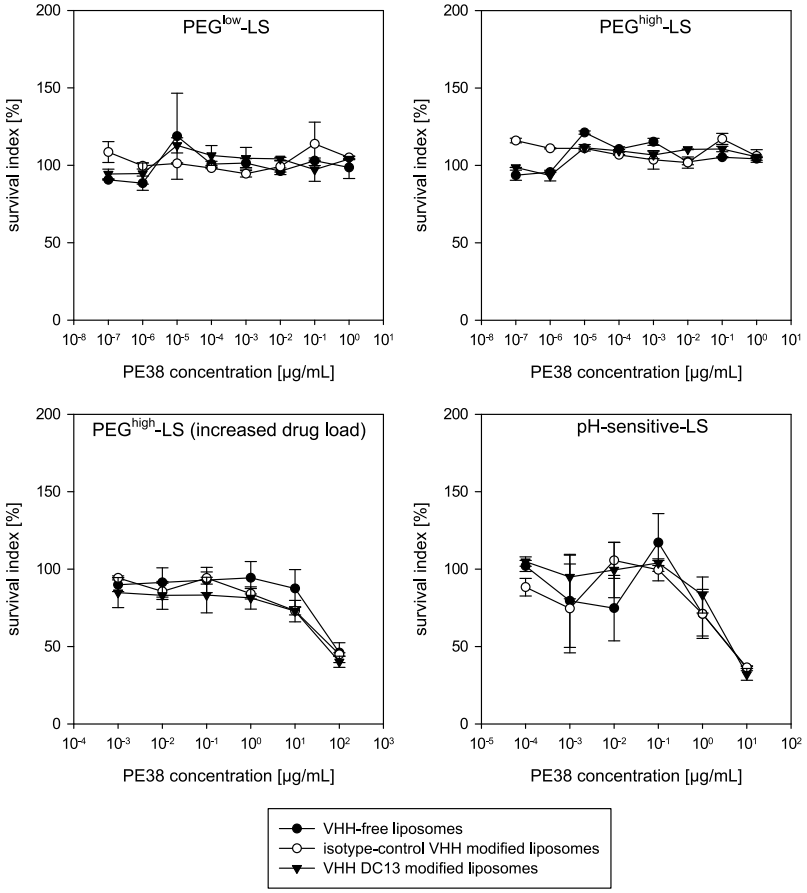

Figure 4: Cytotoxicity of PE38-loaded, actively targeted liposomes. No specific cytotoxicity was observed with VHH DC13-modified liposomes on CD11b^{+}Gr-1^{+} MDSC. The reader is kindly advised to the differently scaled abscissa. Error bars indicate standard deviations of duplicate (upper row) or triplicate (lower row) analyses of single liposomal batches.

Compared with previous reports describing the liposomal delivery of PE38 [8, 9], it is unclear why the here presented systems failed to exhibit target-specific cytotoxicity. The presented results indicate that the drug load as well as the bilayer composition are relevant for the observation of cytotoxic effects, irrelevant whether liposomes are targeted or not. Gao et al. used a combination of egg phosphatidylcholine (transition temperature: -7 to -15 °C [33]), cholesterol and DSPE-mPEG (65 : 32 : 3 mol%) for film hydration with a 2 mg/mL PE38 solution. The group observed an IC_{50} of 36 pM (≈0.0014 µg/mL) for HER2-specific liposomes on target-

positive cells. Zhang et al. prepared anti-hepatoma immunoliposomes composed of soybean phosphatidylcholine, cholesterol (5:4 m/m) and a PEGylated cholesterol derivate (2 to 6 mol%). Here, PE38 loading to the liposomes was described as an incubation step of a 1 mg/mL toxin solution with a non-described amount of already formed liposomes. They reported an IC_{50} of 0.47 µg/mL on target-positive cells. In both reports, significant differences between targeted and non-targeted liposomes were shown. This was not achieved with the here presented CD11b-specifc liposomes and may have eclectic reasons.

First reason is the liposome manufacturing strategy. Although hardly comparable due to different targets, ligands, cell types and experiment conditions, it its noticeable that Gao et al. showed IC_{50} values more than 300fold lower than Zhang et al. and also than the presented data, indicating a much higher cytotoxicity. Film hydration used by Gao et al. usually results in high lipid concentrations after liposome formation, leading to a high ratio of interior to exterior volume. Hence, capacity for passive protein encapsulation is high. This may be advantageous compared to an adsorption-based loading used by Zhang et al. and the here utilized solvent injection. After solvent injection, the liposome concentration is typically low, making additional concentration steps necessary, for example by TFF. Hence, a low liposome-interior acceptor volume is available for encapsulation after the initial liposome formation. Additionally, repulsive effects at the water-alcohol interface may decrease encapsulation and lead to an adsorption-based drug loading. Therefore, total amount of protein inside the liposome may be very low, and high amounts of PE38 are present on the liposome surface (adsorption-based loading, Table 4). Adsorbed cargo may impede uptake of the carrier, or after a potential uptake, be less efficiently delivered into the cytosol compared to encapsulated material, e.g. due to desorption of the cargo in physiological media or degradation during internalization processes.

Secondly, the liposomal bilayer composition is crucial for an effective intracellular delivery of large molecules. Both Gao et al. and Zhang et al. used naturally derived phosphatidylcholines with low transition temperatures as predominant lipid, leading to “fluid” liposomes. Those may have advantageous release properties for large molecules compared to the rigid PEG^{high}-LS and PEG^{low}-LS utilized here. Suggesting such an inadequate release of PE38 from rigid liposomes, a third formulation of low-melting DOPE and CHEMS, which has been described as suitable for the delivery of such proteinaceous toxins was tested [16-18]. However, only minor increases in cytotoxicity and no improvement of specificity of targeted formulations was achieved. To directly compare delivery of large and small molecules, it was additionally tested whether targeted PEG^{high}-LS loaded with the anticancer drug doxorubicin (543.5 Da) can exhibit specific toxicity on $CD11b^{+}$ cells (Figure 5).

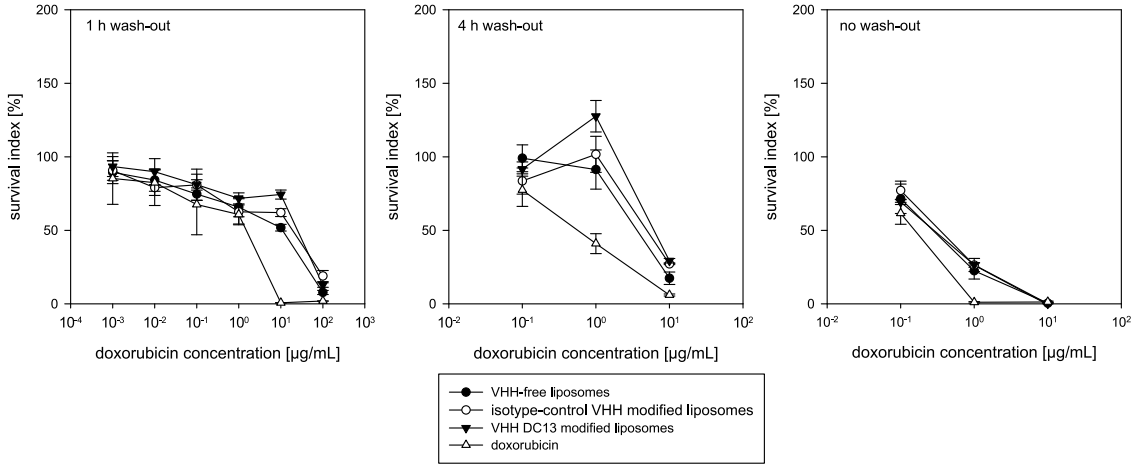

Figure 5: Cytotoxicity of doxorubicin-loaded, actively targeted liposomes. Error bars indicate the standard deviations of triplicate analyses of single liposomal batches.

Due to the small size and higher permeability, it was suggested that doxorubicin may not suffer from poor intracellular release. Interestingly, also no differences between targeted and non-targeted formulations were observed. This was also the case when different incubation times, meaning the time frame in which the liposomes have contact with the cells before the medium is replaced, were investigated to avoid unspecific, drug release related cytotoxic effects. This lack of specificity observed with doxorubicin-loaded liposomes further indicates that an insufficient intracellular PE38 release may not be the sole problem of the presented formulations.

Third possible reason for the lack of specific cytotoxicity may be the target CD11b itself or the corresponding binder VHH DC13. Bachran et al. showed much more effective killing of $CD11b^{+}Gr\text{-}1^{+}$ cells using a PE38 immunotoxin specific for Gr-1 [14]. This may hint towards an insufficient internalization-promoting function of CD11b upon binding or towards an overall low affinity of VHH DC13.

Fourth, observations of a targeted cytotoxicity may be superimposed by the phagocytic activity of the myeloid cells *in vitro*. Here, cells are exposed to the particulate drug delivery system for several hours to days, different to the 4 h exposure applied for targeting experiments with fluorophore-labeled liposomes (Chapter 3 and 4). It may be that, irrespective of a ligand induced cell-liposome interaction, the liposomes are phagocytized by the myeloid immune cells. Therefore, different wash-outs after 1 h and 4 h steps or no wash-out were tested for doxorubicin-loaded liposomes, but also without the observation of a specific cytotoxicity for the targeted systems (Figure 5).

Taken the points raised above together, reasons for the lack of specific cytotoxicity remain elusive. A combination of insufficient drug load, weak internalization-activity of the target or ligand and low intracellular drug release are most likely. Further screenings covering these

parameters would be required to achieve sufficient cell killing, which would exceed the scope of this work.

Additionally, further technological variations may improve specific toxin delivery. This may include usage of a cleavable PEG-coating. PEG was demonstrated to decrease pH-sensitivity of DOPE-CHEMS-based liposomes [27]. This was overcome by usage of linkers between liposome and PEG which are sensitive for a cleavage through lysosomal enzymes [18]. Other strategies may include the co-encapsulation of endosome-disruptive peptides together with proteinaceous toxins, what led to drastic increases in cytotoxicity of diphtheria toxin-loaded immunoliposomes (major lipid: egg phosphatidylcholine) [34]. Furthermore, usage of positively charged lipids [26] or coating of the liposomes with cell-penetrating peptides [35] may exhibit positive effects through an increased internalization, although convincing *in vivo* data for the latter is missing [36].

5. Conclusion

The formulation development of *Pseudomonas* exotoxin A (PE38)-loaded immunoliposomes is presented. Three sortaggable liposomal concepts differing in surface properties and responsiveness against acidic pH were loaded with PE38 during a solvent injection process. All drug-loaded formulations were successfully modified with a ligand specific for the murine myeloid cell marker CD11b by means of Sortase-A technology. Despite promising targeting experiments with fluorophore-labeled liposomes and CD11b-specific immunotoxins, none of the developed immunoliposomes exhibited specific cytotoxic activity on $CD11b^{+}Gr\text{-}1^{+}$ cells. Possible reasons for this unexpected result are evaluated. This chapter therefore discusses the challenges faced during the switch of marker molecules to active ingredients and gives a valuable outlook for further possibilities of formulation improvement.

References

[1] K. Kawakami, O. Nakajima, R. Morishita, R. Nagai, Targeted Anticancer Immunotoxins and Cytotoxic Agents with Direct Killing Moieties, The Scientific World Journal, 6 (2006) 781-790.

[2] P. Wolf, U. Elsässer-Beile, Pseudomonas exotoxin A: From virulence factor to anti-cancer agent, International Journal of Medical Microbiology, 299 (2009) 161-176.

[3] F.M. Foss, DAB389IL-2 (ONTAK): A Novel Fusion Toxin Therapy for Lymphoma, Clinical Lymphoma, 1 (2000) 110-116.

[4] F.M. Foss, P. Bacha, K.E. Osann, M.F. Demierre, T. Bell, T. Kuzel, Biological Correlates of Acute Hypersensitivity Events with DAB389IL-2 (Denileukin Diftitox, ONTAK) in Cutaneous T-Cell Lymphoma: Decreased Frequency and Severity with Steroid Premedication, Clinical Lymphoma, Myeloma and Leukemia, 1 (2001) 298-302.

[5] A. Martin, E. Gutierrez, J. Muglia, C.J. McDonald, C. Guzzo, A. Gottlieb, A. Pappert, W.T. Garland, J. Bagel, P. Bacha, A multicenter dose-escalation trial with denileukin diftitox (ONTAK, DAB389-IL-2) in patients with severe psoriasis, Journal of the American Academy of Dermatology, 45 (2001) 871-881.

[6] B. Weide, T.K. Eigentler, A. Pflugfelder, U. Leiter, F. Meier, J. Bauer, D. Schmidt, P. Radny, C. Pföhler, C. Garbe, Survival after intratumoral interleukin-2 treatment of 72 melanoma patients and response upon the first chemotherapy during follow-up, Cancer Immunology, Immunotherapy, 60 (2011) 487-493.

[7] J. Gao, G. Kou, H. Wang, H. Chen, B. Li, Y. Lu, D. Zhang, S. Wang, S. Hou, W. Qian, J. Dai, J. Zhao, Y. Zhong, Y. Guo, PE38KDEL-loaded anti-HER2 nanoparticles inhibit breast tumor progression with reduced toxicity and immunogenicity, Breast Cancer Res Treat, 115 (2009) 29-41.

[8] W.Z. Jie Gao, Jinqiu He, Huimei Li, He Zhang, Guichen Zhou, Bohua Li, Ying Lu, Hao Zou, Geng Kou, Dapeng Zhang, Hao Wang, Yajun Guo, Yanqiang Zhong, Tumor-targeted PE38KDEL delivery via PEGylated anti-HER2 immunoliposomes, International Journal of Pharmaceutics, 374 (2009) 145-152.

[9] G. Zhang, Y. Liu, H. Hu, Preparation and cytotoxicity effect of anti-hepatocellular carcinoma scFv immunoliposome on hepatocarcinoma cell in vitro, European Journal of Inflammation, 8 (2010) 75-82.

[10] Y. Barenholz, Doxil® – The first FDA-approved nano-drug: Lessons learned, Journal of Controlled Release, 160 (2012) 117-134.

[11] R. Solomon, A.A. Gabizon, Clinical Pharmacology of Liposomal Anthracyclines: Focus on Pegylated Liposomal Doxorubicin, Clinical Lymphoma and Myeloma, 8 (2008) 21-32.

[12] B.S. Pattni, V.V. Chupin, V.P. Torchilin, New Developments in Liposomal Drug Delivery, Chemical Reviews, 115 (2015) 10938-10966.

[13] D.I. Gabrilovich, S. Nagaraj, Myeloid-derived suppressor cells as regulators of the immune system, Nature Reviews Immunology, 9 (2009) 162-174.

[14] C. Bachran, M. Schröder, L. Conrad, J.J. Cragnolini, F.G. Tafesse, L. Helming, H.L. Ploegh, L.K. Swee, The activity of myeloid cell-specific VHH immunotoxins is target-, epitope-, subset- and organ dependent, Scientific Reports, 7 (2017) 17916.

[15] M. Ritzefeld, Sortagging: A Robust and Efficient Chemoenzymatic Ligation Strategy, Chemistry – A European Journal, 20 (2014) 8516-8529.

[16] D.C. Drummond, M. Zignani, J.-C. Leroux, Current status of pH-sensitive liposomes in drug delivery, Progress in Lipid Research, 39 (2000) 409-460.

[17] C.-J. Chu, J. Dijkstra, M.-Z. Lai, K. Hong, F.C. Szoka, Efficiency of Cytoplasmic Delivery by pH-Sensitive Liposomes to Cells in Culture, Pharmaceutical Research, 7 (1990) 824-834.

[18] T. Ishida, M.J. Kirchmeier, E.H. Moase, S. Zalipsky, T.M. Allen, Targeted delivery and triggered release of liposomal doxorubicin enhances cytotoxicity against human B lymphoma cells, Biochimica et Biophysica Acta (BBA) - Biomembranes, 1515 (2001) 144-158.

[19] V.A. Slepushkin, S. Simões, P. Dazin, M.S. Newman, L.S. Guo, M.C.P. de Lima, N. Düzgüneş, Sterically Stabilized pH-sensitive Liposomes: Intracellular delivery of aqueous contents and prolonged circulation in vivo Journal of Biological Chemistry, 272 (1997) 2382-2388.

[20] S. Wöll, S. Schiller, C. Bachran, L.K. Swee, R. Scherließ, Pentaglycine lipid derivates – rp-HPLC analytics for bioorthogonal anchor molecules in targeted, multiple-composite liposomal drug delivery systems, International Journal of Pharmaceutics, 547 (2018) 602-610.

[21] S. Wöll, C. Bachran, S. Schiller, M. Schröder, L. Conrad, L.K. Swee, R. Scherließ, Sortaggable liposomes: Evaluation of reaction conditions for single-domain antibody conjugation by Sortase-A and targeting of CD11b+ myeloid cells, European Journal of Pharmaceutics and Biopharmaceutics, 133 (2018) 138-150.

[22] J. Gubernator, Active methods of drug loading into liposomes: recent strategies for stable drug entrapment and increased in vivo activity, Expert Opinion on Drug Delivery, 8 (2011) 565-580.

[23] G. Haran, R. Cohen, L.K. Bar, Y. Barenholz, Transmembrane ammonium sulfate gradients in liposomes produce efficient and stable entrapment of amphipathic weak bases, Biochimica et Biophysica Acta (BBA) – Biomembranes, 1151 (1993) 201-215.

[24] M. Schröder, S. Loos, S.K. Naumann, C. Bachran, M. Krötschel, V. Umansky, L. Helming, L.K. Swee, Identification of inhibitors of myeloid-derived suppressor cells activity through phenotypic chemical screening, OncoImmunology, 6 (2017) e1258503.

[25] R.L. Biltonen, D. Lichtenberg, The use of differential scanning calorimetry as a tool to characterize liposome preparations, Chemistry and Physics of Lipids, 64 (1993) 129-142.

[26] C.R. Miller, B. Bondurant, S.D. McLean, K.A. McGovern, D.F. O'Brien, Liposome−Cell Interactions in Vitro: Effect of Liposome Surface Charge on the Binding and Endocytosis of Conventional and Sterically Stabilized Liposomes, Biochemistry, 37 (1998) 12875-12883.

[27] J.W. Holland, C. Hui, P.R. Cullis, T.D. Madden, Poly(ethylene glycol)−Lipid Conjugates Regulate the Calcium-Induced Fusion of Liposomes Composed of Phosphatidylethanolamine and Phosphatidylserine, Biochemistry, 35 (1996) 2618-2624.

[28] Y.-B. Hu, E.B. Dammer, R.-J. Ren, G. Wang, The endosomal-lysosomal system: from acidification and cargo sorting to neurodegeneration, Translational Neurodegeneration, 4 (2015) 18.

[29] J.R. Silvius, Thermotropic phase transitions of pure lipids in model membranes and their modifications by membrane proteins, Lipid-protein interactions, 2 (1982) 239-281.

[30] S. Schöttler, G. Becker, S. Winzen, T. Steinbach, K. Mohr, K. Landfester, V. Mailänder, F.R. Wurm, Protein adsorption is required for stealth effect of poly(ethylene glycol)- and poly(phosphoester)-coated nanocarriers, Nature Nanotechnology, 11 (2016) 372.

[31] J.S. Suk, Q. Xu, N. Kim, J. Hanes, L.M. Ensign, PEGylation as a strategy for improving nanoparticle-based drug and gene delivery, Advanced drug delivery reviews, 99 (2016) 28-51.

[32] O.W. Press, E.S. Vitetta, P.J. Martin, A simplified microassay for inhibition of protein synthesis in reticulocyte lysates by immunotoxins, Immunology Letters, 14 (1986) 37-41.

[33] D. Chapman, R.M. Williams, B.D. Ladbrooke, Physical studies of phospholipids. VI. Thermotropic and lyotropic mesomorphism of some 1, 2-diacyl-phosphatidylcholines (lecithins), Chemistry and Physics of Lipids, 1 (1967) 445-475.

[34] E. Mastrobattista, G.A. Koning, L. van Bloois, A.C.S. Filipe, W. Jiskoot, G. Storm, Functional Characterization of an Endosome-disruptive Peptide and Its Application in Cytosolic Delivery of Immunoliposome-entrapped Proteins, Journal of Biological Chemistry, 277 (2002) 27135-27143.

[35] E. Koren, V.P. Torchilin, Cell-penetrating peptides: breaking through to the other side, Trends in Molecular Medicine, 18 (2012) 385-393.

[36] A. Bernkop-Schnürch, Strategies to overcome the polycation dilemma in drug delivery, Advanced drug delivery reviews, 136-137 (2018) 62-72.

Chapter 7

Sortagged anti-EGFR immunoliposomes exhibit increased cytotoxicity on target cells

This chapter is published as: Wöll, S., Dickgiesser, S., Rasche, N., Schiller, S., Scherließ, R.: Sortagged anti-EGFR immunoliposomes exhibit increased cytotoxicity on target cells.
European Journal of Pharmaceutics and Biopharmaceutics, 136 (2019), 203-212.
https://doi.org/10.1016/j.ejpb.2019.01.020

Abstract

Purpose: Conventional chemotherapy is associated with therapy-limiting side effects, which may be alleviated by targeted chemotherapeutics such as immunoliposomes. The targeting ligands of immunoliposomes are commonly attached by unspecific chemical conjugation, bearing risk of structural heterogeneity and therewith related biological consequences. Chemoenzymatic methods may mitigate such risks through site-specific conjugation.

Methods: The formulation parameters for pentaglycine-modified, doxorubicin-loaded liposomes and the reaction conditions for a site-specific, Sortase-A mediated conjugation with monoclonal antibodies were thoroughly evaluated. The cytotoxicity of such sortagged, epidermal growth factor receptor (EGFR)-specific immunoliposomes was tested on human breast cancer cells.

Results: Sortaggable liposomes with a defined size (140 nm, PDI < 0.25) and high encapsulation efficiency (> 90 %) were obtained after manufacturing optimization. A ratio of 1.0-2.5 µM mAb / 100 µM pentaglycine yielded stable dispersions and circumvented carrier precipitation during ligand grafting. The cytotoxicity on $EGFR^+$ MDA-MB-468 cells was up to threefold higher for EGFR-specific immunoliposomes than for the nontargeted controls.

Conclusions: Sortase-A is suitable to generate immunoliposomes with a site-specific ligand-carrier linkage and hence improves chemical homogeneity of targeted therapeutics. However, the sweet spot for manufacturability utilizing mAbs with two Sortase-A recognition sites is narrow, making mono-reactive binders such as scFvs or Fab's preferable for a further development. Despite this, the immunoliposomes demonstrated a targeted delivery of doxorubicin, indicating the potential to increase the therapeutic window during the treatment of $EGFR^+$ tumors.

1. Introduction

The major drawback of conventional anticancer drugs are dose-limiting adverse events that result in a narrowed therapeutic window. One strategy to overcome serious side effects is a targeted drug delivery, which leads to an accumulation of the drug in the tumor while omitting healthy tissues. Today, several concepts for targeted drug delivery have already successfully been applied, e.g. antibody-drug conjugates (ADCs) or drugs encapsulated in a targeted nanoparticulate carrier system such as immunoliposomes [1]. The latter requires the conjugation of a mostly proteinaceous ligand with an appropriate lipid anchor. For that, various chemistry-based coupling techniques, including maleimide-thiol conjugation with cysteines, amine condensation of lysines or N-hydroxysuccineimide-ester-based coupling with carboxylic acid groups have been developed and have recently been extensively reviewed [2]. Although some immunoliposomal formulations have been clinically investigated [3-5], manufacturing hurdles and hence regulatory concerns remain high. Besides causing a tremendous effort in manufacturing a nano-sized drug carrier within the required specifications [6], chemistry-based conjugation methods additionally increase product heterogeneity [7]. Furthermore, stability of the linkers is a critical issue. Especially the widely used maleimide-linker can undergo a retro-Michael addition and exchange with albumin cysteine residues *in vivo* [8]. This includes cleavage between drug carrier and ligand, and thereby a loss of the targeting functionality. Site-specific, chemoenzymatic conjugation methods such as Sortase-A mediated transpeptidation have gained increasing interest for the synthesis of tailored antibody-drug conjugates (ADCs) [9]. The enzyme-catalyzed modification of large protein structures at defined reaction sites leads to homogenous reaction products connected by a stable amide bond [10]. These reaction sites can be introduced by genetic engineering at uncritical parts of monoclonal antibodies such as the C-termini of the Fc part or constant domains of light chains [11]. This avoids the conjugation dependent decrease of antigen recognition in paratope regions observed after lysine-based conjugations [12], or a destabilization of antibodies during or after the reaction, as observed for cysteine conjugations [13, 14]. Hence, deploying a chemoenzymatic method for the site-specific anchoring of targeting ligands would significantly improve the manufacturing process of immunoliposomes.

Doxorubicin (DXR) is a cytotoxic, DNA-intercalating anticancer agent with a broad applicability against many tumors, however also with a dose-limiting anthracycline induced cardiomyopathy as most severe adverse event [6, 15]. The cardiotoxicity was alleviated by encapsulation of DXR into liposomal drug delivery systems [16]. This technology was commercialized as the “first nano-drug” Doxil®, developed by Barenholz and coworkers [6]. It is based on the efficient

encapsulation of DXR by a remote loading technique [17], the use of high melting lipids together with cholesterol and finally a polyethylene glycol coating. Especially the latter leads to a prolonged circulation time and reduced uptake by the mononuclear phagocyte system (MPS) [6]. In addition to the reduced cardiotoxicity, compared to free DXR PEGylated liposomal DXR was found to accumulate to higher extents in human tumor effusions [18] or in human bone metastases of breast carcinoma than in adjacent muscle tissue [19]. This was interpreted as a passive drug targeting via the enhanced permeation and retention effect [6]. However, off-site effects such as mucositis or palmar-plantar erythrodysesthesia (skin toxicity) are still dose-limiting toxicities with PEGylated liposomal DXR [20]. This led to the approach of "active" targeting of liposomal DXR towards tumors by conjugation of tumor-specific ligands on the liposomal bilayer [1]. An established tumor target is the epidermal growth factor receptor (EGFR), whose overexpression is correlated with the pathogenesis of many tumors [21, 22]. Treatments which utilize monoclonal antibodies (mAb) inhibiting the EGFR are efficacious and well-tolerated therapies [21, 23]. One example is cetuximab (C225, Erbitux®), which is currently approved for the treatment of colorectal and head- and neck cancer. A sortaggable variant of cetuximab, on both heavy chains C-terminally conjugated via Sortase-A to the tubulin inhibitor monomethyl auristatin E (MMAE), was recently demonstrated to exhibit specific cytotoxicity on EGFR overexpressing cells [24]. This antibody was therefore regarded as suitable model binder to explore the site-specific Sortase-A conjugation technology on liposomes, with the aim to combine two established concepts – DXR-loaded, PEGylated liposomes and the EGFR-specific mAb cetuximab. Therefore, we first thoroughly evaluated the manufacturing of pentaglycine-modified, PEGylated liposomes by a continuous solvent injection process. We characterized the pentaglycine liposomes regarding liposome stability, doxorubicin loading and particle shape. Engineered monoclonal antibodies carrying a Sortase-A pentapeptide at their heavy chain C-termini specific for EGFR (C_H-LPETG-C225) or hen egg lysozyme (C_H-LPETG-aHEL) were conjugated to the pentaglycine liposomes. The chemoenzymatic transpeptidation was evaluated for reaction kinetics and physical stability of the reaction product. To investigate the *in vitro* targeting ability, the EGFR-specific immunoliposomes were tested for their toxicity on a human breast cancer cell line (MDA-MB-468).

2. Materials

Dimyristyl-modified, PEGylated pentaglycine lipid DMA-PEG-G5 (structure shown in [25]) was from Merck & Cie (Schaffhausen, Switzerland). 1,2-dipalmitoyl-sn-glycero-3-phosphocholine (DPPC), hydrogenated phosphatidylcholine from soybean (HSPC) and 1,2-distearoyl-sn-glycero-3-phosphoethanolamine-N-[methoxy(polyethylene glycol)-2000] (DSPE-mPEG) were acquired

from Lipoid GmbH (Ludwigshafen, Germany). Dulbecco's phosphate buffered saline (DPBS, D1408), cholesterol, 4-(2-hydroxyethyl)piperazine-1-ethanesulfonic acid (HEPES) and Triton X-100 were obtained from Sigma-Aldrich (St. Louis, Missouri, USA). Ammonium sulfate and ethanol were obtained from Merck KGaA (Darmstadt, Germany). MilliQ water (Merck Millipore, Billerica, Massachusetts, USA) was used for preparation and analytical purposes. Doxorubicin was from Ark Pharma (Arlington Heights, Illinois, USA). Ca^{2+}-independent Sortase-A variant SortA7m and a single-domain antibody of camelid heavy chain only antibodies with one LPETG (leucine, proline, glutamic acid, threonine, glycine)-motif (LPETG-VHH) were a kind gift of BioMed X GmbH (Heidelberg, Germany) and prepared as described elsewhere [26].

3. Methods

3.1. Pentaglycine-liposome preparation

Liposomes were prepared by a continuous solvent injection process described in detail in [27]. In brief, DPPC, cholesterol, DSPE-mPEG and pentaglycine-modified DMA-PEG-G5 (59.4 : 34.7 : 5.0 : 1.0, mol%) were dissolved to 90 mM in ethanol. The lipid solution was injected into 250 mM ammonium sulfate buffer pH 5.4 utilizing a binary pumping system combined with a custom-made T-piece at various flow rates. If DPPC was replaced by HSPC (as indicated in results), lipids were dissolved to 100 mM in ethanol and injected at 5 mL/min into 250 mM ammonium sulfate heated to 65 °C (40 mL/min). Buffer was exchanged to DPBS pH 7.4 or 10 mM HEPES pH 7.0 (as indicated in results) by tangential flow filtration (MicroKros® hollow fiber module, 500 kDa cut-off, 20 cm^2 filter area, Spectrum Labs, Los Angeles, CA, USA) to establish a pH and ammonium sulfate gradient over the liposomal membrane [28].

3.2. Liposome characterization

The hydrodynamic diameter and polydispersity index (PDI) were measured by dynamic light scattering (DLS) using a DynaPro Plate Reader II (Wyatt, Santa Barbara, California, USA). The liposome dispersion was diluted to 3 % v/v with surrounding buffer to achieve measurable count rates. The zeta potential (zp) was assessed using a Zetasizer Nano ZS (Malvern Instruments, Worcestershire, UK) after a dilution in 10 mM NaCl to 3 % v/v. Content of each lipid component was determined by an rp-HPLC method with an evaporative light scattering detector as described earlier [25]. The lipid stability of pentaglycine-modified liposomes was evaluated over an eight weeks storage at 2-8 °C.

Differential scanning calorimetry (DSC1, Mettler Toledo, Columbus, Ohio, USA) was used to determine the transition temperature of the liposomal bilayer. Aqueous lipid slurries

(100-200 mg/mL) were prepared by 30 min hydration of preformed lipid films in an ultrasound bath. 100 µL of slurry was transferred to 160 µL aluminum pans. Pans were covered with a pierced lid. DSC measurement was performed with a temperature profile of 5 min equilibration at 5 °C, followed by a heating step (5 K/min) to 75 °C, a plateau phase at 75 °C for 3 minutes and return to 5 °C (-20 K/min). Two cycles were applied per sample, second cycle was used to calculate the melting temperature.

3.3. Doxorubicin loading and quantification

To screen DXR loading into the liposomes, DXR (10 mg/mL in water) and liposomes were mixed to a lipid-to-DXR ratio of 5:1 (m/m). In some cases, 10fold DPBS stock was added to adjust salt concentration to 1fold DPBS as indicated in the results. The liposomes were incubated for 30 min to 24 h in 1.5 mL tubes in an Eppendorf Thermomixer Comfort heating block (1000 rpm, 49 °C). Afterwards, the dispersion was immediately transferred into dialysis bags (Slide-A-Lyzer, MWCO 10 kDa, Thermo Fisher, Waltham, Massachusetts, USA) and dialyzed for at least 24 h with five buffer changes against DPBS pH 7.4 until the concentration of DXR in the dialysis buffer was < 0.2 µg/mL.

DXR content was determined as follows: liposomal samples were diluted in 5 % Triton X-100 (v/v) and incubated for 30 min at 50 °C to ensure a complete vesicle lysis with subsequent dequenching of the encapsulated DXR. Fluorescence intensity (excitation: 485 nm, emission 595 nm) was measured in a 96-well plate reader (M200, Tecan Group, Männedorf, Switzerland) and DXR was quantified using a calibration row in lysis medium (0.06-2 µg/mL). The method typically showed good linearity ($r^2 > 0.999$), accuracy (95-105 % of individually prepared 1 µg/mL samples) and specificity as lipid matrix had negligible influence on DXR quantification. Lipid and DXR content were used to calculate the encapsulation efficiency (EE) according to Equation 1.

Equation 1

$$EE\ [\%] = 100 * \frac{\frac{c(DXR)}{c(Lipid)}(after\ dialysis)}{\frac{c(DXR)}{c(Lipid)}(during\ loading)}$$

3.4. Recombinant expression and purification of monoclonal antibodies

Antibodies for Sortase-A mediated conjugation (C_H-LPETG-mAb) were manufactured using established recombinant expression and purification procedures. Briefly, mammalian expression vectors encoding for EGFR-specific C225 (cetuximab) and a hen egg lysozyme-specific IgG1 (aHEL) fused to a Sortase-A recognition motif (LPETGS) at their heavy chain C-termini were synthesized by GeneArt (Thermo Fisher Scientific, Waltham, MA, USA). Antibodies were

recombinantly expressed in transiently transfected mammalian cells for five days using Expi293 expression system (Thermo Fisher Scientific, Waltham, MA, USA) and afterwards purified from the supernatant by protein A affinity chromatography.

3.5. Ligand conjugation: Reaction conditions and kinetic monitoring

Chemoenzymatic Sortase-A transpeptidation was used to conjugate C_H-LPETG-mAbs to pentaglycine-modified liposomes. The reaction behavior was investigated by spiking different concentrations of C_H-LPETG-C225 to the DXR-LS (100 µM pentaglycine, from which roughly 50 µM were expected to be accessible at the outer leaflet of the bilayer). The mixture was equilibrated at 4 °C, and hydrodynamic diameter, PDI and attenuation-corrected light scattering count rate were determined using a Zetasizer Nano ZS. Detection angle was set to 173° (back scatter), data was analyzed via cumulants fit. After addition of 25 µM Sortase-A, the colloidal stability was tracked during the transpeptidation reaction over 4 h to determine feasible reaction conditions. To further evaluate reaction kinetics and endpoint, 1.0 µM C_H-LPETG-aHEL, DXR free liposomes (100 µM pentaglycine) and 25 µM Sortase-A were incubated at 4 °C. 5 µL of the mixture were sampled in 30 min intervals and analyzed by an rp-HPLC-DAD method published earlier for the analysis of single-domain antibody conjugation to pentaglycine-lipids [27]. The chromatographic conditions, namely the column temperature (60 °C) and the flow rate (1 mL/min) were modified to achieve sharp protein elution. This led to separation of Sortase-A, unmodified C_H-LPETG-aHEL and with one ((DMA-PEG)-C_H-LPETG-aHEL) or two ((DMA-PEG)$_2$-C_H-LPETG-aHEL) lipid anchors modified mAb variants. The reaction progress was calculated as the relative area of each species from the area of 1.0 µM unmodified C_H-LPETG-aHEL at 280 nm (Equation 2; s_n – species of interest, t_i – actual timepoint, A – peak area, A_0 – area of 1.0 µM C_H-LPETG-aHEL). At this wavelength, the influence of amide bonds being introduced by the pentaglycine-modified lipid was negligible. The total sum of the areas of the different mAb species during the reaction did never deviate to more than 6 % from the mean area of a 1.0 µM C_H-LPETG-aHEL standard (n=3, each injected in triplicate). The double-banded peak of mono-modified mAb was treated as single species.

Equation 2

$$reaction\ progress\ [\%]\ of\ s_n = \frac{A_{s_n}(t_i)}{A_0}$$

Liposome batches for *in vitro* cytotoxicity experiments were conjugated with 1.0 or 2.5 µM of C_H-LPETG-aHEL or C_H-LPETG-C225 for 4 h at 4 °C to DXR-loaded liposomes (DXR loading: 4 h at 49 °C, incubation in DPBS buffer), followed by dialysis in Float-A-Lyzer devices (MWCO 1000 kDa, G235037, Spectrum Labs, Los Angeles, California, USA). In case of HSPC-based liposomes, DXR

had been loaded for 1 h at 65 °C from 10 mM HEPES buffer pH 7.0. Liposome-bound mAb concentration was calculated from the peak area of both (DMA-PEG)-C_H-LPETG-mAb and $(DMA\text{-}PEG)_2$-C_H-LPETG-mAb after analysis with above described rp-HPLC method using a 2.5 µM sample of non-lipidated C_H-LPETG-mAb as reference.

3.6. Cryo transmission electron microscopy

Cryo transmission electron microscopy (cryo-TEM) studies were done according to a method described by Klaiber and colleagues [29]. In brief, a thin sample film stretched over the lace holes of a hydrophilized carbon grid was shock frozen by rapid immersion in liquid ethane (97 K). Microscopic examinations utilized a Zeiss / LEO EM922 Omega EFTEM (Zeiss Microscopy GmbH, Jena, Germany) operated at an acceleration voltage of 200 kV and a temperature of 95 K. Images were taken and processed by a digital camera and software system (Gatan, München, Germany).

3.7. *In vitro* cytotoxicity

Cytotoxicity of EGFR- and HEL-targeted liposomes (the latter used as an isotype control) was tested on EGFR-positive cells (MDA-MB-468). 10,000 cells were seeded in 80 µL growth medium (RPMI supplemented with 10 % fetal calf serum, 2 mM L-glutamine and 1 mM Na-pyruvate) in 96-well plates and incubated overnight at 5 % CO_2 and 37 °C in a humidified atmosphere. Dilution series of antibody-modified formulations or control groups were prepared in medium and added to the cells, spanning a final DXR concentration from 100 µg/mL to 1.2 x 10^{-4} µg/mL (5.5fold dilution series, 9 concentrations tested). Wells with cells but without test compound as well as without cells were included as controls. Wells were incubated for 4 h at 37 °C, carefully washed three times with 125 µL fresh medium each and incubated for another 3 days in 100 µL fresh medium. Finally, cell viability was assessed by using CellTiterGlo® luminescent cell viability assay (Promega, Madison, WI, USA) according to the manufacturer's instructions. Data was normalized using wells with cells but without test compound as 100 % and those without cells as 0 %. IC_{50} values and statistics were determined by fitting the viability data to a 4-parameter regression model with GraphPad Prism software (GraphPad Software, La Jolla, CA, USA).

4. Results and discussion

4.1. Liposomal formulation development

Sortaggable, pentaglycine-modified liposomes were prepared by a continuous and scalable solvent injection process utilizing a binary pumping system and a T-shaped mixing element as described earlier [27]. Buffer flow rate was screened for influence on hydrodynamic diameter

(d_h) and PDI (Figure 1). Mean size was reduced with increased buffer flow due to increased shear forces at the injection site [30].

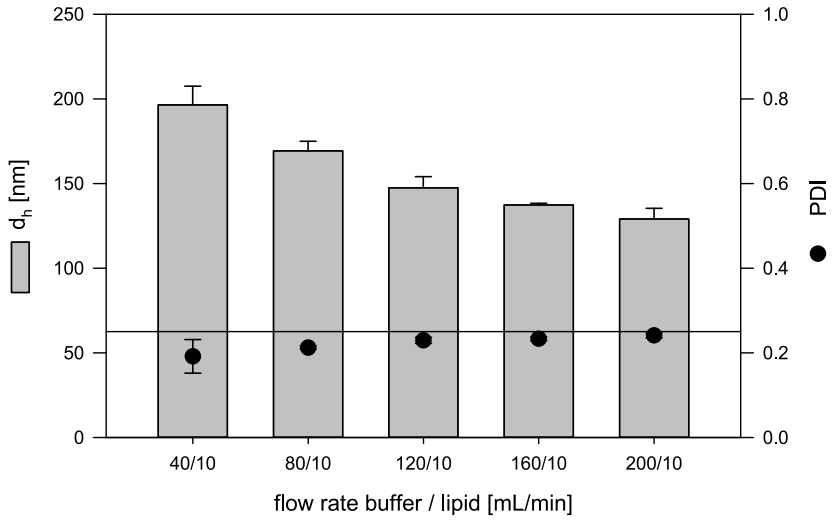

Figure 1: Liposomal size adjustment. The total flow rate was varied to optimize the hydrodynamic diameter (d_h) and polydispersity index (PDI) of the liposomal dispersion obtained from lipid injection into 250 mM ammonium sulfate buffer. Mean size was adjustable between 130 nm and 200 nm, PDI was < 0.25 (reference line) for all settings. Error bars indicate standard deviations of three individual experiments.

Compared to previously reported manufacturing processes, slightly larger (20 nm) d_h were obtained in ammonium sulfate buffer compared to DPBS [27], although other manufacturing parameters (lipid composition and molarity, organic solvent, flow rates) were equal. This indicates the influence of buffer type on the liposome formation mechanism or on the bilayer appearance. Here, lipid headgroups may interact with salts or change their protonation status due to different pH, leading to a change of their headgroup volume. PDI was < 0.25 for all settings, what indicates an acceptable polydispersity of the dispersion. A buffer flow rate of 120 mL/min was chosen for further experiments to prepare liposomes with a mean size of ≈150 nm. This size was previously shown as suitable for effective targeting of myeloid immune cells *in vitro* [27] and *in vivo* [31] with equally composed pentaglycine liposomes. Tangential flow filtration was used to exchange the surrounding buffer to DPBS and to concentrate the liposomal dispersion. These pH and ammonium sulfate gradient pentaglycine liposomes were stable at 2-8 °C for eight weeks regarding physical parameters (size, PDI, zeta potential; Supplementary Figure 1). Furthermore, the liposomes were found to be chemically stable as the bilayer composition was maintained during storage (Supplementary Figure 2). Active loading of drugs to liposomes via a pH and salt gradient typically requires heating to the transition temperature (t_m) of the bilayer [28]. t_m of the lipid blend including the pentaglycine lipids was therefore determined by DSC (Supplementary Figure 3). The measured t_m of 43.7 ± 1.8 °C was comparable to the t_m of the major component DPPC (t_m = 41 °C [32]). As expected, the t_m was not altered by the integrated DMA-PEG-G5 in a relevant manner compared to previous studies. Therefore,

loading experiments were conducted at 49 °C [28]. DXR loading duration was evaluated by dialyzing aliquots drawn from the loading bulk after different time points (Figure 2) in a dialysis bag (10 kDa membrane cut-off). This molecular weight cut-off was suitable to ensure sufficient permeability for the small molecule DXR (543.5 Da). Surprisingly, after lipid and DXR content determination, low encapsulation efficiencies (< 50 %) were obtained for short loading times up to 4 h (Figure 2).

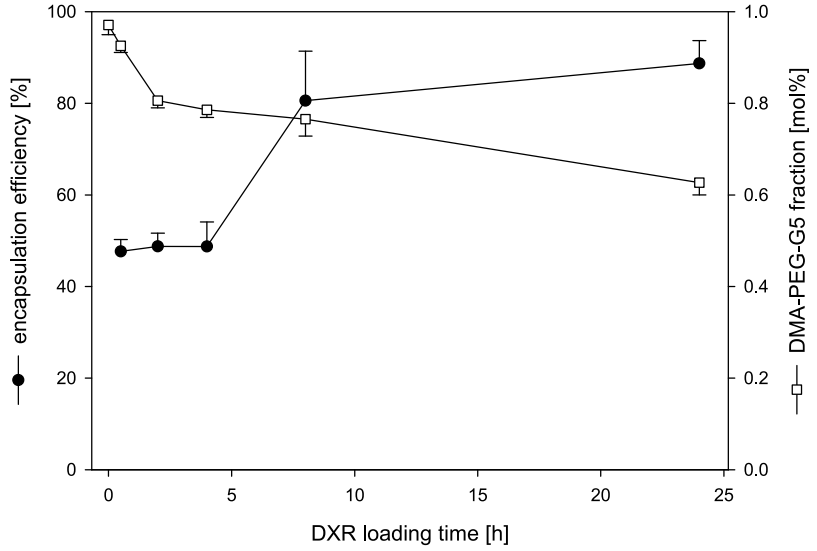

Figure 2: Doxorubicin loading to pentaglycine-modified, PEGylated liposomes. Encapsulation efficiency was low for short incubation times ≤ 4 h and increased up to 89 % after a 24 h loading. The amount of DMA-PEG-G5 in the bilayer concomitantly decreased with prolonged loading at elevated temperature (49 °C), indicating a thermodynamic lability of this amino acid lipid. Data is shown as mean ± standard deviation of loading experiments with three liposome batches.

This was an unexpected result, as typical encapsulation efficiencies for doxorubicin via ammonium sulfate remote loading procedure are > 90 % [6]. We therefore further increased the loading time, achieving encapsulation efficiencies of 89 ± 5 % after 24 h, however with significant impact on chemical and physical stability of the liposomes. DMA-PEG-G5 bilayer fraction decreased upon long lasting incubation at 49 °C, indicating a temperature sensitivity of this lipid (Figure 2). Furthermore, liposome size and PDI increased with continuing incubation (Supplementary Figure 4).

We hypothesized, that the loading buffer was the reason for initially low encapsulation efficiencies. A phosphate buffer was used to obtain a liposomal dispersion ready for Sortase-A conjugation, similar to a previously described protocol for liposome modification [27]. Phosphate salts are known to form a gel-like, viscous dispersion with DXR [33, 34]. This may hinder an efficient and fast DXR diffusion through the liposome membrane, thereby increasing the required time for an exhaustive loading. This was supported by an inverse correlation of loading efficiency and absolute phosphate concentration in the loading mix (Supplementary Figure 5), resulting from different mixing ratios of the DPBS-surrounded liposome dispersion and

the aqueous DXR stock solution. Further increases of loading efficiency were observed when an additional dialysis step was added after TFF, most likely by an enhancement of the salt and pH-gradient by a reduction of ammonium sulfate residuals. These small solutes may underlie a quick reverse diffusion over the TFF-membrane (molecular weight cut-off: 500 kDa) [35], hampering an efficient ammonium sulfate gradient generation. The additional dialysis step prior to DXR loading increased the encapsulation efficiency to 93 % at a phosphate concentration of 0.58 mM (4 h incubation).

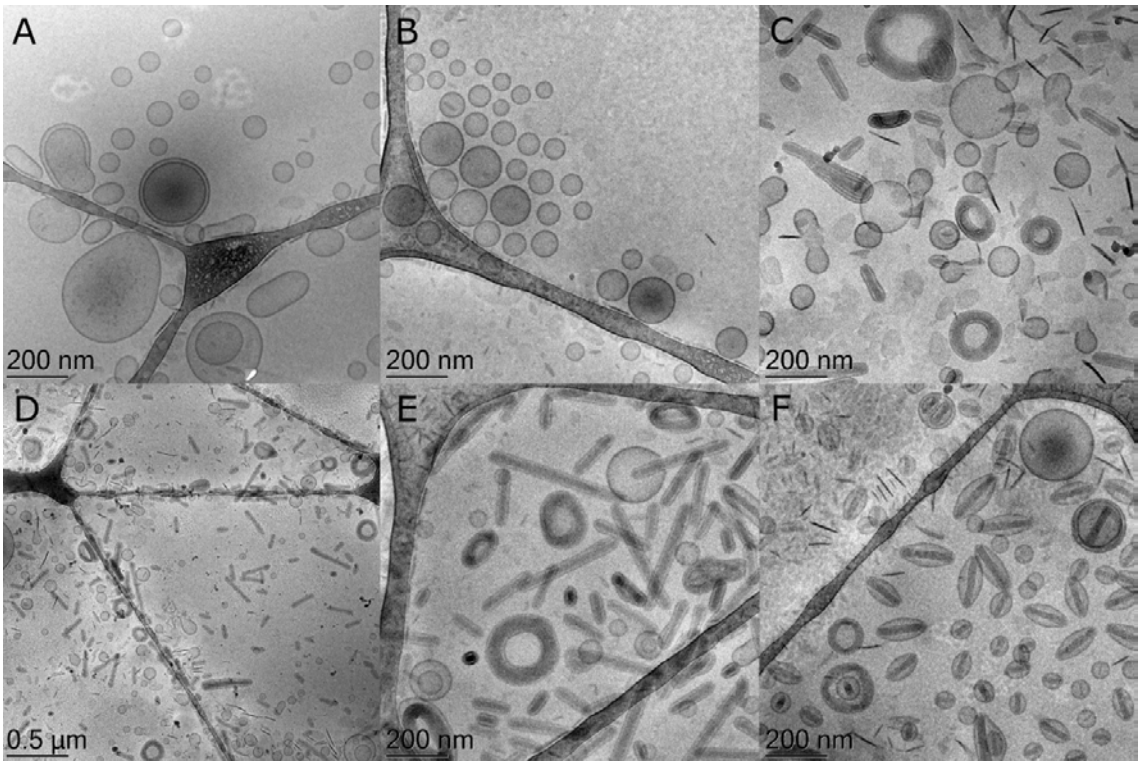

Figure 3: Representative cryo-TEM pictures of pentaglycine liposomes prepared by solvent injection. **A**: After solvent injection in ammonium sulfate buffer. **B**: After rebuffering to DPBS. **C** and **D**: After DXR loading (4 h incubation, from DPBS). **E**: After DXR loading (1 h incubation, from DPBS). **F**: After DXR loading (1 h incubation, from HEPES buffer).

Cryo-TEM was used to image the liposomes individually after solvent injection, tangential flow filtration and doxorubicin loading (Figure 3). Mostly spherical, uni- to bilamellar vesicles were observed after injection and tangential flow filtration. DXR loading had dramatic effects on the liposome appearance: different from frequently reported “coffee-bean” or “rugby” structures [17], many liposomes had a rod-like appearance, probably due to a subsequent growing doxorubicin precipitate in the liposome interior. These rod-like, drug-loaded liposomes had lengths of several hundred nanometers. Furthermore, “donut”-like structures were observed. The precipitate inside the vesicles had a fibrous appearance with a periodicity of about 3 nm, comparable to previous descriptions of such liposomes being loaded via the ammonium sulfate method [36]. Though partly present already after solvent injection and TFF, plenty of disk-like micelle structures were observed especially after doxorubicin-loading. Lasic et al. suggested that the presence of DSPE-mPEG stabilized these flat structures [36, 37]. Subsequent processing such

as tangential flow filtration and DXR loading may enhance their formation by increased stress factors like shearing during pumping and elevated temperature during loading. Thus, we investigated whether loading time or loading medium may influence the liposome appearance. While reduction of the incubation to 1 h did not lead to a homogenous dispersion (Figure 3E), exchanging the loading medium from DPBS to HEPES buffer (as frequently described by various groups [33, 38-41]) had considerable influence on the liposome appearance (Figure 3F). Typical coffee-bean structures were obtained by this method and less rod-like structures were observed. Interestingly, though liposomes appeared quite different in cryo-TEM, dynamic light scattering measurements did not indicate such distinct differences (Supplementary Table 1). It remains unclear why the loading medium has such a high impact on the precipitate dimension inside the vesicles. There might be a co-diffusion of a doxorubicin-phosphate salt inside the liposome interior during the loading at elevated temperature, or slight phosphate "loading" during the shearing caused by the peristaltic pump during TFF. Presence of different anions in the liposome interior are known to have significant impact on the appearance of the precipitate [42]. Low concentrations of phosphate anions inside the liposomes may therefore influence DXR precipitate morphology, thereby leading to the observed rod-like structures.

4.2. Ligand conjugation

Sortase-A was used to graft C_H-LPETG-mAbs on the pentaglycine-modified liposomal surface (Scheme 1). This enzyme promotes a transpeptidation between the threonine of the LPETG-stretch and the N-terminal amino group of the pentaglycine lipid anchor. Since the LPETG-motif was C-terminally attached to both heavy chain C-termini of the homodimeric antibody, two modifications per C_H-LPETG-mAb were distinguishable (mono-modification, termed as (DMA-PEG)-C_H-LPETG-mAb, and a di-modification, termed as (DMA-PEG)$_2$-C_H-LPETG-mAb). Both expected conjugate species were observed as separate peaks in an rp-HPLC analysis (Figure 4).

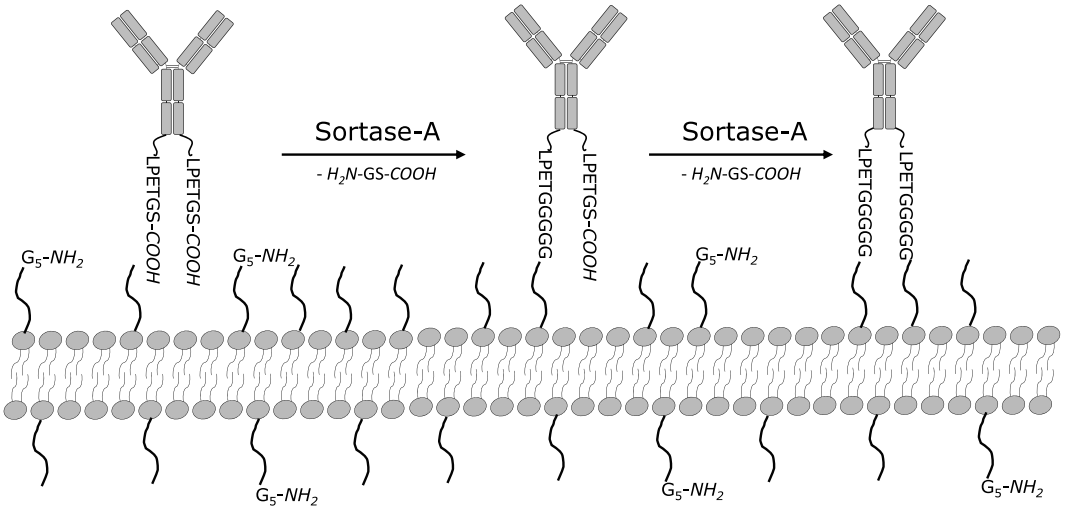

Scheme 1: Schematic conjugation of C_H-LPETG-mAb onto a PEGylated, pentaglycine-modified bilayer.

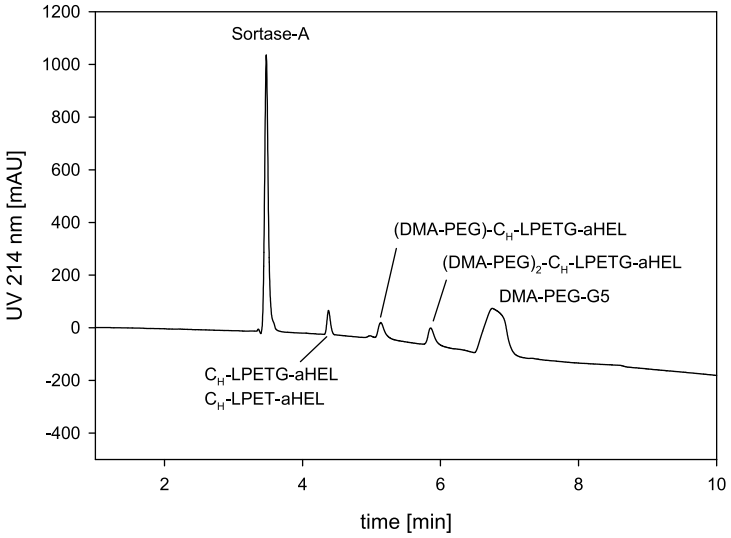

Figure 4: rp-HPLC analysis of Sortase-A mediated C_H-LPETG-aHEL conjugation to pentaglycine-modified liposomes. Reaction conditions: Sortase-A (25 µM), C_H-LPETG-aHEL (1.0 µM) and liposomes (100 µM based on pentaglycine content), incubated for 2 h at 4 °C.

Liposomes equivalent to 100 µM pentaglycine, from which roughly 50 µM were estimated to be accessible for the reaction due to their presence on the outer leaflet of the bilayer (assuming an even distribution in the layers), were incubated with various concentrations of C_H-LPETG-C225. Since macroscopically visible precipitation occurred with initially used high ratios of C_H-LPETG-C225 towards the liposomes (50 µM C_H-LPETG-C225 to 100 µM total pentaglycine), we systematically screened reaction conditions for a stable conjugation protocol (Figure 5).

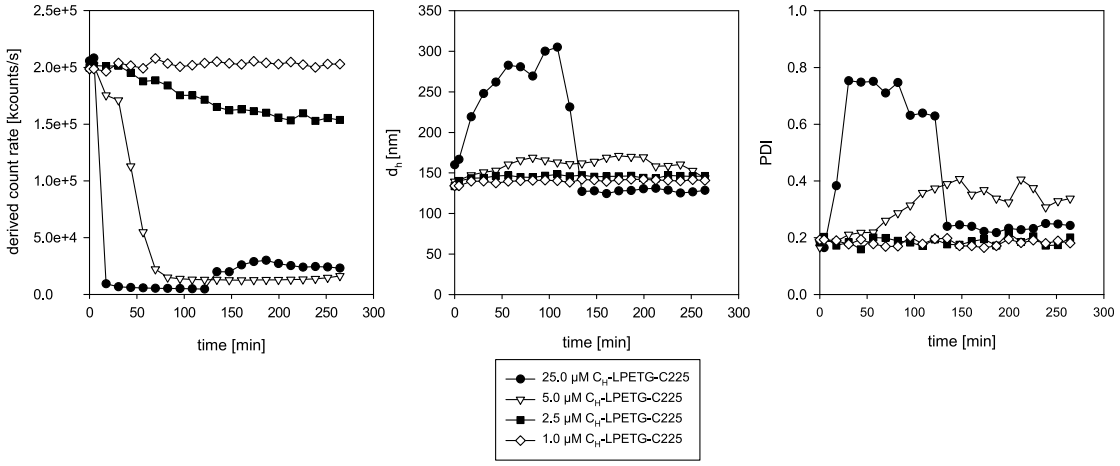

Figure 5: Colloidal stability of the liposomal dispersion during sortagging. C_H-LPETG-C225 was spiked in different concentrations to 100 µM pentaglycine of DXR-loaded liposomes and 25 µM Sortase-A. The reaction progress was monitored by dynamic light scattering for the derived count rate, hydrodynamic diameter and polydispersity index. Strong losses of light scattering intensity indicated aggregation and sedimentation during the reaction.

For that purpose, a cuvette-based dynamic light scattering measurement was deployed and the laser light attenuation corrected ("derived") count rate was used as a parameter for colloidal stability. Here, sedimentation of insoluble aggregates decreases the optical density of the sample in the measurement zone of the cuvette. Monitoring of the derived count rate clearly showed a correlation between the initial C_H-LPETG-C225 concentration and the colloidal

stability. The count rate decreased drastically for 5 µM and 25 µM initial C_H-LPETG-C225 concentration. Only in case of very low C_H-LPETG-mAb concentrations (1.0 µM), a completely stable reaction was observed, indicated by an unchanged count rate, d_h and PDI. The d_h increased especially for the higher concentrations of 5 µM and 25 µM, followed by a decrease down to ≈100 nm due to aggregation and sedimentation. The PDI followed a similar behavior for those two concentrations applied. Liposomes modified with 2.5 µM C_H-LPETG-C225 showed an intermediate behavior. Although the derived count rate decreased significantly for this group, no changes in mean size or PDI were observed. This indicates the formation of a fraction of insoluble and sedimenting aggregates, which are not suitable to be detected by DLS, since they are typically considered as dust by DLS algorithms. Hence, they do not contribute to calculation of the d_h or PDI. Control groups including pure liposomes, a sample of liposomes and 25 µM C_H-LPETG-C225 without Sortase-A as well as a mixture of liposomes, 50 µM LPETG-VHH and Sortase-A did not show aggregation (Supplementary Figure 6). The mass ratio of protein to lipid was similar for the reaction conditions of 50 µM VHH and 5 µM C_H-LPETG-C225. Potentially, the dual mAb modification results in a cross linking of liposomes via Sortase-A and is thereby responsible for the high aggregation propensity at increased antibody concentrations.

To gain deeper insights into the conjugation kinetic of C_H-LPETG-mAbs towards the pentaglycine-modified surface of the PEGylated liposomes, the reaction of 1.0 µM C_H-LPETG-aHEL towards DXR-free liposomes was monitored over 14 h by rp-HPLC. Interestingly, the conversion followed a disproportionation profile (Figure 6). Since the Sortase-A recognition motif LPETG is reformed during the reaction and, hence, also existing in the mAb-liposome product (Scheme 1), the latter can serve as a substrate for another reaction cycle. This reaction can either be the reverse reaction, which would result in deconjugation, or hydrolysis as a general side reaction of sortagging. For up to 4 h, the lipidation of C_H-LPETG-aHEL is the predominant reaction. After 4 h, most C_H-LPETG-aHEL was converted into $(DMA\text{-}PEG)_2$-C_H-LPETG-aHEL (56.3 ± 1.0 mol%), with a minor increase after a prolonged incubation to 14 h (61.8 ± 1.5 mol%). Compared to that, the (DMA-PEG)-C_H-LPETG-aHEL fraction reduced from 22.1 ± 3.2 mol% to 6.7 ± 0.5 mol% in the terminal reaction phase. Interestingly, unconjugated C_H-LPETG-aHEL fraction showed an increase from 21.0 ± 0.5 mol% to 30.5 ± 2.6 mol% between 4 h to 14 h. C_H-LPET-aHEL lacking the hydrolyzed terminal glycine is expected to elute with intact C_H-LPETG-aHEL in the rp-HPLC analysis (Figure 4). Thus, the reaction kinetic indicated that not the di-modification, but a hydrolytic cleavage of (DMA-PEG)-C_H-LPETG-aHEL towards C_H-LPET-aHEL was predominant in the terminal phase of the reaction. The prolonged incubation therefore especially impacts the fraction of mono-modified mAb and reduces the total amount of ligand conjugated to the liposomes. On the other hand, a prolonged sortagging reaction improves chemical homogeneity

of the obtained immunoliposomes, since the intermediate (DMA-PEG)-C_H-LPETG-aHEL fraction is reduced compared to the final product $(DMA\text{-}PEG)_2$-C_H-LPETG-aHEL.

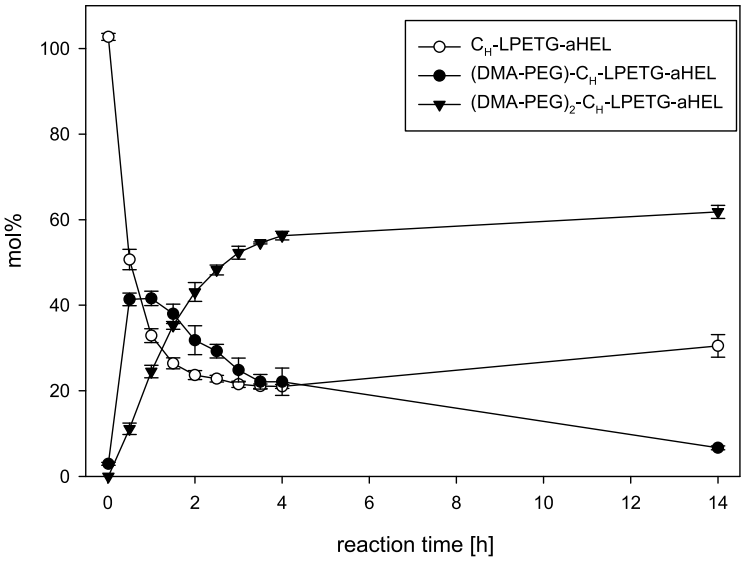

Figure 6: Kinetics of Sortase-A (25 µM) mediated conjugation of C_H-LPETG-aHEL (1.0 µM) to pentaglycine-modified, PEGylated liposomes. The mono-modified (DMA-PEG)-C_H-LPETG-aHEL is the major product for up to 1.5 h incubation, after which the di-modified $(DMA\text{-}PEG)_2$-C_H-LPETG-aHEL is the dominant fraction. A significant reverse reaction can be observed between 4 h and 14 h, indicated by an increase of the non-lipidated C_H-LPETG-aHEL fraction in the terminal reaction phase. The maximum amount of aHEL conjugated to the liposomes (sum of mono- and di-modified mAb) was observed after 4 h (78.4 mol%). Error bars indicate standard deviations of three reactions.

Summarizing the investigations on reaction conditions and kinetics, it can be concluded that the initial concentration of C_H-LPETG-aHEL should not exceed 2.5 µM to prevent extensive aggregation of the liposomal dispersion at the investigated conditions (4 °C incubation temperature, 25 µM Sortase-A, 100 µM pentaglycine). The kinetic investigations identified that the maximal amount (78.4 mol% of 1.0 µM) was conjugated to the PEGylated liposomes after 4 h, either as mono- or di-modified variant. Hence, these conditions were chosen to prepare DXR-loaded immunoliposomes for *in vitro* cytotoxicity tests.

4.3. *In vitro* cytotoxicity of targeted DXR-liposomes on breast cancer cells

In order to evaluate, if doxorubicin encapsulation in functionalized liposomes simultaneously mediated decreased unspecific toxicity but increased targeted activity against $EGFR^+$ cells, we performed *in vitro* cytotoxicity assays. DPPC-based, DXR-loaded liposomes were modified with 1.0 µM or 2.5 µM C_H-LPETG-aHEL or C_H-LPETG-C225, respectively, and purified by dialysis. For that purpose, a dialysis device with a membrane molecular weight cut-off of 1000 kDa was chosen, which should ensure a sufficient permeability for Sortase-A (20.9 kDa) as well as monoclonal antibodies (C_H-LPETG-aHEL: 146.1 kDa, C_H-LPETG-C225: 146.7 kDa). Furthermore, these devices were previously reported to retain the nanoparticulate liposome dispersion in a sufficient manner (lipid recovery > 88 %, [31]).

Table 1: Physico-chemical parameters of EGFR-targeted DXR-liposomes and control groups (standard deviation shown for triplicate analyses).

formulation	d_h [nm]	PDI	zp [mV]	DXR:mAb ratio	nM mAB / µM PL
DPPC-LS	142 ± 1	0.19 ± 0.03	-9.3 ± 0.5	-	-
1.0 µM-aHEL-DPPC-LS	143 ± 1	0.19 ± 0.01	-7.5 ± 0.4	5982	0.057
2.5 µM-aHEL-DPPC-LS	144 ± 0	0.20 ± 0.00	-5.3 ± 0.8	2418	0.138
1.0 µM-C225-DPPC-LS	143 ± 1	0.20 ± 0.01	-8.0 ± 0.3	6334	0.053
2.5 µM-C225-DPPC-LS	145 ± 1	0.19 ± 0.02	-7.2 ± 0.2	2327	0.147
HSPC-LS	120 ± 1	0.22 ± 0.00	-14.8 ± 0.6	-	-
1.0 µM-aHEL-HSPC-LS	101 ± 2	0.23 ± 0.01	-12.6 ± 0.3	4911	0.072
1.0 µM-C225-HSPC-LS	121 ± 1	0.22 ± 0.01	-10.7 ± 0.2	5732	0.062

DPPC-based liposomes modified with 1.0 µM or 2.5 µM C_H-LPETG-C225 or C_H-LPETG-aHEL showed neither changes in the hydrodynamic diameter nor in PDI (Table 1) after the final liposome processing compared to the non-conjugated control. No macroscopically visible precipitation or lipid loss (*data not shown in publication, lipid recoveries ranged from 94-100 %*) was observed.

EGFR$^+$ MDA-MB-468 cells were exposed to the dialyzed formulations for 4 h and, after careful medium exchange, incubated for another 3 days in pure growth medium. It should be tested whether the drug encapsulation firstly decreases the unspecific toxicity of pure doxorubicin, and secondly, whether a selective targeting via the EGF-receptor was able to re-increase the cytotoxicity *in vitro* (Figure 7).

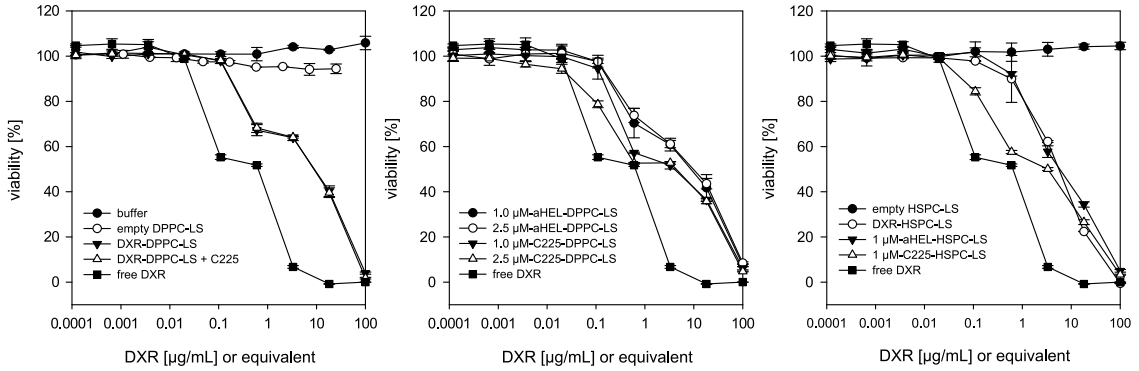

Figure 7: Viability curves of targeted, DXR-loaded DPPC-LS, HSPC-LS and controls. MDA-MB-468 cells were incubated with the liposomal formulations at different DXR concentrations (or equivalent lipid concentrations, according to the DXR:lipid ratio of drug-loaded LS). After 4 h, medium containing unbound liposomes was exchanged, followed by a further incubation of the cells for 3 days, until viability was assessed. Free DXR showed highest cytotoxicity, which was alleviated by drug encapsulation. EGFR-targeting led to a re-increase of cytotoxicity. Data shows mean ± standard deviation of two biological experiments.

Pure doxorubicin had an IC_{50} of 0.3 ± 1.2 µg/mL (Figure 8), which is in line with previously reported IC_{50} values on this cell line (Mamot et al: 0.8 µg/mL [40]). Encapsulation of DXR in the pentaglycine-modified, PEGylated liposomes (DPPC-LS) led to an 18fold decrease of toxicity as indicated by an appropriate increase in IC_{50} (Figure 8A). Similar values were obtained for the

isotype-control C_H-LPETG-aHEL carrying immunoliposomes (19fold and 21fold increase for 1.5 µM-aHEL-DPPC-LS and 2.5 µM-aHEL-DPPC-LS, respectively, not significantly different from mAb-free DPPC-LS). Drug-free (empty) liposomes were not toxic (tested up to 1.3 mM total lipid, Figure 7). Conjugation of C_H-LPETG-C225 mediated an increased cytotoxicity of the liposomes to an IC_{50} of 3.2 µg/mL for 1.0 µM-C225-DPPC-LS and 2.2 µg/mL for 2.5 µM-C225-DPPC-LS, latter significantly different from DPPC-LS ($p < 0.05$, Figure 8A). This indicates a targeted cytotoxicity, that is further amplified at higher ligand densities. Cellular specificity, meaning selective toxicity of C225-targeted liposomes on EGFR-overexpressing cells, but equal toxicity of targeted and non-targeted liposomes on $EGFR^-$ cells has been demonstrated several times with comparable liposomal constructs [40, 43] or C225-based ADCs [24]. The here presented targeted cytotoxicity was also not due to synergistic effects of C_H-LPETG-C225 and liposomal doxorubicin, as a physical mixture (C_H-LPETG-C225 : DXR ratio equal to 2.5 µM-C225-DPPC-LS) showed cytotoxicity comparable to the isotype- or unconjugated liposomes. This underlines the requirement of a stable (covalent) anchoring of the ligand onto the targeted drug delivery system.

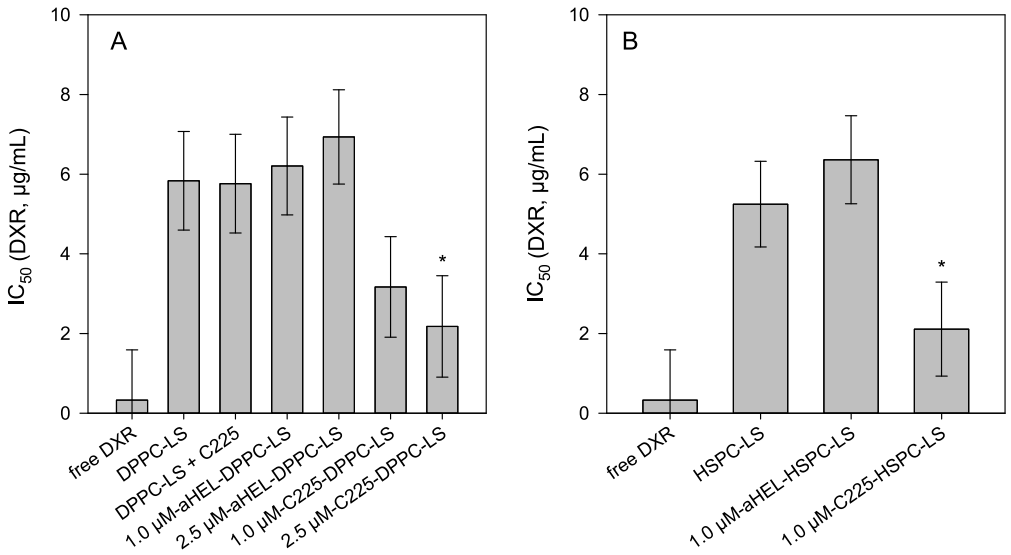

Figure 8: IC_{50} values of EGFR-targeted, DXR-loaded liposomes and controls on MDA-MB-468 cells (data is shown as mean ± standard deviation of two biological experiments; * indicates significant differences ($p < 0.05$) to the ligand free control). **A**: DPPC-based liposomes, loaded with DXR from DPBS buffer and showing significant rod-like morphology. **B**: HSPC-based liposomes, loaded with DXR from HEPES buffer and assumed to have a predominant "coffee-bean" structure. Targeted formulations increased cytotoxicity over non-targeted ones. No relevant differences were observed between the DPPC- and HSPC-based formulations.

Previous reports suggested a density of 0.3-1.2 nM ligand / µM phospholipid for C225 Fab' targeted DXR liposomes, reaching IC_{50} values of 1.1 µg/mL on the same cell line [38, 40]. The ligand density of the presented liposomes ranged from 0.05-0.15 nM ligand / µM phospholipid (Table 1). For direct comparison it should be considered, that monoclonal antibodies provide two ligand binding sites compared to a Fab' fragment. Interestingly, we found only slightly higher IC_{50} values for the 2.5 µM-C225-DPPC-LS constructs (1.1 µg/mL described by Mamot et al. versus 2.2 µg/mL described here). However, more drastic differences were observed for untargeted

DPPC-LS (32 µg/mL versus 5.8 µg/mL). The higher unspecific toxicity of the presented system led to the question whether the particle shape or usage of DPPC (instead of the higher melting HSPC) was the reason for this observation. We therefore prepared HPSC-based liposomes (HSPC-LS) which were loaded with DXR from HEPES buffer to achieve a predominant "coffee-bean" shape based on our morphological investigations (Figure 3) and previously reported cryo-TEM analysis of comparably prepared liposomes [42]. An overview of the different liposomal preparation conditions, the corresponding morphological analyses and link to cytotoxicity read-out is given in Supplementary Table 2. The HSPC-LS were then conjugated with either 1.0 or 2.5 µM C_H-LPETG-aHEL or C_H-LPETG-C225. The reaction behavior was found to be less stable in HEPES compared to DPBS, as strong precipitation was observed for the 2.5 µM group, which was therefore not considered for *in vitro* analyses. Minor aggregates in the 1.0 µM group were removed by centrifugation (5 min at 800 x g), leading to a lipid loss of 10-25 %. Interestingly, negligible impact on IC_{50} values compared to DPPC-LS was observed (5.3 ± 1.1, 6.4 ± 1.1 and 2.1 ± 1.2 µg/mL for ligand free, C_H-LPETG-aHEL and C_H-LPETG-C225-modifed liposomes, respectively, Figure 8B). This suggests a minor influence of DPPC or HSPC usage and also DXR-loading procedure on the *in vitro* performance. The non-targeted DPPC- and HSPC-based formulations showed no significant differences of unspecific toxicity, that could have been caused by the different morphology or bilayer rigidity. The unspecific toxicity was unexpectedly high, expressed in a ratio of 2.5 between the IC_{50} value of non-targeted HSPC-LS and 1.0 µM-C225-HSPC-LS. Mamot et al. reported a ratio of 29 between comparably composed targeted or non-targeted liposomes on the same cell line [40]. This may be explained by different cytotoxicity experiment settings. Especially the longer exposition of cells (2 h in literature compared to 4 h in the presented report) to the formulations prior the wash-out may have led to a drug release and hence higher unspecific toxicity of the liposomes. Comparable observations were previously reported for CD19-targeted, DXR-loaded liposomes [44]. Although the authors obtained only low ratios of 4.6 (for 1 h incubation of cells with the liposomes) or 1.8 (for 24 h incubation) *in vitro*, the targeted liposomes were able to significantly enhance the mean survival time of B-lymphoma model mice. Comparably, Zalba et al. reported a low ratio of 1.5 between the IC_{50} of EGFR-targeted (26 µM) or non-targeted (39 µM), oxaliplatin-loaded liposomes on SW-480 cells (colorectal cancer cells) after 4 h incubation. Nevertheless, the targeted liposomes clearly improved tumor growth inhibition of SW-480 derived xenografts in mice compared to non-targeted ones [43]. These results underline that low ratios in IC_{50} values between targeted and non-targeted liposomes observed *in vitro* are not necessarily predictive for the *in vivo* performance of the drug delivery system.

5. Conclusion and outlook

In the presented work, we thoroughly investigated the loading of doxorubicin into pentaglycine-modified liposomes which were prepared in a controllable and scalable manufacturing process. The pentaglycine lipid anchor was used to conjugate C_H-LPETG-mAbs as targeting ligands on the drug delivery system by sortagging. The conjugation required detailed analyses of reaction conditions and kinetics, as a strong aggregation and precipitation propensity was observed. This was attributed to the presence of two LPETG-motifs per mAb that may lead to cross-linking between liposomes. Precipitation was circumvented by a drastic reduction of the C_H-LPETG-mAb : lipid ratio during reaction. This decrease consequently led to decreased ligand densities < 0.3 nM / µM PL on the liposomal system. Although the ligand density was low, the liposomal drug delivery system increased the specificity of doxorubicin toxicity *in vitro* in a targeted manner. This was firstly indicated by an 18fold increase of the IC_{50} by drug encapsulation in the carrier. Secondly, grafting of cetuximab on the liposomal surface led to a re-decrease of the IC_{50} on breast cancer cells carrying the targeted structure. This drug targeting effect was ligand specific since it was not shown by liposomes functionalized with an isotype control antibody. Increased ligand density may further improve binding efficacy and internalization of the liposomal system [40], which is known to be more effective if multivalent (binding of several receptors) systems are used [45]. Therefore, the use of alternative sortaggable ligands such as Fab's, single-chain variable fragments (scFv) or single-domain antibodies employed with a single LPxTG-motif should be considered for optimization. This would firstly reduce the mass per ligand conjugated to the carrier and secondly avoid liposome cross-linking during conjugation. Furthermore, usage of ligands lacking a Fc-domain would also circumvent pharmacokinetic disadvantages known from full length mAbs used as targeting ligands for immunoliposomes [43, 46-49]. Whether such EGFR-targeted, DXR-loaded drug carriers may improve the treatment of solid tumors in humans was recently investigated in a phase I trial [3]. Interestingly, the authors reported a remarkably low skin cytotoxicity, an issue which is a major concern in the development of EGFR-targeted ADCs [24]. This observation may strengthen the consideration of particulate targeting systems, such as the described nano-sized liposomal system as an alternative to antibody-drug conjugates.

6. Acknowledgement

The authors would like to thank Christopher Bachran and Lee Kim Swee from BioMed X GmbH for supply of Sortase-A. Martina Jeschke is gratefully acknowledged for support during liposome manufacturing. Furthermore, the authors like to thank Markus Drechsler from University of Bayreuth for cryo-TEM pictures.

References

[1] M. Merino, S. Zalba, M.J. Garrido, Immunoliposomes in clinical oncology: State of the art and future perspectives, Journal of Controlled Release, 275 (2018) 162-176.

[2] P. Marques-Gallego, A.I. de Kroon, Ligation strategies for targeting liposomal nanocarriers, Biomed Research International, (2014) e129458.

[3] C. Mamot, R. Ritschard, A. Wicki, G. Stehle, T. Dieterle, L. Bubendorf, C. Hilker, S. Deuster, R. Herrmann, C. Rochlitz, Tolerability, safety, pharmacokinetics, and efficacy of doxorubicin-loaded anti-EGFR immunoliposomes in advanced solid tumours: a phase 1 dose-escalation study, The Lancet Oncology, 13 (2012) 1234-1241.

[4] Y. Matsumura, M. Gotoh, K. Muro, Y. Yamada, K. Shirao, Y. Shimada, M. Okuwa, S. Matsumoto, Y. Miyata, H. Ohkura, K. Chin, S. Baba, T. Yamao, A. Kannami, Y. Takamatsu, K. Ito, K. Takahashi, Phase I and pharmacokinetic study of MCC-465, a doxorubicin (DXR) encapsulated in PEG immunoliposome, in patients with metastatic stomach cancer, Annals of Oncology, 15 (2004) 517-525.

[5] P.N. Munster, K. Miller, I.E. Krop, N. Dhindsa, J. Reynolds, E. Geretti, C. Niyikiza, U. Nielsen, B. Hendriks, T.J. Wickham, V.M. Moyo, P. LoRusso, A phase I study of MM-302, a HER2-targeted liposomal doxorubicin, in patients with advanced, HER2-positive (HER2+) breast cancer, Journal of Clinical Oncology, 30 (2012) TPS663-TPS663.

[6] Y. Barenholz, Doxil® – The first FDA-approved nano-drug: Lessons learned, Journal of Controlled Release, 160 (2012) 117-134.

[7] A.N. Lukyanov, T.A. Elbayoumi, A.R. Chakilam, V.P. Torchilin, Tumor-targeted liposomes: doxorubicin-loaded long-circulating liposomes modified with anti-cancer antibody, Journal of Controlled Release, 100 (2004) 135-144.

[8] S.C. Alley, D.R. Benjamin, S.C. Jeffrey, N.M. Okeley, D.L. Meyer, R.J. Sanderson, P.D. Senter, Contribution of Linker Stability to the Activities of Anticancer Immunoconjugates, Bioconjugate Chemistry, 19 (2008) 759-765.

[9] N. Jain, S.W. Smith, S. Ghone, B. Tomczuk, Current ADC Linker Chemistry, Pharmaceutical Research, 32 (2015) 3526-3540.

[10] M. Ritzefeld, Sortagging: A Robust and Efficient Chemoenzymatic Ligation Strategy, Chemistry – A European Journal, 20 (2014) 8516-8529.

[11] R.R. Beerli, T. Hell, A.S. Merkel, U. Grawunder, Sortase enzyme-mediated generation of site-specifically conjugated antibody drug conjugates with high in vitro and in vivo potency, PloS one, 10 (2015) e0131177.

[12] L.S. Lee, C. Conover, C. Shi, M. Whitlow, D. Filpula, Prolonged Circulating Lives of Single-Chain Fv Proteins Conjugated with Polyethylene Glycol: A Comparison of Conjugation Chemistries and Compounds, Bioconjugate Chemistry, 10 (1999) 973-981.

[13] J. Guo, S. Kumar, M. Chipley, O. Marcq, D. Gupta, Z. Jin, D.S. Tomar, C. Swabowski, J. Smith, J.A. Starkey, S.K. Singh, Characterization and Higher-Order Structure Assessment of an Interchain Cysteine-Based ADC: Impact of Drug Loading and Distribution on the Mechanism of Aggregation, Bioconjugate Chemistry, 27 (2016) 604-615.

[14] Y.T. Adem, K.A. Schwarz, E. Duenas, T.W. Patapoff, W.J. Galush, O. Esue, Auristatin Antibody Drug Conjugate Physical Instability and the Role of Drug Payload, Bioconjugate Chemistry, 25 (2014) 656-664.

[15] O. Tacar, P. Sriamornsak, C.R. Dass, Doxorubicin: an update on anticancer molecular action, toxicity and novel drug delivery systems, Journal of Pharmacy and Pharmacology, 65 (2013) 157-170.

[16] M. Theodoulou, C. Hudis, Cardiac profiles of liposomal anthracyclines, Cancer, 100 (2004) 2052-2063.

[17] J. Gubernator, Active methods of drug loading into liposomes: recent strategies for stable drug entrapment and increased in vivo activity, Expert Opinion on Drug Delivery, 8 (2011) 565-580.

[18] A. Gabizon, R. Catane, B. Uziely, B. Kaufman, T. Safra, R. Cohen, F. Martin, A. Huang, Y. Barenholz, Prolonged Circulation Time and Enhanced Accumulation in Malignant Exudates of Doxorubicin Encapsulated in Polyethylene-glycol Coated Liposomes, Cancer Research, 54 (1994) 987.

[19] Z. Symon, A. Peyser, D. Tzemach, O. Lyass, E. Sucher, E. Shezen, A. Gabizon, Selective delivery of doxorubicin to patients with breast carcinoma metastases by stealth liposomes, Cancer, 86 (1999) 72-78.

[20] R. Solomon, A.A. Gabizon, Clinical Pharmacology of Liposomal Anthracyclines: Focus on Pegylated Liposomal Doxorubicin, Clinical Lymphoma and Myeloma, 8 (2008) 21-32.

[21] C. Yewale, D. Baradia, I. Vhora, S. Patil, A. Misra, Epidermal growth factor receptor targeting in cancer: A review of trends and strategies, Biomaterials, 34 (2013) 8690-8707.
[22] K.M. Riaz, A.M. Riaz, X. Zhang, C. Lin, H.K. Wong, X. Chen, G. Zhang, A. Lu, Z. Yang, Surface Functionalization and Targeting Strategies of Liposomes in Solid Tumor Therapy: A Review, International Journal of Molecular Sciences, 19 (2018) 195.
[23] J. Tol, C.J.A. Punt, Monoclonal antibodies in the treatment of metastatic colorectal cancer: A review, Clinical Therapeutics, 32 (2010) 437-453.
[24] C. Sellmann, A. Doerner, C. Knuehl, N. Rasche, V. Sood, S. Krah, L. Rhiel, A. Messemer, J. Wesolowski, M. Schuette, S. Becker, L. Toleikis, H. Kolmar, B. Hock, Balancing Selectivity and Efficacy of Bispecific Epidermal Growth Factor Receptor (EGFR) × c-MET Antibodies and Antibody-Drug Conjugates, Journal of Biological Chemistry, 291 (2016) 25106-25119.
[25] S. Wöll, S. Schiller, C. Bachran, L.K. Swee, R. Scherließ, Pentaglycine lipid derivates – rp-HPLC analytics for bioorthogonal anchor molecules in targeted, multiple-composite liposomal drug delivery systems, International Journal of Pharmaceutics, 547 (2018) 602-610.
[26] C. Bachran, M. Schröder, L. Conrad, J.J. Cragnolini, F.G. Tafesse, L. Helming, H.L. Ploegh, L.K. Swee, The activity of myeloid cell-specific VHH immunotoxins is target-, epitope-, subset- and organ dependent, Scientific Reports, 7 (2017) 17916.
[27] S. Wöll, C. Bachran, S. Schiller, M. Schröder, L. Conrad, L. Kim Swee, R. Scherließ, Sortaggable liposomes: Evaluation of reaction conditions for single-domain antibody conjugation by Sortase–A and targeting of $CD11b^{+}$ myeloid cells, European Journal of Pharmaceutics and Biopharmaceutics, 133 (2018) 138-150.
[28] G. Haran, R. Cohen, L.K. Bar, Y. Barenholz, Transmembrane ammonium sulfate gradients in liposomes produce efficient and stable entrapment of amphipathic weak bases, Biochimica et Biophysica Acta (BBA) – Biomembranes, 1151 (1993) 201-215.
[29] A. Klaiber, C. Lanz, S. Landsmann, J. Gehring, M. Drechsler, S. Polarz, Maximizing Headgroup Repulsion: Hybrid Surfactants with Ultrahighly Charged Inorganic Heads and Their Unusual Self-Assembly, Langmuir, 32 (2016) 10920-10927.
[30] D. Carugo, E. Bottaro, J. Owen, E. Stride, C. Nastruzzi, Liposome production by microfluidics: potential and limiting factors, Scientific Reports, 6 (2016) 25876.
[31] S. Wöll, C. Bachran, S. Schiller, M. Schröder, L. Conrad, R. Scherließ, L.K. Swee, Sortagging of liposomes with a murine CD11b-specific VHH increases in vitro and in vivo targeting specificity of myeloid cells, European Journal of Pharmaceutics and Biopharmaceutics, 134 (2019) 190-198.
[32] R.L. Biltonen, D. Lichtenberg, The use of differential scanning calorimetry as a tool to characterize liposome preparations, Chemistry and Physics of Lipids, 64 (1993) 129-142.
[33] A. Fritze, F. Hens, A. Kimpfler, R. Schubert, R. Peschka-Süss, Remote loading of doxorubicin into liposomes driven by a transmembrane phosphate gradient, Biochimica et Biophysica Acta (BBA) - Biomembranes, 1758 (2006) 1633-1640.
[34] N. Ohnishi, H. Tomida, Y. Ito, K. Tahara, H. Takeuchi, Characterization of a doxorubicin liposome formulation by a novel in vitro release test methodology using column-switching high-performance liquid chromatography, Chemical & Pharmaceutical Bulletin, 62 (2014) 538-544.
[35] www.spectrum.com, Diafiltration (Buffer Exchange) Using Hollow Fiber Membranes instead of Dialysis Tubing - Automated Diafiltration, http://spectrumlabs.com/lit/hfdial.pdf, access date: 04.03.2018.
[36] D.D. Lasic, P.M. Frederik, M.C.A. Stuart, Y. Barenholz, T.J. McIntosh, Gelation of liposome interior A novel method for drug encapsulation, FEBS Letters, 312 (1992) 255-258.
[37] D.D. Lasic, R. Joannic, B.C. Keller, P.M. Frederik, L. Auvray, Spontaneous vesiculation, Advances in Colloid and Interface Science, 89-90 (2001) 337-349.
[38] C. Mamot, D.C. Drummond, C.O. Noble, V. Kallab, Z. Guo, K. Hong, D.B. Kirpotin, J.W. Park, Epidermal Growth Factor Receptor–Targeted Immunoliposomes Significantly Enhance the Efficacy of Multiple Anticancer Drugs In vivo, Cancer Research, 65 (2005) 11631-11638.
[39] K. Kono, M. Takashima, E. Yuba, A. Harada, Y. Hiramatsu, H. Kitagawa, T. Otani, K. Maruyama, S. Aoshima, Multifunctional liposomes having target specificity, temperature-triggered release, and near-infrared fluorescence imaging for tumor-specific chemotherapy, Journal of Controlled Release, 216 (2015) 69-77.
[40] C. Mamot, D.C. Drummond, U. Greiser, K. Hong, D.B. Kirpotin, J.D. Marks, J.W. Park, Epidermal Growth Factor Receptor (EGFR)-targeted Immunoliposomes Mediate Specific and Efficient Drug Delivery to EGFR- and EGFRvIII-overexpressing Tumor Cells, Cancer Research, 63 (2003) 3154-3161.

[41] R.M. Schiffelers, G.A. Koning, T.L.M. ten Hagen, M.H.A.M. Fens, A.J. Schraa, A.P.C.A. Janssen, R.J. Kok, G. Molema, G. Storm, Anti-tumor efficacy of tumor vasculature-targeted liposomal doxorubicin, Journal of Controlled Release, 91 (2003) 115-122.
[42] T. Li, D. Cipolla, T. Rades, B.J. Boyd, Drug nanocrystallisation within liposomes, Journal of Controlled Release, 288 (2018) 96-110.
[43] S. Zalba, A.M. Contreras, A. Haeri, T.L.M. ten Hagen, I. Navarro, G. Koning, M.J. Garrido, Cetuximab-oxaliplatin-liposomes for epidermal growth factor receptor targeted chemotherapy of colorectal cancer, Journal of Controlled Release, 210 (2015) 26-38.
[44] D.L. Iden, T.M. Allen, In vitro and in vivo comparison of immunoliposomes made by conventional coupling techniques with those made by a new post-insertion approach, Biochimica et Biophysica Acta (BBA) - Biomembranes, 1513 (2001) 207-216.
[45] S. Oliveira, R.M. Schiffelers, J. van der Veeken, R. van der Meel, R. Vongpromek, P.M.P. van Bergen en Henegouwen, G. Storm, R.C. Roovers, Downregulation of EGFR by a novel multivalent nanobody-liposome platform, Journal of Controlled Release, 145 (2010) 165-175.
[46] W.W.K. Cheng, T.M. Allen, Targeted delivery of anti-CD19 liposomal doxorubicin in B-cell lymphoma: A comparison of whole monoclonal antibody, Fab' fragments and single chain Fv, Journal of Controlled Release, 126 (2008) 50-58.
[47] F. Pastorino, C. Brignole, D. Marimpietri, P. Sapra, E.H. Moase, T.M. Allen, M. Ponzoni, Doxorubicin-loaded Fab' Fragments of Anti-disialoganglioside Immunoliposomes Selectively Inhibit the Growth and Dissemination of Human Neuroblastoma in Nude Mice, Cancer Research, 63 (2003) 86.
[48] P. Sapra, T.M. Allen, Improved outcome when B-cell lymphoma is treated with combinations of immunoliposomal anticancer drugs targeted to both the CD19 and CD20 epitopes, Clinical Cancer Research, 10 (2004) 2530-2537.
[49] P. Simard, J.-C. Leroux, In Vivo Evaluation of pH-Sensitive Polymer-Based Immunoliposomes Targeting the CD33 Antigen, Molecular Pharmaceutics, 7 (2010) 1098-1107.

Supplementary Data

Stability of gradient liposomes

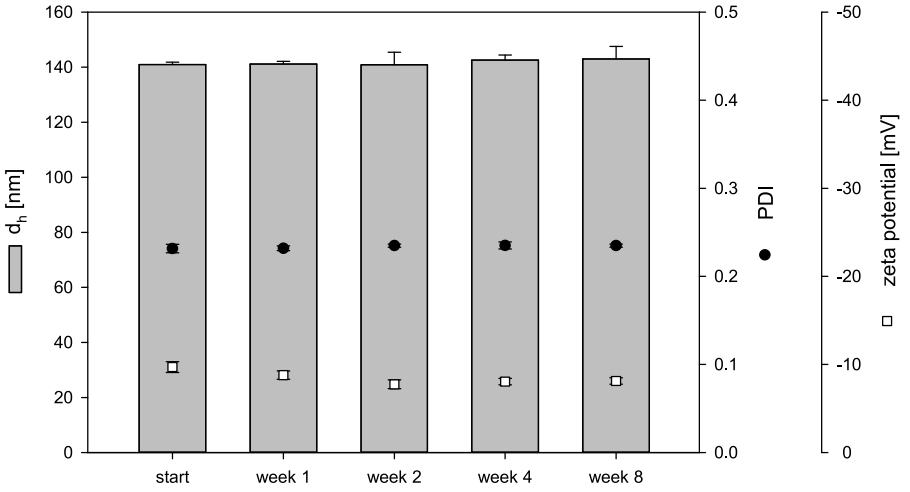

Supplementary Figure 1: Physical stability of pentaglycine-modified gradient liposomes (empty DPPS-LS). No change in d_h, PDI or zeta potential occurred during an 8 weeks storage at 2-8 °C (data shown as mean ± standard deviation of three liposomal batches).

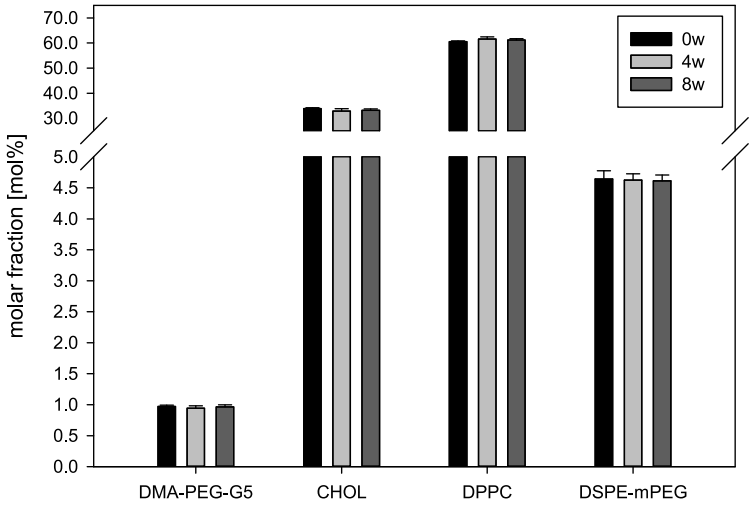

Supplementary Figure 2: Chemical stability of pentaglycine-modified gradient liposomes (empty DPPC-LS). The bilayer composition was maintained over an 8 weeks storage at 2-8 °C (data shown as mean ± standard deviation of three liposomal batches).

Thermal analysis of lipid blend

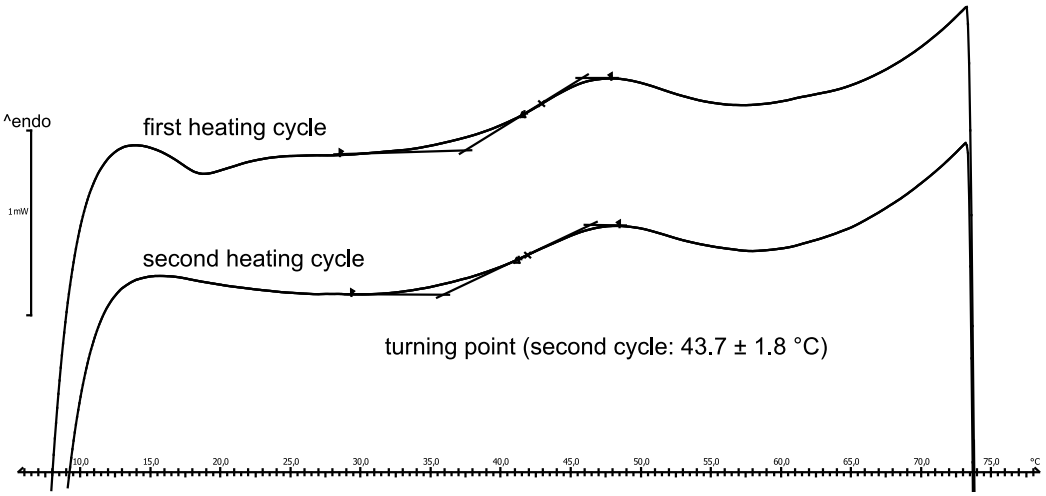

Supplementary Figure 3: DSC thermogram of a hydrated lipid blend consisting of DPPC, cholesterol, DSPE-mPEG and pentaglycine-modified DMA-PEG-G5 (molar ratio 59.4 : 34.7 : 5.0 : 1.0). Transition temperature (t_m) was determined as 43.7 ± 1.8 °C (n=3). A broad phase transition was observed in the thermogram, probably due to the presence of cholesterol.

Influence of doxorubicin loading on physical liposome properties

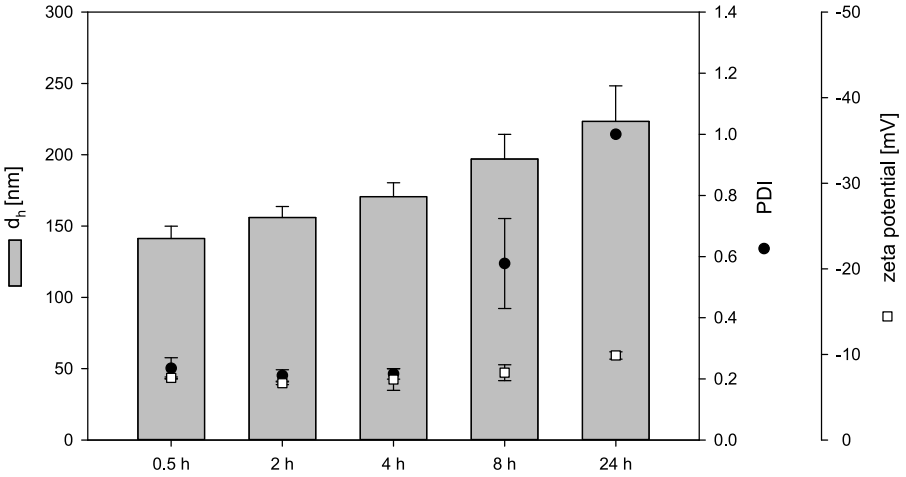

Supplementary Figure 4: Influence of DXR loading on physical liposome properties. Liposomes composed of 59.4 mol% DPPC, 34.7 mol% cholesterol, 5.0 mol% DSPE-mPEG and 1.0 mol% DMA-PEG-G5 were loaded from 1x DPBS as outer buffer (5:1 DXR to lipid m/m). PDI and d_h increased with continuing incubation times. Data shown as mean ± standard deviation of three liposomal batches.

Influence of the phosphate concentration on doxorubicin loading

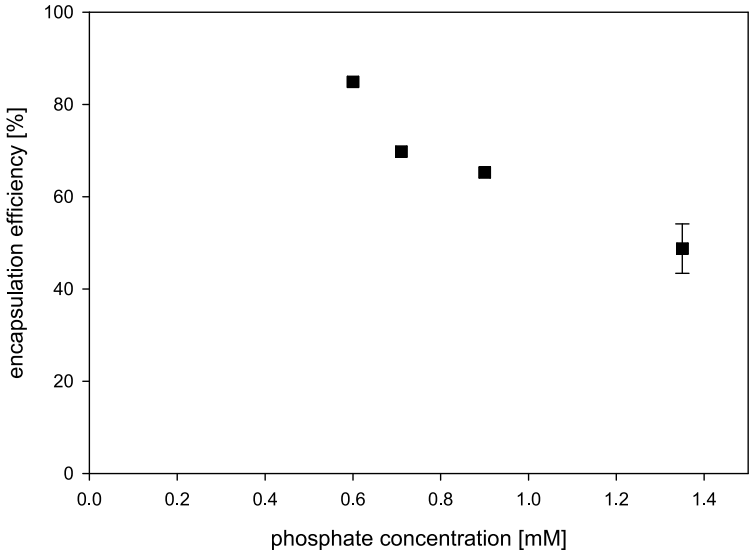

Supplementary Figure 5: DXR encapsulation efficiency after loading from differently composed buffer systems. A loading mix was prepared from DXR (10 mg/mL in water), liposomes (ad 30 mM; in DPBS) and water to adjust a doxorubicin to lipid ratio of 5:1 m/m. Due to variation of lipid concentration in different liposomal batches, absolute phosphate concentration varied between different loading experiments, which was only in one case (1.35 mM) corrected by addition of 10x DPBS stock. There was an inverse correlation between phosphate concentration and encapsulation efficiency. If shown, error bar indicates mean ± standard deviation of results obtained from three liposomal batches, otherwise experiment was conducted with one single batch.

Colloidal stability during sortagging

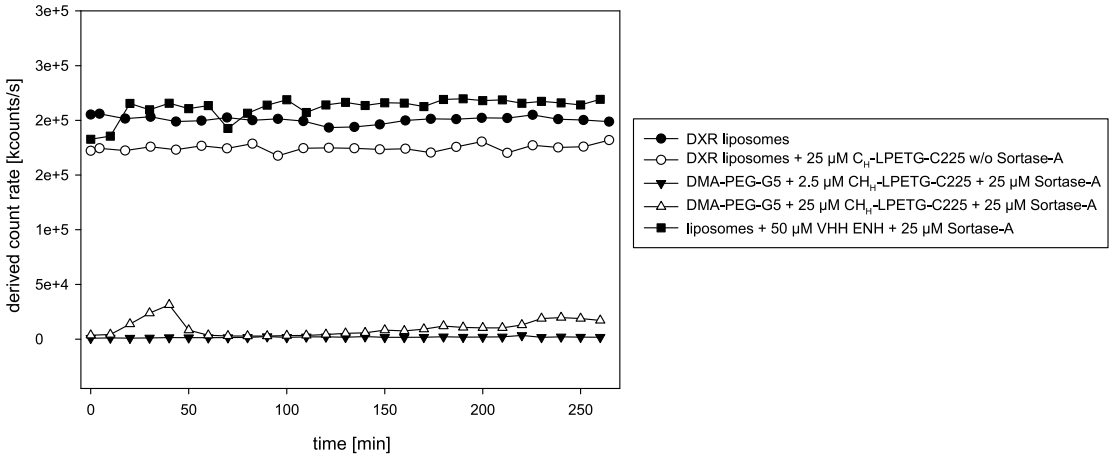

Supplementary Figure 6: Control groups for investigation of colloidal stability of pentaglycine-modified PEGylated liposomes during Sortase-A reaction. Sole DXR-loaded liposomes or a Sortase-A free mixture with 25 µM C_H-LPETG-C225 did not show sedimentation over the experiment duration (270 min). Gradient liposomes (100 µM pentaglycine) incubated with 50 µM of a single-domain antibody (VHH ENH) were stable during the reaction time. 100 µM non-liposomal DMA-PEG-G5 obtained from a film-hydration showed no aggregation when incubated with Sortase-A and 2.5 µM C_H-LPETG-C225, but with 25 µM C_H-LPETG-C225.

Supplementary Table 1: Physico-chemical parameters of liposomes analyzed by cryo-TEM (data from one batch, analyzed in triplicate).

formulation	d_h [nm]	PDI	zp [mV]
after injection	151 ± 4	0.23 ± 0.01	-3.0 ± 0.3
after TFF	141 ± 1	0.23 ± 0.00	-8.4 ± 0.5
after DXR loading (4 h, from DPBS)	152 ± 2	0.17 ± 0.01	-7.0 ± 0.5
after DXR loading (1 h, from DPBS)	147 ± 2	0.19 ± 0.01	-6.5 ± 0.6
after DXR loading (1 h, from HEPES)	138 ± 0	0.21 ± 0.01	-8.0 ± 0.5

Supplementary Table 2: Overview of liposome compositions and manufacturing conditions for DXR-loaded liposomes analyzed by cryo-TEM and tested for *in vitro* cytotoxicity.

measured lipid composition	interior buffer	exterior buffer	incubation conditions	predominant structures observed in cryo-TEM	description in cytotoxicity assay
DPPC: 60.5 mol% CHOL: 34.2 mol% DSPE-mPEG: 4.5 mol% DMA-PEG-G5: 0.8 mol%	250 mM $(NH_4)_2SO_4$	DPBS, pH 7.4	4h, 49 °C	rod-like, "donut"-structures	"DPPC-LS" or derivatives (equivalent batch used for cytotoxicity assay)
DPPC: 60.7 mol% CHOL: 34.1 mol% DSPE-mPEG: 4.2 mol% DMA-PEG-G5: 0.9 mol%	250 mM $(NH_4)_2SO_4$	DPBS, pH 7.4	1 h, 49 °C	rod-like, "donut"-structures	not analyzed
DPPC: 60.7 mol% CHOL: 34.1 mol% DSPE-mPEG: 4.3 mol% DMA-PEG-G5: 0.9 mol%	250 mM $(NH_4)_2SO_4$	10 mM HEPES, pH 7.0	1 h, 49 °C	"coffee beans" / "rugby-like"	not analyzed
HSPC: 59.9 mol% CHOL: 35.0 mol% DSPE-mPEG: 4.2 mol% DMA-PEG-G5: 0.9 mol%	250 mM $(NH_4)_2SO_4$	10 mM HEPES, pH 7.0	1 h, 65 °C	HSPC-based liposomes were not analyzed via cryo-TEM. Typical "coffee bean" / "rugby-like" appearance is expected, comparable to previous reports that analyzed similar prepared liposomes [1]	"HSPC-LS" or derivatives

References

[1] T. Li, D. Cipolla, T. Rades, B.J. Boyd, Drug nanocrystallisation within liposomes, Journal of Controlled Release, 288 (2018) 96-110.

Chapter 8
Summary and conclusion

1. Comprehensive discussion and summary

Eight actively targeted liposomal drug formulations, called immunoliposomes, have been investigated in human trials so far. This underlines the clinical relevance of such drug delivery systems [1]. Therefore, targeted liposomes are an important part of the formulation scientist's toolbox to enable a safe and effective administration of drugs with suboptimal pharmacokinetic (e.g. distribution in healthy tissues) and pharmacodynamic (e.g. toxicity) profiles. They are one attempt to realize Paul Ehrlich's idea of a "magic bullet", a tailored medicine that precisely targets disease-affected tissues without impairment of healthy cells. Immunoliposomes are complex multi-component systems, and the utilized excipients like lipids and antibodies are mainly derived from biological systems. Those heterogeneous precursors already indicate that reproducible and homogenous manufacturing of drug products is a complicated and demanding task. Hence, protein conjugation of targeting ligands to the liposomes potentially multiplies heterogeneity. It is therefore of utmost technological interest to provide methods that promote a defined, site-specific conjugation between the liposomal carrier and the targeting ligand.

Staphylococcus aureus derived Sortase-A is a transpeptidase with a great potential as chemoenzymatic "swiss army knife" [2]. It offers a site-specific conjugation between LPxTG (leucine, proline, any amino acid, threonine, glycine)-modified proteins and N-terminal glycine-carrying motifs, such as other proteins and peptides, but also towards synthetic lipids. Hence, the application of the Sortase-A transpeptidase for the surface modification of liposomal drug carriers and therewith related analytical, technological and biological questions was set as focus of this scientific thesis.

Pentaglycine-modified dimyristyl lipids were investigated to serve as targeting ligand anchors in different liposomal constructs. Since liposome manufacturing and purification includes numerous steps, a suitable rp-HPLC method was developed to cover in process and final quality control of the liposome composition (**Chapter 2**). The method was validated regarding linearity, specificity, precision, accuracy and sample stability for the quantification of two pentaglycine lipids and selected helper lipids. The method represents a highly flexible tool to determine the exact lipid composition of various sortaggable liposomal formats, including liposomes with different surfaces charges, PEGylation, rigidity or pH-sensitivity. This helped to control liposome compositions during manufacturing and guaranteed batch consistency, setting the basis for the following physico-chemical and biological experiments.

Considering the chemical composition of liposomes, PEGylation was shown to have tremendous impact on the pharmacokinetic behavior of the carrier [3]. However, also physical properties like

the hydrodynamic diameter, polydispersity and zeta potential are important factors influencing the biological fate [3]. A comprehensive investigation to control the liposomal hydrodynamic diameter of differently PEGylated liposomes during manufacturing by a solvent injection process was therefore conducted in **Chapter 3**. This manufacturing method offers an easily scalable way to prepare small to medium sized unilamellar liposomes. Such a scalability is of particular importance when translating the manufacturing of nanomedicines from lab-scale to batch sizes sufficient to meet clinical demands, thereby maintaining quality attributes of preclinical batches. Especially the commonly preclinically applied thin film hydration with subsequent extrusion represents a procedure with challenging scalability, e.g. due to distinct limits in vessel or extruder size. The here investigated solvent injection process is a promising alternative that demonstrated controllability of the liposomal size as well as an easy scalability. Increase of the flow rates, especially of the aqueous anti-solvent, led to a decrease of the liposome diameter. Diameters ranging from 95 nm to 230 nm were covered for differently PEGylated liposomal formulations with a pentaglycine-modified surface.

The pentaglycine modification was inevitable for a subsequent conjugation of LPxTG-modified targeting ligands by Sortase-A. Enzymatic reactions require steric accessibility of the recognition motifs, which greatly varies between differently PEGylated liposomal surfaces. Pentaglycine motifs shielded by a surrounding 2 kDa PEG layer were suppressed from reaction with a single-domain antibody, whereas pentaglycines exposed via a 2 kDa PEG spacer showed comparable behavior on PEGylated or non-PEGylated bilayers. Temperature increase also enabled the sortagging of PEG-shielded pentaglycines, which may allow the selective sortagging of disparately accessible glycines by using different reaction conditions. This may open the door for a convenient manufacturing of multi-layered liposomes. Additionally, the relative efficiency of transpeptidation was improved from 40 % to 80 % by increasing the ratio of pentaglycine nucleophile to the LPETG-modified antibody.

A potential pitfall for the use of Sortase-A is the reverse reaction, or more precisely, a product hydrolysis by water molecules acting as alternative nucleophiles. The depletion of Sortase-A from immunoliposomal reaction bulks was therefore investigated in **Chapter 4**, combined with stability studies covering the kinetic cleavage of the targeting ligand from the liposomes. PEGylated bilayers adsorbed Sortase-A in an unspecific fashion. However, those PEGylated liposomes were not prone for ligand cleavage by enzyme residuals. Although Sortase-A residuals were much lower for non-PEGylated bilayers, these formulations lost 20 % of the ligand bound to the liposome during eight weeks of cooled storage. This contrary result was explained by steric prevention of the reverse reaction on PEGylated bilayers. The ligand-cleavage from non-PEGylated bilayers was prevented by an additional Sortase-A removal step via poly-histidine

affinity beads. This indicates the necessity of an elaborated purification strategy for usage of the Sortase-A technology on liposomal carriers (Figure 1).

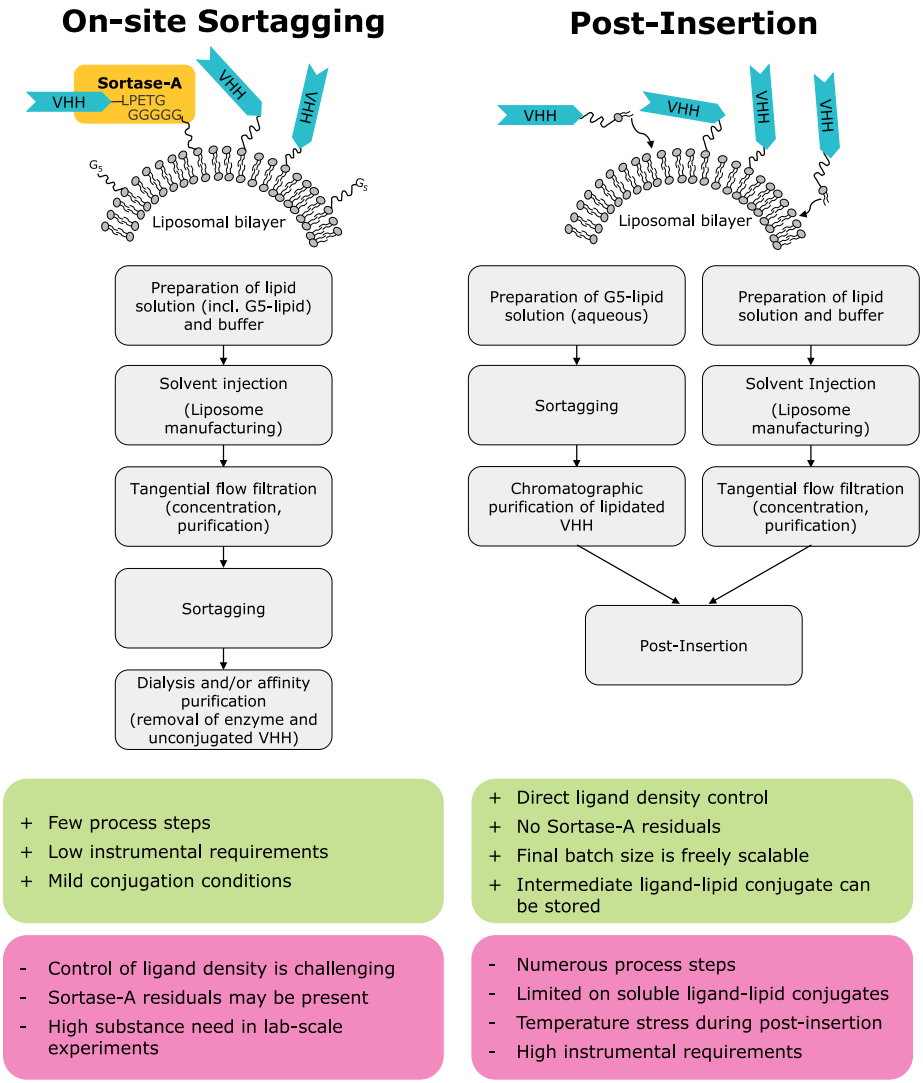

Figure 1: “On-site sortagging” or “post-insertion” – manufacturing routes for immunoliposomes with ligands conjugated to the lipid anchor by means of Sortase-A.

An alternative to extensive purification of reaction bulks is the avoidance of Sortase-A exposure to the liposomal surface during manufacturing. This was realized by separation of the ligand lipidation from liposome manufacturing (**Chapter 5**Figure 1)**.** Single-domain antibodies were lipidated using Sortase-A and a pentaglycine-PEG-dimyristyl motif. The water-soluble reaction product was successfully purified by reversed-phase chromatography without loss of antigen binding capacities. The lipidated antibodies were inserted into the bilayer of preformed, fluorophore-loaded liposomes (“post-insertion”). This enabled a specific targeting of antigen-positive cells. Hence, an alternative to the “on-site sortagging” manufacturing for single-domain antibody-based immunoliposomes was developed (Figure 1).

An overview of both manufacturing routes and a comparison of their advantages and disadvantages is given in Figure 1. Although the sortagging on the liposomal surface is a

straightforward approach without requirement of additional equipment, it has several drawbacks. The most important one is the above discussed retention of Sortase-A, which requires the use of elaborated purification techniques. The post-insertion strategy avoids unfavorable Sortase-A residuals by circumventing enzyme exposure to the liposomal surface. Another drawback is the high dependency of the reaction efficiency during on-site sortagging from the liposomal surface, making the ligand density on the carrier hard to predict. Since the insertion process of lipidated ligands into liposomes is very efficient, the post-insertion strategy offers an easy way to adjust this ratio just by the mixing ratio of the liposome precursor and the purified lipidated ligand. Also, the batch volume of the immunoliposomal bulk can be freely adjusted and does not depend on minimal required volumes determined e.g. by dialysis devices. This is of importance during the early research phase, where only limited amounts of especially proteinaceous components such as targeting ligands are available. Besides these advantages, the post-insertion strategy has also several drawbacks. This is firstly an overall higher demand on equipment, since a suitable instrumentation for a (typically chromatographic) purification of the lipidated ligand is required. Secondly, the obtained product should be compatible with the purification process, meaning it should not show degradation (e.g. loss of binding) and it should be water-soluble. This was demonstrated in Chapter 5 for the combination of a PEGylated lipid anchor and single-domain antibodies and may be also feasible with other binders such as monoclonal antibodies or fragments thereof (scFv, Fab'). Thirdly, the post-insertion process is typically conducted at elevated temperatures above the transition temperature of the lipid mix, what may be incompatible with temperature-sensitive drugs. Finally, the post-insertion strategy includes numerous additional steps, leading to increased demands on process characterization and analytics for the intermediates in commercial manufacturing. This higher effort in the value chain should also be considered during evaluation of the manufacturing route.

Not only liposomal bilayers, but also biological membranes were modified with the isolated, lipidated single-domain antibodies. Insertion of lipidated compounds into cell membranes ("hydrophobic insertion") represents one of three currently described non-genetic methods for cell membrane engineering. This hydrophobic insertion is, compared to covalent conjugation or on electrostatic interaction-based cell surface modifications, a very gentle approach due to the negligible toxicity, the maintenance of normal cellular activities and the participation of the inserted molecules in the cell membrane dynamics [4]. Cell surface modifications have drawn increasing interest in the field of cell therapies e.g. for regenerative medicine or cancer immunotherapy. These therapies were revealed to be much more effective when the administered cells were engineered with target-specific binders, e.g. due to increased cell homing effects, greater tissue retention rates or improved *in vivo* persistency [4]. In this thesis,

the membranes of murine T cells were engineered with a CD11b-binding single-domain antibody. This promoted supraphysiological cell-cell interactions with myeloid cells in a co-culture assay (**Chapter 5)**. The demonstrated membrane engineering may enable novel forms of autologous therapies, in which endogenous cells are redirected towards specific tissues by exogeneous ligands.

Variants of myeloid cells, characterized by a $CD11b^{+}Gr\text{-}1^{+}$ phenotype, are attractive targets in immuno-oncology due to their suppressive influence on the immune response in the tumor microenvironment. A single-domain antibody specific for the human myeloid cell surface receptor CD11b was conjugated on fluorophore-labeled liposomes (**Chapter 3**). The immunoliposomes showed a specific binding towards antigen-positive monocytes and granulocytes *in vitro*, but not towards target-negative T or B cells. An internalization of the drug carrier by target-positive cells was observed with confocal microscopy. Comparable results were obtained with equally composed liposomes equipped with a single-domain antibody specific for CD11b on murine myeloid cells (**Chapter 4**). Moreover, after an intravenous injection of CD11b-specific liposomes into mice, a significant threefold increase in mean fluorescence intensity of $CD11b^{+}Gr\text{-}1^{+}$ splenocytes was observed compared to control liposomes carrying a non-specific ligand. For the first time, immunoliposomes which were prepared from a sortagging process demonstrated a targeting proof of principle in an animal experiment.

These promising results led to the decision to encapsulate cytotoxic payloads into the drug carriers. *Pseudomonas* exotoxin A is a proteinaceous ribosylase that inhibits the protein biosynthesis in picomolar concentrations when delivered to the cytosol of eukaryotic cells. A truncated variant lacking the endocytosis-promoting domain was loaded into liposomes, which were then targeted against $CD11b^{+}Gr\text{-}1^{+}$ cells. However, no target-specific cytotoxicity was observed, although several liposomal formulations varying in PEGylation, drug load and lipid composition were screened. Also liposomes loaded with an established toxic chemical entity (doxorubicin) failed to exhibit specific toxicty on $CD11b^{+}Gr\text{-}1^{+}$ cells. Reasons for this failure and further possible strategies were extensively discussed in **Chapter 6**.

Doxorubicin is clincally applied as a liposomal anti-cancer drug. The active encapsulation of doxorubicin into pentaglycine-modified, PEGylated liposomes was investigated in **Chapter 7**. The epidermal growth factor receptor (EGFR) was utilized as an alternative and established target compared to the myeloid cell target CD11b. Liposomes were directed towards $EGFR^{+}$ cancer cells using a sortaggable variant of an approved anti-EGFR monoclonal antibody (C225, cetuximab). The targeted liposomes exhibited a significant higher cytotoxicity compared to their non-targeted counterparts. This indicated the suitability of the developed liposomal carriers to

act as targeted drug delivery system for doxorubicin on an established target, and suggested that cell line-, target- or ligand-related aspects impeded specific toxicity on myeloid cells. Similar doxorubicin-loaded, EGFR-targeted immunoliposomes prepared with a maleimide-based coupling chemistry have been successfully investigated in a clinical phase I study [5]. The same group is currently recruiting patients for a subsequent phase II study [6]. The site-specific conjugation approach demonstrated within this thesis offers an important alternative to manufacture such EGFR-targeted immunoliposomes. The defined reaction product obtained here from chemoenzymatic coupling may exhibit benefits from a toxicological and immunological, but also from an analytical and finally regulatory perspective.

It is especially the lack of such a defined reaction product, or *vice versa* product heterogeneity that was associated with toxic side effects of ADCs, that led to batch recalls of PEGylated enzymes or that decreased the bioactivity of therapeutic proteins [7]. Sortase-A mediated site-specific transpeptidation is one approach to mitigate such risks during protein modification, however it should not remain unmentioned that also other enzymatic or chemical methods have been developed to address these problems. Especially transglutaminases are considered as powerful alternative to Sortase-A due to the vastly lower K_M and the irreversible reaction mechanism [7]. Also, chemical conjugation techniques such as the Huisgen cycloaddition, the strain-promoted azide-alkyne cycloaddition or the Staudinger ligation allow a site-selective derivatization of proteins, although side reactions have been described [7]. Comparing chemical and enzymatic techniques, it is important to state that many chemical methods require the introduction of novel functional groups like unnatural amino acids into the protein. Similarly, enzymes rely on genetically introduced recognition tags. Both recognition tags or unnatural amino acids may influence expression yields or potentially alter the protein structure. Chemical methods may additionally require catalysts such as copper that can be responsible for toxicity related concerns or lead to protein precipitation [7]. Thus, especially sensitive proteins may favor enzymatic coupling methods due to the mild reaction conditions that help to maintain protein conformation and activity.

Altogether, a broad variety of conjugation methods are meanwhile available for site-selective protein modification [7] and thus display potential options for a defined anchorage of targeting ligands on liposomes. Such bioorthogonal reactions may subsequently replace the still predominantly applied unspecific techniques, including e.g. thiol-maleimide-based or carbodiimide-based coupling strategies [8]. Hence, increased elucidation of bioorthogonal conjugation techniques for the design of targeted liposomes can contribute to an improved developability, increased safety and possibly enhanced efficacy of such nanotherapeutics. The within this thesis described investigation of the Sortase-A technology for liposomal surface modification strived to contribute to this elucidation.

2. Conclusion and future perspectives

The present work reveals the vast potential, but also important drawbacks of the Sortase-A technology used for chemoenzymatic surface modification of liposomes. Sortagging offers a facile approach for an efficient and highly defined conjugation of targeting ligands onto drug carriers. However, Sortase-A depletion from the reaction bulk was demonstrated to be a critical process step with a significant impact on the stability of the obtained product. Strategies to mitigate this risk, either by improved purification or by post-insertion manufacturing routes were disclosed. This work enables now the preparation of immunoliposomes with chemoenzymatically anchored ligands in suitable stability and decreased material consumption.

CD11b-specific immunoliposomes prepared with Sortase-A efficiently targeted human and murine myeloid cells *in vitro*. For the first time, such sortagged liposomes were also demonstrated to specifically reach myeloid $CD11b^{+}Gr\text{-}1^{+}$ target cells *in vivo*. This shows the great potential for these formulations to act as drug carriers that may regulate immune responses, e.g. in the tumor microenvironment. The specific toxicity of doxorubicin to cancer cells using a sortagged, immunoliposomal formulation highlighted the capacity of the system to not only deliver marker molecules, but also actual drugs. However, the specific delivery of a proteinaceous toxin to $CD11b^{+}Gr\text{-}1^{+}$ cells was not successful. This challenge may be subject to further investigations. Those should especially relate liposomal formulation aspects, such as the bilayer composition, to the cellular fate of the carrier. In particular, thorough analysis of parameters promoting the intracellular release of large molecules from a targeted immunoliposomal system would provide essential benefit for a wide variety of therapeutic applications. Latter may not only include the targeted delivery of proteinaceous toxins to cancer or immuno-oncological cells, but also antigen delivery for vaccination or ribonucleic acid delivery for gene therapy.

This broad potential applicability underlines that the drug carriers and the related surface modification strategies developed within this thesis provide an essential benefit in the field of targeted drug delivery – from a technological, but also from a therapeutic perspective.

References

[1] M. Merino, S. Zalba, M.J. Garrido, Immunoliposomes in clinical oncology: State of the art and future perspectives, Journal of Controlled Release, 275 (2018) 162-176.
[2] M. Ritzefeld, Sortagging: A Robust and Efficient Chemoenzymatic Ligation Strategy, Chemistry – A European Journal, 20 (2014) 8516-8529.
[3] Y. Barenholz, Doxil® – The first FDA-approved nano-drug: Lessons learned, Journal of Controlled Release, 160 (2012) 117-134.
[4] D.Y. Lee, B.-H. Cha, M. Jung, A.S. Kim, D.A. Bull, Y.-W. Won, Cell surface engineering and application in cell delivery to heart diseases, Journal of Biological Engineering, 12 (2018) e28.
[5] C. Mamot, R. Ritschard, A. Wicki, G. Stehle, T. Dieterle, L. Bubendorf, C. Hilker, S. Deuster, R. Herrmann, C. Rochlitz, Tolerability, safety, pharmacokinetics, and efficacy of doxorubicin-loaded anti-EGFR immunoliposomes in advanced solid tumours: a phase 1 dose-escalation study, The Lancet Oncology, 13 (2012) 1234-1241.
[6] ClinicalTrials.gov, Ralph Winterhalder (MD): Anti-EGFR-immunoliposomes Loaded With Doxorubicin in Patients With Advanced Triple Negative EGFR Positive Breast Cancer. ClinicalTrials.gov Identifier: NCT02833766, https://clinicaltrials.gov/ct2/show/NCT02833766, access date: 06.01.2018.
[7] A.C. Braun, M. Gutmann, T. Lühmann, L. Meinel, Bioorthogonal strategies for site-directed decoration of biomaterials with therapeutic proteins, Journal of Controlled Release, 273 (2018) 68-85.
[8] P. Marques-Gallego, A.I.P.M. de Kroon, Ligation Strategies for Targeting Liposomal Nanocarriers, BioMed Research International, (2014) e129458.

Synopsis

Bibliographic Abstracts

Abstract (English)

Drugs are encapsulated in nano-sized drug delivery systems to refine their pharmacokinetic, pharmacodynamic or physico-chemical behavior upon administration. Immunoliposomes are conjugates of targeting ligands and lipid-based drug carriers. These ligands are designed to specifically direct the encapsulated drug to the disease-affected target tissue. The conjugation reaction combining the carrier and ligand is a critical step since it is a possible source of product heterogeneities. In this work, Sortase-A transpeptidase was investigated as a chemoenzymatic tool to provide a site-specific anchoring of antibodies on liposomes. Liposomes bearing pentaglycine lipids that serve as Sortase-A acceptor motifs ("sortaggable liposomes") were manufactured via a scalable solvent injection process. This process yielded small to medium sized liposomes differing in lipid composition, PEGylation or charge. Flow rate alterations were identified as suitable parameter to align the hydrodynamic diameter of the differently composed liposomes between 140 nm and 180 nm. A newly developed rp-HPLC method with evaporative light scattering detection helped to monitor the exact lipid composition of these liposomal formulations. This was indispensable for subsequent downstream processes like ligand conjugation and liposome purification steps, but also for physico-chemical and biological characterization.

Both single-domain antibodies and whole monoclonal antibodies were successfully conjugated to the liposomes. Differently PEGylated liposomes demonstrated a high dependency of the reaction efficiency on the steric accessibility of the pentaglycine motif. Also, the efficiency of transpeptidation was improved from 40 % to 80 % by increasing the ratio of pentaglycine nucleophile to the antibody. Sortase-A depletion from the reaction bulk by dialysis was insufficient and led to a loss of liposome-associated ligand during storage. This was explained by the enzymatic reverse reaction. Alternative purification strategies from Sortase-A and manufacturing options such as a post-insertion process were disclosed.

Sortase-A mediated conjugation of CD11b-specific single-domain antibodies led to a targeting of liposomes to human and murine myeloid cells *in vitro*. For the first time, sortagged liposomes were demonstrated to specifically deliver fluorescent marker molecules towards murine splenic $CD11b^{+}Gr\text{-}1^{+}$ cells *in vivo*. However, these liposomes did not exhibit specific cytotoxicity when loaded with cytotoxic molecules (*Pseudomonas* exotoxin A, doxorubicin). This was not circumvented through formulation optimization regarding drug load or lipid composition. Opposed to that, epidermal growth factor receptor targeted liposomes loaded with the anti-cancer drug doxorubicin exhibited a specifically higher cytotoxicity on a breast cancer cell

line compared to their non-targeted counterparts. This hinted at cell line-, ligand- or target-specific circumstances that impeded specific cytotoxicity on myeloid cells.

In this thesis, it became obvious that Sortase-A transpeptidation is a suitable technology to anchor targeting ligands on liposomes. The obtained results contribute therefore to the elucidation of site-selective conjugation strategies utilized for the design of targeted nanotherapeutics.

Abstract (German)

Arzneistoffe werden in nanoskalierte, partikuläre Trägersysteme verkapselt, um pharmakokinetische, pharmakodynamische oder physikochemische Eigenschaften des Wirkstoffs zu verbessern. Immunoliposomen sind Konjugate zwischen Liganden und lipid-basierten Arzneistoffträgern (Liposomen), durch die der verkapselte Stoff zielgerichtet zu krankheitsbefallenen Geweben und Zellen transportiert werden kann. Die Konjugationsreaktion, die Ligand und Träger vereint, ist ein kritischer Schritt in der Herstellung solcher Systeme, da sie eine mögliche Ursache für Produktheterogenität darstellt. In dieser Arbeit wurde daher eine chemo-enzymatische Transpeptidierung über das Enzym Sortase-A für das molekular ortsselektive Verankern von Liganden auf Liposomen untersucht.

Dabei wurden Pentaglycin-tragende Liposomen über eine einfach skalierbare Herstellungsmethode („solvent injection“) produziert. Die Pentaglycin-Modifikation dient hier als Erkennungssequenz für Sortase-A zur Konjugation von LPETG-tragenden (Leucin, Prolin, Glutaminsäure, Tyrosin, Glycin) Liganden. Die Flussraten der für die Liposomenherstellung genutzten Methode wurden als geeignete Parameter identifiziert, durch deren Variation sich verschiedenste Formulierungen auf einen Größenbereich zwischen 140 nm und 180 nm einstellen ließen. Es wurde weiterhin eine rp-HPLC-Methode basierend auf massensensitiver Lichtstreuungsdetektion zur adäquaten chemischen Charakterisierung der Pentaglycin-Liposomen hinsichtlich ihrer Lipid-Komposition entwickelt.

Sowohl Einzeldomänen-Antikörper als auch intakte monoklonale Antikörper wurden erfolgreich an die Liposomen konjugiert. Hierbei zeigte sich eine starke Abhängigkeit der Reaktionseffizienz von der sterischen Akzessibilität des Pentaglycin-Nukleophils, welche sich durch verschiedene PEGylierungsmuster der Liposomen unterschied. Eine Verbesserung der Konjugationseffizienz von 40 % auf 80 % konnte durch eine Erhöhung des Verhältnisses des nukleophilen Pentaglycins zum LPETG-Liganden erreicht werden. Die Abreicherung von Sortase-A aus dem Reaktionsansatz über Dialyse war unzureichend und führte zu einem Verlust von Liposomen-gebundenen Liganden während der Lagerung. Dies wurde durch die von Sortase-A ebenfalls katalysierte Rückreaktion begründet. Eine verbesserte Aufreinigungsstrategie als auch eine optimierte Herstellungsoption (Post-Insertion) wurden experimentell dargelegt.

Die Konjugation von CD11b-spezifischen Einzeldomänen-Antikörpern auf Fluorophor-beladene Liposomen führte zu einer erfolgreichen Targetierung von humanen und murinen myeloischen Zellen *in vitro*. Mittels Sortase-A hergestellte Immunoliposomen wurden erstmalig auch in einem Tierexperiment getestet, in dem die spezifische Färbung von $CD11b^{+}Gr\text{-}1^{+}$ Zellen in der Milz gezeigt werden konnte. Eine spezifische *in vitro* Zytotoxizität von Toxin-beladenen

Liposomen auf myeloischen Zellen konnte jedoch nicht bestätigt werden, obwohl Parameter wie Beladungsgrad, Lipidkomposition und Art des Toxins (*Pseudomonas* Exotoxin A und Doxorubicin) verändert wurden. Im Gegensatz dazu zeigten mit dem Zytostatikum Doxorubicin beladene und gegen den epidermalen Wachstumsfaktor-Rezeptor gerichtete Immunoliposomen eine spezifisch höhere Toxizität auf einer Brustkrebs-Zelllinie als ungerichtete Formulierungen. Dies deutet darauf hin, dass Zelllinien-, Ligand- oder Target-spezifische Eigenschaften für die fehlende spezifische Toxizität auf myeloischen Zellen verantwortlich sein können.

Die vorliegende Arbeit demonstriert die Eignung der Sortase-A katalysierten Transpeptidierung als Methode zum Verankern von Liganden auf Liposomen aus technologischer wie auch biologischer Perspektive. Die hier erarbeiteten Resultate tragen daher zur Erforschung von selektiven Konjugationsstrategien für das Design von zielgerichteten Nanotherapeutika bei.

Appendices

Curriculum Vitae

Personal information

Name:	Steffen Wöll
Date of birth:	12.12.1988
Place of birth:	Diez
Nationality:	German

Scientific education

Since 10/2017	Research scientist, Chemical and Pharmaceutical Development, Merck KGaA, Darmstadt
07/2014 – 09/2017	PhD candidate, Chemical and Pharmaceutical Development, Merck KGaA, Darmstadt in collaboration with the Department of Pharmaceutics and Biopharmaceutics, Kiel University, Kiel
05/2014	Licensure as pharmacist
11/2013 – 04/2014	Pharmaceutical internship, Fasanen-Apotheke, Berlin
05/2013 – 10/2013	Pharmaceutical internship, Chemistry, Manufacturing and Controls, Merck KGaA, Darmstadt
04/2009 – 04/2013	Study of Pharmacy, Johannes Gutenberg-University Mainz (8 semesters)

School education

04/2008 – 03/2009	Civilian service and temporary employee, Hospital of the Red Cross, Diez
03/2008	General qualification for university entrance
07/1999 – 03/2008	Sophie-Hedwig-Gymnasium, Diez
07/1995 – 06/1999	Primary school, Esterauschule Holzappel

Publications

Peer-reviewed publications contributing to this thesis

Wöll, S., Dickgiesser, S., Rasche, N., Schiller, S., Scherließ, R.: Sortagged anti-EGFR immunoliposomes exhibit increased cytotoxicity on target cells. *European Journal of Pharmaceutics and Biopharmaceutics, 136 (2019), 203-212*.

Wöll, S., Bachran, C., Schiller, S., Schröder, M., Conrad, L., Scherließ, R., Swee, L. K.: Sortagging of liposomes with a murine CD11b-specific VHH increases *in vitro* and *in vivo* targeting specificity of myeloid cells. *European Journal of Pharmaceutics and Biopharmaceutics, 134 (2019), 190-198.*

Wöll, S., Bachran, C., Schiller, S., Schröder, M., Conrad, L., Swee, L. K., Scherließ, R.: Sortaggable liposomes: Evaluation of reaction conditions for single-domain antibody conjugation by Sortase-A and targeting of $CD11b^{+}$ myeloid cells. *European Journal of Pharmaceutics and Biopharmaceutics, 133 (2018), 138-150.*

Wöll, S., Schiller, S., Bachran, C., Swee, L. K., Scherließ, R.: Pentaglycine lipid derivates – rp-HPLC analytics for bioorthogonal anchor molecules in targeted, multiple-composite liposomal drug delivery systems. *International Journal of Pharmaceutics, 547 (2018), Issues 1-2, 602-610.*

Other publications

Sterner, B., Harms, M., **Wöll, S.**, Weigandt, M., Windbergs, M., Lehr, C.M.: The effect of polymer size and charge of molecules on permeation through synovial membrane and accumulation in hyaline articular cartilage. *European Journal of Pharmaceutics and Biopharmaceutics, 101 (2016), 126-136.*

Wöll, S., Kim S.H., Greten H.J., Efferth, T.: Animal plant warfare and secondary metabolite evolution. *Review article: Natural Products and Bioprospecting, 3 (2013), Issue 1, 1-7.*

Conference contributions

Wöll, S., Schiller, S., Scherließ, R.: Targeted Toxin Carriers – Bioorthogonal Ligand Conjugation. *Poster Contribution to the 44th Annual Meeting & Exposition of the Controlled Release Society, Boston, Massachusetts, USA (2017).*

Wöll, S., Gockel, L. M., Schiller, S., Scherließ, R.: Spray Drying of Liposomes: Surface Stabilizer Relationship. *Poster Contribution to the 21th Annual Meeting of the German Chapter of the Controlled Release Society, Marburg, Germany (2017).*

Wöll, S., Schiller, S., Scherließ, R.: Sortase-A mediates VHH-conjugation to differently PEGylated liposomes. *Poster Contribution to the Annual Meeting of the German Pharmaceutical Society, Munich, Germany (2016).*

Wöll, S., Schiller, S., Scherließ, R.: Directional liposome functionalization using enzyme-mediated single-domain antibody conjugation. *Poster Contribution to the 9th World Meeting on Pharmaceutics, Biopharmaceutics and Pharmaceutical Technology, Glasgow, United Kingdom (2016).*

Wöll, S., Schiller, S., Scherließ, R.: Spray Drying of antigen-loaded DOTAP liposomes as dry powder pulmonary vaccine. *Poster Contribution to the 4th International Symposium on Phospholipids in Pharmaceutical Research, Heidelberg, Germany (2015).*

Statement in lieu of an oath

Erklärungen nach § 8 und § 9 der Promotionsordnung

Hiermit erkläre ich gemäß § 9 der Promotionsordnung der Mathematisch-Naturwissenschaftlichen Fakultät der Christian-Albrechts-Universität zu Kiel, dass ich die vorliegende Arbeit, abgesehen von der Beratung durch meine Betreuerin, nach Inhalt und Form selbstständig und ohne fremde Hilfe verfasst habe. Weiterhin habe ich keine anderen als die angegebenen Quellen oder Hilfsmittel benutzt und die den benutzten Werken wörtlich oder inhaltlich entnommenen Stellen als solche kenntlich gemacht. Die vorliegende Arbeit ist unter Einhaltung der Regeln guter wissenschaftlicher Praxis entstanden und wurde weder ganz noch in Teilen an einer anderen Stelle im Rahmen eines Prüfungsverfahrens vorgelegt, veröffentlicht oder zur Veröffentlichung eingereicht. Weiterhin wurde mir weder ein akademischer Grad entzogen, noch habe ich an dieser oder einer anderen Fakultät einen früheren Promotionsversuch unternommen.

Teile der Arbeit sind in wissenschaftlichen Zeitschriften veröffentlicht, eingereicht oder zur Einreichung vorbereitet worden. Die dies betreffenden Abschnitte sind entsprechend gekennzeichnet. Die vorliegende Dissertation wurde daher als teilkumulative Arbeit verfasst. Im Folgenden wird der Eigenanteil des Promovenden an den veröffentlichten oder zur Veröffentlichung angestrebten Kapiteln gemäß § 8 Absatz 2 der Promotionsordnung dargestellt.

1) Wöll, S., Schiller, S., Bachran, C., Swee, L. K., Scherließ, R.: Pentaglycine lipid derivates – rp-HPLC analytics for bioorthogonal anchor molecules in targeted, multiple-composite liposomal drug delivery systems. *International Journal of Pharmaceutics, 547 (2018), Issues 1-2, 602-610.*

    - Konzeptionierung: 70 %
    - Planung: 70 %
    - Durchführung: 100 %
    - Manuskripterstellung: 90 %

2) Wöll, S., Bachran, C., Schiller, S., Schröder, M., Conrad, L., Swee, L. K., Scherließ, R.: Sortaggable liposomes: Evaluation of reaction conditions for single-domain antibody conjugation by Sortase-A and targeting of $CD11b^+$ myeloid cells. *European Journal of Pharmaceutics and Biopharmaceutics, 133 (2018), 138-150.*

    - Konzeptionierung: 50 %
    - Planung: 60 %
    - Durchführung: 80 %
    - Manuskripterstellung: 80 %

3) Wöll, S., Bachran, C., Schiller, S., Schröder, M., Conrad, L., Scherließ, R., Swee, L. K.: Sortagging of liposomes with a murine CD11b-specific VHH increases *in vitro* and *in vivo* targeting specificity of myeloid cells. *European Journal of Pharmaceutics and Biopharmaceutics, 134 (2019), 190-198.*

   - Konzeptionierung: 50 %
   - Planung: 60 %
   - Durchführung: 70 %
   - Manuskripterstellung: 80 %

4) Wöll, S., Dickgiesser, S., Rasche, N., Schiller, S., Scherließ, R.: Sortagged anti-EGFR immunoliposomes exhibit increased cytotoxicity on target cells. *European Journal of Pharmaceutics and Biopharmaceutics, 136 (2019), 203-212*.

   - Konzeptionierung: 50 %
   - Planung: 60 %
   - Durchführung: 80 %
   - Manuskripterstellung: 80 %

5) Wöll, S. and Bachran, C., Schiller, M., Conrad, L., Scherließ, R., Swee, L.K.: Sortase-A mediated chemoenzymatic lipidation of single-domain antibodies for cell membrane engineering. *Intended for submission to a pharmaceutical journal in 2019.*

   - Konzeptionierung: 80 %
   - Planung: 50 %
   - Durchführung: 40 %
   - Manuskripterstellung: 80 %

Ort Datum Unterschrift (Steffen Wöll)

Danksagungen

Die vorliegende Arbeit entstand unter der Leitung von Frau Prof. Dr. Regina Scherließ der Christian-Albrechts-Universität zu Kiel und Herrn Stefan Schiller der Firma Merck KGaA im Rahmen meiner Tätigkeit als Doktorand bei der Firma Merck KGaA. In diesem Abschnitt möchte ich mich bei all jenen bedanken, die mich beim Anfertigen dieser Arbeit fachlich oder zwischenmenschlich unterstützt haben.

Mein besonderer Dank gilt meiner Doktormutter, Prof. Dr. Regina Scherließ, für ihre Betreuung während der praktischen Forschung, dem Anfertigen von Postern, Präsentationen, Publikationen und nicht zuletzt dieser Arbeit. Regina, ich danke dir sehr für deine kompetente Unterstützung, Diskussionsbereitschaft und die wertvollen Hinweise mit Blick auf die Wissenschaft, die mich stets vorangebracht haben. Auch danke ich dir für die offene Art, mit der du mich in den Kieler Arbeitskreis trotz der weiten Distanz integriert hast, sei es durch die tollen Klassenfahrten, das Doktorandenseminar inklusive Besuch der Kieler Woche oder durch die jährliche Weihnachtsfeier.

Ebenfalls danke ich Prof. Dr. Susanne Sebens sowie Prof. Dr. Ulrich Massing für die Übernahme der weiteren Gutachten.

Ein ganz besonders herzliches Dankeschön gilt Stefan Schiller. Stefan, du hast durch dein strikt logisches Denken, deine Methodenkenntnisse und Erfahrung in der Präsentation von Daten die Arbeit immer wertvoll und hochkompetent unterstützt. Ganz besonders danke ich dir jedoch dafür, dass du inmitten der strategischen Neuausrichtung der Doktorarbeit ein für mich spannendes Forschungsfeld aus dem Hut gezaubert hast. Auch möchte ich dir und in diesem Zusammenhang allen weiteren PharmTech-Kollegen danken, die die Doktorandenzeit in Darmstadt zu einem schönen und prägenden Abschnitt meines Lebens gemacht haben:

Dr. Markus Weigandt danke ich für die Möglichkeit, bei der Firma Merck und innerhalb von Pharmaceutical Technologies promovieren zu können, an internationalen Kongressen teilzunehmen, vor allem aber für die Unterstützung einer Forschungsarbeit ohne direkten Projektbezug. Dies ist in Zeiten knapper Budgetierung nicht selbstverständlich. Auch die Winter- und Sommerfrische darf an dieser Stelle nicht unerwähnt bleiben.

Dr. Andrea Hanefeld, ich danke dir für die anfängliche Betreuung dieser Arbeit. Dr. Simon Geißler, danke, dass auch du von dem Wert dieser Arbeit immer überzeugt warst, nötige Ressourcen zur Verfügung gestellt hast und vor allem auch fachlich wichtigen Input geben konntest. Ohne dein reibungslos funktionierendes DDI wäre manches Experiment deutlich schwerer gefallen. Dr. Meike Harms – Meike, du hast mich im Praktikum von der

Pharmazeutischen Technologie überzeugen können und bist mit Bernd der eigentliche Grund, wie es überhaupt zu dieser Arbeit kommen konnte – dafür danke ich auch dir.

Dr. Mira Oswald – ich danke dir für die tolle Einarbeitung in die Welt der Liposomen, die du mir am Anfang meiner Promotionszeit gegeben hast, für die Läufe durch Darmstädter Wälder und die vielen Zugfahrten nach Mainz, die das Pendeln angenehm gemacht haben. Dr. Markus Riehl, als Mitglied der „Vakzinierungsboygroup“ danke ich auch dir für die intensive Einarbeitung und Reviews von Publikationen. Dr. Magdalena Münster, Dr. Robert Hennig, Carolin Auch, Christian Jede, ich danke euch sehr für eure engagierte Unterstützung bei Korrekturlesungen. Dirk Schiroky danke ich besonders für seine Expertise und Einarbeitung an der MS. Auch allen weiteren Mitdoktoranden und Kollegen (Dr. Melanie Hofmann, Karsten Flügel, Dr. Corinna Schoch, Katrin Grieser und Vicky Schmitt) danke ich für ihre ständige Hilfs- und Diskussionsbereitschaft auf der Arbeit und noch viel mehr für die schönen gemeinsamen Stunden danach, sei es beim Laufen, im Kessel, am Rosenmontag oder auf den Wasn. Danke für eure Freundschaft.

Ich möchte weiter Lukas Maria Gockel und Martina Jeschke für die praktische Unterstützung bei aufwendigen Experimenten, sowie Reiner Vonderschmitt für seine Unterstützung bei Basteleien und die angenehmen gemeinsamem drei Jahre in der Laborbox danken. Dem Kieler Arbeitskreis, besonders Dr. Mathias Mönckedieck, Dr. Judith Heidland, Dr. Fabian Stahlkopf und Marie Hellfritzsch danke ich für die warmherzige Aufnahme in Kiel und unvergessliche Stunden an der Kieler Förde.

Forschung in interdisziplinären Bereichen kommt nicht ohne exzellente Kollaborationspartner aus. Ich danke daher ganz herzlich den Kollegen von BioMed X (Dr. Lee Kim Swee, Dr. Matthias Schröder, Lena Conrad sowie besonders Dr. Christopher Bachran) für die zahlreichen durchgeführten Experimente, die wertvollen Diskussionen und die tollen Ergebnisse der Zusammenarbeit im Bereich des MDSC-Targeting. Ebenso herzlich danke ich Dr. Stephan Dickgießer und Dr. Nicolas Rasche für die Bereitstellung von Antikörpern, die erfolgreiche Durchführung von Zellversuchen für das EGFR-Targeting und die Unterstützung beim Schreiben der zugehörigen Publikation.

Arbeit ist nicht alles. Daher danke ich dir, Julian, besonders für deine unvergleichliche Art, mir die schönen Seiten des Lebens neben der Arbeit zu zeigen – nur eine von deinen vielen Eigenschaften, die ich schmerzlich vermisse. Auch wenn du nie ganz verstanden hast, wie man Tag für Tag viele Stunden in Forschung investieren kann – am Ende habe ich es auch dafür getan, damit sich vielleicht irgendwann einmal dein Schicksal nicht wiederholen muss. Dies ist aber nur ein unbedeutender Trost für eine Menge Zeit, die uns auch durch diese Arbeit genommen wurde.

Ich danke an dieser Stelle meinen Geschwistern, welche mir durch ihre Präsenz in der Heimat in vielen wichtigen Punkten den Rücken freigehalten haben. Ebenso danke ich meinen Eltern, die mir ein naturwissenschaftlich-offenes Denken in die Wiege gelegt und mich in Studium und Promotion bedingungslos unterstützt haben. Auch meinen drei (!) Omas möchte ich hier ausdrücklich danken. Ich bin davon überzeugt, dass ohne eure Entbehrungen vieles in meinem Leben nicht möglich gewesen wäre – daher ist diese Arbeit konsequenterweise euch gewidmet.

Zu guter Letzt danke ich meiner Freundin Katharina. Kathi, ich danke dir für deine Geduld, die du mit mir hattest, wenn ich mürrisch spät abends nach Hause gekommen bin, wenn ein ganzes Wochenende zum Schreiben verplant oder die Merck-Welt mal wieder allzu einnehmend war. Danke, dass du auch in den schwierigsten Phasen dieses Lebensabschnitts immer zu mir gestanden und mich unterstützt hast.